THE TABBERABBERAN OROGENY

IN NORTHWEST TASMANIA

by

DAVID BRUCE SEYMOUR, B.Sc. (Hons)

Submitted in partial fulfilment of the
requirement for the degree of
Doctor of Philosophy

UNIVERSITY OF TASMANIA
HOBART

(March 1980)

Except as stated herein this thesis contains no material which has been accepted for the award of any other degree or diploma in any university, and, to the best of my knowledge and belief, this thesis contains no copy or paraphrase of material previously published or written by another person, except when due reference is made in the text of the thesis.

D.B. SEYMOUR

FRONTISPIECE

Alpine moorland surrounding the
Vale River at the southern end
of the Vale of Belvoir.

ABSTRACT

In the Black Bluff region of Northwestern Tasmania, Cambrian sedimentary and volcanic rocks are distributed in an arcuate belt around the northwest margin of the Tyennan Geanticline, which is composed of Precambrian greenschist-grade metaquartzites and metapelites. The volcanics, which are dominated by heavily altered intermediate to acid pyroclastics, are concentrated in the southern part of the belt which borders the margin of the geanticline. The Cambrian rocks are unconformably overlain by Lower Ordovician quartzose clastics and Middle Ordovician limestones. Movements responsible for the angular discordance are inferred to have been dominantly vertical and responsible for steep tilting of the Cambrian sequences and considerable uplift of the Tyennan Geanticline, which became the source area for the sediments immediately overlying the unconformity. The quartzose clastics were mainly deposited in terrestrial alluvial fan environments, although marginal marine sedimentation became progressively more important upwards in the sequence. Intertidal sedimentary environments persisted during deposition of the limestone sequence, but relief of the Precambrian source areas had by early Middle Ordovician time been reduced to such an extent that terrigenous influx was insignificant.

Middle Devonian deformation of the Palaeozoic rocks, at high crustal levels, produced open, upright, horizontal to gently plunging folds of variable trend. The Tyennan Geanticline behaved as a relatively rigid block during this deformation, which has been correlated with the Tabberabberan Orogeny, of regional importance in southeastern Australia. The structural development now recognized involves a progressive sequence of regional folding on axes which trend east (D1), northeast (D2), north (D3) and northwest to north-northwest (D4). The last three phases of folding were associated with development of axial plane cleavage in the more ductile lithologies. Localized folding on east-northeast axes and associated cleavage postdates D2, and may have occurred between D2 and D3. The relative timing of fold and cleavage development on west-northwest trends in the limestone at Loongana and Gunns Plains is uncertain. Previous conclusions regarding dating of the Tabberabberan deformation may need reconsideration in view of the newly proposed structural sequence.

Development of tectonite fabrics in the altered volcanics was mainly by syntectonic recrystallisation and new grain growth of fine sericitic mica and chlorite. Quartz phenocrysts deformed variously by brittle fracturing, pressure solution processes and/or development of intragranular deformation lamellae. Pressure dissolution/solution transfer/reprecipitation processes

were also important in the formation of spaced cleavage domains in the Ordovician quartzose clastics and limestones. The deformation took place at burial depths probably no greater than 4-5 km, although temperatures of >300°C may have been attained at the base of the limestone.

Analysis of total strain, using various types of elliptical particles in incipiently to strongly cleaved Ordovician limestones indicates a shortening across the cleavage of 19% to 71%, with concomitant maximum extensions within the cleavage plane of 26% to 163%. The appearance of obvious cleavage at outcrop scale in the limestone corresponds to a measured shortening of 30-35%. Coincidence of cleavage with the XY plane of the finite strain ellipsoid has been demonstrated with a confidence of ±5° in the oolitic limestones. Consideration of all three principal strains reveals that the rocks generally lie in the flattening field of deformation with the total strain ellipsoid being such as to indicate either approximately plane strain or a deformation process intermediate between plane strain and pure flattening.

In evaluating the strain, several of the commonly available analytical methods have been used. In doing so, it has been possible to critically assess these methods and to quantify their variable dependence upon initial fabric.

LIST OF CONTENTS

CHAPTER 3. (contd.)

CHAPTER 4. STRUCTURAL GEOLOGY

CHAPTER 4. (contd.) Page

(Reprint of paper):

Seymour, D.B. and Boulter, C.A. (1979): Tests of computerized strain analysis methods by the analysis of simulated deformation of natural unstrained sedimentary fabrics. *Tectonophysics, 58:* 221-235.

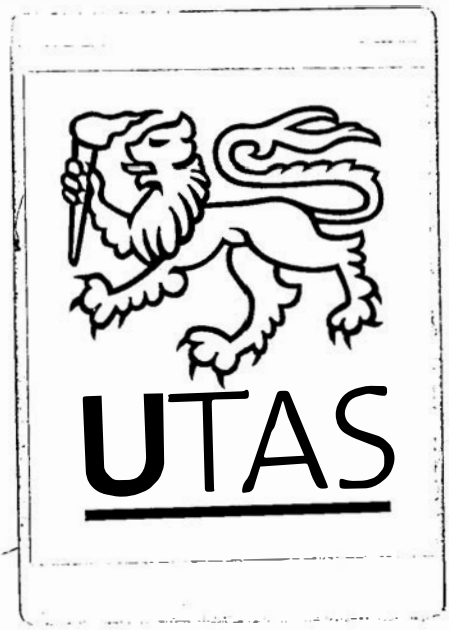

LIST OF FIGURES

Page

* * * *

LIST OF TABLES

CHAPTER 1

INTRODUCTION

1.1 LOCATION AND SCOPE OF PROJECT

This thesis summarizes the results of geological field mapping at a scale of 1:20,000 in an area of some 500 sq.km. in northwest Tasmania, southeast Australia (see Fig. 1.1). The research has concentrated on detailed stratigraphic, sedimentological and structural analysis of Lower Palaeozoic rocks deformed by folding on several different trends during the Devonian Tabberabberan Orogeny (see Map 1, in pocket). The location and coverage of the study area outlined in Fig. 1.2 was determined mainly from consideration of the best area in which to examine the intersection of the main Tabberabberan fold belts, and from the fact that little detailed structural mapping had previously been carried out in this area, in comparison with areas to the east, north and southwest.

As a consequence of analysis of the effects of the Tabberabberan Orogeny, interest has also been focussed in the fields of geological strain analysis and deformation mechanisms associated with the development of rock cleavage. The results of this work are of more general interest in structural geology, and are reported in separate chapters.

1.2 ACCESS AND TERRAIN

Most of the high areas in the central part of the region covered by Fig. 1.2 are underlain by quartzose clastic rocks of probable Lower Ordovician age. This lithology together with the fact that the region was at least periglacial at some time in the Pleistocene, has resulted

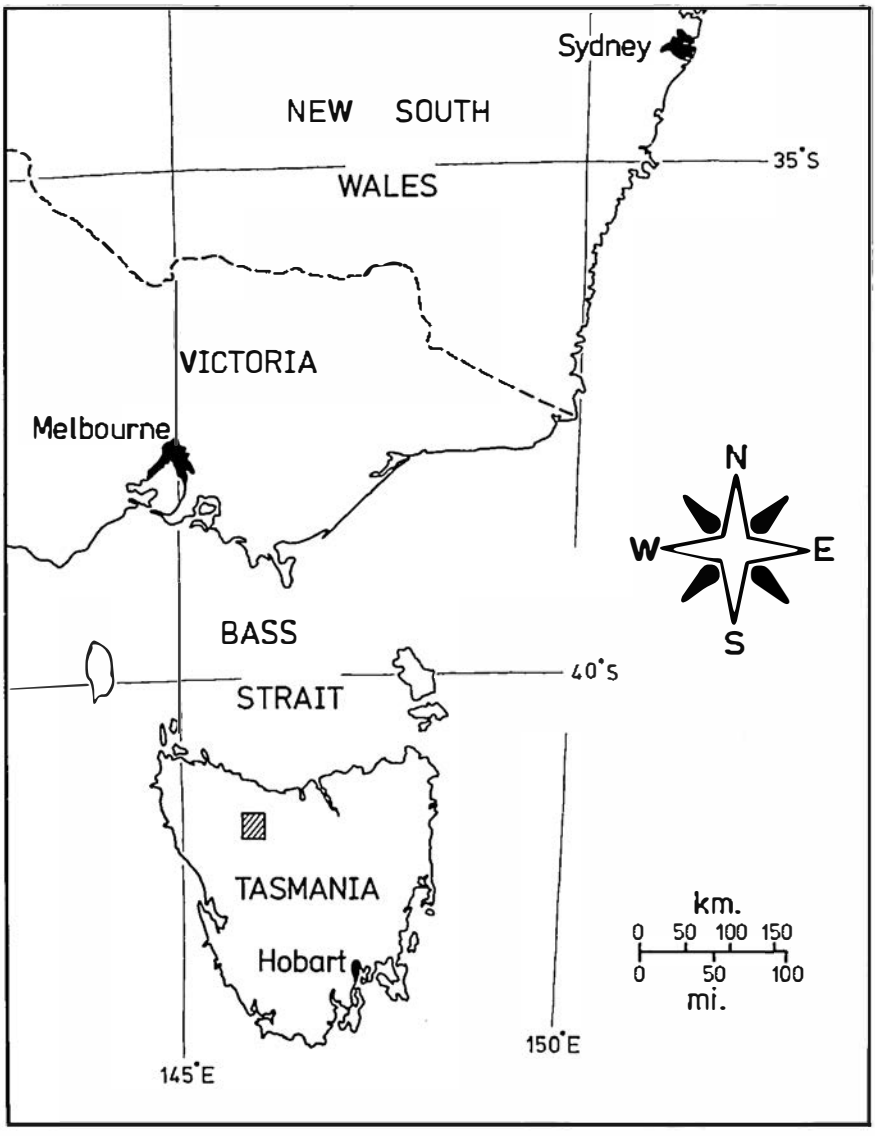

REGIONAL LOCATION

Southeast Australia

FIGURE 1.1

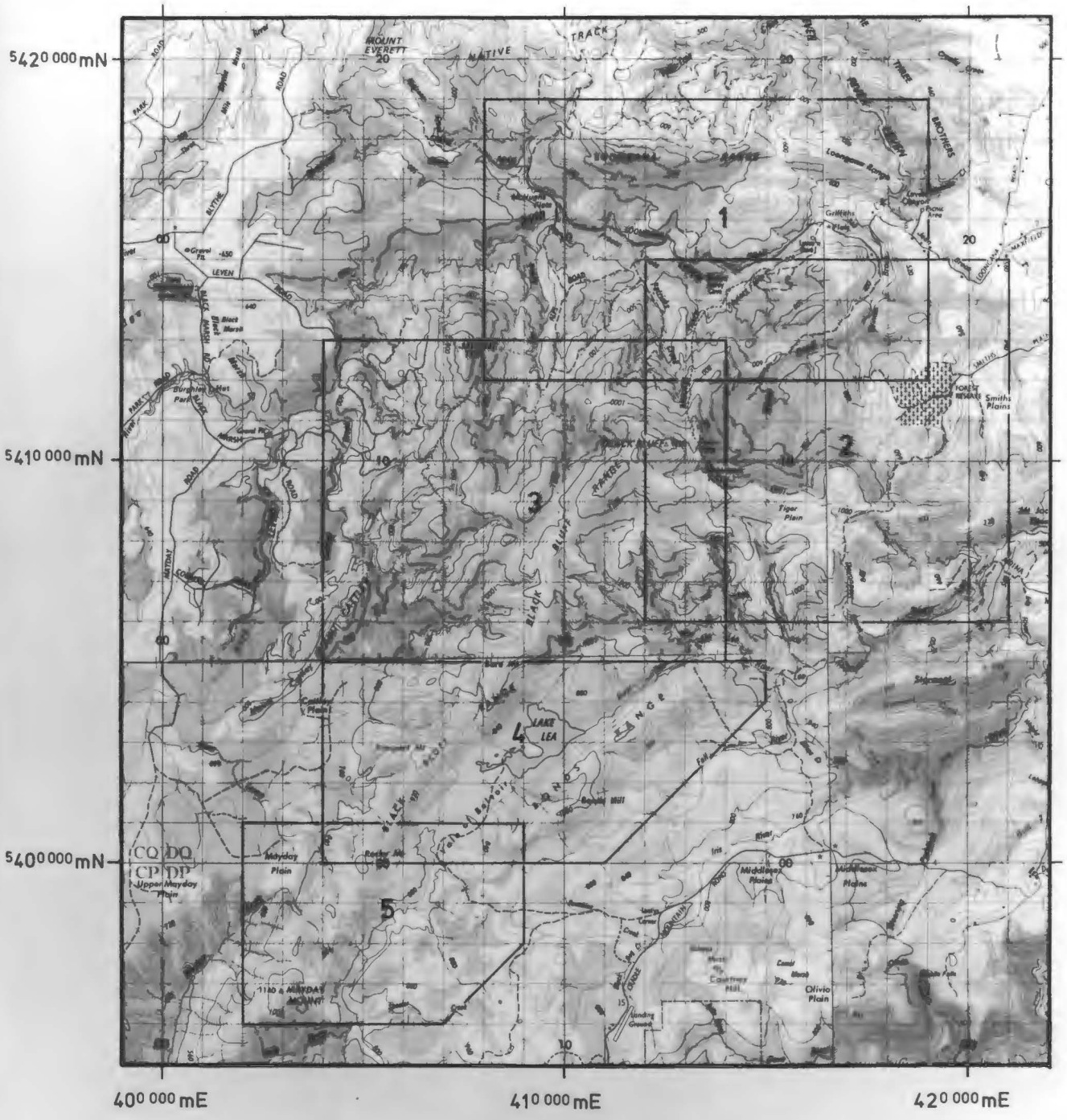

1:150,000 LOCALITY MAP

Showing coverage of structural maps

1. Loongana
2. Smiths Plain
3. Black Bluff
4. Vale of Belvoir (North)
5. Vale of Belvoir (South)

FIGURE 1.2

in thin soil cover and dominant alpine moorland vegetation in the high areas (see Frontispiece). Maximum topographic relief in the region is about 960 m, the highest peak being Black Bluff at 1339 m. The thin soil cover has resulted in reasonably good outcrop, particularly along ridge crests.

Topographic low areas are mainly occupied by less resistent rocks of probable Cambrian age (mainly altered volcanics, pyroclastics and flysch-facies sediments), by Ordovician limestone, or by Tertiary flood basalts. Areas underlain by these lithologies are often heavily forested, although considerable clearfelling has been carried out in many places. An exception is the Vale of Belvoir in the central southern part of Fig. 1.2, which is underlain by Ordovician limestone and has natural alpine grassland vegetation similar to that developed on the quartzose clastics. Outcrop in the topographic low areas is generally poor, and geological mapping often necessarily relies heavily on creek and road sections and quarries.

Access to the area was mainly via the Loongana road in the north, a network of forestry roads in the west, and a four-wheel-drive track connecting the Cradle Mt. road with the Vale of Belvoir in the south (see Fig. 1.2). These generally provided access only to the marginal parts of the area, most of the mapping being accomplished by long traverses on foot. Reliable weather for field mapping in much of north-western and western Tasmania is restricted to the summer months, December to early March. Parts of three such summer field seasons have been occupied with the field mapping, a total of some four and a half months having been spent in the field.

1.3 ACKNOWLEDGEMENTS

I wish to acknowledge the following individuals and institutions who have provided academic, financial or logistical support during the course of the project:-

(1) Dr. C.A. Boulter (now of the Geology Department, University of Western Australia), Dr. E. Williams, Supervising Geologist of the Geological Survey Section of the Tasmanian Department of Mines, and Associate Professor S.W. Carey of the Geology Department, University of Tasmania, for acting as supervisors of the research.

(2) Other staff members of the Geology Department, University of Tasmania, particularly Drs. M.R. Banks, C.P. Rao and C.F. Burrett for many helpful academic discussions.

(3) Griff Weste and Paul Askins of Comalco Limited Exploration Office, Spreyton, Tasmania, for helpful discussions on the geology of the Cambrian rocks of the Smiths Plains area, to the east of Black Bluff.

(4) Associated Forest Holdings of Burnie, for allowing access to the forestry roads in the western part of the area.

(5) Mr. Jim Charleston of Wilmot, Tasmania, for allowing the use of a hut in the Vale of Belvoir for accommodation during some of the fieldwork.

(6) The Australian Government for providing financial assistance through the Commonwealth Postgraduate Research Awards scheme.

1.4 NOTATION

Maps 1 to 6 inclusive refer to folded maps included in the pocket at the back of the thesis. The mapping was carried out and compiled on base maps at scales of 1:20,000 and 1:15,840. Grid coordinates are given in the order (east, north) to either the nearest kilometre

(e.g. 402397), which refer mainly to Map 1, or to the nearest 100 metres (e.g. 4197/4121), which refer mainly to Fig. 1.2, which is constructed from parts of the Tasmanian Government Lands Department 1:100,000 Tasmaps HELLYER, SOPHIA, FORTH and MERSEY.

Specimen numbers are prefixed UTGD and refer to the collection of the University of Tasmania Geology Department. Photomicrographs are labelled with respect to lighting conditions, i.e. PPL for plane polarized light and XPL for crossed polarizers.

1.5 GEOLOGICAL SETTING

The large amount of data available on the Palaeozoic geology of western Tasmania has in recent years lead to attempts at compilation, the most notable being those of Corbett (1970) and Williams (1976, 1978). The map produced by Corbett is included for comparison (Fig. 1.3), but as Williams' compilation is the most recent, and is also part of a published work, the more rigorous terminology used on it will be adhered to herein (Map 1, in pocket).

1.5.1 Precambrian elements

The Precambrian rocks of western Tasmania occupy regions between which Lower Palaeozoic deposition took place in elongate troughs. These regions became geanticlines during the Cambrian, i.e. they were topographic high areas which supplied detritus to the developing troughs. Williams made a strict distinction between the term "geanticline" and the term "block", which he used to identify regions of Precambrian rocks which acted passively, with little internal deformation, during the Devonian Tabberabberan Orogeny, responsible for most of the deformation in the pre-Carboniferous Palaeozoic rocks of western Tasmania. Thus the Tyennan Block was subdivided by Williams into a northern Cradle Mountain

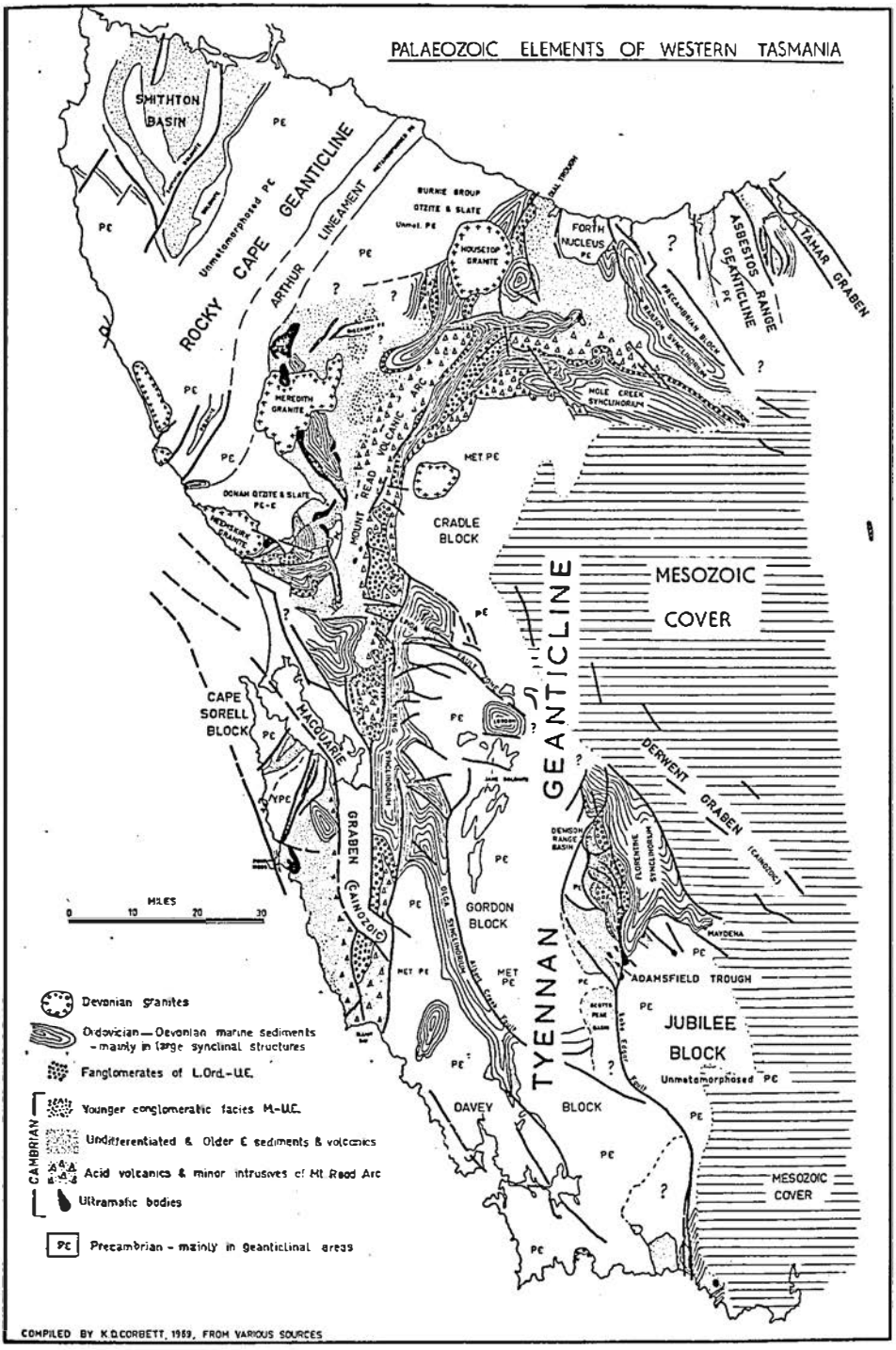

(after Corbett, 1970)

FIGURE 1.3

Block and a southern Prince of Wales Range Block, on the basis of a zone between the two which yielded by folding and faulting during the final major phase of the Tabberabberan Orogeny (see Map 1). Corbett showed similar subdivisions of the Precambrian on his compilation (Fig. 1.3), but was less rigorous in his terminology, mixing the terms "geanticline", "block" and "nucleus". To attempt to avoid confusion, the term "geanticline" will be used herein in reference to the Precambrian areas in all cases except where specific reference is made to the behaviour of these areas during the Tabberabberan deformation.

The Precambrian rocks can be subdivided into two groups, based on relative degrees of metamorphism. Both groups have suffered polyphase deformation, but only one has reached relatively high grades of metamorphism. The latter group predominates in the Tyennan Geanticline, consisting of "deformed and metamorphosed sequences of interbedded siltstone and orthoquartzite" (Williams, 1978, p.177). Metamorphic grade is as follows:-

(1) reaching upper greenschist facies with growth of pre-kinematic almandine garnet, in the Cradle Mountain area (415385) at the northern end of the geanticline (Gee *et al.*, 1970a).

(2) pre-kinematic and early syn-kinematic growth of chlorite, biotite, almandine and kyanite in a zonal sequence, at the Raglan Range (400335; Gee, 1963) and Frenchmans Cap (405320; Spry, 1963) in the central part of the geanticline.

(3) an early main phase of garnet grade metamorphism at Davey River (415225; McClean, 1974) in the southwestern part of the geanticline.

Multiple folding together with this early main period of metamorphism were used by Spry (1962, pp.107-126) to define the Frenchman Orogeny, the imprint of which was in turn used as the identifying

characteristic separating this group of rocks from the relatively unmetamorphosed Precambrian. Spry (1962, p.124) also introduced the terms "older" Precambrian (Spry's quotation marks), to cover all those rocks apparently formed prior to the Frenchman Orogeny, and "younger" Precambrian for all those apparently formed later.

The southeastern part of the presently exposed area of the Tyennan Geanticline is occupied by relatively unmetamorphosed probable Precambrian sequences of dolomite and quartzite. Williams (1978, p.188) seems to have considered this feature as a geanticline separate from the Tyennan Geanticline. Corbett (1972, p.11) named it the Jubilee Block (Fig. 1.3) and made a definitive statement separating it from the definition of the Tyennan Geanticline. The eastern limit of the Tyennan Geanticline is thus defined by the western margin of the Palaeozoic Adamsfield Trough (labelled 6 on Map 1), and by the faulted contact with the Jubilee Block of Corbett.

Deformation and metamorphism attributed to the Frenchman Orogeny also appear in the Forth Geanticline (Burns, 1965) on the north coast. Quartzite, schist and amphibolite display metamorphism to almandine garnet grade accompanying the earlier deformation.

The large area of Precambrian rocks occupying most of the northwest corner of Tasmania has been termed the Rocky Cape Geanticline. Three suites of deformed but relatively unmetamorphosed Precambrian rocks are separated by a linear belt (the Arthur Lineament, Map 1) which appears to consist of their more metamorphosed equivalents (Williams, 1978, p.179, after McNeil, 1961; Longman and Matthews, 1962). The unmetamorphosed suites are the Rocky Cape Group on the northwest side of the Arthur Lineament, consisting of supermature orthoquartzite and siltstone; the Burnie Formation to the east of the lineament, containing black mudstone turbidite quartz-wacke and rare altered pillowed spilite; and the Oonah

Formation in the southeast corner of the geanticline, comprising dominantly siliceous siltstone and fine-grained sandstone. The Penguin Orogeny has been defined as constituting the movement resulting in the folding and the development of the metamorphic belt in the Rocky Cape Geanticline (Williams, 1978, p.179; Spry, 1962, p.124). The Penguin Orogeny is regarded as younger than the Frenchman Orogeny.

1.5.2 Cambrian elements

Williams (1976, 1978) subdivided areas of Cambrian sedimentation into five main elements:-

(1) the Dundas Trough, situated between the Tyennan and Rocky Cape Geanticlines (see 1 on Map 1).

(2) the Fossey Mountain Trough, between the Tyennan and Forth Geanticlines (5, Map 1).

(3) the Dial Range Trough, between the Forth and Rocky Cape Geanticlines (4, Map 1).

(4) the Adamsfield Trough, which developed at the southeastern margin of the Tyennan Geanticline (6, Map 1).

(5) the Smithton Trough, which developed within the Rocky Cape Geanticline (3, Map 1).

In this study interest has been concentrated on correlates of rocks which formed in the first three of these troughs.

In the Dundas Trough (Campana and King, 1963) lithologically distinctive groups of Cambrian sedimentary and volcanic rocks are distributed in belts approximately parallel to the margins of the trough (Map 1). The sedimentary rocks are chiefly in the western part of the trough and comprise two main sequences: a lower unfossiliferous sequence (including the Crimson Creek Formation of dominantly mudstone) and an upper fossiliferous Middle and Late Cambrian usually greywacke-type

turbidite sequence, including the Dundas Group. In the eastern part of the trough, along the western and northwestern margins of the Tyennan Geanticline, the stratigraphic interval covered by these two sequences is occupied by a pile of dominantly acid-intermediate volcanic and associated rocks, the Mount Read Volcanics (see 2 on Map 1).

In the Fossey Mountain Trough (Jennings, 1958, 1963) the large scale distribution of Cambrian rocks is similar to that in the Dundas Trough, with volcanic rocks being concentrated towards the northern margin of the Tyennan Geanticline (Map 1). The Dial Range Trough, however, contains a high proportion of tholeiitic basic volcanics. In the Dundas Trough similar basic volcanics often occur in close association with tectonically emplaced ultramafic complexes. Williams (1978, p.190) associated these basic volcanics with an early extensional rifting stage of development of the Dundas Trough. Further details of stratigraphy in the Dundas, Fossey Mountain and Dial Range Troughs are discussed in a later section.

1.5.3 Ordovician and Siluro-Devonian elements

The base of the Ordovician System in many places in western and central northern Tasmania is represented by an erosional, and sometimes recognizably angular, unconformity against Cambrian sedimentary or volcanic rocks, or against Precambrian rocks (Carey and Banks, 1954). The basal Ordovician beds are often molasse-facies terrestrial conglomerates (Owen Conglomerate and correlates) deposited as alluvial fans and consisting of detritus derived from the underlying Cambrian rocks and/or from the metamorphic rocks of the geanticlines. The occurrence of the unconformity and/or the nature of the immediately overlying sediments has lead to the proposal of a tectonic movement or series of movements towards the end of the Cambrian, involving reactivation and uplift of the

geanticlines and also of parts of the Cambrian sequence close to the margins of the geanticlines. The newly uplifted areas then became source areas for the following phase of sedimentation.

The conglomerates are succeeded conformably by finer grained siliceous clastics, shallow marine Early to Late Ordovician limestones of the Gordon Subgroup and shallow marine interbedded quartz sandstone and mudstone (Eldon Group and correlates), the youngest known beds of the latter being of middle-Early Devonian age (Williams, 1978, p.194, after Flood, 1974). The sequence up to the top of the Gordon Subgroup has been referred to in the past as the Junee Group, but problems have arisen with this nomenclature; these are discussed in a later section. Deposition of the conformable beds following the conglomerates extended over much of the areas which had earlier been geanticlines.

In the late-Early to early-Middle Devonian the Cambrian to Early Devonian rocks of western Tasmania suffered widespread deformation, producing upright flattened parallel folds on several different trends (Williams, 1978). The early phase folds trended parallel to the margins of the areas of Precambrian rocks, which acted as relatively competent blocks during the deformation. The deformation is correlated with the Tabberabberan Orogeny, which has regional significance in southeastern Australia.

The Palaeozoic rocks occupying the northeast corner of Tasmania east of the Tertiary Tamar Trough (Map 1) are markedly different to those of central northern and western Tasmania. These have been termed the Mathinna Beds, and consist of sequences of interbedded mudstone and quartz-wacke ranging in age from Early Ordovician to Early Devonian. They are also affected by folding correlated with the Tabberabberan Orogeny. The folds have northwest trending hingelines parallel to

trends of folds produced in the last phase of Tabberabberan deformation in Palaeozoic rocks to the west of the Tamar Trough. However the indicated direction of tectonic transportation is opposite on either side of the Tamar Trough. Williams (1978, p.201) stated:

> "The abrupt change in sedimentary rock types and structural characteristics between western and northeastern Tasmania indicates that the Tamar River is the site of a fracture along which lateral movements brought the contrasting regions into juxtaposition (Williams and Threader, 1971; Williams *et al.*, 1976)."

Attempts to fit such movements into a large scale tectonic framework have been reported by Crawford and Campbell (1973) and Harrington *et al.* (1973).

The folded rocks of both northeastern and western Tasmania have been intruded by granitic rocks of Devonian age. They are essentially post-kinematic to the Tabberabberan structures. In western Tasmania they have a range in minimum ages of 335-365 m.y., while in northeastern Tasmania the age range is 360-375 m.y. (Williams, 1978, p.199).

Most of central and southeastern Tasmania is covered by little-deformed flat-lying strata of Late Carboniferous and younger age, intruded by dykes, sills and transgressive sheets of Jurassic dolerite. This makes comment on the southeasterly extension of the Fossey Mountain Trough difficult (Map 1). However, the occurrence of probable Cambrian basic intrusives and/or volcanics near Connorville (508365, Map 1), the Cambrian sediments and volcanics of the Adamsfield Trough, and poorly known Cambrian rocks near Surprise Bay (472173) on the south coast, have been cited as evidence suggesting that there may have been a continuous belt of Cambrian sedimentation and volcanism around the Tyennan Geanticline (Corbett *et al.*, 1972).

CHAPTER 2

STRATIGRAPHIC BACKGROUND

2.1 THE DUNDAS GROUP AND STRATIGRAPHIC EQUIVALENTS

2.1.1 Type area

The Dundas Group was defined in the Dundas area (369362, Map 1), 7 km east of Zeehan, by Elliston (1954). In the Dundas Trough the base of the Group is a structurally concordant but erosional boundary with the underlying Crimson Creek Formation to the west, consisting of unfossiliferous mudstone and of inferred Early Cambrian age (Banks, 1962a, pp.127-131). The boundary is often marked by faults, or by an ultramafic/mafic complex with thrust faulted contact against the Crimson Creek Formation and erosional contact with the Dundas Group (as at Serpentine Hill, 368368).

An amended type section (after Elliston, 1954) for the Dundas Group was given by Banks (1962a, p.132):-

(Misery Hill to Mt. Razorback)		(South Comet Creek)	
TOP			
Mt. Zeehan Conglomerate (Ordovician)			
——— (conformable boundary) ———			
Dundas Group	(m)		
Misery Conglomerate	150		
*Climic Siltstone and Greywacke	610		
Fernflow Greywacke and Conglom.	145		
*Comet Siltstone and Greywacke	320		
Fernfields Greywacke and Conglom.	595		
Brewery Junction Slate and Tuff	745		
Razorback Conglomerate	75		
*Hodge Slate	185		
Greywacke Conglomerate	120	=? Red Lead Conglom.	75
		Severn Slate	245
—— (contact with serpentinite) ——		South Comet Greywacke	45
		*Judith Slate & Greywacke	60
BASE		— (contact with Carbine Group, U. Proterozoic-L. Cambrian) —	
		TOTAL	3295 m

* indicates Formation for which biostratigraphic information is available.

This type section was revised by Blissett (1962, p.32) who rejected some of the formations. Blissett's section is as follows:-

TOP Junee Group

Misery Conglomerate

Dundas Group	(m)
Climie Formation	460
Fernflow Formation	150
Comet Formation	150-300
Fernfields Formation	?0-590
Brewery Junction Formation	610
Razorback Conglomerate	80-230
Hodge Slate	150-180
Red Lead Conglomerate	50-120
Judith Formation	60
TOTAL	1710-2700 m

BASE

Blissett removed the Misery Conglomerate from the definition of the Dundas Group because he considered it equivalent to the Mt. Zeehan Conglomerate and other basal conglomerates of the Junee Group in western Tasmania (Blissett, 1962, pp.36, 49).

The following notes summarize the known biostratigraphy of the Dundas Group in its type area:-

(1) Judith Formation

contents: *Peronopsis, Ptychagnostus, Pagetia* and other trilobites

correlation: *Ptychagnostus gibbus* Zone

age: early-Middle Cambrian

reference: Banks (1962a, p.132, after Opik, 1956, p.251).

(2) Hodge Slate

contents: *Archaeolafoea serialis, Archaeocryptolaria skeatsi,* other "dendroids", trilobites and cystoids

correlation: upper part of *P. atavis* Zone or the *P. punctuosis* Zone

age: middle-Middle Cambrian

reference: Banks (1962a, p.132, after Opik, in Banks, 1956, p.191).

(3) Comet Formation

contents: agnostids including *Oidalagnostus* and many other trilobites including numerous "*Blackweldaria* cf. *biloba*".

age: Lower Dresbachian (early-Late Cambrian)

reference: Banks (1962a, p.132).

(4) Climie Formation (200 m below top)

contents: inarticulate brachiopods *Angulotreta* (?) sp. and *Lingulella* (?) sp.
trilobites *Olenus* sp., *Neoagnostus* sp., *Agnostus* sp., Ceratopygidae, gen. et sp. indet.

age: early post-Idamean (early-Late Cambrian)

reference: Jago (1978).

Two important pieces of biostratigraphic information from Dundas Group correlates elsewhere in the Dundas Trough are as follows:-

(1) In a section on the Huskisson River (372375, Map 1), the correlate of the Dundas Group is once again separated from the Crimson Creek Formation by an ultramafic body (Blissett, 1962, pp.36-39). The agnostid trilobite *Glyptagnostus reticulatus* is found about 25 m below the conformable contact with the Junee Group (Jago, 1973; Blissett, 1962, pp.38-39). This indicates correlation with one of the two lower Idamean zones (middle-Late Cambrian) from Queensland.

(2) The youngest fossiliferous horizon recorded from correlates of the Dundas Group outside the type area to date is that containing *Lotagnostus*, from near Birch Inlet, south of Macquarie Harbour in the central west coast (Jago, 1972, 1973). The indicated age is the late-Franconian stage of the late-Late Cambrian.

There has been some argument as to the assigned position of the top of the Dundas Group in its type area. Elliston (1954) included the Misery Conglomerate as part of the Group, while Blissett (1962) regarded this formation as equivalent to the basal conglomerates of the Junee Group. Blissett (1962) and Williams (1975) both considered that the contact between the Climie Formation and the Misery Conglomerate was conformable, however the possibility of it being a paraconformity was raised by Jago (1973). This possibility appears to have also been considered by Banks (1962a, pp.132-133):

> "Between the Comet Slate and the Mt. Zeehan Conglomerate only 900 m of sediment, some of it greywacke conglomerate, represents most of the Upper Cambrian. It seems likely that a major interval of non-deposition or of erosion occurs within the sequence between these formations."

The main problem which has arisen with respect to the Dundas Group is the lithofacies-based correlation with it which has been used by workers in other areas, particularly the Fossey Mountain and Dial Range Troughs. Blissett (1962, p.31) stated:

> "... the use of the term Dundas Group, as defined, should be restricted to units which can be placed with certainty within this time range, as proposed by Campana *et al.* (1960)."

Here, Blissett refers to the interval between the *Ptychagnostus gibbus* Zone (early-Middle Cambrian) and the *Glyptagnostus reticulatis* Zone (middle-Late Cambrian). Unfortunately in making this restriction Blissett appears to be mixing lithostratigraphic and biostratigraphic concepts.

The lithofacies correlation problem is compounded by rapid facies changes, both vertically and laterally, in the sedimentary and volcanic rocks of the Dundas Group.

2.1.2 Fossey Mountain Trough

A definitive statement on the Cambrian rocks of this trough has not yet been published. The main publications to date are those of Jennings (1958, 1963), however the most complete statement on the stratigraphy of the trough as a whole was given by Jennings in Banks (1962a, pp.135-136). The following stratigraphy is compiled from the latter:-

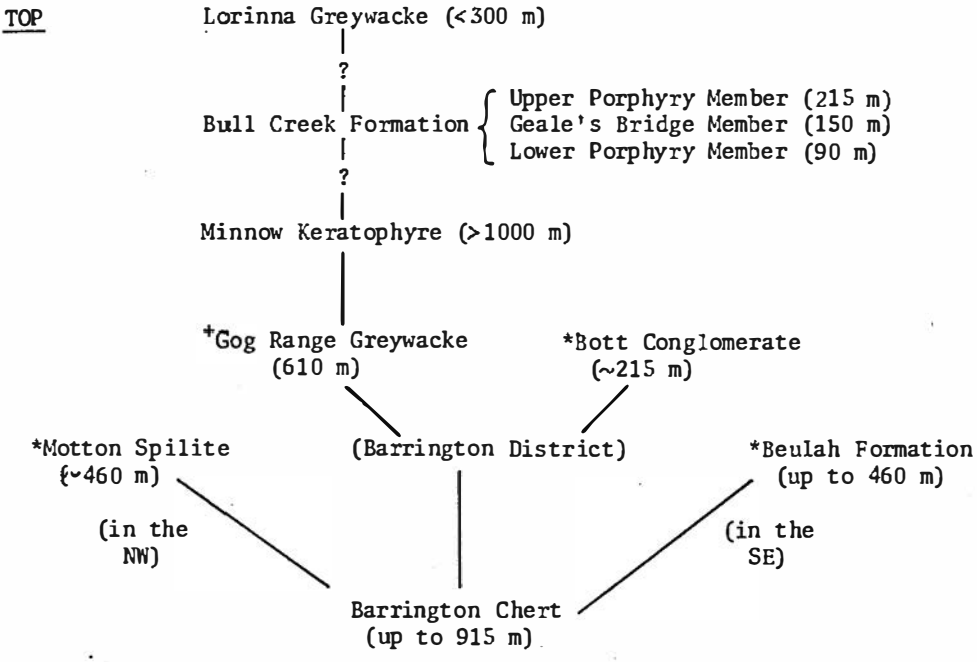

+ biostratigraphic data available
* restricted areal distribution.

In the first of his publications on the Fossey Mountain Trough, Jennings (1958) actually used the term "Dundas Group" for rocks of inferred Cambrian age in the Round Mount area (429407, Map 1), although he introduced no new formation names. His justification was (Jennings, 1958, p.22):

> "The definition of the Dundas Group includes similar rock types to those which occur here, and it occupies a similar stratigraphic position. Therefore, to avoid coining unnecessary new names this association of volcanic and pyroclastic rocks together with their associated greywacke type sediments shall be referred to tentatively as the Dundas Group."

This is almost correct use of lithofacies correlation, i.e. technically the rocks should be referred to as "correlates of the Dundas Group".

Jennings later dropped the Dundas Group term but still regarded the rocks as correlates of the Dundas Group (Jennings, 1963, p.38). Biostratigraphic information is conspicuously lacking from Cambrian rocks of the Fossey Mountain Trough, the only useful data being from the Gog Range Greywacke. Loose specimens inferred to have come from this formation contained *Pseudagnostus*, other agnostids and trilobites which suggest a Late Cambrian age (Jennings, after Opik, in Banks, 1962a, p.136).

Jennings (in Banks, 1962a, p.135) considered that deposition of the Barrington Chert was interrupted by uplift along the centre of the basin accompanied by widespread volcanic activity, all formations above the chert containing fragments of chert.

2.1.3 St. Valentines Peak area

Cambrian rocks in the vicinity of St. Valentines Peak are exposed in the core of an approximately N-S trending anticline (395422, Map 1). The Cambrian rocks here paas upwards with apparent conformity but probable disconformity into correlates of the basal conglomerates of the Junee Group (Jago *et al.*, 1975). The exposed succession on the western limb of the anticline as given by Jago *et al.* is:-

(Locality: PMG Road-Black Pit Road area

		(m)
TOP	Basal Junee Group conglomerate	
	—— (contact very sharp but slightly uneven) ——	
	Very fine grey siltstone	0.05-0.1
	Poorly fossiliferous micaceous grey-green siltstone and interbedded fine breccia beds	3.5
	Lens of chert/quartzite breccia	0.15-0.45
	—— (? disconformable contact) ——————	
	Grey siltstone	1
	Microbreccia	0.5
	Grey siltstone	11
	Deeply weathered brown siltstone	1.5
	Laminated and non-laminated slightly pyritic pale grey chert (hornfels)	230-375
	(?) Contact metasomatic rock (originally impure limestone or dolomite ?)	100
	Metasandstone and metasiltstone	75-100
	Welded tuff (welding incipient to moderate, rhyolitic to rhyodacitic)	100
	Massive, cherty, pyritic metasandstone and metasiltstone	100+
BASE	TOTAL	623-793 m

Fossils described by Jago *et al.* are from a locality 3 km south of the section listed. The fauna, which included agnostid trilobites, indicated a late-Middle Cambrian age (Jago *et al.*, 1975, p.87). The outcrop at the locality was poor, and the stratigraphic position of the fauna with respect to the above section could only be inferred. Structural mapping in the area indicated that the fauna occurs stratigraphically slightly below the lowest unit of the measured section. Other possibilities considered were that the sediments at the fossil locality corresponded to either the unit above the welded tuff, or to the chert unit above the (?) contact metasomatic rock.

2.1.4 Dial Range Trough

Burns (1963, 1964) described predominantly sedimentary rocks which he correlated with the Dundas Group, occupying a meridional belt (the Dial Range Trough) extending from east of Gunns Plains (419430), north to Bass Strait (see 4, Map 1). The slightly amended composite succession listed by Burns (1964) is as follows:-

TOP	(m)
(Jukesian Unconformity)	
Beecraft Megabreccia and correlates (Teatree Point Megabreccia, Westbank Beds) equivalent to, or unconformably overlying, the Radfords Creek Group	150
Radfords Creek Group	
Mudstone, sandstone and conglomerate	60++?
Applebee Volcanics (intermediate)	60
Mudstone, sandstone and conglomerate	120-150
(Disconformity ?)	
Motton Spilite	0?-460
Barrington Chert	75-850+
(Hardstaff Unconformity)	
Cateena Group	
Mudstone, sandstone and conglomerate	320
Wilsonia Volcanics (acid)	0-110
Mudstone and sandstone	170
Kerrison Volcanics (intermediate)	35-120
Mudstone, sandstone, claystone and conglomerate	305+
Isandula Conglomerate	180+
(Disconformity)	
Lobster Creek Volcanics (acid to intermediate)	305+
BASE	

The following notes (1) and (2) summarize known biostratigraphic data on Cambrian rocks in the Dial Range Trough:-

(1) Cateena Group

locality: Cateena Point

formation: the unnamed Formation beneath the Kerrison Volcanics

contents: trilobites, dendroids, brachiopods

correlation: *Ptychagnostus gibbus* Zone (A.A.Opik)

age: early-Middle Cambrian

reference: Burns (1964, p.34).

(2) Radfords Creek Group

Biostratigraphic information is available from the unnamed formation underlying the Applebee Volcanics, and is summarized in the following notes a), b) and c).

a) Burns (1964, p.47) compared a measured section in the Sugarloaf Gorge on the Leven River east of Gunns Plains (421431, Map 1) with the same section as measured by Banks (1956, p.184). A slightly modified version from Jago (1976) is as follows:-

TOP

	(m)
Gordon Limestone (Junee Group)	
(Fault)	
1. "West Conglomerate" (Junee Group)	37
(Inferred unconformity)	
2. Brecciated greywacke	26
(Major fault)	
3. "Middle Conglomerate"	13
4. Mudstone with *Ptychagnostus* near top	22
5. Tuff	5.5
6. Mudstone	18
7. Greywacke	4
8. Mudstone	33
9. Greywacke sandstone, conglomerate and tuff	14
(Major fault)	
10. "East Conglomerate"	23
11. Mudstone	19
12. Tuff, lava	19
13. Argillite with *Lejopyge*, *Ptychagnostus*, *Pianaspis(?) leveni*, etc.	90
14. Tuff and lava	19
15. Argillite with *Tasagnostus* (near top)	460
(break??)	802.5m
Sprent Formation	

BASE

Jago retained the unit numbers of Burns (1964) for uniformity. He correlated the fauna of unit 13 with either the *Lejopyge laevigata* II or III Zone of the late-Middle Cambrian. Burns (1964, p.48) correlated the unit with the Comet Formation of the Dundas Group type succession. Banks (1956, p.184) reported *Clavagnostus* from unit 15, but Jago was unable to confirm this, finding *Tasagnostus* sp. instead, about 10 m from the top of the unit. Jago's discovery of *Ptychagnostus* near the top of unit 4 supported Burns' (1964, p.48) suggestion of tectonic repetition by faulting within the section. Jago (1976) considered that units 10 to 14 and the upper part of 15 (a thickness of > 200 m) are in continuous sequence with only minor

faulting, while Burns suggested continuity of units 3 to 9 and 10 to 12.

An interesting piece of absolute chronological information has emerged from the identification by Jago *et al.* (1977) of unit 14 in the above section as a body intrusive into the surrounding sediments. Sixteen whole-rock samples of this intrusion produced a perfect-fit Rb-Sr isochron indicating an Early Ordovician age of 490 ± 18 m.y.

b) Banks (1956, p.185) listed the following succession in an old timber road along the west side of the Leven Gorge (422433), 2 km NE of the section referred to in a) above, and stratigraphically above the fauna with *Lejopyge*:-

TOP

Quartz biotite keratophyre (Applebee Volcanics?)
Argillite
Greywacke with *Pseudagnostus*, a dikelocephalid, and another trilobite with affinities to *Monocheilus* (Opik, 1951).

——————————— (gap) ———————————

Argillite
Greywacke

——————————— (gap, 100 m +) ———————————

Chert and argillite, thin-bedded
Argillite (12-15 m)
Argillite with greywacke beds up to 0.5 m thick.

BASE

The fossiliferous horizon was dated as basal Dresbachian (early-Late Cambrian; Opik, 1951, see Banks, 1956, p.185), which is younger than the *Lejopyge* horizon (Burns, 1964, p.48).

Jago (1976, p.5) described the following additional fossils from this section:-

From the lowest exposed bed (a siltstone):

inarticulate brachiopods, trilobites, *Nepea* sp., *Aspidagnostus* sp., *Valenagnostus* sp., *Clavagnostus* sp., possible *Peronopsis*.

From slightly higher in the section:

Agnostascus sp., *Nepea* and other trilobites.

Jago correlated this fauna with either the *Lejopyge laevigata* III Zone or *Damesella torosa-Ascionepea janitrix* Zone.

A fauna from the formation underlying the Applebee Volcanics was also extracted from a quarry near Riana (416438, Map 1). The fauna was age equivalent to the *Lejopyge laevigata* Zone of the late-Middle Cambrian (Burns, 1964, p.47, after A.R. Palmer, U.S. Geol. Survey).

c) From the information in a) and b) above, Burns (1964, p.48) listed the following generalized succession for the southern end of the Dial Range:-

TOP	(m)
Mudstone	61
Applebee Volcanics	61
Mudstone with *Pseudagnostus* Mudstone, conglomerate, chert and tuffs with *Lejopyge* Barrington Chert *or* Motton Spilite	122-168
BASE	

The western wall of the Dial Range Trough has been interpreted as a fault scarp resulting from normal faulting (Burns, 1963, p.13), support for this being the presence of megabreccias derived from the high side, which appear to have been emplaced consequent upon tilting. Current direction, thickness variations within formations and their manner of transgression indicated that the trough axis sloped southwards at 30 m/km and currents travelled down it from a northern source. Burns (1963, pp.14-15) listed the following hiati in the succession as evidence of tectonic movements during sedimentation:-

(1) The Cateena Group rests on the Precambrian in places, on the Lobster Creek Volcanics in others, probably due to transgression of the Group over a submarine volcanic pile.

(2) The Barrington Chert rests on the Cateena Group in places and transgresses across almost a full thickness of that Group. In other places it rests on Lobster Creek Volcanics.

(3) The base of the Radfords Creek Group rests on Motton Spilite in the southeastern part of the trough and on Barrington Chert in the southwest. At the northern end of the trough the Group is represented by the Beecraft Megabreccia and correlates which transgress across all earlier-deposited formations of the Dundas Group to rest on basement in places. This transgression represents southward tilting of the axis of the trough of at least 30m/km, before or during deposition of the Group.

Burns (1964, p.155) identified the base of the Barrington Chert as an unconformity, the Hardstaff Unconformity, primarily on the basis of evidence of truncation of underlying stratigraphic units at the base of the chert. The construction of an interpretive palaeogeologic map at the base of the chert enabled Burns to deduce that the expression of the movements resulting in the Hardstaff Movement was broad, gentle folding with minor faulting, the folds having limb dips $\leq 20^{o}$.

A palaeogeologic map of the base of the Ordovician constructed by Burns (1964, p.160) showed that at this time the Barrington Chert had been deformed into a gentle geanticline (limb dips $\sim 15^{o}$, structural relief $\sim$300 m) and tight synclines. Burns correlated the movements responsible for this deformation with the Jukesian Movement, which was defined by Carey and Banks (1954) to mean those movements represented by the unconformity between the Cambrian Dundas and Ordovician Junee Groups.

2.2 MOUNT READ VOLCANICS

The Mount Read Volcanics were defined by Campana and King (in Banks, 1962a, p.131) on a type section in the Mt. Read/Red Hills area, southeast of Rosebery (380367, Map 1). They consist of a pile of dominantly acid to intermediate calc-alkaline volcanic and pyroclastic rocks with minor sediments, distributed in an arcuate belt fringing the Tyennan Geanticline, and which accumulated between the Geanticline and the troughs in which the Dundas Group and correlates were deposited (Map 1). Campana and King (1963) estimated their total thickness to be at least 2400 m. The volcanic types include lavas, volcanic breccias, ash-fall and ash-flow tuffs and intrusives, compositions being dominantly of altered rhyolite and dacite, with subordinate andesite and basalt. Post-emplacement alteration has usually lead to quartz-albite-chlorite-sericite assemblages ("spilite-keratophyre" mineralogy).

There has been considerable argument over the age of the Mount Read Volcanics. As pointed out by Banks (1962a, p.131) they have been variously regarded as:-

(1) essentially younger than the Dundas Group (Campana *et al.*, 1958)

(2) more-or-less contemporaneous with the Dundas Group (Carey, 1953; Banks and Solomon, 1961).

(3) older than the Dundas Group (Campana *et al.*, 1960; Campana, 1961a).

Banks (*ibid.*) stated: "They are clearly pre-Ordovician as they are overlain unconformably by Ordovician rocks." Blissett (1962, p.41) recorded the presence of lavas and tuffs interbedded with the Dundas Group *sensu stricto*. He concluded that at least part of the Mount Read Volcanics is older than the Dundas Group, and considered it likely that part may be equivalent in age to the Dundas Group. Loftus-Hills *et al.* (1967) also considered the volcanics to be partly older and partly contemporaneous with the Dundas Group.

At Que River (390396, Map 1), 17 km north of Tullah, Gee *et al.* (1970b) described acid volcanic agglomerates, breccia and massive pyroclastics practically identical to Mount Read Volcanics in the Rosebery area (379374), interlayered with fossiliferous marine carbonaceous shales. The sediments yielded an agnostid trilobite fauna indicating correlation with the *Ptychagnostus punctuosis* Zone or the *Ptychagnostus nathorsti* Zone (late-Middle Cambrian on the Swedish time scale) (Gee *et al.*, 1970b; Jago, 1977). This part of the Mount Read Volcanics is therefore laterally equivalent to the Dundas Group.

Within the Mount Read Volcanics at Comstock (383346), close to the margin of the Tyennan Geanticline near Queenstown, Corbett *et al.* (1974) distinguished a Late Cambrian sequence of volcanic and sedimentary rocks (the Tyndall Group), unconformably overlying older schistose pyroclastics which contain the major ore mineralization in the area. The sequence contains a basal limestone with trilobites indicating a late-Middle or early-Late Cambrian age (Jago *et al.*, 1972). In most areas the Tyndall Group is conformable with overlying siliceous Owen Conglomerate, the basal formation of the Junee Group. In fact, in their definition of the Tyndall Group, Corbett *et al.* included the Jukes Formation, a coarse locally-derived volcaniclastic conglomerate and breccia unconformably resting on volcanics in places and passing transitionally upwards into Owen Conglomerate, and which was considered by previous writers as part of the Junee Group (Campana and King, 1963; Wade and Solomon, 1958; Banks, 1962b, p.149). Corbett *et al.* justified making it part of the Mount Read Volcanics on the basis of its probable Cambrian age, the presence of pyroclastic units in its lower part in the Comstock area, and the observation that it is intruded by a quartz-feldspar porphyry body, with strong affinities with the Mount Read Volcanics, near Lake Dora (388354, Map 1).

Corbett *et al.* (1974) noted that in the Queenstown area the great bulk of the Mount Read Volcanics lies below the Tyndall Group, and must therefore be of Middle or Early Cambrian age. However, they also pointed out the occurrence of volcanic units similar to the Mount Read Volcanics in the Rosebery Group at Rosebery (Loftus Hills *et al.*, 1967; Brathwaite, 1972), which is apparently overlain by the Crimson Creek Formation (pre-Dundas Group). Corbett *et al.* therefore concluded that the Mount Read Volcanics span the complete time range of the Cambrian sedimentary sequences.

2.3 THE JUKESIAN UNCONFORMITY: THE CONTACT BETWEEN DUNDAS GROUP/MOUNT READ VOLCANICS AND THE JUNEE GROUP

Carey and Banks (1954, pp.264-5) defined the following Lower Palaeozoic unconformities in Tasmania:-

(1) The Tyennan Unconformity: defined as the angular discordance between pre-Dundas rocks below and the Junee Group above as revealed on the southeastern slope of Tim Shea, at the head of the Tyenna Valley (457273, Map 1). The rocks underlying the Junee Group at this locality are now identified as probable Precambrian rocks of the Jubilee Geanticline. On the basis of suggested tectonic control of cycles of sedimentation in the Dundas Group (*sensu stricto*), Carey and Banks considered the unconformity to be the expression of eight or more orogenic movements, the earliest being older than late-Middle Cambrian and the latest being younger than early-Late Cambrian but older than Early Ordovician, together with a period of erosion or non-deposition prior to the deposition of the Junee Group. The orogenic movements occurring within the span of time represented by the Tyennan Unconformity are referred to as the Tyennan Orogeny. The time span is at least that during which the Dundas Group was deposited.

(2) The Jukesian Unconformity: defined as the angular discordance between the Dundas Group below and the Junee Group above as revealed at the northern end of Mt. Jukes, south of Queenstown. Carey and Banks considered it to be the expression of an orogenic movement of post-early-Late Cambrian but pre-Early Ordovician age, followed by a period of erosion or non-deposition prior to the deposition of the Junee Group. The movement is referred to as the Jukesian Movement of the Tyennan Orogeny.

As pointed out by Corbett *et al.* (1974, p.185) the Jukesian Movement has in the past been thought of as separating the Cambrian and Ordovician Systems in Tasmania. However, in the Queenstown area Corbett *et al.* were able to demonstrate equivalence of the Jukesian Unconformity with the unconformity at the base of the Tyndall Group (the Comstock Unconformity). This implies a minimum age of late-Middle or early-Late Cambrian for the unconformity at Queenstown. Jago *et al.* (1975, p.88) noted that it has become apparent that the basal parts of the Junee Group in different parts of Tasmania are probably Late Cambrian, which supports the conclusion that the Jukesian unconformity may not generally represent a boundary between rocks of Cambrian and Ordovician ages.

Unconformities of the Jukesian type are common in western and central northern Tasmania, but are not always present. Examples of localities where the basal conglomerates of the Junee Group are structurally concordant with an underlying Upper Cambrian sedimentary sequence are:-

(1) Misery Hill near Zeehan, where the Mt. Zeehan Conglomerate overlies the Dundas Group *sensu stricto* (i.e. in its type area). The conglomerate contains rounded cobbles and bounders of purple quartzite, purple, grey and green chert, pink quartz and hematized siltstone in a matrix of pebble grit formed of similar material (Blissett,

1962, p.56). It seems possible that some of this material was derived from erosion of the underlying Dundas Group beds.

(2) On the Denison Range near Adamsfield (440290, Map 1; Corbett, 1970, 1972).

(3) St. Valentines Peak, where the basal conglomerate of the Junee Group is a poorly sorted chert conglomerate with pebbles of white and grey chert set in a sandstone matrix (Jago *et al.*, 1975).

Jago (1973) has presented biostratigraphic evidence suggesting that such apparently conformable contacts between the fossiliferous Dundas Group correlates and the Junee Group correlates in northern and western Tasmania are in reality paraconformable. Proof of this is often frustrated by the unfossiliferous nature of the basal conglomerates of the Junee Group.

The contact between correlates (or probable correlates) of the Dundas Group/Mount Read Volcanics and basal beds of the Junee Group in the Fossey Mountain and Dial Range areas is generally an erosional, and sometimes recognizably angular, unconformity (unconformity of Jukesian type). Unfortunately in exposures of the unconformity there is often evidence of disturbance by thrust faulting along or very close to the contact, sometimes making relationships difficult to interpret. Jennings (1963, p.S5) regarded this as evidence of decollement action between the rocks above and below the contact, due to their difference in competence.

A good example of an erosional angular unconformity is exposed on the old road to Cethana, near Claude Creek (429407, Map 1). Although a small thrust fault runs through this outcrop close to the contact the unconformable nature of the contact can be clearly seen (Fig. 2.1; see also photograph in Jennings, 1958, p.24). The rocks below the contact are steeply dipping greywacke siltstones, while the basal beds of the

FIGURE 2.1

Outcrop of angular unconformity of Jukesian type at 429407, near Claude Creek. Coarse quartzose conglomerate above contains pebbles derived from the steeply dipping greywacke siltstones below.

FIGURE 2.1

gently dipping overlying conglomerate contain porphyry and greywacke pebbles (Jennings, 1958, p.28). Some of the latter pebbles are cleaved, and this was cited by Jennings (1963, p.56) as part of his evidence that the Dundas Group correlates in the area had suffered deformation before the beginning of Junee Group deposition. However, examination of this outcrop by the present author both during the present study and during the course of an unpublished B.Sc. Honours study (Seymour, 1975) has favoured the conclusion that the cleavage in the pebbles is parallel to a subvertical strongly developed cleavage in the thin bedded sedimentary rocks underlying the contact. The latter cleavage in turn is parallel in strike and subparallel in dip to axial surfaces of folds in quartz sandstones (the Moina Sandstone) conformably overlying the basal siliceous conglomerate of the Junee Group, and is also approximately parallel to strongly developed cleavage in limestones which conformably overlie the Moina Sandstone. The development of the folds and cleavage in the Junee Group correlates in this area is associated with the youngest phase of the Tabberabberan Orogeny in northern Tasmania (Seymour, 1975; Williams, 1978). It therefore seems reasonable to suggest that the cleavage in the Dundas Group correlates below the unconformity at this locality developed during the Devonian deformation, and not as a result of Jukesian movements. The effect of the latter was therefore restricted to the tilting and/or folding of the Dundas Group correlates which lead to the discordance in bedding attitudes across the boundary. It is suggested that the porphyry and greywacke pebbles in the conglomerate were less competent than the rest of the rock, thus selectively absorbing the strain and forming cleavage, while the rest of the rock adjusted mainly by movements including grain-boundary sliding.

It is instructive to compare this line of reasoning with that of Jennings (1963, p.96) who lists the following evidence that the Dundas

Group correlates had suffered deformation before Junee Group deposition began:

> "(1) In the Iris River, on the Gog Range, at Cethana, Tin Spur and other places there is a well marked unconformity above the Cambrian sequence.
> (2) The basal Ordovician sediments contain sheared pebbles of Cambrian rocks.
> (3) The strong axial plane schistosity of the Cambrian rocks does not persist into the Ordovician system except locally near demonstrably Tabberabberan structures.
> (4) There is a contrast in fold style from similar type folds with accommodation by axial plane schistosity in the Cambrian rocks to concentric folds with bedding plane slip in the Ordovician sediments.
> (5) The schistosity in the Dalcoath Anticline (Burns, 1961) appears to fan, indicating refolding."

Jennings' terminology here indicates that he is making an assumption which is common in earlier literature on the Palaeozoic of Tasmania, namely that an unconformity of Jukesian type represents a boundary between rocks of Cambrian and Ordovician age. (2) to (4) may be readily explained by competence contrast between the Dundas Group correlates and the basal Junee Group beds. The fanning referred to in (5) is a common feature in single-phase Tabberabberan fold structures elsewhere (Seymour, 1975) and does not necessitate refolding.

In some cases the lack of bedding or other reference surfaces in rocks underlying the Jukesian Unconformity preclude identification of the surface as an angular unconformity, and it may only be possible to distinguish it as an erosional contact. This is particularly the case where the contact is underlain by rocks similar to the Mount Read Volcanics. A well-exposed example of such a situation is described by Jennings (1963, p.56) on the north facing slopes of the Gog Range (446405, Map 1):-

> "... the conglomerate overlies purple Cambrian keratophyre. Here the basal beds are composed of boulders of keratophyre set in a matrix of keratophyric material. Passing upward, the beds contain fewer boulders of keratophyre until a normal quartz conglomerate without keratophyre is reached. This occurs abruptly some 9 m above the base but as the keratophyre

conglomerate is so similar to its parent rock, the precise base of the conglomerate is difficult to ascertain within a metre. The exposure is regarded as illustrating the inclusion of Cambrian soil horizons in the conglomerate and strengthens the suggestion of a terrestrial origin for the formation. However, this exposure is somewhat atypical for the area and elsewhere the transition from Cambrian rocks into the Roland Conglomerate is abrupt, although the lowest bed of the conglomerate is usually more argillaceous than the rest of the formation."

2.4 THE JUNEE GROUP: NOMENCLATURAL PROBLEMS

As discussed by Corbett and Banks (1974, pp.211-214) Lower Palaeozoic stratigraphic nomenclature in Tasmania has been wrought with problems involving confusion over what is referred to by the term "Junee Group". Lewis (1940) introduced the term "Junee Series" for sedimentary rocks of demonstrated Ordovician age in the Tim Shea-Maydena area (between 457273 and 469267, Map 1). Carey (1947) suggested that sedimentary sequences of Ordovician age similar to those described by Lewis occurred throughout the State. This lead to the proposal of a generalized sequence, termed the "Junee Group", by Hills and Carey (1949), composed of five formations which had been defined in different areas:-

TOP

Crotty Sandstone
Gordon River Limestone
Caroline Creek Sandstones and Shales
West Coast Range Conglomerate (inc. Owen Conglomerate)
Jukes Breccia and correlates

BASE

The basal beds of this succession often overlie unconformities of Tyennan or Jukesian type, as defined by Carey and Banks (1954). The Crotty Sandstone has since been assigned to the Siluro-Devonian Eldon Group, but the remainder of the sequence is essentially that identified as composing the Junee Group by Banks (1962b, p.147):-

TOP

Formation	Location of type section
"Fenestella Shale"	Linda Valley, Queenstown (388340)
Gordon Limestone (L.-U.Ord.)	Florentine Valley (454280)
Florentine Valley Mudstone	Florentine Valley (")
Caroline Creek Sandstone	Melrose-Railton (453424)
Owen Conglomerate	Queenstown (383338)
Jukes Conglomerate	Lake Jukes (382331)

BASE

The most common usage of the term "Junee Group" prior to the publication of Corbett and Banks (1974) referred to the above sequence. The main problem with this nomenclature is that the formations are defined from widely separated areas and not from a single type section. With the aid of new mapping, Corbett and Banks (1974) attempted to remove this problem by re-defining the Junee Group on the basis of formations defined within the Florentine Valley-Denison Range area. In this nomenclature the Gordon Limestone was elevated to Subgroup status with three recognizable formations. The Junee Group, however, was still not defined from a *single* type section. In fact, the introduction of an unproved (and possibly unprovable) correlation between the Reeds Conglomerate and the Tim Shea Sandstone, which were defined as the basal formations of the Group on the Denison Range (441290, Map 1), and in Lewis' original type area at Tim Shea (456273) respectively, lead to an objection to the new terminology by Brown *et al.* (1975).

To accommodate this objection, Corbett and Banks (1975) discarded the term "Junee Group" altogether. because of the confusion associated with its use and because Lewis' original type area was considered unsuitable for definitive stratigraphy and correlation with other areas in Tasmania. Two Subgroups were set up, the Denison Subgroup and the Gordon Subgroup, together approximately taking the place of the Junee Group. The Denison Subgroup is defined in the Denison Range, including all the beds between a basal unconformity of Jukesian type and the base

of the limestone sequence. As such it includes fossiliferous Upper Cambrian sequences conformably underlying the Reeds Conglomerate, whereas the Junee Group of Corbett and Banks (1974) began at the base of this formation. Under this new nomenclature, the Tim Shea Sandstone and Florentine Valley Formation together in the original Junee Group type area were considered to be probable correlates of the Denison Subgroup (Corbett and Banks, 1975, p.124). The only change made to the Gordon Limestone Subgroup was to rename it the Gordon Subgroup and include within it at the top the fossiliferous siltstone and sandstone of the Westfield Beds, thus including all formations between the top of the Denison Subgroup and the base of the Eldon Group correlates within a single Subgroup. Thus, the stratigraphic interval approximately covered by the Junee Group is now divided into two parts, comprising a lower clastic unit and an upper limestone unit. This is essentially the subdivision used on recent Tasmanian Department of Mines large scale compilations, including Map 1 and Fig. 2.2 herein.

Stratigraphic equivalents of both the Denison Subgroup and the Gordon Subgroup occur within the main area of interest of this project. Correlates of the Denison Subgroup display the greater amount of variation between different localities in Tasmania, so some detailed discussion of these is included, in the following section.

2.5 THE DENISON SUBGROUP AND STRATIGRAPHIC EQUIVALENTS

2.5.1 Type area

On the Denison Range, the Reeds Conglomerate consists of quartzose conglomerate and conglomeratic sandstone, usually red to purplish in colour, and varies greatly in thickness, occurring as four large wedges with a maximum thickness of 1560 m (Corbett and Banks, 1974). Its upper boundary is transitional with sandstone at the base of the Florentine Valley Formation, which consists predominantly of fossiliferous marine quartzose and calcareous sandstones and micaceous and calcareous siltstones. Intercalations of marine sandstone with abundant worm burrows occur in places. Lensing of beds occurs down to outcrop scale, particularly in the conglomerates. Sandstones have abundant trough cross-bedding, while finer conglomerates display scour and fill structures, interlensing of sand and gravel, rare large scale tabular cross-bedding and numerous channel structures (up to 10 m across). Coarse conglomerates are thick bedded and massive, with large scale channel structures and cross-bedding in places. The most common clast compositions are quartzite and quartz-schist, which together with palaeocurrent data indicate derivation from the Tyennan Geanticline to the west.

Corbett and Banks (1974) interpreted the Reeds Conglomerate as an alluvial fan complex with deposition mainly by shallow braided streams, on the basis of the following evidence:-

(1) prevailing red colour of the sediments
(2) abundance of cross-bedding and channel structures
(3) pronounced lateral variability of the sequence
(4) rounding and imbrication of clasts
(5) bimodal nature of the conglomerates (i.e. pebbles in a sand matrix)

(6) absence of very fine-grained material

(7) absence of fauna except for worm burrows in the rare marine intercalations.

The Tim Shea Sandstone, interpreted by Corbett and Banks as a lateral equivalent of the Reeds Conglomerate at Tim Shea, consists mainly of quartzose sandstone and conglomeratic sandstone with lesser pebble conglomerate and some basal breccia and chocolate shale in places. Its thickness is variable to a maximum of 300 m. The bulk of the formation consists of alternations of zones up to 100 m thick of unfossiliferous red cross-bedded sandstone (probably non-marine) and gray flat-bedded bioturbated sandstone (probably marine) with gastropods at some horizons. Corbett and Banks suggested the sedimentary environment was a flat coastal plain at the seaward edge of the alluvial fans of the Reeds Conglomerate, with alternating shallow marine and alluvial floodplain deposition.

2.5.2 Queenstown area

Banks (1962b) listed the Owen Conglomerate, defined in the Queenstown area, as one of the basal formations of his generalized sequence comprising the Junee Group (see previous discussion). The type section is as follows (Banks, 1962b, p.154, after Wade and Solomon, 1958; Solomon, 1957):-

Central part of Owen Spur

Upper Owen:	220 m	
Middle Owen:	12 m	yellow, medium grained, thickly bedded siliceous conglomerate
	61 m	red sandstone
	(73 m)	

Below summit of Mt. Owen

Middle Owen:	49 m	cross-bedded, red sandstone with pebble bands, becoming more conglomeratic upwards
	12 m	dark, medium grained conglomerate, mainly yellow siliceous pebbles in hematitic matrix
	15 m	red sandstone
	(76 m)	
Lower Owen:	104 m	coarse grained, grey, siliceous conglomerate with red sandstone bands mostly less than 0.6 m thick; sandstone commoner in upper part of unit than in lower; pebbles mainly banded quartzite, vein quartz; quartzite, chert, etc.
	12 m	very coarse grained conglomerate, boulders up to 0.6 m long.
	107 m	yellow grey, coarse grained siliceous conglomerate with lenticular sandy beds.
	61 m	pink-grey, very coarse grained, siliceous conglomerate with thin sandstone beds; pink sandy matrix.
	(214 m)	

Banks (1962b, p.155) noted that the "Upper Owen" is marine, and considered it to be a correlate of the Caroline Creek Sandstone. He therefore proposed that the Owen Conglomerate be considered to consist only of the Lower and Middle units listed above, which he renamed "Member A" and "Member B", respectively. Note that conglomerate is concentrated in the lower part of the sequence, Member B apparently containing more than 80% of sandstone.

Banks (1962b, p.156) gave the following petrographic description of the Owen Conglomerate:

"The formation is dominantly siliceous with fragments of vein quartz, quartzite, quartz schist, chert and rarely other rock types in a matrix of quartz grains with a siliceous and/or ferruginous cement. The colour varies from white or grey to purple or greenish. The larger fragments, with a maximum length of about 0.6 m in Member A are characteristically well-rounded but the sand grains in the matrix are angular or sub-angular. Most of the larger fragments have a fairly high sphericity, varying somewhat with rock type, and in a few beds almost discoidal particles occur. The grains in the matrix have a high sphericity. Sorting is good both in the conglomerates and sandstones and the framework is closed. Member A is poorly-bedded, no cross-bedding has been recorded, but imbrication may be present. Member B is more clearly bedded than Member A and shows cross-bedding and cut-and-fill structure (Wade and Solomon, 1958, p.387). The beds, especially those of conglomerate, tend to be lenticular."

Solomon (1957) recorded the presence of local unconformities in or at the base of Member B southeast of Mt. Jukes (384329, Map 1). Banks favoured an origin for the Owen Conglomerate as alluvial fans, flood-plains or playas, with an envisaged palaeogeography of a plain overlying Cambrian rocks with piedmont deposits against a highland of Precambrian rocks to the east.

2.5.3 Fossey Mountains area

The terminology set up by Jennings (1963) is as follows:-

strat. equiv. (Corbett & Banks, 1975)		(m)	lithology
Gordon S.G.	Gordon Limestone	915	pure limestone with some calcareous sandstone.
Denison S.G.	Magog Group		
	Moina Sandstone	245	sandstone, quartzite, shale.
	Roland Conglomerate	245-	quartz conglomerate and quartzite.

The Roland Conglomerate attains its maximum thickness of 245 m at its type locality at Mt. Roland (439410, Map 1). but displays rapid lateral thinning, particularly towards the south, with thinning ratios

of up to 7:1 (Jennings, 1958, p.30). Jennings (1963, p.55) described a typical rock from the formation as a "dense recrystallized quartz conglomerate, generally but not invariably coloured pink, composed of sub-rounded fragments of quartz, quartzite, and quartz schist in a fine grained siliceous matrix. The pinkish colouration is due to finely divided haematite disseminated throughout the rock and also to the predominance of pink pebbles among the phenoclasts." Jennings proposed a terrestrial origin for the formation on the basis of presence of cross-bedding, grain-supported fabric sometimes present in the pebbles, absence of fossils and grading, subordinate matrix, and provenance of the clasts from the Precambrian rocks to the south.

The Moina Sandstone in the Fossey Mountains area is a formation of marine sandstone, quartzite, shale and conglomerate, often with transitional boundaries with both the underlying Roland Conglomerate and overlying Gordon Limestone (Jennings, 1963, p.56). Banks (1962b) substituted the term "Caroline Creek Sandstone" for "Moina Sandstone". At Caroline Creek (453424, Map 1) ferruginous sandstones of the formation contain orthid brachiopods and trilobites indicating Early Ordovician age (Banks, 1962b, p.167, after Kobayashi, 1940). Abundant bedding-perpendicular worm burrows in some of the lithofacies lead to use of the term "Tubicolar Sandstone" by some early workers. Jennings (1963, p.59) considered the deposition of the Moina Sandstone to mark a change in sedimentation from the well-sorted, probably terrestrial gravels of the Roland Conglomerate into finer grained marine sediments. The composition of the sediments and thinning of the formation to the south is consistent with their derivation from the same source as the Roland Conglomerate.

2.5.4 Dial Range area

Burns (1964) used the following terminology:-

strat. equiv. (Corbett & Banks, 1975)		(m)
Gordon S.G.	Gordon Limestone	600
Denison S.G.	Dial Group	
	Moina Sandstone	max. 245
	Duncan Conglomerate	0-550
	Gnomon Mudstone	min. 9

The Dial Group in the Dial Range area is equivalent in stratigraphic position to the Magog Group of Jennings, overlying Dundas Group correlates with proven or inferred angular unconformity. However, certain important lithological differences are apparent. Occurring between the unconformity and the Duncan Conglomerate in places is a thin sequence of interlaminated purple mudstone and fine sandstone with thin conglomerate bands termed the Gnomon Mudstone by Burns. This formation is similar in some respects to certain lithologies in the Dundas Group correlates, but is distinguished from the latter in having a high proportion of detrital hematite, and by the presence of conglomerate bands similar in composition to the Duncan Conglomerate.

The Duncan Conglomerate is markedly dissimilar to the Roland, Owen and Reeds Conglomerates in that, except in its uppermost parts, the pebbles are derived from the Barrington Chert, a formation within the Cambrian sequence of the Dial Range Trough (Burns, 1964, p.67). These often constitute 100% of the pebbles in the lower parts of the formation. Other pebble compositions are quartzite and vein quartz derived from the Precambrian rocks of the Rocky Cape Geanticline, hematite and limonite

from Precambrian and Cambrian orebodies, and rare boulders of Cambrian lava and mudstone. The conglomerate is poorly sorted (as opposed to the Owen Conglomerate) and bimodal, with separated, subangular to rounded pebbles in a granular matrix. It forms two thick fans centred on Mt. Montgomery (421444, Map 1) and Mt. Duncan (419439, Map 1). Currents were generally to the southwest, material being mainly derived from the Barrington Chert source immediately to the east (Burns, 1964, p.79). Burns interpreted the deposit as a fanglomerate mantling high areas of Cambrian rocks just east of Mts. Duncan and Montgomery. The contribution from source areas to the west was relatively minor.

Burns described the Moina Sandstone equivalent in the Dial Range area as a well-bedded sandstone, shale and conglomerate dominantly derived from the Precambrian rocks, with fossils and bioturbation indicating a marine origin. In the Dial Group it underlies, overlies and interfingers with the terrestrial Duncan Conglomerate (Burns, 1964, p.73). This is in contrast to the situation in the Magog Group in the Fossey Mountains area, where the Moina Sandstone everywhere succeeds the Roland Conglomerate and overlaps it into basement highs (Jennings, 1958, 1963).

CHAPTER 3

STRATIGRAPHY AND SEDIMENTOLOGY

3.1 STRATIGRAPHIC NOMENCLATURE IN THE BLACK BLUFF REGION

Fig. 3.1 shows the main area of interest of the field mapping carried out during the course of this project, outlined on a section of the Tasmanian Department of Mines 1:250,000 Burnie geological map sheet (Williams and Turner, 1973). The key to this map makes five main subdivisions of the Palaeozoic rocks:-

Cambrian

(1) Undifferentiated Cambrian sequences (light blue-green with "u" overprint).

(2) Middle-Upper Cambrian, fossiliferous, usually greywacke turbidite sequences (light green with horizontally lined overprint).

(3) Acid with intermediate volcanic and associated rocks dominant (solid medium green).

(Unconformity in northern Tasmania and parts of western Tasmania attributed to Cambrian movements; apparent conformity in Adamsfield region and parts of western Tasmania.)

Ordovician

(4) Siliceous terrestrial conglomerate, marine quartzwacke and siltstone.

(5) Limestone sequence.

It should be re-emphasized at this point that, at least within the area of interest marked on Fig. 3.1, the ages indicated in the key to this map are only approximate for most of the sequence. That is,

FIGURE 3.1

A section of the Tasmanian Department of Mines 1:250,000 Burnie geological map sheet with the areal coverage of Fig. 1.2 outlined. See pocket at back of thesis for key.

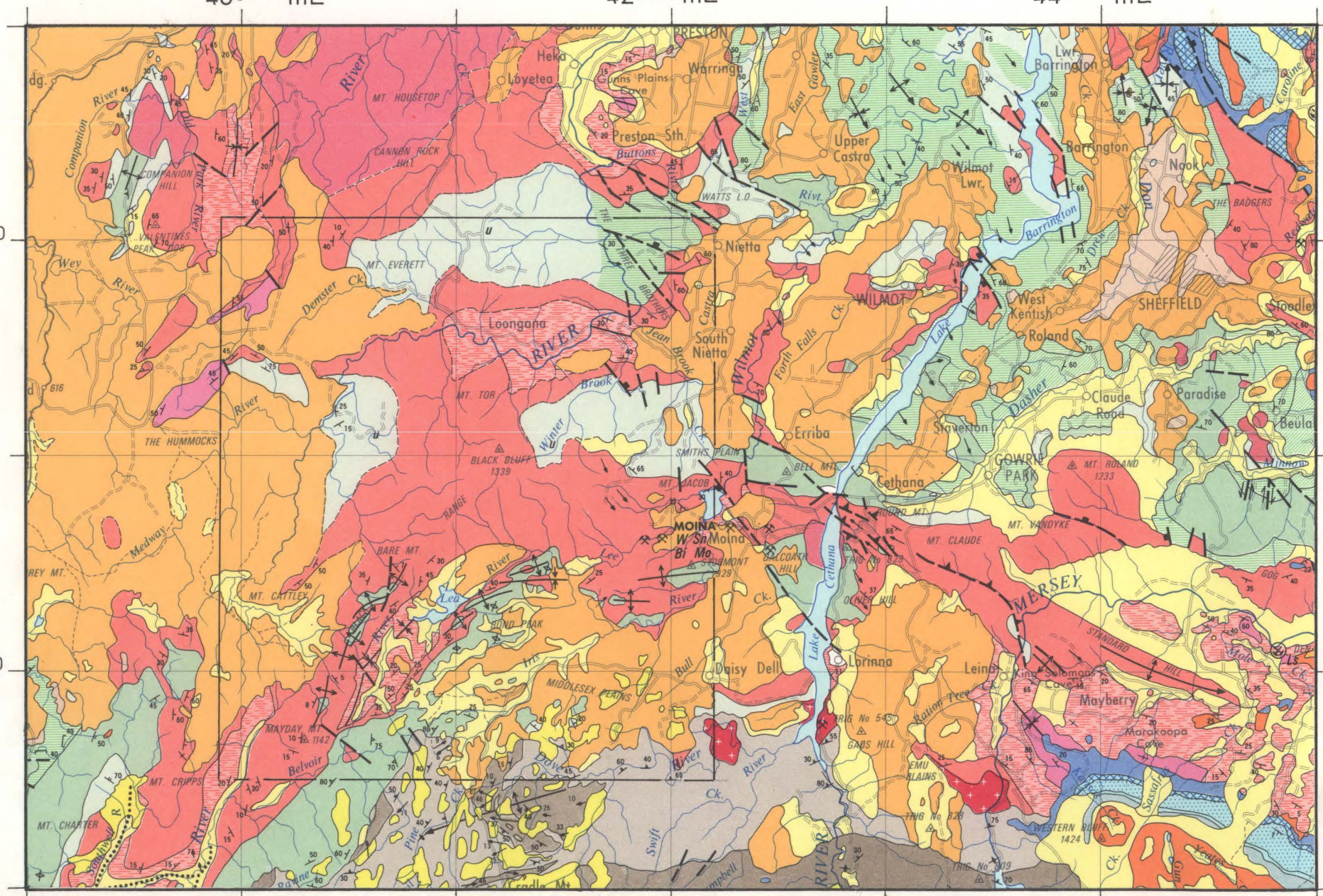
400 000 mE
420000 mE
440 000 mE
5420000 mN
5400 000 mN
PRESTON
Heka
Loyetea
Gunns Plains Cave
Warrington
Lwr Barrington
Upper Castra
Barrington
Nook
Wilmot Lwr.
Preston Sth.
Buttons
WATTS L.O.
Nietta
South Nietta
WILMOT
West Kentish
Roland
SHEFFIELD
Claude Road
Paradise
Beulah
Erriba
Staverton
Cethana
GOWRIE PARK
MOINA
W Sn Mo
Bi Mo
Lorinna
Leina
Daisy Dell
Mayberry
Marakoopa Cave
MT. HOUSETOP
CANNON ROCK HILL
COMPANION HILL
VALENTINES PEAK
MT. EVERETT
Loongana
RIVER
MT. TOR
THE HUMMOCKS
BLACK BLUFF 1339
MT. JACOB
SMITHS PLAIN
BELL MT.
MT. ROLAND 1233
MT. CLAUDE
MT. VANDYKE
BARE MT.
MT. CATTLEY
MAYDAY MT. 1142
MT. CRIPPS
MT. CHARTER
MIDDLESEX PLAINS
GADS HILL
EMU PLAINS
WESTERN BLUFF 1424
STANDARD HILL
MERSEY
Lake Cethana
Wilmot
Forth Falls Ck.
Dasher
Barrington
Dove
Caroline
Jean Brook
Winter Brook
Medway
Lee
Belvoir
Swift
Pine
Sandfly R.
Companion
Wey
Demster Ck.
Rayton Tree
Yeates
Cradle Mt.

the basal parts of the sequence identified as "Ordovician" may be Upper Cambrian in places, and much of the "Cambrian" sequence is volcanic and unfossiliferous, and is of unknown age at present. Subdivisions (2) and (3) are probable stratigraphic equivalents of the Dundas Group and Mount Read Volcanics respectively. Subdivision (4) is approximately stratigraphically equivalent to the Denison Subgroup, and subdivision (5) to the Gordon Subgroup. Because of outcrop problems in the definitions of type sections, no new formal stratigraphic nomenclature has been introduced herein, and the main units are referred to by inferred stratigraphic equivalence in the manner listed above.

3.2 MOUNT READ VOLCANICS/(?)DUNDAS GROUP STRATIGRAPHIC EQUIVALENTS

3.2.1 Introduction

Rocks stratigraphically underlying unconformities of Jukesian type in the Black Bluff region occupy three main outcrop areas (Fig. 3.1):-

(1) an elongate E-W trending belt between Smiths Plains and Black Bluff
(2) an arcuate area appearing between the Tertiary flood basalts in the vicinity of The Hummocks and the Denison Subgroup stratigraphic equivalents in the Mt. Tor area
(3) outcrops in the cores of structural domes on the ridges to the northwest and southeast of the Vale of Belvoir, northeast of Mayday Mt.

Sequences in areas (1) and (2) consist partly of sedimentary rocks lithologically similar to those of the Dundas Group, and partly of intermediate to acid volcanics and pyroclastics having lithological affinities with the Mount Read Volcanics. In area (3) however, coarse acid quartz porphyries and acid pyroclastics predominate. The large

scale rock distribution pattern therefore is similar to that recorded in the Dundas Trough, with volcanic and pyroclastic rocks being concentrated towards the margin of the Tyennan Geanticline. Despite close examination of the sedimentary parts of the sequence, the rocks in areas (1), (2) and (3) have so far proven unfossiliferous.

3.2.2 The Smiths Plains area

The available structural information from this area (see Map 3, in pocket) indicates that a consistently steeply southeast to southward dipping and younging stratigraphic sequence may be present, at least in the northern half of the outcrop belt. In the southeastern part of the belt this situation becomes more complicated with strikes in the sedimentary rocks being similar but local steep overturning occurring (i.e. dips steep but reversed, and younging direction still to the SSE). On the Devonport Mine track near 4180/4095, on a creek just east of Tiger Plain near 4166/4087, and also in a small isolated outcrop area of volcanics and pyroclastics south of Tiger Plain at 4153/4077 (see Fig. 1.2 for localities), strikes of steeply dipping poorly defined compositional layering and flow banding in tuffs and lavas are approximately at right angles to strikes in the rest of the belt. Excluding the last two of these latter localities, the bones of a composite stratigraphy for the belt can be extracted from the remaining data. The compilation assumes no repetition or foreshortening of the succession by faulting:-

TOP of exposed composite section, near 4181/4090 on Devonport Mine track

	Unit		(m)
	6	Altered andesitic lava	800+
↑	5	Mainly thin bedded argillaceous siltstones, some thin ashflow units	250
		(Interval covered by Tertiary basalt)	1100
Crystal vitric ashflow tuffs in SW part of belt.	4	Rhyolitic agglomerate or volcanic wacke conglomerate, crystal lithic lapilli tuff and volcanic wacke	650
	3	Interlayered thin bedded argillaceous siltstone and lithic crystal ashfall tuff (andesitic composition)	350
↓	2	Rhyolitic crystal vitric ashflow tuffs (some welded)	700
	1	Interlayered thin bedded argillaceous siltstone and sandstone and crystal vitric tuffs, with large rhyolite masses (domes or intrusions ?) at 4181/4132 and 4187/4136.	250
		TOTAL	4100 m

BASE of exposed composite section at 4163/4128 in Winterbrook Creek.

Most of these rocks have a characteristic strong alteration to mineralogies of quartz-sericite-chlorite-albite-(±carbonate)-(±iron oxides), which is most noticeably developed in the ashflow tuffs, the lithic crystal tuffs of unit 3, the coarse agglomerates and lapilli tuffs of unit 4 and the andesites of unit 6. These alteration products however, have often been recognizably deformed or recrystallized during cleavage development associated with the Tabberabberan deformation and therefore formed prior to it. The alteration was most probably of hydrothermal origin.

The degree of alteration often makes identification of original lithologies difficult. This is illustrated by Fig. 3.2B which shows a quartz porphyry from 4132/4115 (Fig. 1.2), 1.3 km northeast of the summit

FIGURE 3.2

A. Lithic crystal ashfall tuff from Mount Read Volcanics stratigraphic equivalent, 4187/4129, Smiths Plains area. Note lithic fragments: (1) feldspar porphyry, (2) quartz-mica schist. Specimen UTGD 48372. PPL.

B. Altered quartz-felspar porphyry or crystal vitric tuff from Mount Read Volcanics stratigraphic equivalent, 4132/4115, 1.3 km northeast of Black Bluff. Specimen UTGD 48398. XPL.

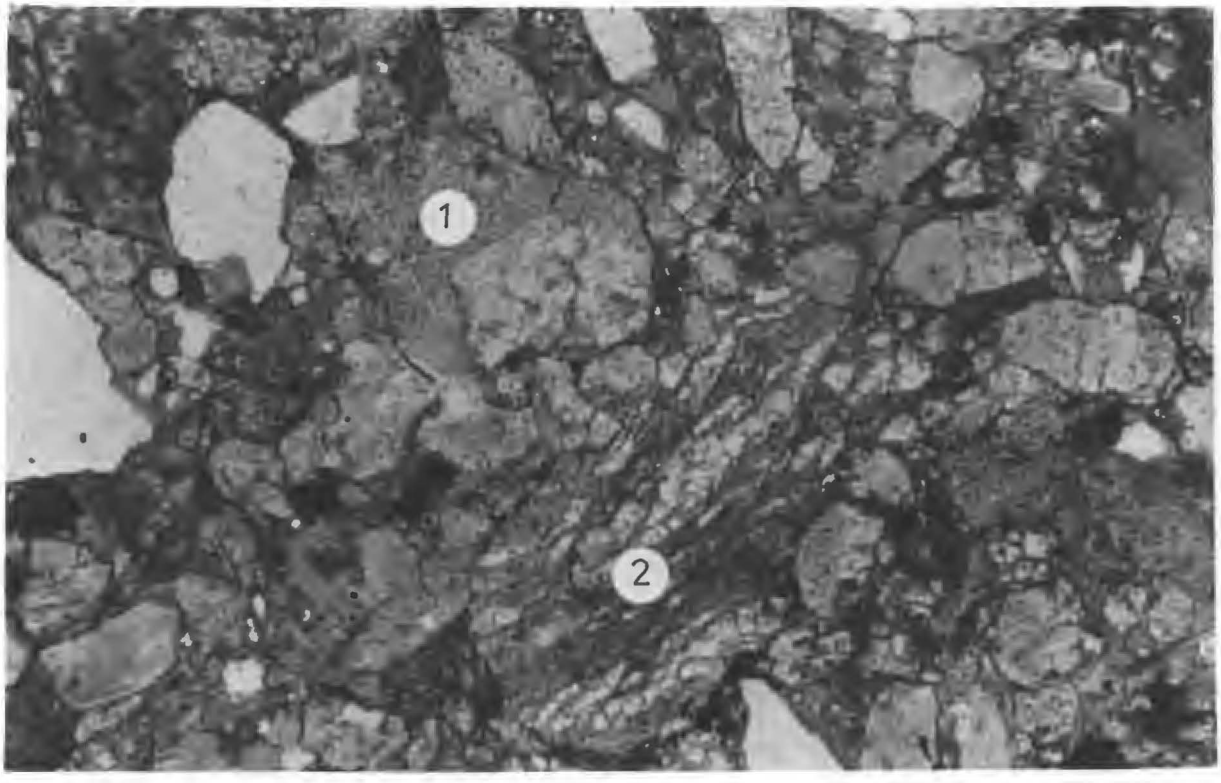

FIGURE 3.2A

1 mm

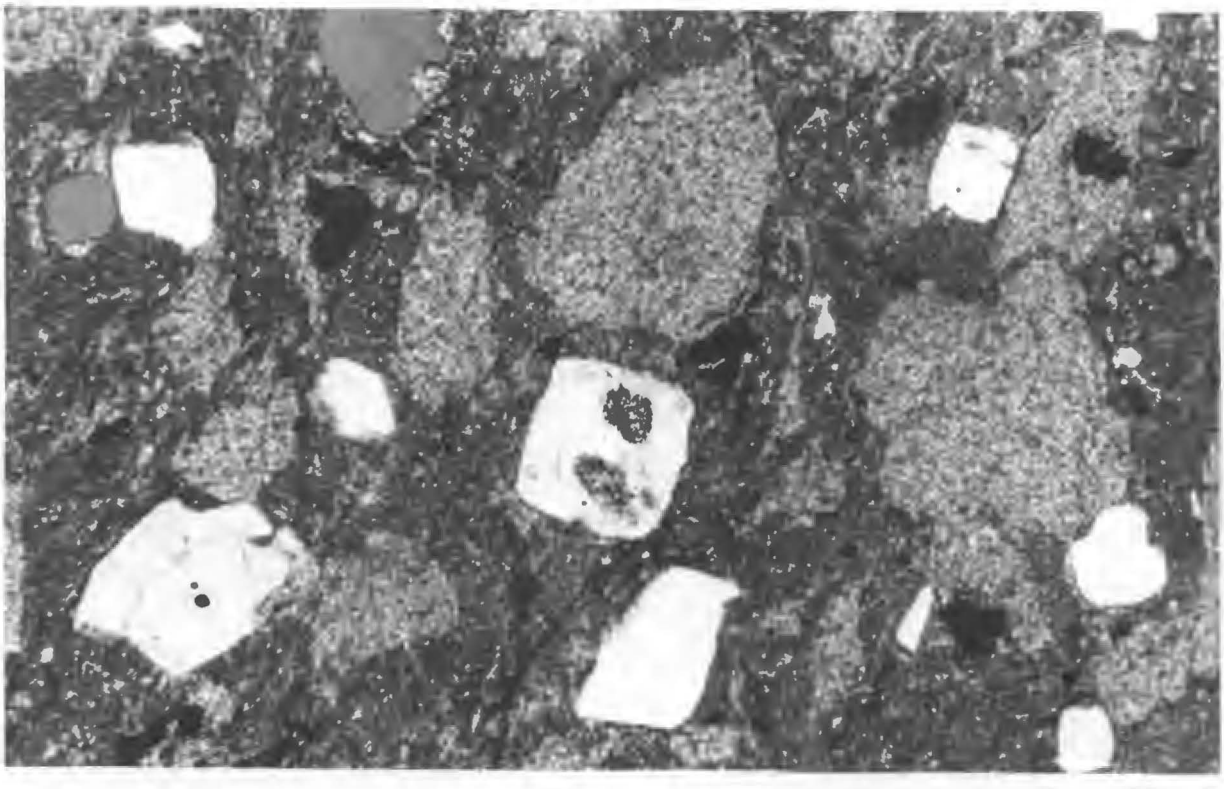

FIGURE 3.2B

1 mm

of Black Bluff. It is a probable lateral equivalent of part of unit 1 or unit 2 in the listed section. Unaltered quartz phenocrysts have the equant shape due to the bipyramidal habit inherited from the high temperature β form. This and commonly observed embayment are characteristic of quartz phenocrysts in tuffs, lavas and other porphyries in the Mount Read Volcanics stratigraphic equivalents in the area of this study. The light-coloured irregular blebs visible in Fig. 3.2B are now composed almost entirely of very fine sericite, while the matrix appears to consist of very fine quartz, (?) felspar and sericite. The blebs represent either altered felspar phenocrysts (in which case the original rock was a quartz-felspar porphyry) or sericitized devitrified glass shards, whereby the original rock may have even been an ashflow tuff! The outline shape of some of the blebs is almost that of euhedral felspar, which favours the first interpretation, but many are also very irregular and cuspate. Crystal shape, however, could be distorted due to volume change associated with the alteration.

Fig. 3.2A illustrates a lithic (felspar > quartz) crystal tuff from unit 3, outcropping in a quarry at 4187/4129 in a thin bedded sequence, interlayered with laminated fine argillaceous siltstones. The deposit represents an ashfall tuff which may be slightly reworked. Note the two lithic fragments visible, 1 being composed of felspar porphyry, while 2 is a foliated quartz-mica schist. Fragments such as 2 indicate the presence of Precambrian basement below this area at the time of volcanism. The dominant alteration of this rock is mainly confined to the matrix and has produced chlorite. Iron oxide grains are common and seem to be associated with the chloritic alteration. The felspars have a less altered appearance but are turbid and are all of albite composition. Unless a lot of Fe and Mg has been introduced it seems likely that the original bulk composition of the rock was andesitic.

An altered probable original ashflow tuff is illustrated in Fig. 3.3B. This is a sample from 4193/4103 on the Devonport Mine track, from one of the units constituting a minor part of unit 5. The discontinuous elongate light coloured areas consist now of mainly fine anhedral quartz and felspar, and alternate with the darker matrix which has a dominantly sericitic alteration. Heavily embayed quartz and occasional strongly sericitized felspar phenocrysts are present and the layering tends to wrap around them. In addition to the 'primary' embayment of the quartz phenocrysts, some initial dissolution of them and later optically continuous overgrowth of quartz on them appears to have taken place during the (probably hydrothermal) alteration. The present layering may be due to the original presence of flattened fragments of pumice or vesicular lava, and its appearance has been considerably enhanced by development of cleavage, which is subparallel to the layering in this section. The effect of the deformation has been mainly to produce a preferred orientation in the fine sericite of the matrix. Examination of the fine structure of the matrix favours the conclusion that the mechanism responsible for the development of the tectonic fabric was dominantly recrystallization rather than reorientation of existing grains.

The original porphyritic texture of the altered andesites of unit 6 is still discernible in most samples (Fig. 3.3A) and relict flow banding is sometimes visible at outcrop scale (e.g. UTGD 48378). The fine groundmass has a patchy chloritic alteration, and all the phenocrysts except for large embayed quartz crystals have been almost completely altered. The felspars are now composed of fine sericite-(?)carbonate assemblages, while rarer, darker phenocrysts with crystal outlines similar to hornblende have a fine chloritic alteration. Iron oxide grains are scattered throughout the rock, and appear to be at least partly a product of the alteration of the ferromagnesian phenocrysts.

FIGURE 3.3

A. Altered andesitic lava from Mount Read Volcanics stratigraphic equivalent, 4180/4091, Devonport Mine track, Smiths Plains area. Note altered felspar and embayed quartz phenocrysts. Specimen UTGD 48375. XPL.

B. Altered banded ashflow tuff from Mount Read Volcanics stratigraphic equivalent, 4193/4103, Smiths Plains area. Specimen UTGD 48383. PPL.

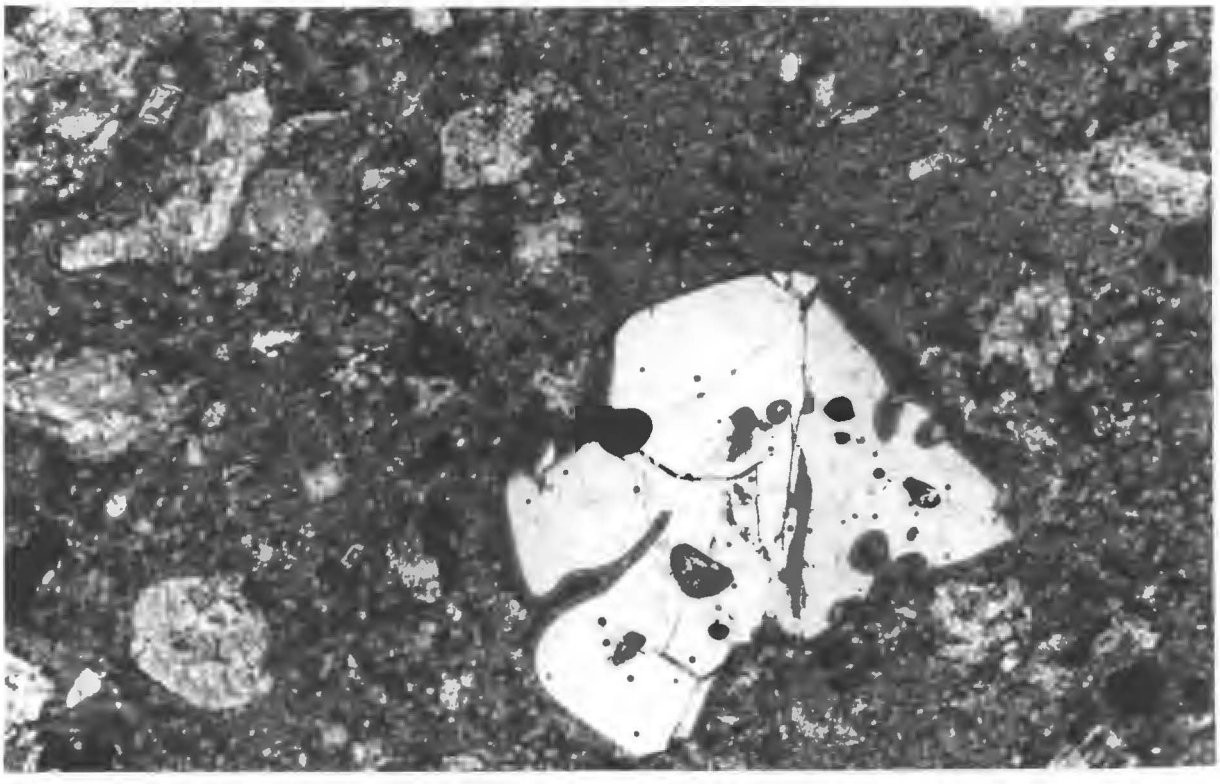

FIGURE 3.3A

2 mm

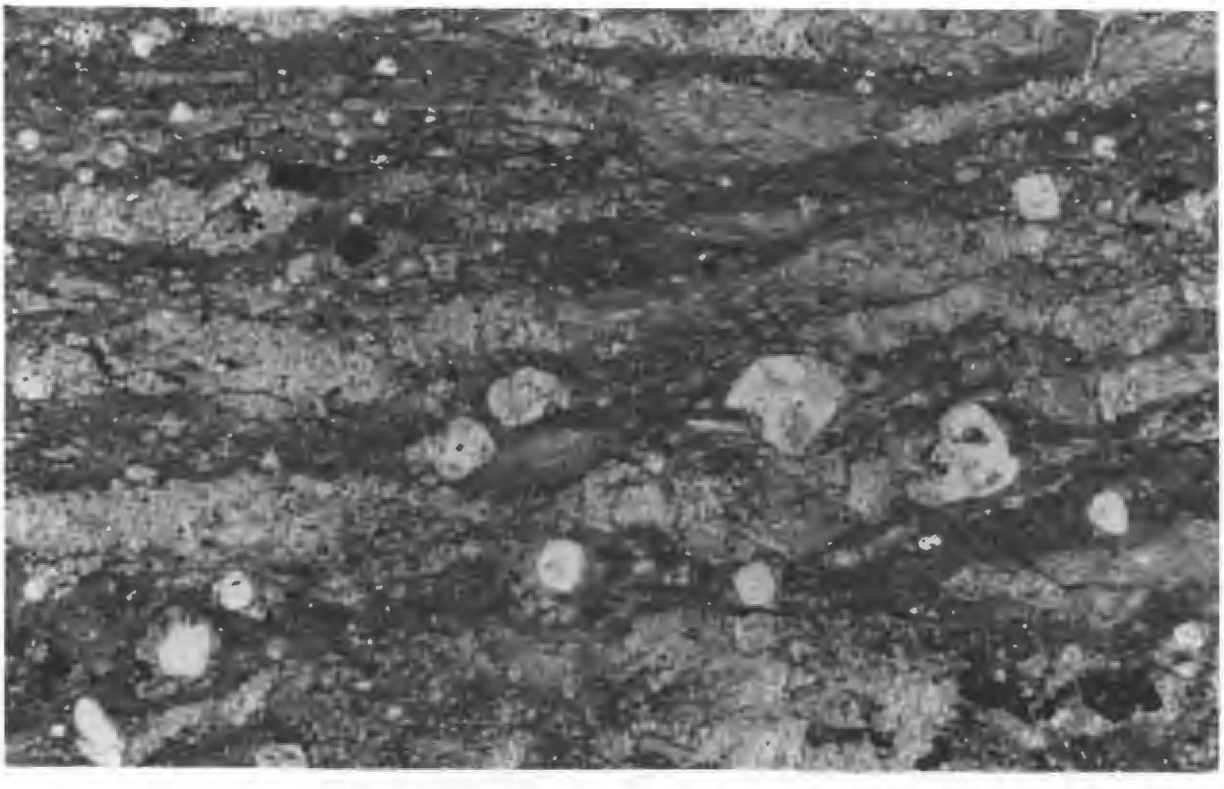

FIGURE 3.3B

2 mm

Examination of the fine sediments within the Smiths Plains sequence has so far failed to yield any biostratigraphic information. The absence of fossils may be due to the fact that the sediments (in units 1, 3 and 5) essentially represent thin intercalations within a stratigraphy otherwise dominated by probably violent volcanism. Even in the quiescent periods the environment may not have been favourable to marine organisms. Alternatively the sediments need not have been marine at all; they may have been deposited in lakes situated in depressions in the volcanic topography which were closed off from the sea. The sediments are nevertheless apparently similar in some respects to those of late-Middle Cambrian age described by Burns (1964, p.47; section 2.1 herein) from a section in the Leven River Gorge just northeast of Gunns Plains, at the southern end of the Dial Range Trough 20 km north of the Smiths Plains area. In that section mudstones and greywackes were interbedded with tuffs and lavas, although the volcanics made up only a small part (about 6%) of the sequence. The predominance of volcanics and pyroclastics (probably >80%) in the Smiths Plains section supports its identification as a stratigraphic equivalent of part of the Mount Read Volcanics, as the Tasmanian Department of Mines has done from more limited evidence on Map 1.

3.2.3 The Hummocks-Mt. Tor area

This area is split into two parts by a remnant strip of Tertiary basalt just east of the bridge over the Leven River at 404412 (see Fig. 3.1). Available information indicates that the structure of the Mount Read Volcanics/Dundas Group stratigraphic equivalents in the two subareas may be different, and they will be treated separately in the discussion to follow.

In the eastern and larger of the two subareas, available structural data indicates that a continuous moderately to steeply southeastward dipping and younging sequence is probably present (see Map 4). The following section was observed on the southern of the two roads leading southeast from the Leven Bridge, from the eastern end of the bridge (4044/4122, Fig. 1.2) to the base of the slopes leading northeast to the summit of Mt. Tor, at 4064/4108:-

TOP of measured section

Unit		(m)	
5	Interlayered thin bedded laminated blue-grey argillaceous siltstones, massive lithic wacke, and coarse lithic wacke conglomerate or agglomerate. Minor lithic crystal tuff.	250+	
4	Altered thin bedded green vitric quartz-felspar-crystal tuffs (chloritic alteration). Some probable ashflows.	700	(?) ↑
3	Interlayered massive very fine blue-grey siliceous sediments (fine ashfall tuff ?), and thin bedded laminated blue-grey argillaceous siltstone.	400	|
2	Altered basic volcanic (chloritic alteration)	400	|
1	Interlayered thin bedded light green laminated argillaceous siltstone, and altered felspar-crystal vitric tuff (chloritic alteration). Minor massive very fine grey siliceous sediment (fine ashfall tuff ?).	200+	
	TOTAL	1950 m	

BASE of measured section.

(The arrow indicates the vertical extent of massive pink-green rhyolite, welded crystal vitric (?) ashflow tuffs and minor agglomerate which are probable lateral equivalents of units 2 to 4, to the northeast of the measured section.)

In comparison to the Smiths Plains section, this sequence contains a somewhat lower proportion (about 60%) of volcanics (including pyroclastics), and correspondingly higher proportion of fine grained sediments

similar to those in the Dundas Group. A major difference is the presence of basic volcanics in this section. There appears to be some indication of cyclicity in the volcanism, both on a large scale with units dominated by fine sediments interspersed with the volcanic units, and also on a smaller scale, for example within units 1 and 4 which in parts display thin alternations of laminated siltstone and felspar-crystal vitric tuff. Many of the fine sediments may in fact contain a fairly high contribution of very fine ashfall material, particularly the massive fine grained siliceous parts of units 1 and 3.

Mount Read Volcanics/Dundas Group stratigraphic equivalents occur in a limited exposed section in quarries on Black Marsh Road, just southeast of The Hummocks (4009/4142, Fig. 1.2), and appear to form a moderately to steeply ENE-dipping and younging sequence. This is in contrast to the section to the east of the Leven River described above, and suggests that there may be a structural break between the two areas. The following short succession was observed on Black Marsh Road:-

TOP

Unit		(m)
	Coarse siliceous conglomerate (basal unit of Denison Subgroup strat. equivalents)	
	(Inferred angular unconformity)	
4	Thin bedded finely and very strongly laminated dark grey shale and argillaceous siltstone	20+
	(Possible structural discontinuity)	
3	Interlayered thin bedded light green claystone and shale	52
2	Foliated light green crystal vitric tuff (ash flow) with well preserved devitrified glass shards and eutaxitic texture (chloritic alteration)	48
1	Interlayered thin bedded light green argillaceous siltstone and shale.	54
	TOTAL	174 m

BASE of exposure.

FIGURE 3.4

Altered ashflow tuff from the Mount Read Volcanics/ Dundas Group stratigraphic equivalents, 4008/4143, near The Hummocks. Note the delicately preserved devitrified glass shards. S is layering which is parallel to bedding in enclosing sediments. Specimen UTGD 48414. PPL.

FIGURE 3.4

Pike (1964, pp.27-28) reported an altered (?)rhyolitic lava outcropping on Black Marsh Road south of the quarries, and apparently underlying unit 1 above. The tuff of unit 2 contains very delicately preserved devitrified glass shards (Fig. 3.4), now composed of mosaics of fine grained anhedral quartz. The rock also has a foliation which is parallel to bedding in the sediments above and below unit 2. The foliation is defined by discontinuous elongate chloritic layers, one of which can be seen in Fig. 3.4, and which probably represent an original eutaxitic texture produced by compaction of an ashflow tuff deposit. Parts of unit 1 contain what appear to be accretionary lapilli composed of fine grained material and up to 4-5 cm in diameter, and both this unit and unit 3 may include a significant contribution from very fine ashfall material. No fossils have been found in any of the sediments in this section.

3.2.4 Bonds Range and southern Black Bluff Range

On these two ranges which flank the Vale of Belvoir, to the northeast of Mayday Mt. (see Figs. 1.2 and 3.1), stratigraphic equivalents of the Mount Read Volcanics outcrop mainly in the cores of structural domes formed by the interference of folds on various trends attributed to the Tabberabberan Orogeny. The dominant lithology in these areas is altered coarse rhyolitic quartz-minor felspar porphyry, with a light coloured quartz-felspar rich fine grained matrix. The alteration is sericitic, with felspar phenocrysts in particular often completely pseudomorphed and almost unrecognizable. Quartz phenocrysts, which reach 1 cm in diameter in porphyries on the northern part of Bonds Range, are commonly embayed and have the compact bipyramidal habit inherited from the high temperature form. The porphyries are often massive and structureless and some of them may be intrusives. However, flow banding is present

in UTGD 48421 from 4071/4038 in the northernmost of the three outcrops on the Black Bluff Range, and in UTGD 48426 and UTGD 48431 from 4112/4030 on Bonds Range. Possible autobrecciation textures were identified in UTGD 48424, from 4051/4015 in the middle outcrop on the Black Bluff Range, and in UTGD 48430 from 4067/4038 in the northern outcrop. This suggests that some of the porphyries may be lavas.

The only detected variations from the almost uniform lithology described above are as follows:-

(1) A moderately altered flow-banded quartz-felspar porphyry (UTGD 48422) from 4059/4032 in the northern outcrop on the Black Bluff Range has a pronounced chloritic alteration in its matrix, and may have originally been andesitic in composition.

(2) Strongly altered quartz-crystal vitric tuffs (e.g. UTGD 48434), possibly of ashflow origin, occur near 4051/3972 on the southernmost extension of Bonds Range, about 2 km east-northeast of Mayday Mt.

(3) One of only two observed occurrences of sedimentary rocks is a quartz wacke (UTGD 48427) from 4123/4040 on the northern part of Bonds Range. This locality is stratigraphically almost immediately below the basal clastic unit of the Denison Subgroup stratigraphic equivalent. This together with the fact that the quartz in the rock is of volcanic type suggests that the occurrence represents a small pocket of volcaniclastic sediment formed in a topographic depression in the top of the volcanic pile.

The only other recorded occurrence of sediments in these areas is thin bedded laminated maroon argillaceous siltstone at 4057/4022 at the northern end of the middle outcrop on the Black Bluff Range.

3.3 UNCONFORMITIES OF JUKESIAN TYPE

Unconformities between Mount Read Volcanics/Dundas Group stratigraphic equivalents and the Denison Subgroup stratigraphic equivalent occur at a number of localities in the Black Bluff region. They are generally erosional in character, and sometimes an angular relationship between rocks above and below can at least be inferred. The following summary is subdivided depending on the map sheet on which the unconformities occur.

3.3.1 Smiths Plains map (see Map 3)

(1) On the Devonport Mine track at 4180/4091, flow banding in an altered andesitic lava dips ENE at 40°; some 100 m further south-southeast and about 50 m vertically above this point, bedding in quartz arenites close to the base of the Denison Subgroup stratigraphic equivalent dips SE at about 30°. The contact is not exposed but an angular discordance, and possible angular unconformity, is suggested.

(2) On the banks of a creek just east of Tiger Plain near 4166/4087 a short sequence of fine volcaniclastic sediments is exposed overlying altered crystal vitric tuffs with inferred angular unconformity. The exact contact is not exposed but its inferred stratigraphic position can be very closely approached (i.e. within 1-2 m) from above and below. Compositional layering in the tuffs dips steeply to the SW at 70°, while thin bedded red-brown laminated pebbly hematitic quartz wacke siltstones immediately overlying the inferred unconformity dip to the SSE at 20°. Angular pebbles in the latter are composed of volcanic quartz and volcanic lithic fragments. The siltstones persist for a stratigraphic interval of some 20 m and are then abruptly but conformably overlain by thin bedded slightly

hematitic quartz arenites typical of the Denison Subgroup stratigraphic equivalent throughout the Black Bluff region.

(3) At the northern edge of a small 'window' of Mount Read Volcanics stratigraphic equivalents just south of Tiger Plain at 4155/4082 (see Map 3 and Fig. 1.2), thin compositional layering in altered crystal vitric tuff dips to the SSW at 85°. Immediately overlying the tuffs (i.e. within 1-2 m), thick bedded coarse pebbly quartz arenites dip NE at 22°, although the actual contact is not exposed.

3.3.2 Black Bluff map (see Map 4)

(1) Angular unconformity between Mount Read Volcanics/Dundas Group stratigraphic equivalents and the basal siliceous clastics of the Denison Subgroup stratigraphic equivalent is suggested but cannot be proven, in the vicinity of 4064/4108, approximately 2 km south-southeast of the summit of Mt. Tor (see Map 4 and Fig. 1.2). The closest approach to the contact here is however, about 250 m. Interlayered thin bedded laminated siltstones and massive lithic wackes of unit 5 (see Section 3.2.3 herein) below the contact dip to the SE at 60-70°, while interlayered chert breccias and quartz arenites above the contact have almost the same strike but dip SE at 30-35°.

(2) Angular unconformity can again be inferred in the vicinity of The Hummocks (4009/4142, Fig. 1.2), where the contact is again unexposed but can be approached to within a few metres. Thin bedded fine sediments and tuffs of the Mount Read Volcanics/Dundas Group stratigraphic equivalents form a sequence dipping ENE at 50-60°, except for the uppermost exposed unit (unit 4, see Section 3.2.3 herein), which dips in the same direction but at 30° and may have a fault between it and the rest of the sequence below it.

Siliceous conglomerate on The Hummocks, representing the basal unit of the Denison Subgroup stratigraphic equivalent, dips to the NNE at about 45°, suggesting structural discordance and probable angular unconformity with the sequence listed in Section 3.2.3 herein.

3.3.3 Vale of Belvoir (North) map (see Map 5)

(1) The only good outcrops of Jukesian-type unconformities in the Black Bluff region occur in excellent exposures around the northern end of the northern-most of the three 'windows' on the southern Black Bluff Range (see Fig. 3.1 and Map 5). Here the unconformity is markedly erosional, displaying considerable relief over short distances, and the basal overlying beds contain detritus derived from the rocks below. Unfortunately, however, the underlying rocks are generally massive structureless quartz porphyries and angularity of the unconformity cannot be demonstrated (Fig. 3.5). However, minor thin bedded laminated maroon wacke siltstones occurring at 4058/4023, at the northern end of the middle outcrop on the Black Bluff Range, are within 20 m of the contact and dip NW at 75°, while the basal siliceous clastics just above the contact dip NNW at 20°. Compositional layering in tuffs near the southeastern end of the northern-most outcrop on the Black Bluff Range at 4079/4033, and in the centre of the southernmost outcrop at 4038/3983, dips 70° NW and 65° SE respectively, but both of these localities are some distance both on the ground and stratigraphically from the contact.

(2) At the northern end of Bonds Range at 4139/4045, flow layering in coarse quartz porphyry within 1-2 m vertically of the contact, dips at 85° to the SSE, while bedding in coarse pebbly quartz arenites overlying the contact dips at 7° to the WNW.

FIGURE 3.5

Outcrop of unconformity of Jukesian type between massive altered quartz porphyry of Mount Read Volcanics stratigraphic equivalent and overlying basal quartzose conglomerate of Denison Subgroup stratigraphic equivalent, 4067/4038, southern Black Bluff Range. Some of the material in the matrix of the conglomerate has been derived from the underlying bedrock.

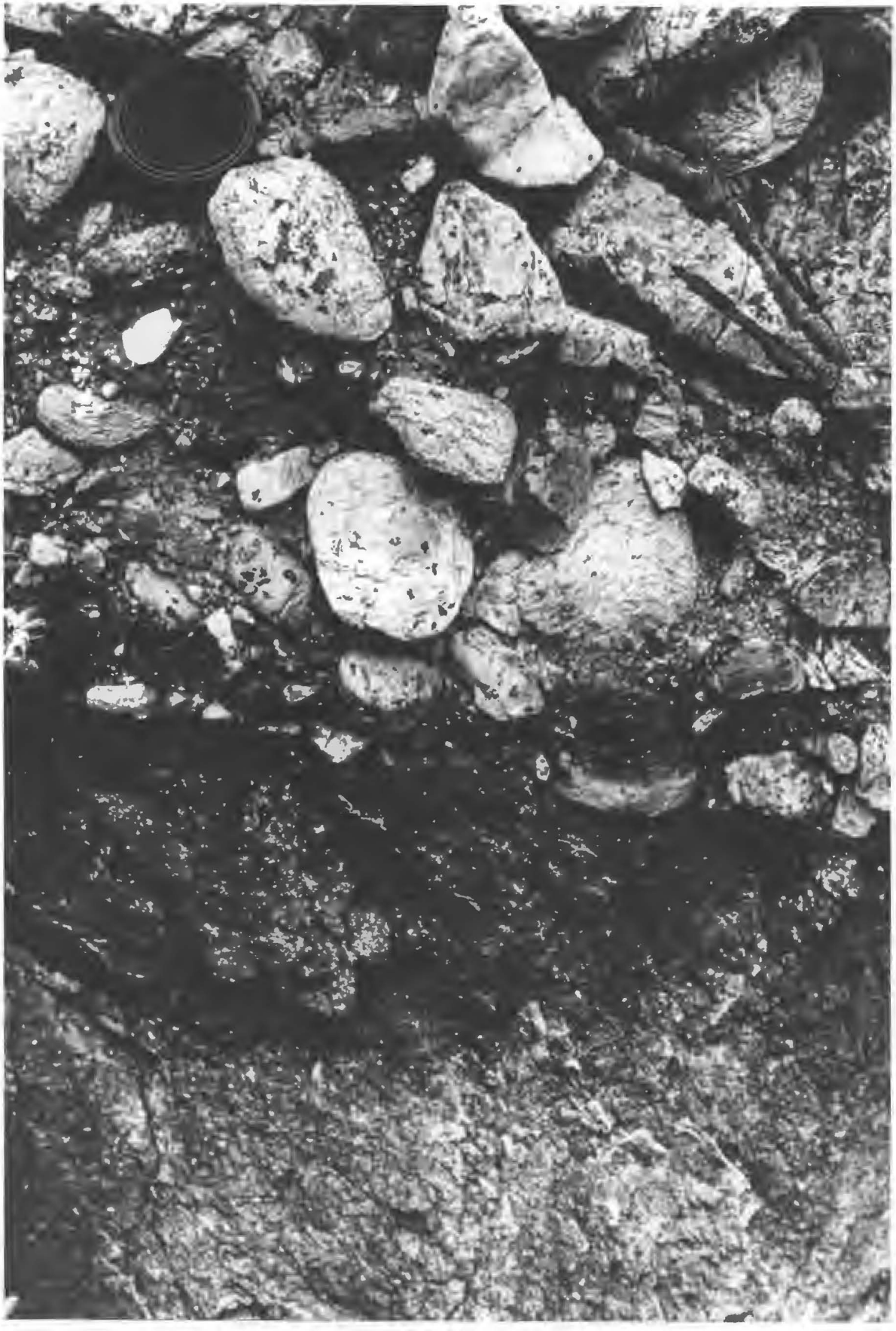

FIGURE 3.5

10 cm

3.4 DENISON SUBGROUP STRATIGRAPHIC EQUIVALENT

3.4.1 Introduction

In the Black Bluff region, quartzose clastic sedimentary rocks occupying the stratigraphic interval between unconformities of Jukesian type and the base of limestone sequences stratigraphically equivalent to the Gordon Subgroup, generally do not fall naturally into a lower terrestrial conglomerate sequence and an upper marine sandstone sequence. This is the case in several other areas, for example the Fossey Mountains area (Mt. Claude-Mt. Roland-Gog Range, see Fig. 3.1) where Jennings (1958, 1963) defined the Roland Conglomerate and Moina Sandstone, which together would now be considered to be stratigraphically equivalent to the Denison Subgroup. No attempt has therefore been made herein to subdivide the Denison Subgroup stratigraphic equivalent in the Black Bluff region into formations, although lithofacies similar to those recorded in, for instance, the Roland Conglomerate and the Moina Sandstone, are present. The main difference compared with the Fossey Mountains and Dial Range areas is the relative unimportance of coarse quartzose conglomerates, and the fact that where they do occur it is not always at the base of the sequence.

The Denison Subgroup stratigraphic equivalent displays considerable variation in thickness within the Black Bluff region, as summarized in the following notes:-

(1) In the northern part of the region, on the Loongana Range in the vicinity of Leven Canyon (4175/4170, Fig. 1.2), the sequence is 280 m thick.

(2) In the central part of the region, the greatest thicknesses are developed -

a) just south of Tiger Plain (vicinity of 4157/4070), it is 800 m thick,

b) a section due east from just west below the summit of Mt. Tor (4074/4128) is at least 700 m thick, the top being in faulted relationship with Mount Read Volcanics/Dundas Group stratigraphic equivalents to the east (see Map 4).

(3) In the southern part of the area, thicknesses decrease markedly again -

a) on the southern part of the Black Bluff Range (4072/4029), the sequence is 480 m thick,

b) on Bonds Range in the vicinity of 4097/4022 it is 100 m thick,

c) near the southernmost extension of Bonds Range at 4062/3988 it is 280 m thick.

The following distinctive lithofacies have been recognized within the Denison Subgroup stratigraphic equivalent in the Black Bluff region:-

I Volcanic wacke (in grainsize from coarse conglomerate to siltstone) and lithic wacke (mainly fine conglomerate).

II Medium to coarse grained hematitic quartzose conglomerate.

III Fine chert with quartz arenite matrix (overall bimodal fabric).

IV Pebbly quartz arenite with trough and (minor) planar cross-lamination.

V Pebbly quartz arenite and wacke with very abundant bedding-normal worm burrows.

VI Thin bedded interlayered laminated hematitic siltstone and fine quartz arenite with bioturbation and marine trace fossils in the siltstone layers.

3.4.2 Lithofacies I

This lithofacies is restricted to the basal parts of the sequence. Three kilometres east of the summit of Mt. Tor, near 4103/4128 (see Fig. 1.2 and Map 4), coarse volcanic wacke conglomerate occurs in a small remnant situated on an upthrown fault block and immediately overlying an inferred unconformity of Jukesian type on altered volcanics of the Mount Read Volcanics stratigraphic equivalent. Most of the pebbles in this rock are volcanic (quartz porphyry), a few are composed of hematitic sandstone and the matrix is a fine hematitic sandstone. The conglomerate is very poorly sorted and the pebbles are angular, subangular or subrounded and up to 6-8 cm in maximum diameter. The lithology is very similar to published descriptions of the Jukes Conglomerate (e.g. Banks, 1962b, p.149), a unit with patchy distribution which underlies the Owen Conglomerate in the Queenstown area in the Dundas Trough.

Fine volcanic wacke conglomerate also occurs in a few thin beds close to the base of the Denison Subgroup stratigraphic equivalent on the southwest shore of Paddy's Lake, just over 0.5 km east of the summit of Black Bluff (4131/4103, Fig. 1.2; specimen UTGD 48406). This rock is hematitic and red-brown in colour. The most common clast compositions are altered quartz-felspar porphyry and volcanic quartz, the former being sub-rounded and the latter sub-angular. There is a continuous variation in grainsize from the largest grains (about 1 cm in diameter) down to the matrix, which is in places visibly a result of degradation of the lithic fragments. Minor thin beds of quartzose conglomerate of Lithofacies II occur in close association with this lithology at this locality, and the sequence passes rapidly upwards into thin bedded pebbly quartz arenites of Lithofacies IV.

FIGURE 3.6

A. Hematitic fine lithic wacke conglomerate of Lithofacies I of the Denison Subgroup stratigraphic equivalent, from 4169/4080, east of Tiger Plain. Considerable tectonic strain has lead to distortion of grain shapes of the lithic clasts. Specimen UTGD 48403. PPL.

B. Pebbly medium-grained quartz arenite of Lithofacies IV of the Denison Subgroup stratigraphic equivalent, from 4174/4083, east of Tiger Plain. Note the metaquartzite composition of one of the large clasts. The other is composed of chert. Specimen UTGD 48399. XPL.

FIGURE 3.6A

2 mm

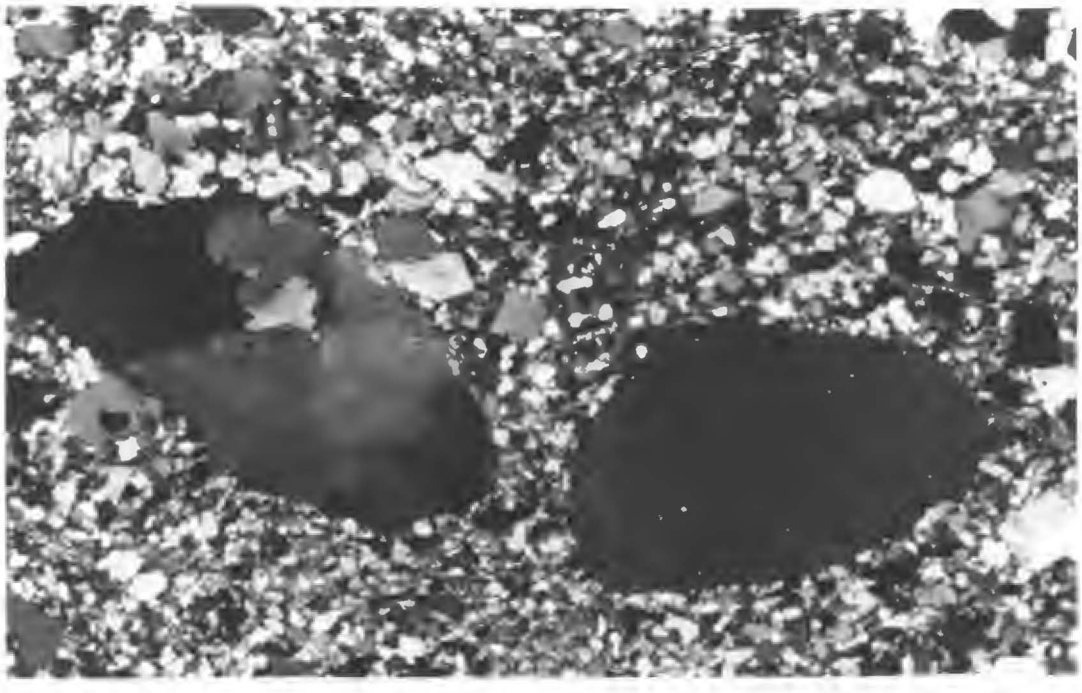

FIGURE 3.6B

2 mm

As defined herein, Lithofacies I also includes lithic wackes containing lithic fragments which are not recognizably of volcanic derivation, but may still have been derived from the sedimentary parts of the Mount Read Volcanics/Dundas Group stratigraphic equivalents. An example is a red-brown hematitic fine lithic wacke conglomerate (specimen UTGD 48403) from within 100 m of the base of the sequence, at 4169/4080, about 1 km southeast of Tiger Plain (see Fig. 1.2). Clast compositions in decreasing order of importance are hematitic siltstone, metamorphic quartz, metaquartzite and quartz-mica schist, and volcanic quartz (Fig. 3.6A). Nearly all the clasts are subangular, maximum grainsize is about 1 cm and sorting is very poor. Considerable tectonic strain has been absorbed mainly by the matrix and the siltstone clasts, and so grain shapes of the latter in Fig. 3.6A are not original.

The short sequence of volcaniclastic wacke siltstones occurring in the basal part of the Denison Subgroup stratigraphic equivalent just east of Tiger Plain (4166/4087), described in Section 3.3.1 herein, may also be considered part of Lithofacies I.

3.4.3 Lithofacies II

This lithofacies includes medium to coarse grained quartzose conglomerates similar to conglomerates described from the Roland Conglomerate in the Fossey Mountains area (Jennings, 1958, 1963), Member A of the Owen Conglomerate in the Queenstown area (Banks, 1962b), and the Reeds Conglomerate in the type section of the Denison Subgroup on the Denison Range (Corbett and Banks, 1974, 1975) (See Section 2.5 herein for summaries). However, in the Black Bluff region such conglomerates are never thickly developed, and often do not occur right at the base of the sequence, as is the case in other areas.

Coarse quartzose conglomerates do occur at the base of the sequence around the boundaries of the two northernmost 'windows' of Mount Read

Volcanics stratigraphic equivalents on the southern Black Bluff Range southwest of Bare Mt. (see Fig. 3.1), where they immediately overlie erosional unconformities of Jukesian type. These basal conglomerates are always less than 50 m, and generally of the order of 10 m or less, in thickness. There has been tectonic movement in some places along the boundary with the underlying volcanics, no doubt a result of the competence difference evidenced by the stronger development of cleavage in the volcanics, but generally the erosional unconformity is relatively undisturbed. Fig. 3.5 shows a typical example of the conglomerate close to the unconformity, from the northern end of the northernmost 'window' on the Black Bluff Range. The pebbles and cobbles in this rock constitute only about 50-60% of the deposit, and the overall fabric is bimodal, the matrix consisting of coarse hematitic quartz-lithic arenite containing at least some material derived from the altered quartz porphyry underlying the unconformity. It is notable that almost none of the pebbles and cobbles are derived from the latter material. Rather, they comprise subrounded to subangular clasts of metaquartzite, foliated metaquartzite and quartz-mica schist, and vein quartz, in order of decreasing importance. The massive metaquartzite and vein quartz clasts tend to be more angular, and the clasts with tectonic foliations more rounded. The foliation in the latter is disoriented from clast to clast, indicating that it was a feature of the source rock, and not developed during the Tabberabberan deformation after the deposition of the conglomerate. The clasts seem to have random orientation except right at the base, where some alignment parallel to the contact is apparent (Fig. 3.5). Nearly all of the clasts of pebble size and above in this deposit appear to have been derived from the Precambrian metamorphic rocks of the Tyennan Geanticline to the southeast (see Fig. 3.1).

The presence of a thin unit of coarse quartzose conglomerate at the base of the sequence has also been inferred along the southern

boundary of the belt of Mount Read Volcanics/Dundas Group stratigraphic equivalents west of Smiths Plains (See Fig. 3.1). The steep north-facing slopes here are often covered by talus deposits and bedrock outcrop is very poor; the presence of conglomerate is mainly inferred from its occurrence as boulders in the talus. The conglomerate unit was shown on the Tasmanian Department of Mines 1 mile series Sheffield Sheet (Jennings *et al.*, 1959) as about 100-150 m thick.

Thin units of coarse quartzose conglomerate also commonly occur some distance above the base of the Denison Subgroup stratigraphic equivalent in the Black Bluff region. Where this is the case the conglomerate commonly overlies one of the finer grained lithofacies. Some examples are:-

(1) At 4112/4110 (Fig. 1.2), 1.5 km west-northwest of the summit of Black Bluff, a 10 m thick unit of very coarse quartzose conglomerate conformably overlies interlayered thin bedded hematitic fine quartz arenites and laminated siltstones with flame structures and ball and pillow structure (Lithofacies VI?). The latter are in turn underlain by fine quartzose conglomerate, while the coarse conglomerate is overlain by thin bedded ferruginous pebbly quartz arenites with ripple marks (Lithofacies IV). It consists of fairly well sorted subrounded to rounded clasts of massive metaquartzite, foliated metaquartzite and vein quartz up to 30 cm or so in long dimension, with a grain supported fabric. The subordinate matrix consists of quartz arenite. Many of the clasts, particularly those composed of foliated metaquartzite, are disc-shaped. The clasts have a well-developed bedding-parallel preferred orientation, with some tendency to imbrication. The conglomerate unit includes a few thin quartz arenite layers.

(2) At 4142/4091, 2 km southeast of the summit of Black Bluff, thin bedded coarse quartz arenites with ripple marks are overlain by about 10 m of medium grained quartzose conglomerate. The contact is a low angle angular unconformity of up to about 20^{o}, the arenites having the steeper dip. The base of the conglomerate at this locality is about 300 m above the base of the sequence. The conglomerate appears to grade upwards into fine conglomerates and coarse pebbly quartz arenites of Lithofacies IV.

(3) A similar situation to (2) also occurs at 4142/4082, 1 km to the south, where thin bedded pebbly quartz arenites (Lithofacies IV) are overlain by fine to medium grained quartzose conglomerate, once again with low angle angular unconformity.

The quartzose conglomerates occupying the basal parts of the Denison Subgroup stratigraphic equivalent in other areas have been interpreted as the deposits of terrestrial alluvial fans by various authors (Sections 2.4 and 2.5 herein). The conglomerates described above are similarly interpreted, on the basis of:

(1) their oxidized nature

(2) apparent lack of lateral continuity of individual units

(3) their bimodal fabrics (pebbles and cobbles in sand matrix)

(4) absence of silt and clay-size material

(5) their unfossiliferous nature.

It should be re-emphasized at this point that the conglomerates make up only a minor part of the Denison Subgroup stratigraphic equivalent in most of the Black Bluff region. However, two of the other lithofacies, namely Lithofacies III and IV, have also been interpreted as terrestrial deposits (see later discussion), and may have also been deposited in an alluvial fan environment. Together, Lithofacies I to IV inclusive make up a major part of the sequence throughout the Black Bluff region.

Bull (1972) recognized the following modes of sedimentation in alluvial fans:-

(1) water laid sediments

a) channel deposits

b) sheetflood deposits

c) sieve deposits

(2) debris-flow deposits.

The coarse quartzose conglomerates in the Black Bluff region appear to represent more than one of these modes. Thus, the deposit shown in Fig. 3.5 is devoid of bedding, stratification and grading, and has a bimodal fabric consisting of randomly oriented (except right at the base) subangular to subrounded clasts in an abundant poorly sorted matrix containing a significant contribution from the immediately underlying bedrock. Under the criteria listed by Bull (1972, p.69) the final mode of emplacement of this deposit was almost certainly as a debris flow, although the metaquartzite clasts may have undergone other modes of transport in the journey from their source area. In contrast to this example, the conglomerate described from 4112/4110 in example (1) above has a more well sorted population of rounded large clasts with grain-supported fabric, having either bedding-parallel preferred orientation or slight imbrication, the pore space being filled by quartz arenite. This deposit most probably represents channel lag material. Channel fill may also be represented by some of the more fine grained quartzose conglomerates transitional between Lithofacies II and IV, and which sometimes display trough cross-stratification.

3.4.4 Lithofacies III

This lithofacies comprises fine to medium grained lithic breccias with usually hematitic matrix varying from quartz arenite to quartz-lithic wacke. Two examples are shown in Fig. 3.7A and 3.7B. Most of the quartz in the matrix is of metamorphic origin. The dominant composition of the larger clasts is white, pink and brown chert, which is often slightly argillaceous. Less common are clasts of foliated and unfoliated metaquartzite (Fig. 3.7). All the large clasts are angular or subangular, but the chert clasts tend to be somewhat more angular than the metaquartzite clasts. The overall fabric is distinctly bimodal.

Rocks transitional between this lithofacies and fine-medium grained quartzose conglomerate occupy the basal 50 m or so of the sequence at Mt. Tor (4074/4128, Fig. 1.2). However, the lithofacies does not only occur in the basal part of the sequence. Fine to medium grained quartzose conglomerate overlying the minor angular unconformity within the sequence at 4142/4082 (see discussion under Lithofacies II) grades upwards into rocks characteristic of Lithofacies III. Occurrences of Lithofacies III at 4104/4062 in the central part of the Black Bluff Range are high in the sequence, within approximately 100-150 m of the base of the Gordon Subgroup stratigraphic equivalent.

Rocks of Lithofacies III are often red-brown in colour, mainly due to the hematitic nature of the matrix. This together with the lack of fossils and common occurrence of trough cross-bedding indicates that the lithofacies represents terrestrial deposition. It may fit into the alluvial fan model as representing deposits of braided distributary streams (sheetflood sediments of Bull, 1972, p.66). The provenance of the chert clasts, however, remains a problem.

FIGURE 3.7

A. Hematitic fine chert breccia of Lithofacies III of the Denison Subgroup stratigraphic equivalent, from 4138/4089, 2 km southeast of summit of Black Bluff. Note quartz arenite matrix and bimodal fabric. Specimen UTGD 48405. PPL.

B. Same lithology as A, above, from 4104/4062, central Black Bluff Range. Note clast of foliated meta-quartzite. Specimen UTGD 48417. PPL.

FIGURE 3.7A

2 mm

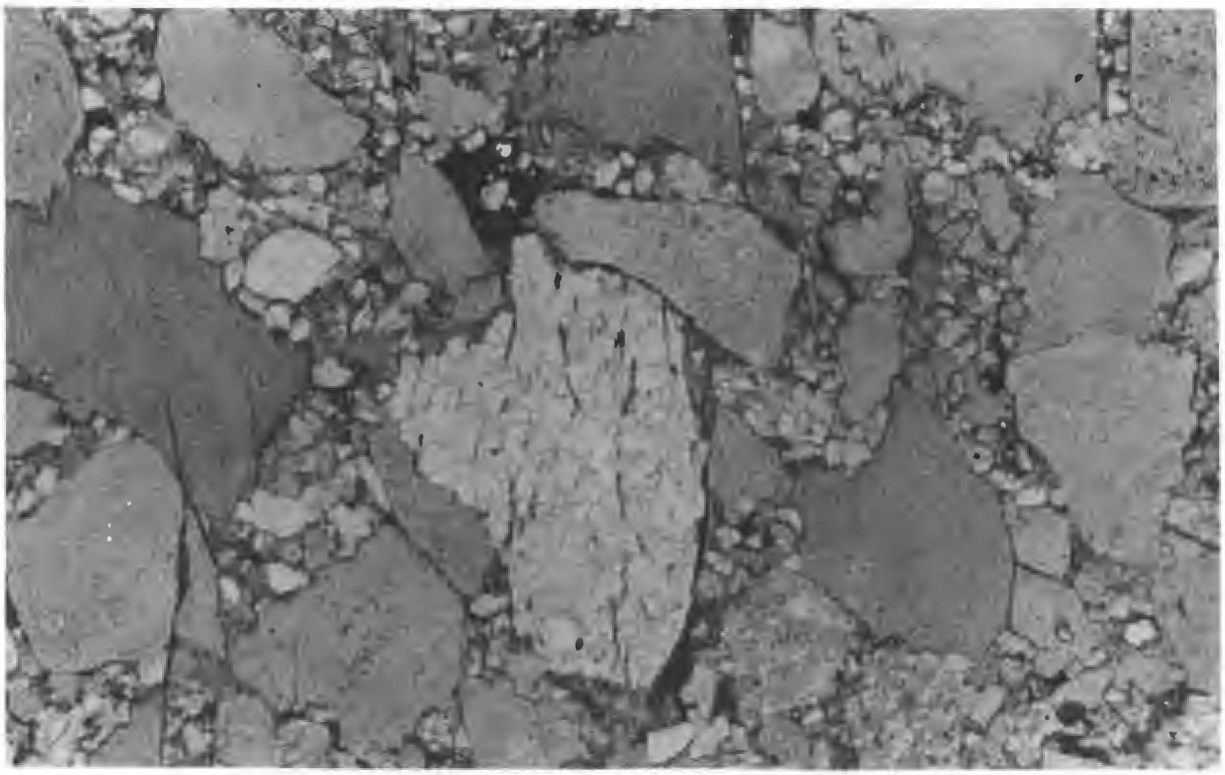

FIGURE 3.7B

2 mm

3.4.5 Lithofacies IV

Pebbly medium to coarse quartz arenite is typical of this lithofacies. An example from 4174/4083, 2 km east-southeast of Tiger Plain, is illustrated in Fig. 3.6B. The pebbles are subrounded to subangular, are generally up to about 0.7 cm in diameter, and are often concentrated at certain horizons. They constitute up to about 10% of the rock, and are composed of metaquartzite and chert, with the former predominating. The remainder of the rock is a poorly to moderately sorted slightly hematitic quartz arenite consisting of mostly subangular grains of metamorphic quartz having low sphericity, with an argillaceous matrix. Blue-green tourmaline is a common accessory mineral.

In outcrop, the rock is often thick bedded, and trough cross-lamination is a common sedimentary structure. Marine fossils are apparently absent. The colour is usually light grey to mottled light grey-brown, indicating a lower degree of oxidation than is present in Lithofacies III. This lithofacies may perhaps be considered as a more mature, less pebbly variant of Lithofacies III, while the less oxidized nature suggests that it is a more marginal marine facies. Lithofacies IV occurs at or very close to the base of the Denison Subgroup stratigraphic equivalent on Bonds Range near 4111/4032. The mineralogy indicates that the sediment was predominantly derived from the Precambrian rocks of the Tyennan Geanticline.

3.4.6 Lithofacies V

This lithofacies consists of bioturbated quartz arenite and quartz wacke, characteristically containing abundant bedding-perpendicular worm burrows, the density of which is often so great that it is difficult to identify original undisturbed sediment. This is a characteristic common to certain lithofacies within the Moina Sandstone in the Fossey Mountains area to the east (Jennings, 1958, 1963), which lead early

workers to refer to that formation as "the Tubicolar Series". The higher percentage of argillaceous matrix compared with the arenites of Lithofacies IV may be at least partly a result of the bioturbation, as evidenced by higher matrix:grain ratios within burrow fill in those examples where unburrowed material is still present (e.g. specimen UTGD 48402). The dominant clast composition is metamorphic quartz, and, as was the case with Lithofacies IV, blue-green tourmaline is again a common accessory mineral (see Fig. 3.8A). The sorting of the quartz clasts is somewhat better than in Lithofacies IV, but they are still dominantly subangular (see Fig. 3.8A and 3.8B). Rocks of Lithofacies V are nearly always mottled light grey to grey-green in colour, indicating a lack of oxidation.

The characteristics of Lithofacies V summarized above suggest a marine-dominated environment of deposition. The environment suggested is an intertidal one. The factor which differentiated the deposition of Lithofacies V from that of intertidal burrowed dolomicrites within the limestone sequence of the Gordon Subgroup stratigraphic equivalent was a much higher degree of terrigenous influx, which must point to still considerable relief of the source area in the Precambrian terrain at the time.

Lithofacies V tends to be more dominant in the upper parts of the Denison Subgroup stratigraphic equivalent sequence in the Black Bluff region, but this is by no means a universal rule. Hence, sediments characteristic of the lithofacies occur very close to the base of the sequence on Bonds Range near 4111/4032.

FIGURE 3.8

A. Bioturbated argillaceous quartz wacke of Lithofacies V of the Denison Subgroup stratigraphic equivalent, from 4169/4075, near Devonport Mine, southeast of Tiger Plain. Note detrital tourmaline grain (t). Specimen UTGD 48402. PPL.

B. As for A, above, but XPL.

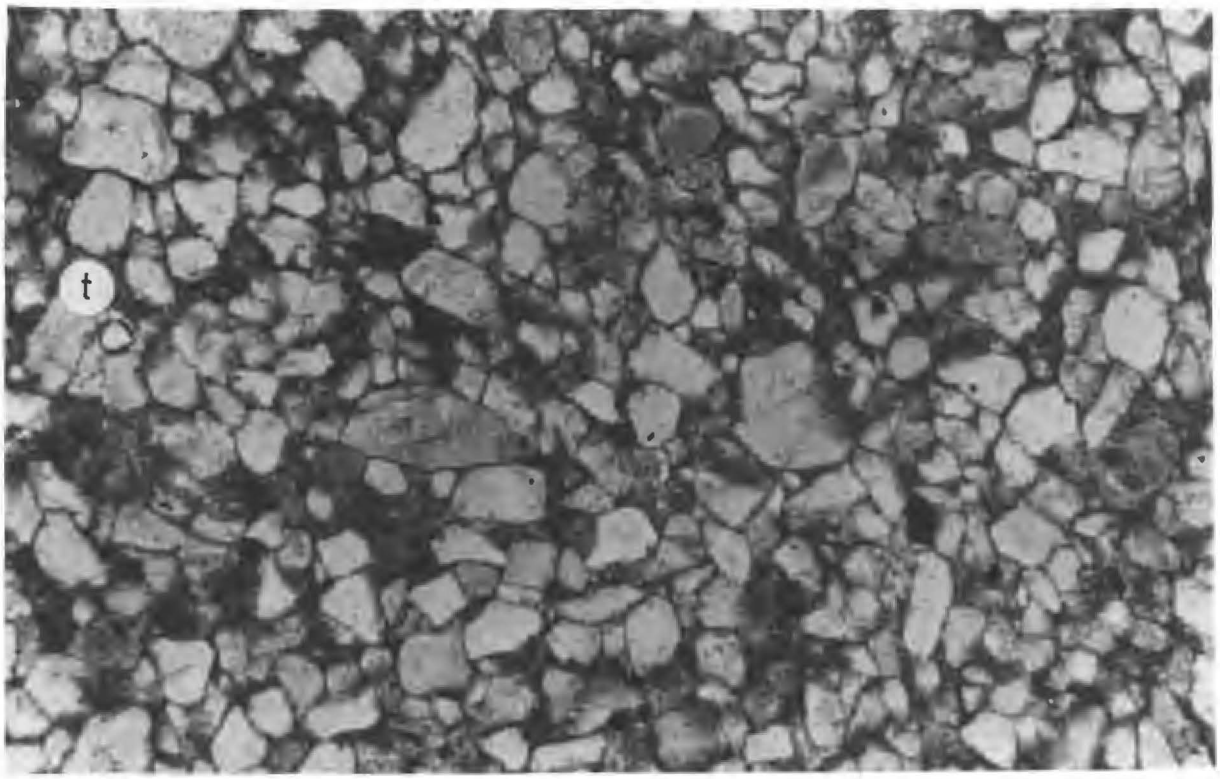

FIGURE 3.8A

1 mm

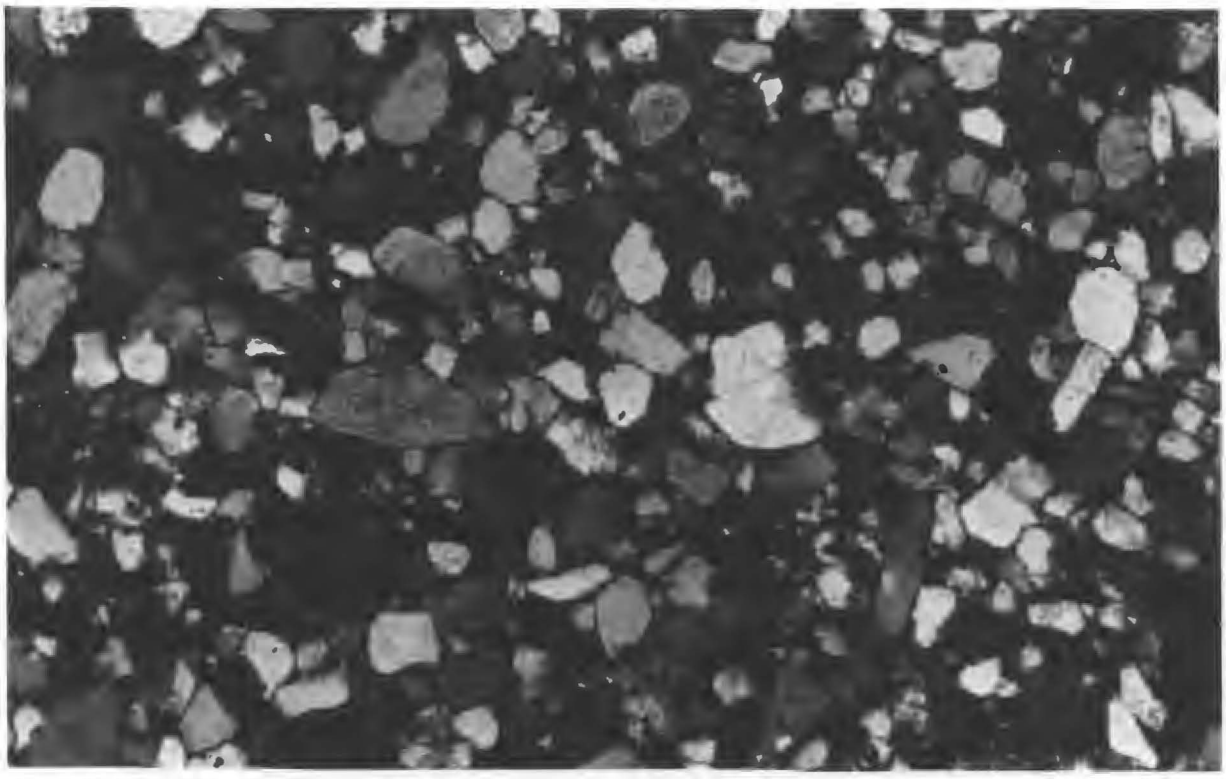

FIGURE 3.8B

1 mm

3.4.7 Lithofacies VI

This lithofacies makes up only a minor part of the Denison Subgroup stratigraphic equivalent in the Black Bluff region. It consists of thin bedded interlayered laminated dark red-brown hematitic siltstone and pale-coloured fine quartz arenite. The siltstone beds are sometimes very minor or absent. Where they are present they are sometimes bioturbated. At 4077/4056 on the Black Bluff Range 1 km northwest of Bare Mt., trace fossils which have been identified as trilobite feeding burrows have been found in the top surface of one of these siltstone beds (specimen UTGD 48419). The arenite beds are much less hematitic and often contain ripple marks, ripple-drift cross-lamination and occasionally small scale trough cross-lamination.

Lithofacies VI sometimes forms the upper part of a sequence consisting of Lithofacies II-III-IV-VI. It is interpreted herein as a marginal lower intertidal to subtidal facies, with the siltstone forming in shallow lagoon or bay conditions and the arenite representing laterally migrating shallow bars. An alternative is that the assemblage formed in intertidal conditions, with the siltstone representing intertidal mudflats and the arenite representing intertidal channels. The presence of trilobite feeding burrows, however, argues against intertidal conditions.

3.4.8 Palaeocurrents

Interpretation of palaeocurrent lineations in the Denison Subgroup stratigraphic equivalent in the Black Bluff region is made difficult by the fact that many areas have been through two episodes of folding on different trends during the Tabberabberan Orogeny, leading to complications in the unwinding of the tectonic structure. The following notes summarize results from areas where the structure is relatively simple and unwinding could be reliably carried out:-

(1) At 4053/3976, 2.5 km east-northeast of the summit of Mayday Mt. in the southern part of the region, asymmetric straight ripples in Lithofacies VI indicate currents directed from the SE (mode, 133°).

(2) At 4106/4017 in the vicinity of Bonds Hill on Bonds Range, planar cross-bedding in Lithofacies IV indicates currents directed from between ESE and SE (mode, 126°).

(3) At 4086/4051, close to Bare Mt. in the central Black Bluff Range, similar current indicators to those in (2) indicate currents directed from the SE (mode, 125°).

(4) At 4084/4057, 1.2 km northwest of Bare Mt., current indicators similar again to those in (2) indicate currents directed from between E and ESE (mode, 106°).

(5) At 4113/4109, 1.4 km west-northwest of the summit of Black Bluff, asymmetric slightly sinuous ripples in thin bedded hematitic quartz arenites of Lithofacies IV indicated currents directed from between 120° and 150° when simple removal of the dip was carried out. However, recognition of two phases of folding in this area indicated that a strike rotation was required prior to removal of the dip, and this yielded currents directed from between 150° and 180° (SSE to S).

(6) At 4142/4091, 2 km southeast of the summit of Black Bluff, asymmetric straight ripples in thin bedded quartz arenites of (?)Lithofacies VI indicate currents directed from approximately WSW (mode, 255°).

(7) At 4149/4067, 2 km south-southwest of Tiger Plain, planar cross-lamination in thin bedded quartz arenites of Lithofacies IV indicate currents directed from almost due E (mode, 084°).

3.4.9 Provenance and sedimentary environment

Palaeocurrent data and the mineralogy of the sediments indicates that the main source area during deposition of the Denison Subgroup stratigraphic equivalent was the Tyennan Geanticline to the south and southeast. This conclusion is consistent with the lenticular shape of the overall sequence, being thickest in the Mt. Tor-Black Bluff-Tiger Plain area and thinning both to the north and to the south. The initiation of the deposition appears to have been due to uplift of the Tyennan Geanticline, probably accomplished at least partly by reactivation of old basement faults which formed during the initial rifting of the Precambrian areas which lead to the formation of the Palaeozoic troughs. Uplift was probably not restricted only to the Tyennan Geanticline, parts of the Mount Read Volcanics/Dundas Group stratigraphic equivalents also being involved.

These mainly vertical tectonic movements lead to tilting of parts of the Mount Read Volcanics/Dundas Group stratigraphic equivalents sequence, leading to formation of angular unconformities with the overlying rocks. The surface on which deposition of the basal beds of the Denison Subgroup stratigraphic equivalent was to take place probably initially had considerable relief, which was partly an original topographic feature and partly a result of differential uplift (by way of block faulting) of the volcanosedimentary terrain. Topographic highs on this surface may have initially been sites of erosion, while immediate deposition took place in topographic lows. This is the depositional situation envisaged for the essentially terrestrial volcaniclastics of Lithofacies I. As deposition progressed the Tyennan Geanticline supplied a progressively greater proportion of the detritus. Continued tectonic movements during deposition of the Denison Subgroup stratigraphic equivalent is evidenced by the presence of minor angular unconformities

within the sequence; significantly, these are overlain by quartzose conglomerate derived from the Precambrian rocks.

The characteristics of the bulk of the sediments within the sequence indicate that they were deposited in alluvial fan environments. However, marine and marginal marine facies begin to predominate in the upper parts of the sequence. In a few places (e.g. in parts of Bonds Range), marine-influenced conditions may have prevailed even in the earliest stages of deposition.

3.5 GORDON SUBGROUP STRATIGRAPHIC EQUIVALENT

3.5.1 Loongana area

Carbonate lithofacies stratigraphically equivalent to the Gordon Subgroup occur in a large syncline in the Loongana area in the northern part of the Black Bluff region (see Fig. 3.1). The axis of the syncline is horizontal and trends ESE-WNW, and it is an asymmetric structure with a long northern limb and short southern limb. The southern boundary of the limestone may be faulted against the Denison Subgroup stratigraphic equivalent (see Map 2). An early report on the limestone at Loongana was that by Hughes (1957), although he have no details of the lithofacies present.

The maximum exposed section of limestone at Loongana is estimated herein to total about 1150 m. The top of the limestone is missing. The base is exposed in the Leven River near 4179/4164 where lithofacies transitional between the limestone and bioturbated quartz arenites of the Denison Subgroup stratigraphic equivalent are only developed to a minor extent. The basal 10-15 m of the limestone sequence consists of micrite containing sparse oncolites and small specimens of the gastropod *Maclurites*, and may have been deposited in a lower intertidal to shallow subtidal environment. Most of the remainder of the sequence consists of

dolomicrites which are often bioturbated, with dolomitized bedding-perpendicular burrows being common. These are interpreted as intertidal sediments. They include a few minor shell beds and calcarenite beds which may represent intertidal channels. Towards the upper part of the sequence dolomitization becomes better developed and algalaminated dolomicrites appear. Some of these may have been deposited in supratidal environments. Stromatolitic algalaminated dolomicrites occur near the top of the exposed section at Taylors Flat, 4143/4143.

Burrett (1978, pp.88-90) obtained the following biostratigraphic information from the limestone at Loongana, based on conodont microfaunas:-

(1) Location: the oncolitic micrite close to the base of the sequence

Contents: *Phragmodus flexuosus* Moskalenko

Panderodus serpaglii sp. nov.

Indicated age: Chazyan (early-Middle Ordovician).

(2) Location: about 220 m above base of sequence

Contents: *Phragmodus flexuosus* Moskalenko

Belodina compressa (Branson and Mehl)

Indicated age: Blackriveran (middle-Middle Ordovician).

(3) The youngest indicated age obtained by Burrett from the Loongana sequence was Rocklandian (late-Middle Ordovician).

3.5.2 Vale of Belvoir area

Limestones representing the stratigraphic equivalent of the Gordon Subgroup outcrop in the southern part of the Vale of Belvoir in a markedly asymmetric SE-verging syncline with a horizontal NE-trending axis (see Figs. 1.2 and 3.1, and Map 6). The total section present is estimated at just over 400 m, although the base is obscured and the top has been removed by erosion. The following is a composite section based on the available outcrop, from the top of siliceous clastics of the

Denison Subgroup stratigraphic equivalent, on a traverse northwest across the Vale from near 4075/3992:-

TOP

unit		(m)
4	Calcareous mudstone	20
3	Chert nodular micrite	100
2	Thin bedded bioturbated dolomicrite with abundant vertical and horizontal worm burrows	90
1	Thin bedded dolomicrite with calcarenite channels	70
	(Gap in outcrop)	150
BASE	TOTAL	430 m

Unit 1 of the Vale of Belvoir section contains thinly bedded dolomicrite with dolomite stringers parallel to bedding. In its upper parts it includes laterally discontinuous beds of cross-stratified calcarenite containing silicified orthid brachiopod and gastropod fragments in a coarse spar cement. Unit 1 is interpreted as a lower intertidal facies, with the calcarenite units representing the well-washed infilling of intertidal to subtidal channels. The channel-like form of the calcarenite units can actually be seen in some outcrops (Fig. 3.9A).

Unit 2 consists mainly of thin bedded dolomitic micrite which is extensively bioturbated, dolomitized worm burrows with both bedding-parallel and bedding-normal orientations being common, the former tending to predominate (see Fig. 3.9B). Unit 2 is interpreted as representing a high intertidal sedimentary environment.

Unit 3 consists of slightly dolomitic micrites containing abundant very elongate chert nodules which are parallel or subparallel to bedding and tend to be concentrated on certain bedding planes.

FIGURE 3.9

A. Calcarenite-filled channel in thin bedded dolomicrites, Gordon Subgroup stratigraphic equivalent, Vale of Belvoir. Lower intertidal facies.

B. Burrowed dolomicrite, Gordon Subgroup stratigraphic equivalent, Vale of Belvoir. Upper intertidal facies.

FIGURE 3.9A

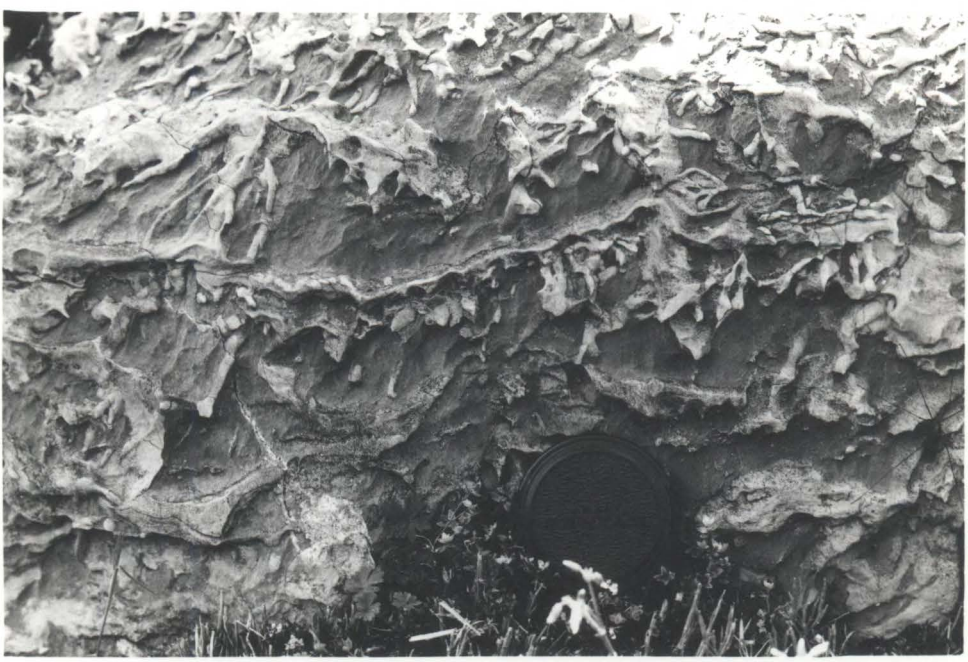

FIGURE 3.9B

10 cm

The nodules are up to 4 cm in cross-section diameter but are up to 0.5 m in length. Those with high length:width ratios are often sinuous, and there is no preferred orientation within the bedding plane. In many places the chert is visibly a result of replacement, and also appears to post-date dolomitization. The depositional environment of Unit 3 is problematical.

Burrett (1978, p.112) recorded the following conodont assemblages from the Vale of Belvoir section:-

(1) Locality: near lowermost exposure of unit 1

Contents: rare *Chirognathus monodactyla* Branson and Mehl.

(2) Locality: close to top of unit 1

Contents: *C. monodactyla* Branson and Mehl

Panderodus gracilis (Branson and Mehl)

Belodina compressa (Branson and Mehl)

Plectodina aculeata (Stauffer).

Burrett found that the Vale of Belvoir section ranged in age from Blackriveran (middle-Middle Ordovician) to Kirkfieldian (late-Middle Ordovician).

CHAPTER 4

STRUCTURAL GEOLOGY

4.1 PREVIOUS WORK ON THE TABBERABBERAN OROGENY IN TASMANIA

The existence of several different fold trends attributed to the Devonian Tabberabberan Orogeny has been recorded for some time in previous literature on the Palaeozoic geology of western Tasmania (Carey, 1953; Bradley, 1956; Jennings, 1958, 1963; Solomon, 1962, 1965; Burns, 1963, 1964; Williams, 1976, 1978). As noted by Williams (1978, p.195), the geanticlines of Cambrian times behaved as relatively competent blocks during the Devonian deformation. The folds are generally open, upright, horizontal to gently plunging and symmetrical, but locally tighter structures occur in a number of places, and folds are often asymmetric around the margins of the Tyennan Block, with vergence towards it (see the cross-sections on Map 1). Strong cleavage development is mostly restricted to the less competent lithologies, for example those occurring within the Mount Read Volcanics/Dundas Group and Gordon Subgroup stratigraphic equivalents.

Solomon (1962, p.324) noted the dominant N-trending folds close to the margin of the Tyennan Block in the "West Coast Structural Unit" north and south of Queenstown (see Map 1). Williams (1978, p.195) stated that these folds have approximately 2 km half-wavelength, have an axial cleavage and are often asymmetrical and overturned with axial surfaces dipping steeply to the west, indicating tectonic transportation from the west. Solomon also recognized WNW to NW trending folds and faults, the latter being particularly strongly developed in the Linda Fault System, just northeast of Queenstown (385342, Map 1). He suggested that these structures are probably later than the N-trending structures.

This conclusion was supported by the work of Baillie and Williams (1975) in the Zeehan area northwest of Queenstown (365355, Map 1), where interference of the two deformation phases has produced folds which change markedly in trend and plunge along their hingelines. They found that primary cleavage associated with the N-trending phase had been crenulated during the deformation event which produced the NW-trending structures. Folds and faults of NW trend also occur in the Precambrian rocks of the central part of the western margin of the Tyennan Block (see Map 1). Williams (1978, p.197) identified all of these NW-trending structures in central western Tasmania as the "Zeehan/Gormanston trend", which he grouped together with the similar "Deloraine/Railton trend" in the central north, the two groups of structures together representing the effect of the late phase of the Tabberabberan Orogeny in Tasmania. It was envisaged that during this late phase the Tyennan Block had yielded in a NW-trending narrow zone and behaved as two blocks - hence the subdivision into a Cradle Mountain Block to the north and Prince of Wales Range Block to the south, on Map 1.

Solomon (1962, p.327) seemed to consider that NNE- to NE-trending folds and cleavage close to the northwest margin of the Tyennan Block (vicinity of 402397, Map 1) are an extension of the early N-trending structures north and south of Queenstown, the change in trend being controlled by the margin of the block. This is one of the suggestions which has been tested by the mapping carried out during the course of this project. It is notable that at St. Valentines Peak (396421), away from the margin of the block, the folds are almost N-trending again. On the basis of mapping in the region between St. Valentines Peak and Black Bluff (412410), Pike (1964) recognized folds on three distinct trends:-

(1) E-W, parallel to the northern margin of the Tyennan Block

(2) NE, parallel to the northwest edge of the Tyennan Block

(3) NW cross-folds unrelated to the margins of the block.

Pike favoured the conclusion that these sets of structures developed in a distinct sequence, (1) being the earliest and (3) the latest, as opposed to the alternative hypothesis that they developed contemporaneously and their trends were controlled by the margins of the Tyennan Block.

In the Fossey Mountains area at the northern margin of the Tyennan Block, Jennings (1958, 1963) recognized sets of folds analagous to the first and third of the sets recognized by Pike, above. The early E-W trending folds were identified as broad, gentle, upright low amplitude structures with no associated cleavage development, and half-wavelengths of the order of 5 km. The main evidence for the existence of this set of structures came from examination of the large scale outcrop pattern in central northern Tasmania (e.g. on the scale of Map 1), and from the fact that the later WNW- to NW-trending crossfolds are doubly plunging, with a tendency to show sigmoidal outcrop patterns. An example of such a crossfold is the WNW-trending Standard Hill Anticlinorium (440401, Map 1 and Fig. 3.1), the hingelines of which change from sub-horizontal to ESE-plunging at about 20^{o} along an east-west line just south of 5400000 mN (see Fig. 3.1). Thus, Jennings (1963, p.100) explained this change of plunge as being due to intersection of the WNW-trending folds at this point with a large scale flexure on the limb of one of the earlier E-W trending folds. Williams (1978, p.196) termed the large E-W trending folds in central northern Tasmania the "Loongana/Wilmot trend", and grouped them together with the N-trending folds in central western Tasmania ("West Coast Range/Valentines Peak trend") as the "Early fold phase" of the Tabberabberan Orogeny.

The later set of folds recognized by Jennings in the Fossey Mountains area are smaller scale structures, having half-wavelengths of about 2.5 km. They are asymmetric, with vergence to the southwest and axial surfaces and associated thrust faults dipping to the northeast, indicating tectonic transportation from the latter direction (see Section I-J, Map 1). They are often associated with moderately to strongly developed steeply dipping primary cleavage in the less competent lithologies. Williams (1978, p.196) termed this set of structures the "Deloraine/Railton trend". The trends of folds, cleavage and faults of this association actually change gradually from WNW in the vicinity of Mole Creek (451399, Map 1) to NNW near Smiths Plains (420411). Structures of the Deloraine/Railton trend appear to die out southwest of the latter point. The swing in trends may be an effect of deflection against the rigid northern margin of the Tyennan Block. Solomon (1962, p.330) seemed to suggest an alternative explanation, namely that the swing was due to refolding during the deformation responsible for the NNE- to NE-trending folds at the northwest margin of the Tyennan Block. However, if this was true, it would presumably imply that the latter are the youngest Tabberabberan structures present in northwest Tasmania, which contradicts Williams (1978), and also Pike (1964, p.80) who identified NE-trending folds cut by later NW-trending faults.

The fact that evidence for the early E-W trending fold phase in the Fossey Mountains area is almost absent on the scale of minor structures was confirmed by detailed mapping by Seymour (1975) in the Mayberry (441398, Fig. 3.1) and Claude Creek (429407) areas. The simplicity of the structural data is evident in Figs. 4.1 and 4.2, the only clue to the existence of more than one phase of folding being a small amount of variation in plunge of the WNW- to NW-trending folds. In fact, the gentle NW plunge of folds in the Moina Sandstone (part of the Denison

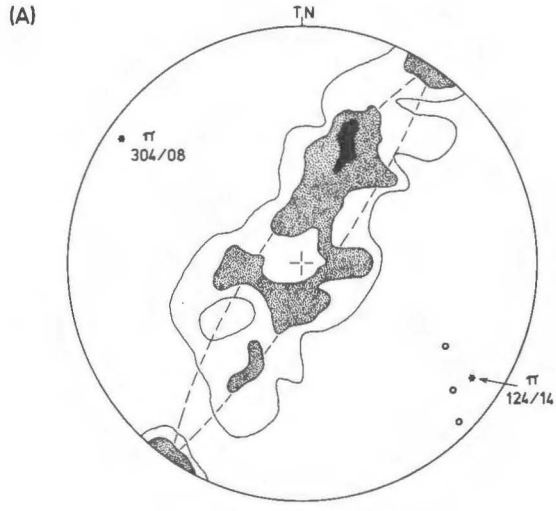

Liena Gorge, Mayberry area
55 poles to bedding
Contours 2,5,10% per 1% area
o Minor fold hinges

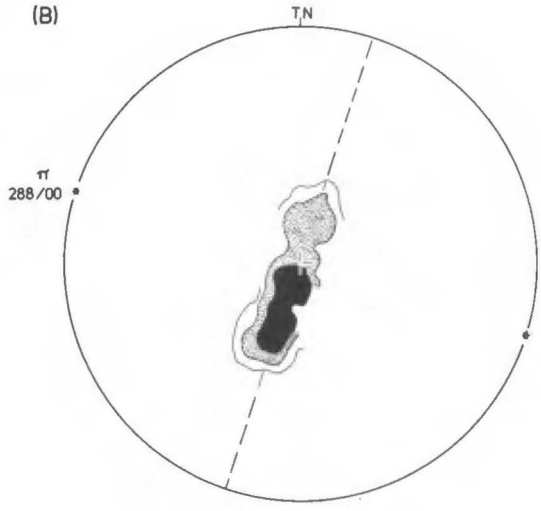

Sensation Gorge, Mayberry area
67 poles to bedding
Contours 5,10,20% per 1% area

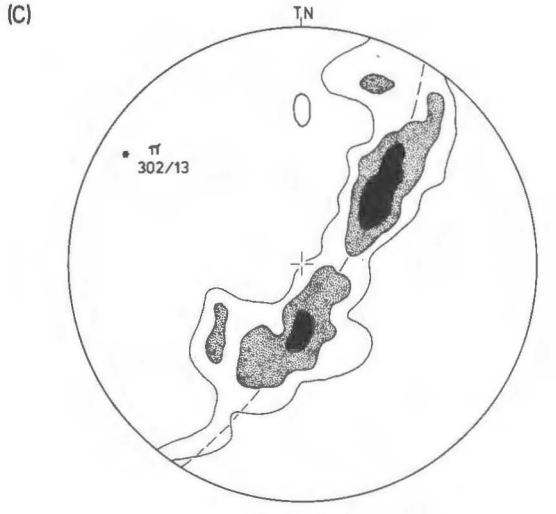

Claude Creek
52 poles to bedding
Contours 2,5,10% per 1% area

STRUCTURAL DATA

MOINA SANDSTONE

Mayberry & Claude Creek areas

FIGURE 4.1

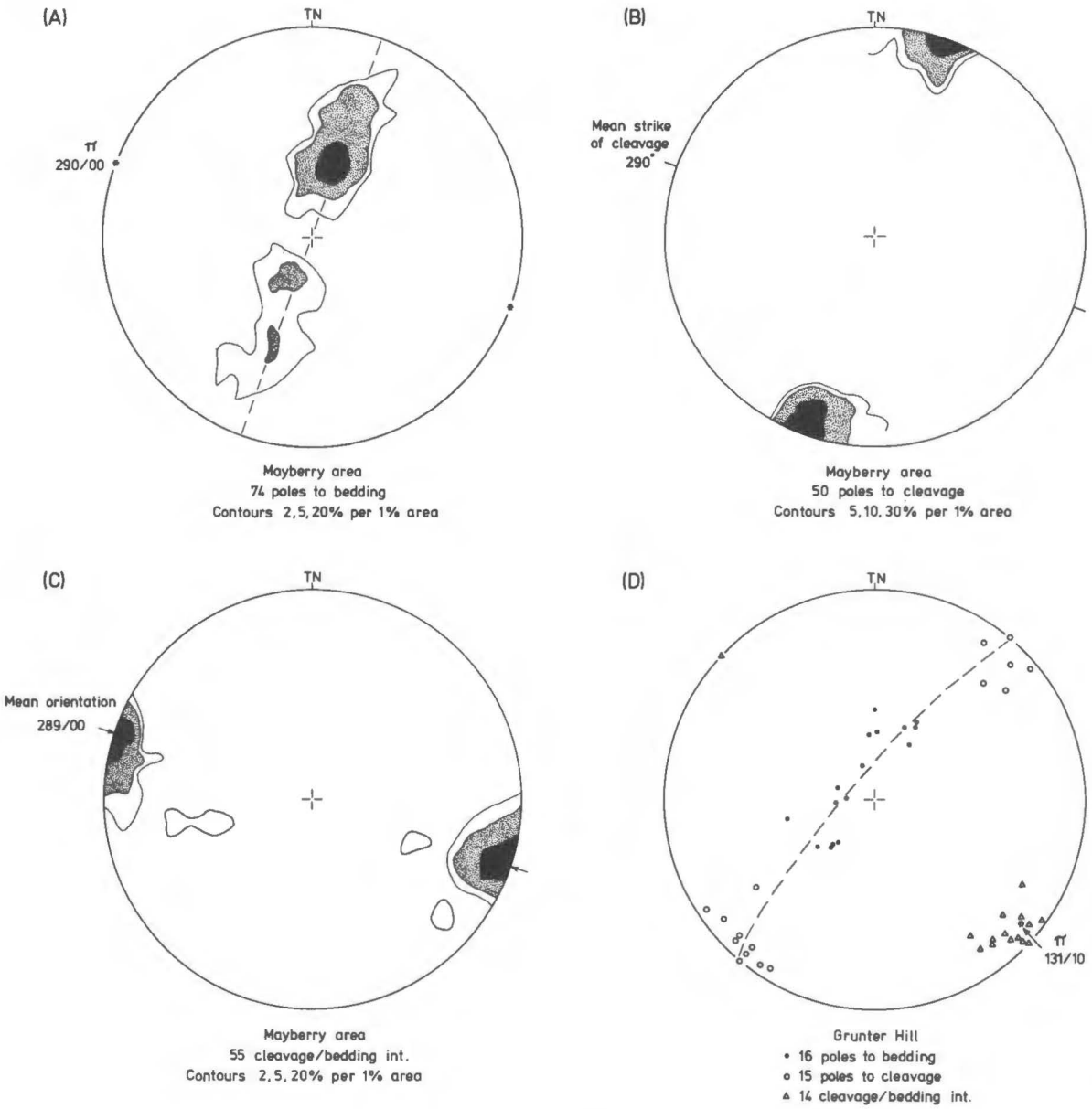

STRUCTURAL DATA

GORDON LIMESTONE S.G.

Mayberry area

FIGURE 4.2

Subgroup stratigraphic equivalent) at Claude Creek (Fig. 4.1C) was suggested by Jennings (1963, p.99) to be due to disturbance associated with the intrusion of the Dalcoath Granite (406427, Fig. 3.1).

Burns (1963, 1964), in a study covering the area between the Dial Range (420440, Map 1) in the west and Eugenana (441434) in the east, recognized two main phases of deformation associated with the Tabberabberan Orogeny. The first ("Eugenanan phase") produced horizontal to gently plunging N-trending open upright folds with associated well developed steeply dipping cleavage in incompetent lithologies, while the second ("Loonganan phase") produced superposed oblique cross-folds with NE trends. It is tempting to suggest that the latter structures represent the same deformation phase which produced the NNE- to NE-trending folds at the northwest margin of the Tyennan Block. However, during the course of the present study structures of the latter trend have not been detected any further northeast than Black Bluff (412410, Map 1), and they may in fact die out at about this point. The relationship between the Eugenanan phase of Burns and the trends defined by Williams (1978) is somewhat uncertain. That is, it may represent either the northerly extension of the N-trending structures in central western Tasmania and at St. Valentines Peak, or it may represent the Deloraine/Railton trend of Williams, which may have continued its progressive swing in azimuth from WNW through NW and NNW to be N-trending near the north coast of Tasmania.

The most important information reported by Burns relates to the dating of the Tabberabberan Orogeny in Tasmania. Quarrying at Eugenana had revealed tectonically undeformed fossil spelean deposits which had been deposited in pockets and cavities in a cave breccia, containing blocks of limestone of the Gordon Subgroup stratigraphic equivalent with the primary tectonic cleavage disoriented from block to block

FIGURE 4.3

Tectonically undisturbed fossil cave infilling of the Eugenana Beds, deposited in a cavity in a collapse breccia containing blocks of limestone of the Gordon Subgroup stratigraphic equivalent, with the tectonic cleavage disoriented from block to block. Hallets Quarry, Eugenana.

FIGURE 4.3

5 m

(see Fig. 4.3). The total lack of tectonic disturbance of the deposits (which were referred to as the Eugenana Beds), together with the fact that both the Eugenanan and Loonganan deformation phases were represented in the limestone bedrock at the locality, lead Burns to conclude that the deposition of the spelean deposits post-dated all the Tabberabberan tectonic movements in the region. Spore analysis of carbonaceous siltstone from the deposits yielded a flora of late-Middle Devonian age (Balme, 1960). This information together with the age of the youngest beds affected by the Tabberabberan Orogeny (the Lower Devonian Bell Shale, of the Eldon Group) sets upper and lower limits to the age of the deformation.

4.2 INTRODUCTION (INCLUDING NOMENCLATURE)

SUMMARY MAP - see pocket

As noted in the statement on scope of the project (Section 1.1), the area outlined on Fig. 3.1 was chosen mainly on the basis of projection of a potential area of intersection of the main fold trends defined by Williams (1978). It was hoped that information leading to a clearer understanding of the sequence of development of the Tabberabberan structures could be obtained from mapping in this area. Five structural maps are included, the coverage of which is indicated on Fig. 1.2. Maps 2, 3 and 4 are at a scale of 1:20,000, but due to the unavailability of metric base maps at the time of compilation, Maps 5 and 6 are at 4 inches to the mile (1:15,840). A standard metric grid has been used on all maps, however. The coverage of smaller subareas used for structural analysis of the Denison Subgroup stratigraphic equivalent is shown on Fig. 4.4.

Following the procedure of Williams (1978), the association of Tabberabberan structures into groups in the Black Bluff region has been based mainly on trend. This is considered valid because of the relatively

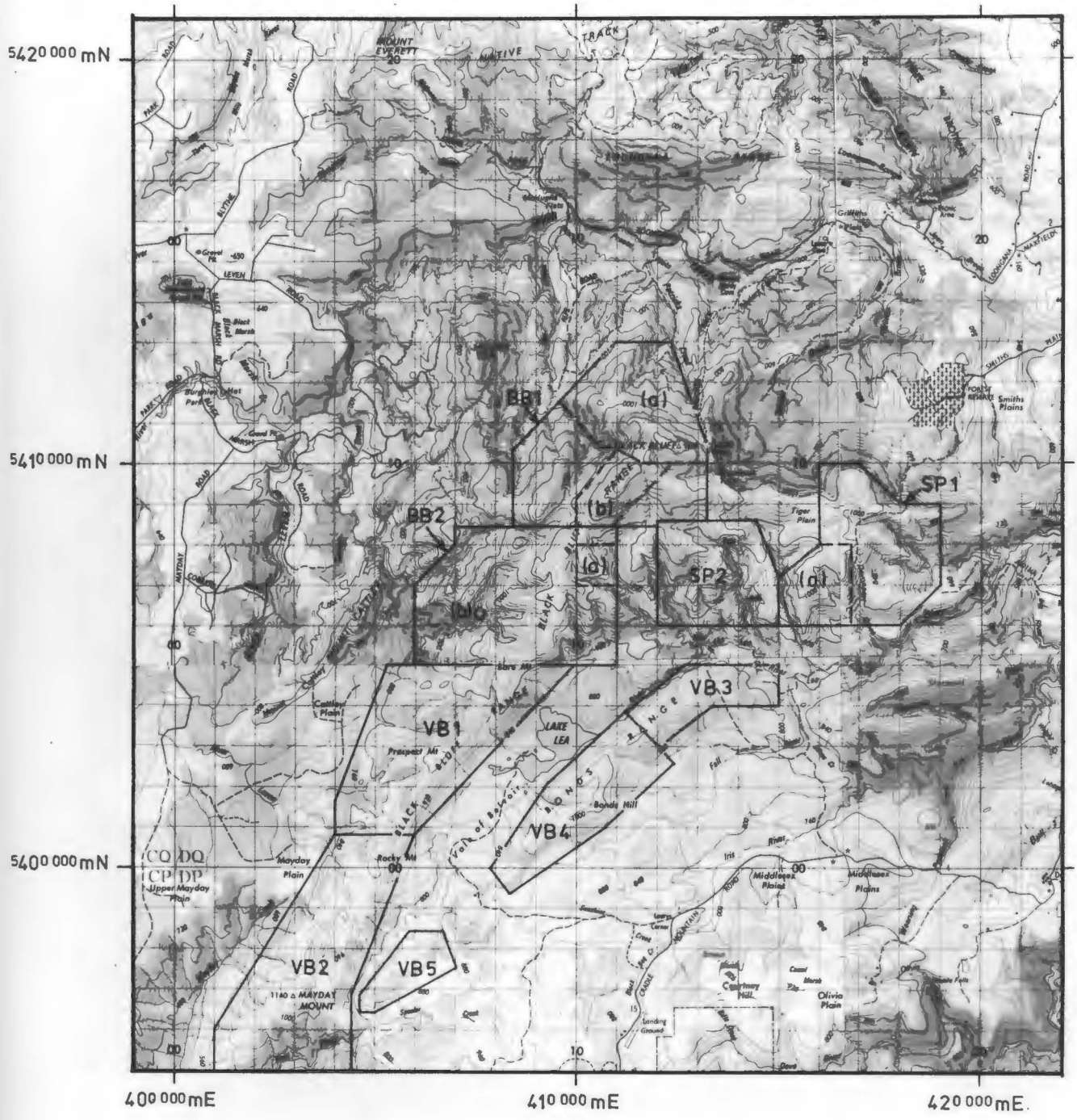
5420 000 mN
5410 000 mN
5400 000 mN
400 000 mE
410 000 mE
420 000 mE
BB1
BB2
SP1
SP2
VB1
VB2
VB3
VB4
VB5
(a)
(b)
(c)
CQ DQ
CP DP
Mayday Plain
Upper Mayday Plain
Smiths Plains
Middlesex Plains
Olivia Plain
Lake Lea
Bonds Hill
Rocky Hill
1140 MAYDAY MOUNT
TN MN
LOCATION OF SUBAREAS
Denison Subgroup strat. equiv.
0
5
km

FIGURE 4.4

simple open, generally upright folding on horizontal to gently plunging hingelines on several different trends, with associated development of steeply dipping axial cleavage. Subdivision on the basis of style groups has generally proved less successful because of very similar style development of most of the phases. Because of the gentle folding on several trends (often producing dome and basin pattern) and the type of cleavage development, it has not always been possible to determine the temporal sequence of development of structures at individual localities. Rather, the structures have been initially grouped as outlined above, and the temporal sequence inferred from information from a number of localities. The symbolism used on the structural maps distinguishes cleavages associated with each of the trend groups, rather than indicating a temporal sequence, e.g. S_1, S_2, etc. (see Fig. 4.5). The latter notation is only used in the text or in figures to indicate the local sequence of development of cleavages in a particular outcrop, rock specimen or thin section. Evidence for the regional temporal sequence is discussed in the text. Correlation with the trend groups of Williams (1978) has been indicated wherever possible.

For consistency with previous mapping practice by the Tasmanian Department of Mines, the follwing symbolism for rock types has been used on the structural maps:-

Tertiary

Tb	Basalt

Ordovician

Og	Limestone stratigraphically equivalent to the Gordon Subgroup
Osc	Siliceous clastics (conglomerates and sandstones) stratigraphically equivalent to the Denison Subgroup

Bedding (facing known or inferred):

vert. horiz. airphoto interp.

Flow banding (lavas):

vert.

Compositional layering (tuffs):

vert.

Minor folds in bedding:

asymm. symm.

Plunge indicated (axis horizontal if no number shown). Asymmetry looking in direction of arrow.

Cleavages:

vert.

West Coast Range/Valentines Peak trend (Williams, 1978)

Belvoir trend

Bonds Range trend

Deloraine/Railton trend (Williams, 1978)

Loongana trend

FIGURE 4.5 STRUCTURAL MAP SYMBOLS

Cambrian

Ɛpv	Stratigraphic equivalents of the Mount Read Volcanics/Dundas Group, pyroclastics and other volcanics dominant
Ɛspv	Stratigraphic equivalents of the Mount Read Volcanics/Dundas Group, sediments dominant, pyroclastics and other volcanics minor
Ɛ	Undifferentiated rocks of probable Cambrian age.

Except for the limestone sequence, this notation is based on probable age only.

All of the stereoplots used to present structural data are lower hemisphere equal-area projections. True north is used as reference for all azimuthal data.

An attempt has been made to standardize rock cleavage nomenclature by utilizing the new morphological classification of Powell (1979), who brought attention to the plethora of often ill-defined terms previously in use. This classification is especially useful because it completely avoids genetic terminology. The subdivisions are as follows:-

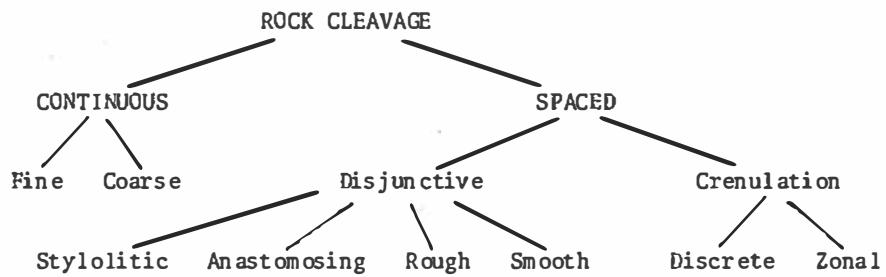

The "disjunctive cleavage" types are illustrated in Fig. 4.6. The only parts of this nomenclature where more detail has sometimes been required is in the description of "stylolitic disjunctive" cleavages which are common in deformed limestones of the Gordon Subgroup stratigraphic equivalent, and of "rough disjunctive" cleavages which occur in the quartzose clastics of the Denison Subgroup stratigraphic equivalent. Alvarez *et al.* (1978) provided a finer subdivision of equivalents of Powell's "stylolitic disjunctive" cleavage in limestones, based on

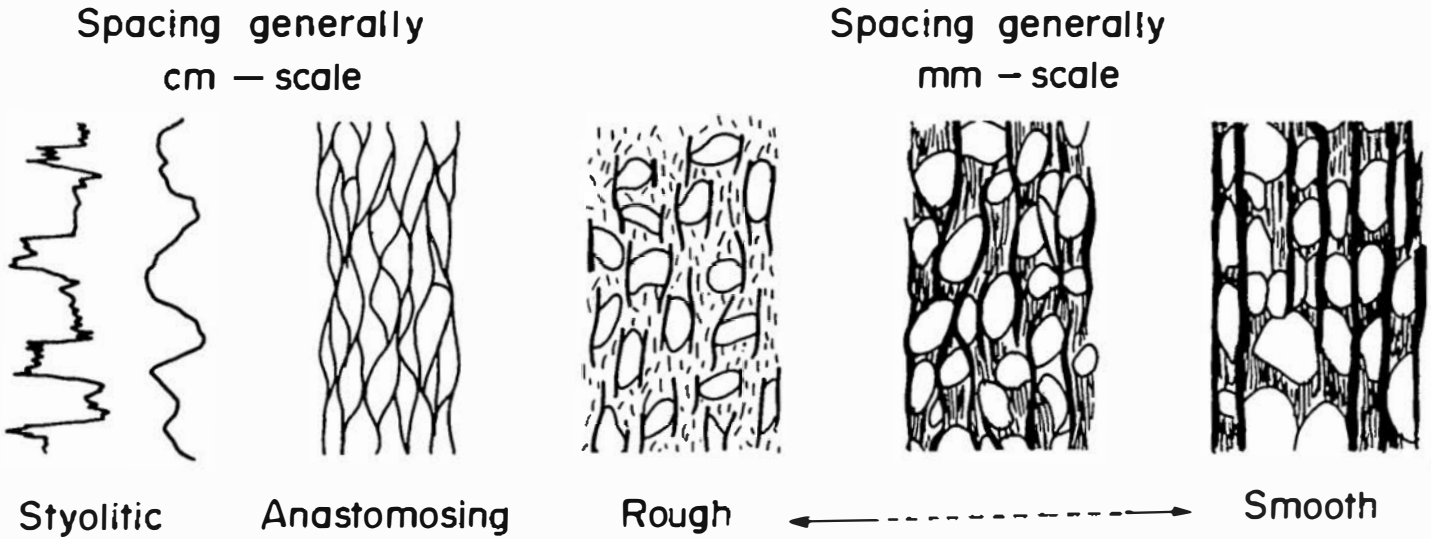

FIGURE 4.6

Cleavage classification scheme of Powell (1979).

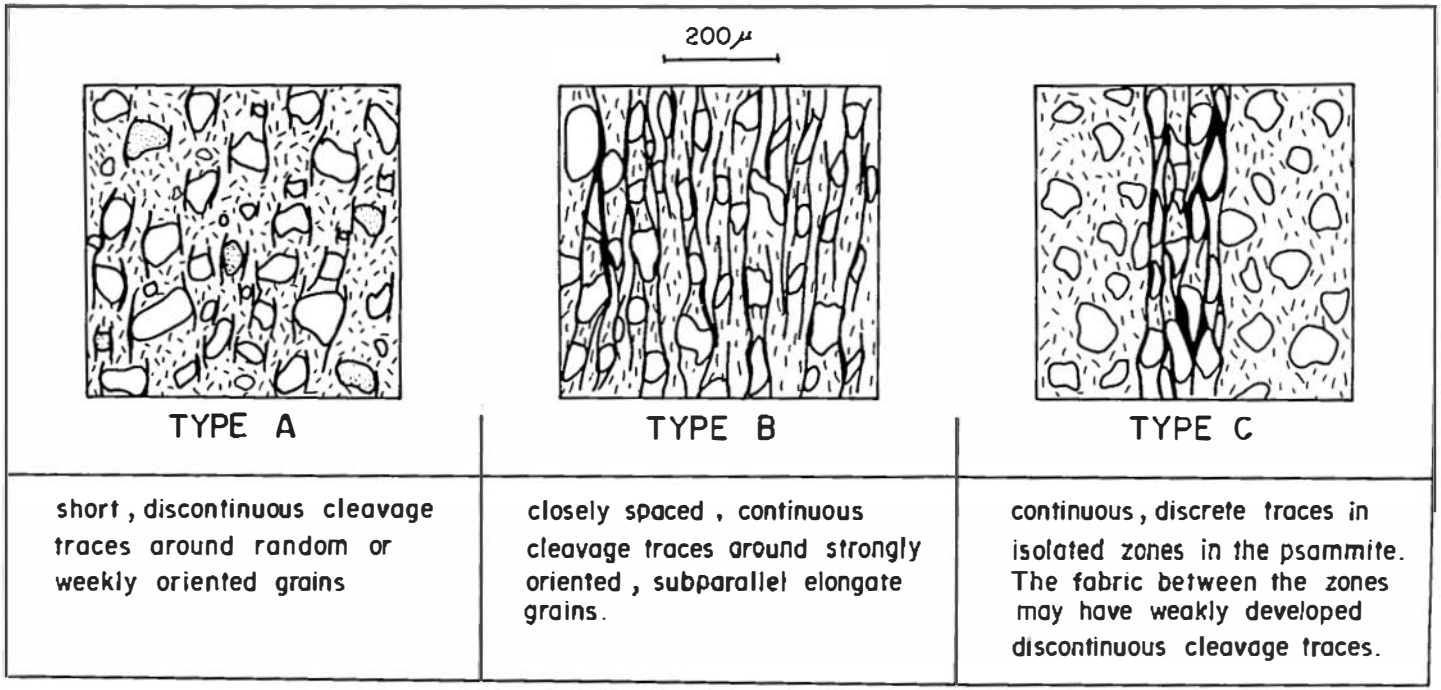

FIGURE 4.7

Types of "rough cleavage" in psammitic rocks defined by Gray (1978).

intensity of development, although they unfortunately used the genctic term "solution cleavage". A more detailed classification of equivalents of Powell's "rough disjunctive" cleavage in deformed psammites was given by Gray (1978), and is illustrated in Fig. 4.7.

Wherever reference is made to the finite strain ellipsoid representing the flattening strain associated with cleavage development, the notation $X \geq Y \geq Z$ is used for the principal axes of the ellipsoid.

4.3 LOONGANA STRUCTURAL MAP

4.3.1 Structure of the Gordon Subgroup stratigraphic equivalent

The main structural feature in the Loongana area is an asymmetric NNE-verging syncline with 3 km half-wavelength and a horizontal WNW-trending axis, in the limestone of the Gordon Subgroup stratigraphic equivalent. This is referred to herein as the "Loongana Syncline". Hughes (1957, p.139) stated that the axis is exactly E-W trending, but detailed mapping has shown this to be some 20° in error (see Fig. 4.8). Convergence of the structure in the limestone with that in the Denison Subgroup stratigraphic equivalent to the south suggests that there is a fault boundary between the two (see Map 2).

The limestone is bounded at its western limit by a major NNW-trending vertical or steeply dipping fault, which has upthrown Mount Read Volcanics/Dundas Group stratigraphic equivalents to the west. This fault was first recognized by Hughes (*ibid.*), and is named herein the "Loongana Fault". It may extend for at least 16 km, from east of Mt. Everett (4092/4200, Fig. 1.2), through Paddy's Lake (4132/4104), to south of the Lea River, between Stormont and the northeast end of Bonds Range (4152/4040). The fault appears to have had considerable dextral strike-slip movement, possibly of the order of 1-2 km, and the swing in strike in the Denison Subgroup stratigraphic equivalent at the

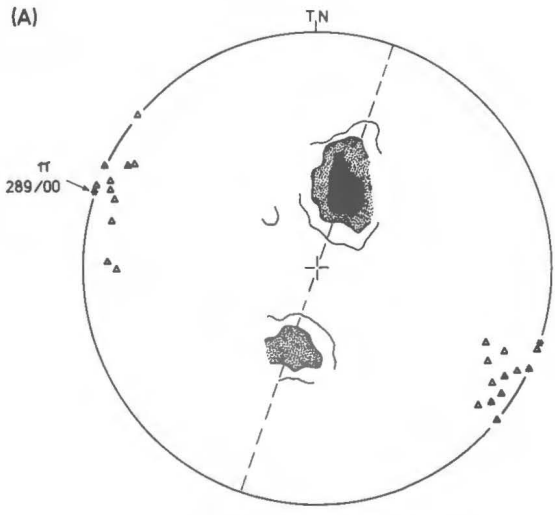

35 poles to bedding
Contours 5, 10, 20% per 1% area
▲ 20 cleavage/bedding int.
(Excludes Taylors Flats area)

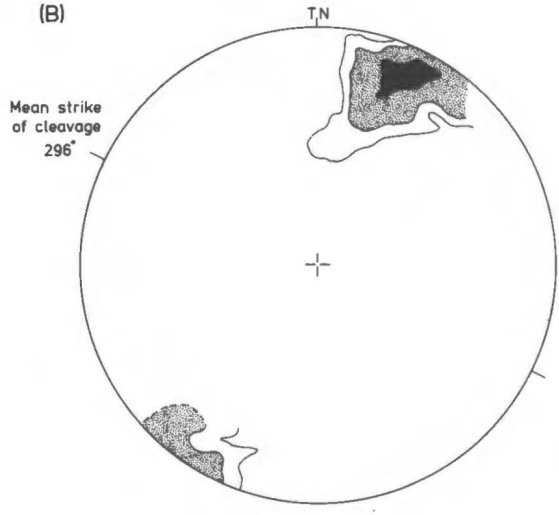

32 poles to cleavage
Contours 5, 10, 20% per 1% area
(Excludes Taylors Flats area)

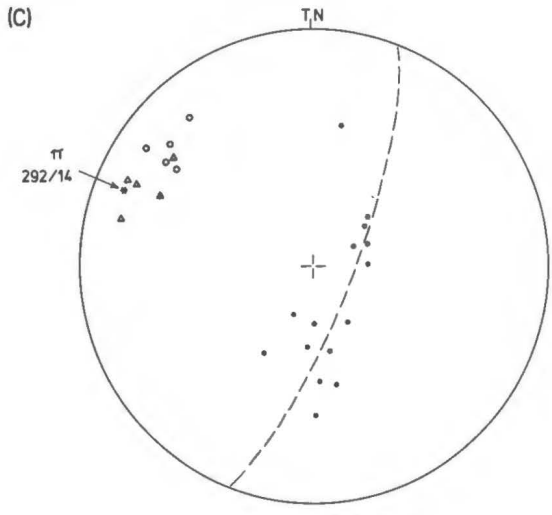

Taylors Flats area
• 15 poles to bedding
▲ 5 cleavage/bedding int.
○ 5 minor fold hingelines

STRUCTURAL DATA

GORDON LIMESTONE S.G.

Loongana area

FIGURE 4.8

western end of the Loongana Range is possible a drag effect of this movement. Substantial vertical movement on the fault is also indicated by the apparently large amount of relative uplift of Mount Read Volcanics/ Dundas Group stratigraphic equivalents to the west. Other smaller faults in the southeast quadrant of Map 2 are apparently similar in sense of vertical movement to the Loongana Fault.

Structural relationships to the west of the Loongana Fault have proven difficult to decipher because of poor outcrop and thick vegetation cover. The faults shown in this area are mainly interpretive, and are associated with an upthrown block of Mount Read Volcanics/Dundas Group stratigraphic equivalents faulted into the core of a NE-plunging syncline south of the Leven River, and with a small isolated downthrown block of limestone of the Gordon Subgroup stratigraphic equivalent to the north of the river.

The relative simplicity of the internal structure of the limestone can be seen in Fig. 4.8. There is a suggestion of slight transection of the synclinal structure by the cleavage, reflected in a small clockwise divergence of the mean strike of cleavage and mean cleavage/bedding intersection from the π-pole (see Fig. 4.8A and 4.8B). The bedding and cleavage plots both reflect the overall NNE-verging asymmetry of the structure, the former reflecting the long SSW-dipping limb (Fig. 4.8A), and the latter showing the dominantly steep SSW-dipping cleavage (Fig. 4.8B). Figure 4.8C is a plot of data from a small area at Taylors Flats (4143/4143), in the hinge zone of the Loongana Syncline, where symmetric second order parasitic folds with half-wavelengths of 100 m are exposed. These data were excluded from the plots in Figs. 4.8A and 4.8B because they indicate a WNW plunge at about 15^{o}. The hinges of small third order parasitic folds exposed across the closure of a second order anticline at Taylors Flats deviate by approximately 18^{o} in trend

clockwise from the π-pole derived from bedding attitudes in the same area.

4.3.2 Minor structures in the Gordon Subgroup stratigraphic equivalent

Tectonic fabric elements in cleaved limestones of the Gordon Subgroup stratigraphic equivalent at Loongana are similar to those recognized in similar lithologies in the Mayberry and Claude Creek areas by Seymour (1975, 1977). They can be subdivided into three groups, various combinations of which produce the overall appearance of cleavage in outcrop or hand specimen:-

(1) Tectonic stylolites

These were described by Seymour (1975) as fairly closely and regularly spaced, somewhat wavy and anastomosing dark seams having a strong preferred orientation close to the overall cleavage attitude. They are distinguished from diagenetic stylolites by the following characteristics:-

	Tectonic stylolites	Diagenetic stylolites
a) Composition:	Never dolomitized	Commonly partially dolomitized
b) Orientation:	Usually at high angles to bedding; parallel or sub-parallel to overall cleavage attitude	Most commonly parallel to bedding (in many cases they actually follow bedding surfaces)
c) Morphology:	Commonly irregularly but smoothly sinuous.	Commonly having sharp small wavelength box-like indentations.

These characteristics are not absolutely definitive, so that in low strain situations where cleavage is at a high angle to bedding, the possibility of mistaken identification of bedding-perpendicular diagenetic stylolites as tectonic features exists, especially if only the plane normal to the cleavage/bedding intersection is examined.

The spacing of tectonic stylolites appears to depend at least partly on strain. Thus, in very low strain examples where the stylolites

are just beginning to appear they tend to have spacings ≥5 cm. In medium strain examples, such as found in the limestone at Loongana, shortening during flattening associated with the cleavage development is of the order of 25-35% (Seymour, 1975; Chapter 5 herein), and spacing of stylolites is mostly in the range 0.5-2 cm. In micritic lithologies at these states of strain, variably developed grain elongation fabrics with preferred orientation parallel to the tectonic stylolites are usually present in the microlithons between the stylolites. At the highest states of strain, such as found in limestones at Claude Creek (430406, Fig. 3.1) and the Vale of Belvoir (407400), shortening during flattening is probably > 60% (Chapter 5 herein), and tectonic stylolites when present are usually much more planar features with spacing ≤ 0.5 cm. In micrites, grain elongation fabrics in the microlithons are very strongly developed at these strain states.

Apart from the lack of dolomitization, tectonic stylolites in the limestone appear to be identical in composition to the diagenetic types, that is, they are 'residue seams' consisting of concentrations of the least soluble components of the bulk rock, namely clays, iron oxides, bituminous matter and quartz. Their dissolution-related origin is evidenced by the frequent observation of fossil fragments which are truncated against them. They are therefore suggested to have a similar mode of origin to that of diagenetic stylolites, in that they formed as a result of dissolution and removal of the more soluble components of the rock under non-hydrostatic stress ("pressure solution", or more correctly, "pressure dissolution", Park and Schot, 1968; Durney, 1972, 1976).

(2) Grain elongation fabrics

Tectonic S-fabrics defined by grain elongation of extremely fine grained calcite in micrites, are almost ubiquitous in the limestones at Loongana. Study in other areas (Seymour, 1975) has indicated that the

first appearance of such fabrics postdates that of tectonic stylolites in the strain history. Thus, at very low strain states (<15% shortening in X), cleavage may be defined by tectonic stylolites alone ("stylolitic disjunctive cleavage" of Powell, 1979), while at medium to high strains both tectonic stylolites and microlithon grain elongation fabrics may be present ("rough" to "smooth disjunctive cleavage" of Powell). Not all cleaved lithologies in the Gordon Subgroup stratigraphic equivalents contain tectonic stylolites, and Seymour (1975, p.54) suggested that the purity of the limestone may be a controlling factor here. Thus, a micrite with a very low or absent insoluble residue component may be expected to develop a tectonite fabric defined only by grain elongation and preferred orientation, without stylolites. Such a fabric would be termed a "fine continuous cleavage" in the classification of Powell (1979).

The very fine grained nature of the micrite fabrics has presented difficulties in interpretation of the deformation mechanism(s) responsible for their development. Seymour (1975, p.54) suggested that pressure dissolution on grain boundaries facing the maximum principal compressive normal stress (σ_1), with diffusion transfer and redeposition on boundaries facing the minimum principal compressive normal stress (σ_3) may have played an important role, in the manner described by Durney (1972, 1976) and Elliott (1973). However, intragranular strain may have also played a part. The extremely small grainsize of these micrites (commonly 2-4 μ) has lead to a more recent suggestion by Seymour (in press), that superplastic flow (Schmid *et al.*, 1977) may have been an important deformation mechanism.

(3) Calcite fibre veins

These are narrow veins up to 5 mm wide, composed of acicular crystals of pure calcite whose long axes are usually at a high angle to the overall trend of the vein. The veins sometimes have overall

trends at a high angle to cleavage, but they more often appear to have been constrained to follow the boundaries between parts of the rock of differing competence, especially between bedding-parallel dolomite layers or diagenetic stylolites and the surrounding micrite matrix. The growth direction of the calcite fibres at each instant of growth has been assumed to be parallel to the long axis of the incremental strain ellipsoid, in the manner of Wickham and Elliott (1970), Durney and Ramsay (1973) and Philips (1974). Three groups of veins have been recognized, based mainly on internal geometry as observed in sections normal to the cleavage/bedding intersection:-

a) Those with overall trends often parallel to bedding, and calcite fibres sub-perpendicular to the walls of the vein. These veins can sometimes be traced around fold closures, and have occasionally developed microfolds, the limbs of which are attenuated and truncated by tectonic stylolites. They are believed to have formed by extension normal to the early layer-parallel shortening, prior to the bulk of the folding and cleavage development.

b) Those having fibres with curved geometry from one side of the vein to the other. Usually the fibre orientation on one side of the vein is parallel to cleavage in the surrounding matrix. They are assumed to preserve a record of the changing relative orientation of the incremental strain ellipsoid during progressive deformation. Thus, curved fibres tend to be common on fold limbs where the progressive strain increments are non-coaxial, while straight fibres are found in hinge zones, where cleavage is perpendicular to bedding. The formation of this type of vein covers a significant fraction of the total strain history.

c) Some veins found on fold limbs have straight fibres which are not perpendicular to the vein walls, but are nevertheless parallel or

sub-parallel to cleavage in the surrounding matrix. These are assumed to have formed late in the strain history, thus not recording a sufficient amount of non-coaxial strain to develop curved fibre geometry.

The formation of the groups of veins a), b) and c) therefore covers a large part of the strain history. Durney (1972) interpreted such veins as the product of the opposite of pressure dissolution, namely reprecipitation in areas of low compressive stress of the soluble components of the rock which had been removed from areas of high compressive stress. It is therefore inferred that "pressure solution processes" (a term used herein to include dissolution, diffusion transfer and reprecipitation under non-hydrostatic stress) operated during the whole strain history associated with cleavage development in limestone of the Gordon Subgroup stratigraphic equivalent.

The comments on vein types a), b) and c) above can also be applied to "beard" structures ("pressure shadows") which formed on those surfaces of large competent grains (e.g. pyrite, quartz) which are at a high angle to the X direction of the finite strain ellipsoid. These are often found in association with the fibre veins.

The only other important tectonic fabric element in the limestone is intragranular strain expressed mainly as twinning and kinking in coarse calcite spar infilling desiccation vugs ("birdseyes") in dismicrites and forming the cement in sparites. The analysis of deformation mechanism maps by White (1976) supports a suggestion that this is a grainsize effect, the coarse spar falling in the field of dislocation creep and dislocation glide, while the fine grained micrite matrix is in the field of pressure solution (or perhaps superplastic flow), at the same conditions of temperature and differential stress.

Most of the deformed limestone at Loongana has well-developed cleavage, with tectonic stylolites with spacing in the range 0.5-2 cm, well developed microlithon grain elongation fabrics and calcite fibre veins all being present. In the more strongly cleaved micrites, well developed grain elongation fabrics are occasionally seen on the cleavage surfaces, their pitch being down the dip. The presence of these indicates that the microlithon fabric is of L-S type in at least some cases, and suggests that the shape of the finite strain ellipsoid more closely approaches that indicative of plane strain than being of purely oblate type.

Some indication of the magnitude of strain associated with the cleavage development in the limestone at Loongana has been obtained from analysis of stromatolites deformed homogeneously with their matrix, from the top of the exposed stratigraphic section at Taylors Flats (4143/4143). Cross-sections of the columnar stromatolites are exposed on a sub-horizontal bedding surface (approximate YZ section of the finite strain ellipsoid) at the closure of a second order upright horizontal symmetric anticline in the hinge zone of the Loongana Syncline. The degree of cleavage development at this locality was judged to be average for the limestone in the Loongana area. Elliott (1970) and Dunnet (1969) plots of axial ratio/orientation data of the stromatolite cross-sections are shown in Fig. 4.9A-C. The reference direction is the cleavage trace in all the plots. Using the assumption that the axial ratio/orientation fabric of the stromatolites in bedding-parallel section in the unstrained state was random, the tectonic strain ratios derived from the two methods are $R_{S_1} = 1.68$ and $R_S = 1.65$ respectively. In the Elliott method, the derivation of R_S involved finding the geometric centre of the contoured plot (Fig. 4.9B), assuming this to be the "initial circle point" (Elliott, 1970) and measuring its distance from the plot origin.

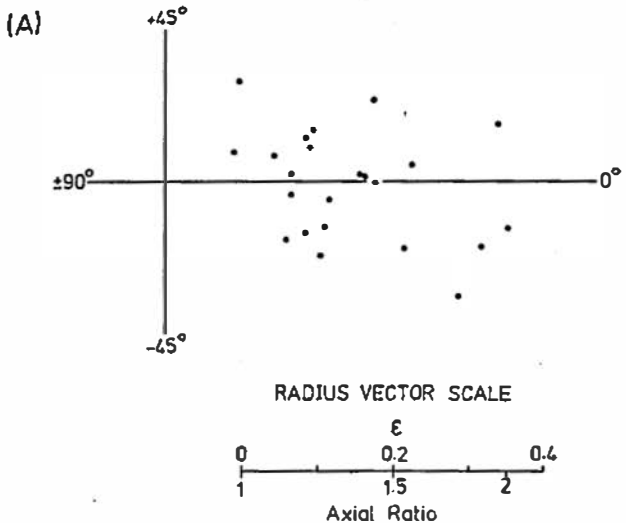

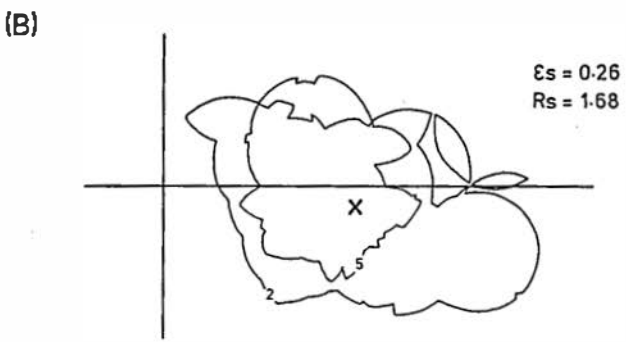

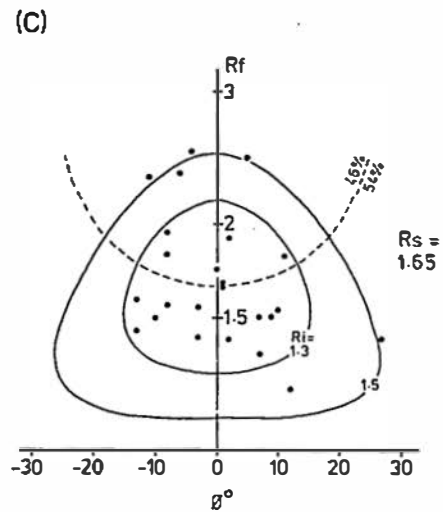

FIGURE 4.9

Elliott, 1970 (A, B) and Dunnet, 1969 (C) plots of axial ratio/orientation data from cross-sections of deformed stromatolites in Gordon Subgroup stratigraphic equivalent, Loongana (4143/4143). Approximate YZ section of finite strain ellipsoid.

In the case of the Dunnet method, the procedure involved fitting of standard curves of constant initial axial ratio (R_i) to the data (solid lines, Fig. 4.9C). A "50% of data" curve is also used, and should have half of the data points above it and half below (dashed line). The precision of the Dunnet method is commonly very good at low to moderate strains, in this case to 0.05 R_s units. Note that the curve fit implies that most of the stromatolite cross-sections in the tectonically unstrained state had axial ratios < 1.3. The data obtained are two-dimensional only, but boundary limits can be calculated for the three-dimensional strain based on assumptions about the shape of the finite strain ellipsoid. The figure R_s = 1.65 has been used, and is assumed to be the strain ratio of the YZ section of the finite strain ellipsoid:-

assumption	X	Y	Z
plane strain (const. vol.)	+65%	0	-39%
pure flattening (const. vol.)	+19%	+19%	-28%
intermediate between plane strain and pure flattening.	+35%	+10%	-33%

4.4 SMITHS PLAINS STRUCTURAL MAP

4.4.1 Structure of the Mount Read Volcanics/Dundas Group stratigraphic equivalent

The main outcrop area of these rocks is a 3-5 km wide approximately E-W trending belt east of Black Bluff (see Fig. 3.1 and Map 3). Structural information from this area is rather sketchy due to limited outcrop, but the available data indicate a relatively simple structure with bedding geometry apparently unrelated to Tabberabberan structures. Bedding mostly dips steeply S or SSE (see Fig. 4.10F) with stratigraphic younging in the same direction. Even where these dip directions are reversed, e.g. near 4192/4102, younging is still to the S or SSE.

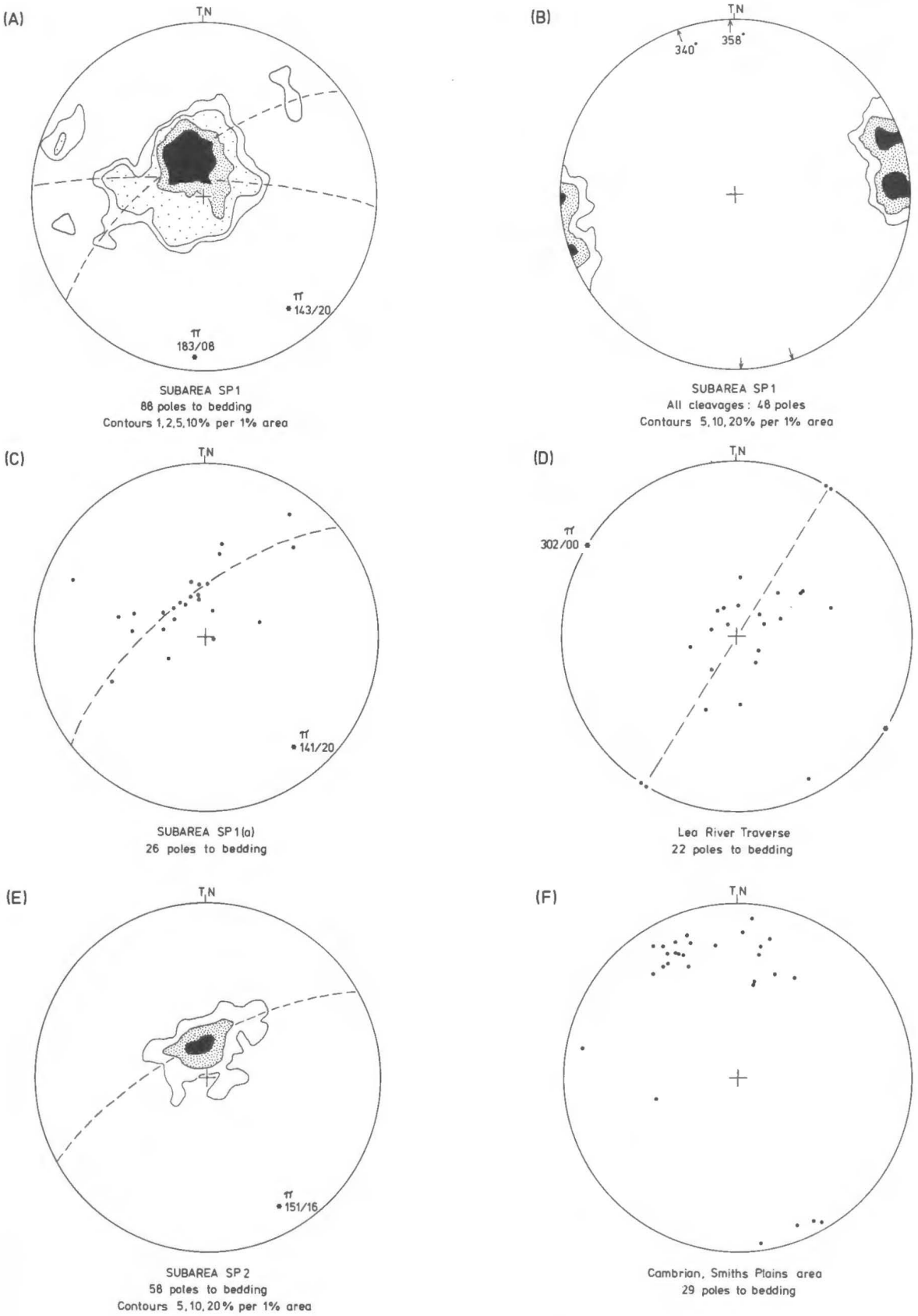

STRUCTURAL DATA

L.Ord. Siliceous Clastics & Cambrian rocks

Smiths Plains map

FIGURE 4.10

Cleavage in the Mount Read Volcanics/Dundas Group stratigraphic equivalents in this area is usually expressed as patchy development of preferred orientation in fine sericite mica in the matrix of altered tuffs and lavas. Cleavages belonging to two generations have been recognized:-

(1) Weakly to moderately developed steeply dipping to vertical N-striking cleavage occurs in altered coarse tuffs and agglomerates near 4195/4120, and in altered andesitic lavas on the Devonport Mine track near 4181/4094. At both of these localities two steeply dipping cleavages are developed, the other being of NW-NNW strike and generally more strongly developed. The N-striking cleavage is earlier, and is correlated with the group of structures of "West Coast Range/Valentines Peak trend" of Williams (1978). Cleavage of similar strike also occurs in the Denison Subgroup stratigraphic equivalent at many localities in the southern part of the Smiths Plains map.

(2) Moderately to strongly developed steeply dipping to vertical cleavage of NW to NNW strike is present in most outcrops of Mount Read Volcanics/Dundas Group stratigraphic equivalents in the Smiths Plains area. Usually this is the only cleavage developed but where the weaker cleavage described in (1) above is also present, the cleavage of NW to NNW strike is later. Cleavage of this strike is also widespread in the Denison Subgroup stratigraphic equivalent on the Smiths Plains map, and it is correlated with the "Deloraine/Railton trend" of Williams (1978). Particular localities where this cleavage can be observed in closely spaced outcrops lying above and below unconformities of Jukesian type are:-

a) near 4180/4088 on the Devonport Mine track 2 km east of Tiger Plain,

b) around the northern boundary of a small 'window' of Mount Read Volcanics/Dundas Group stratigraphic equivalents just south-southwest of Tiger Plain (near 4154/4082),

c) on the crest of a ridge 1.7 km northeast of the summit of Black Bluff (near 4125/4119).

4.4.2 Minor structures in the Mount Read Volcanics/Dundas Group stratigraphic equivalents

Fig. 4.11 illustrates the style of development of two subvertical cleavages in a very strongly altered quartz-felspar porphyry (possibly originally an andesitic lava), from 4180/4094 on the Devonport Mine track. The orientation of the section is horizontal, normal to the intersection of the two cleavages. Both cleavages are defined by somewhat zonal development of preferred orientation of very fine sericitic mica. The sericite almost certainly formed originally as a product of hydrothermal alteration, a considerable time before the onset of the Tabberabberan deformation. Examination of the tectonite fabric defining the first cleavage at high magnification indicates that it formed mainly by recrystallization of this sericite. The zonal nature of the fabric may have been partly controlled by variable sericite content of the rock matrix, due to patchiness of the hydrothermal alteration. The preferred orientations defining the two cleavages are quite critically developed, to the extent that either cleavage can be made virtually invisible in thin section by aligning it with the polarizers. For this reason, two orientations of the thin section with respect to the polarizers were needed to illustrate the two fabrics in Fig. 4.11. Both photomicrographs cover the same field of view, however.

These cleavages do not fit precisely into the classification scheme of Powell (1979). However, they probably most closely approximate to his "rough disjunctive cleavage", and are perhaps transitional between

FIGURE 4.11A and B

Two views of same field of view of horizontal section of cleaved altered quartz-felspar porphyry from Mount Read Volcanics/Dundas Group stratigraphic equivalent, 4180/4094, 3.5 km southwest of Smiths Plains. Two preferred orientations of fine sericite define the two cleavages. S_2 fabric is at extinction in A, S_1 fabric at extinction in B. Specimen UTGD 48380. XPL.

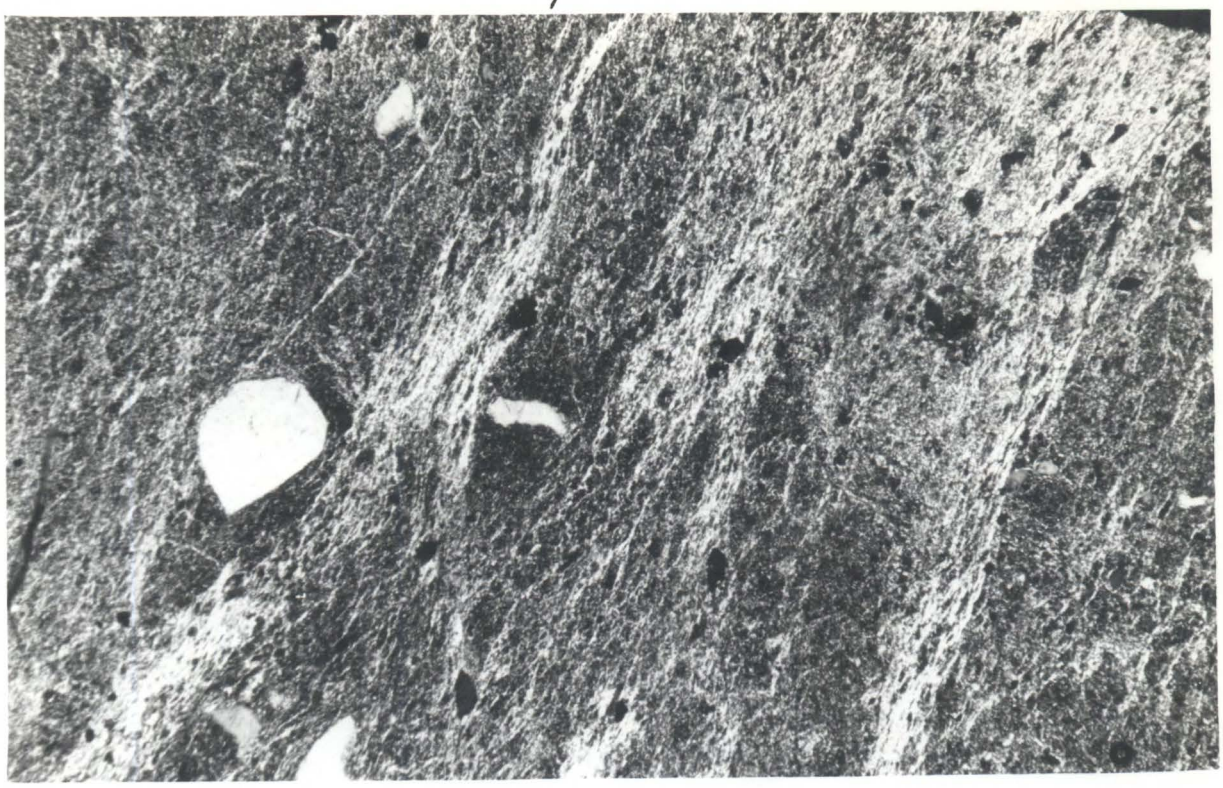

S_1

FIGURE 4.11A

0.5 mm

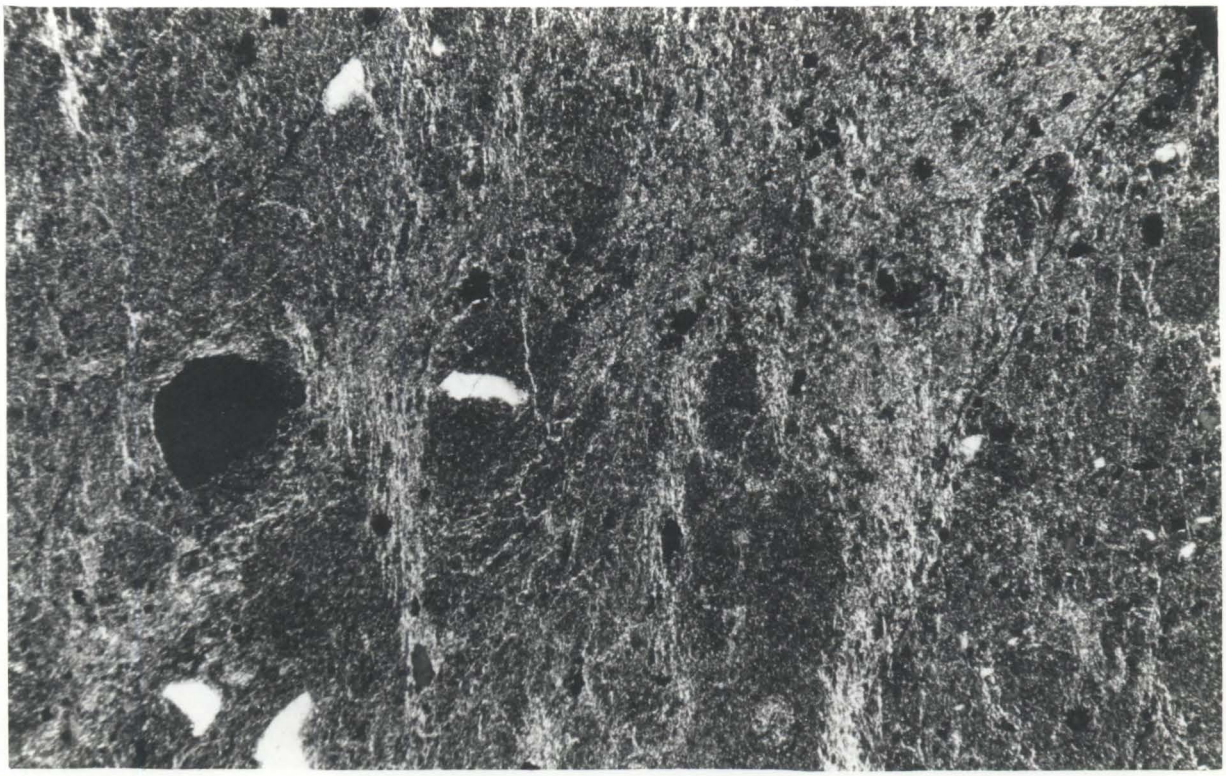

S_2

FIGURE 4.11B

0.5 mm

this and "fine continuous cleavage". Note that the formation of the second cleavage in Fig. 4.11 has produced a slight but noticeable asymmetric crenulation of S_1. The sericite fabric defining S_2 appears to have originated in a similar manner to S_1, i.e. by recrystallization both of pre-existing matrix sericite, and of sericite which had already once been recrystallized during formation of S_1. The latter can be seen particularly in the matrix just to the right of the large quartz phenocryst.

Where two steeply dipping but non-vertical cleavages are present, a small angular difference between them can often be detected on a vertical section bisecting the obtuse angle between their strikes. Such a section is illustrated in Fig. 4.12. This is a strongly cleaved altered volcanic wacke conglomerate or agglomerate from a road cutting at 4195/4121, 1 km west-northwest of Smiths Plains. The pre-tectonic alteration once again appears to have been strongly sericitic. The preferred orientation of fine sericite defining the second cleavage in this rock is very strongly developed, closely approaching a "fine continuous cleavage" of Powell (1979), and the first cleavage is almost obliterated (Fig. 4.12A). However, if S_2 is adjusted to optical extinction under crossed polars, the weak discontinuous traces of the S_1 sericite fabric can be clearly seen at about 30° to S_2 (Fig. 4.12B). Examination of horizontally oriented thin sections of oriented specimens from this locality has shown that S_1 strikes N and S_2 strikes NW-NNW.

In some of the tuffs, particularly those of ashflow origin, a strong pre-tectonic bedding-parallel foliation of compactional origin was apparently present. Where tectonic cleavage has developed obliquely to such a "primary" foliation, the first such cleavage sometimes has a crenulation morphology. An example of such cleavage development is illustrated in Fig. 4.13, which shows a possible ashflow tuff from

FIGURE 4.12A and B

Preferred orientation of fine sericite defining two steeply dipping cleavages in the matrix of an altered volcanic wacke conglomerate or agglomerate in the Mount Read Volcanics/ Dundas Group stratigraphic equivalent, 4195/4121, 1 km west-northwest of Smiths Plains. This section is vertical and bisects the obtuse angle between the cleavage strikes. S_1 is best seen when S_2 is at optical extinction, as in B. Black grains are iron oxides. Both photos cover same field of view. Specimen UTGD 48364. XPL.

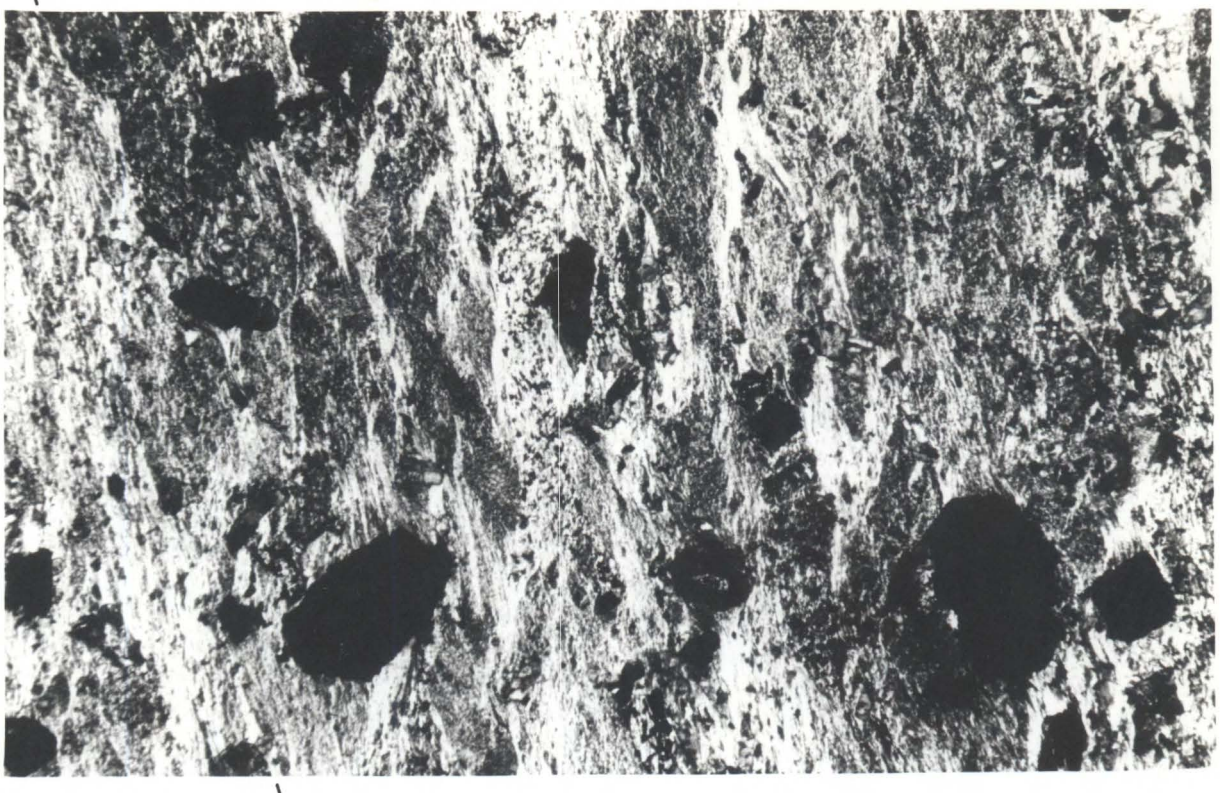

S_2

FIGURE 4.12A

1 mm

S_1

FIGURE 4.12B

1 mm

FIGURE 4.13

Vertical tectonic cleavage crossing steeply dipping bedding foliation in an ashflow tuff at an acute angle, producing asymmetric crenulation morphology. Section is sub-horizontal and shows strikes of S_0 and S_1. Specimen UTGD 48374 from 4196/4103, 1.8 km southwest of Smiths Plains. PPL.

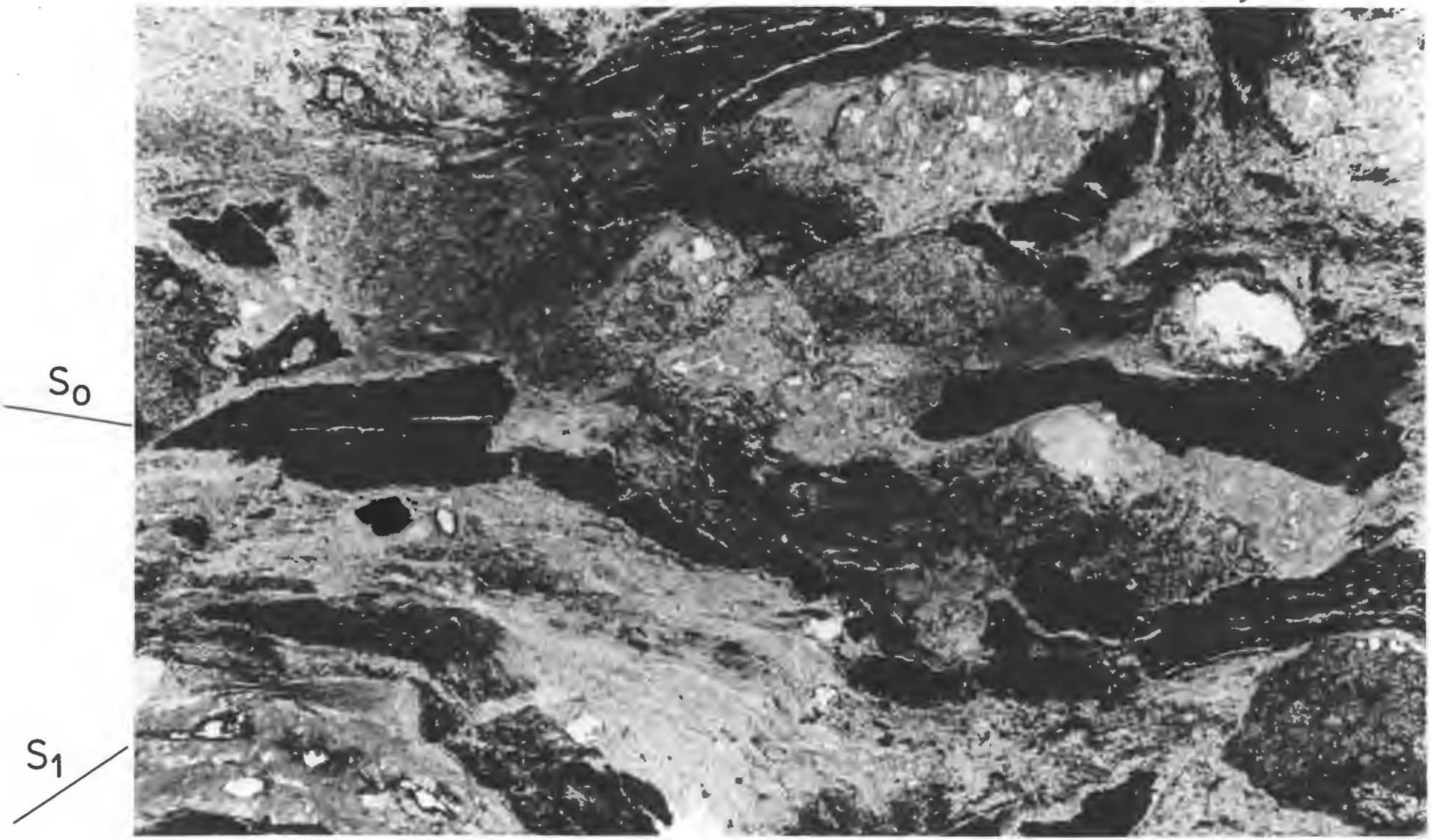

FIGURE 4.13

4196/4103, 1.8 km southwest of Smiths Plains. Notice the flattened pumice fragments present in this rock. The section illustrated has sub-horizontal orientation. The bedding foliation dips at 78° to the SSE, and the vertical cleavage crosses it with WNW strike. This cleavage has been correlated with the "Deloriane/Railton trend" of Williams (1978). The crenulation of the bedding foliation is clearly seen in Fig. 4.13. The cleavage is also accompanied by a patchily developed preferred orientation of fine sericitic mica both in the matrix and in the pumice fragments.

In some crystal tuffs, the pre-tectonic alteration caused complete sericitization of felspar phenocrysts. During the tectonic deformation these have often selectively absorbed the strain, resulting in strongly developed preferred orientation of fine sericite within the altered phenocrysts. This fabric is usually constant in orientation from phenocryst to phenocryst, such that when observed in thin section they all go to optical extinction together between crossed polars. A typical example is shown in Fig. 4.14, which is a vertical section perpendicular to the dominant cleavage in a crystal lithic tuff from 4195/4121, 1 km west-northwest of Smiths Plains. The sericite fabric, which parallels the long dimension of the altered phenocryst, is set at 45° to the polarizing directions, so that the interference colours are at their brightest.

Apart from the fine mica preferred orientation described above, other tectonic fabric elements present in deformed Mount Read Volcanics/ Dundas Group stratigraphic equivalents in the Smiths Plains area include tectonic stylolites and "mica beards" (e.g. Williams, 1972; Powell, 1969, 1977) on crystals and lithic fragments in tuffs. These mostly occur as roughly triangular areas projecting from the ends of grains, and are best seen in vertical sections normal to cleavage. The mica within the beards generally has an overall preferred orientation of

FIGURE 4.14

Well developed cleavage-parallel preferred orientation of fine sericite in a completely altered felspar phenocryst which has selectively absorbed the strain in a deformed crystal lithic tuff in the Mount Read Volcanics/Dundas Group stratigraphic equivalent at 4195/4121, 1 km west-northwest of Smiths Plains. Section is vertical and normal to dominant cleavage. Polarizers adjusted so that interference colours in the mica are at their brightest.
Specimen UTGD 48365. XPL.

S_1

FIGURE 4.14

0.2 mm

FIGURE 4.15

A. Preferred orientation of chlorite in "beards" on ends of a felspar phenocryst, and also infilling a fracture along the crystal cleavage of the phenocryst, in an altered lithic crystal tuff in the Mount Read Volcanics/Dundas Group stratigraphic equivalent, 4187/4128, 2 km west-northwest of Smiths Plains. Section vertical and normal to single weakly developed vertical cleavage. Chlorite preferred orientation parallel to cleavage trace.
Specimen UTGD 48372. PPL.

B. Same rock as in A but section vertical and parallel to cleavage, showing chlorite beard on a lithic fragment composed of metaquartzite. Preferred orientation of chlorite in beard pitches at 90^{o} in cleavage. PPL.

S_1

FIGURE 4.15A

0.25 mm

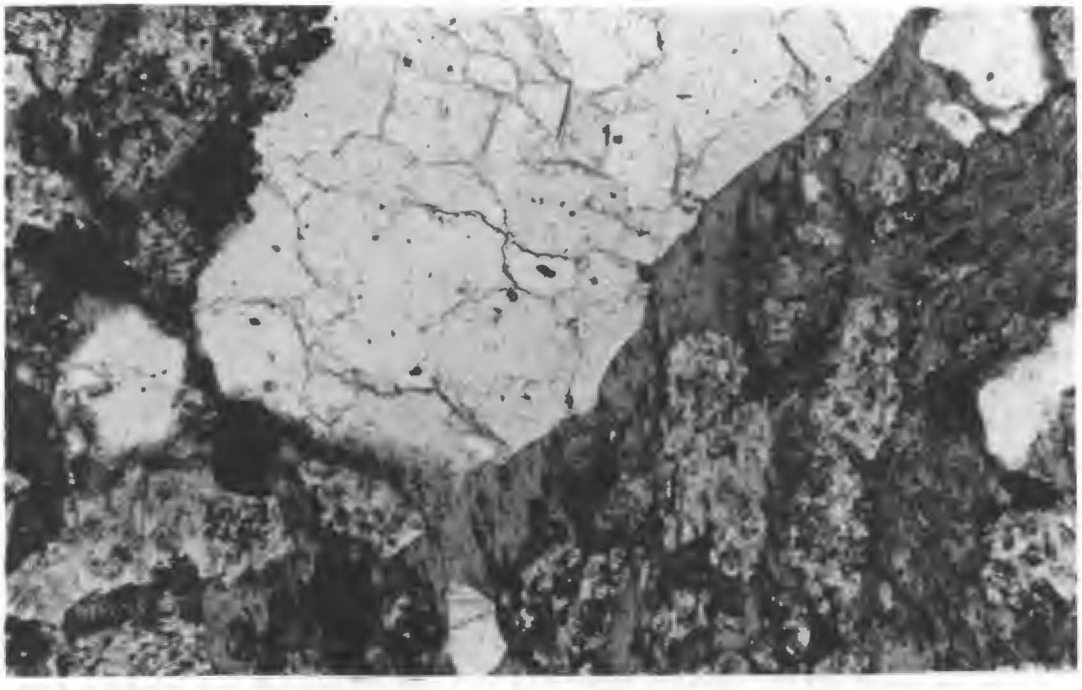

FIGURE 4.15B

0.25 mm

{001} traces parallel to the cleavage trace; in fact, when the beards are strongly developed they may be the main fabric element responsible for the appearance of cleavage in outcrop and hand specimen. The beards apparently formed mainly on surfaces inclined at a moderate to high angle to cleavage.

Fig. 4.15 shows chlorite beards in an altered lithic (felspar > quartz) crystal tuff with a single weakly developed vertical cleavage of NW-NNW strike, from a quarry at 4187/4128, 2 km west-northwest of Smiths Plains. This rock has a strong chloritic matrix alteration which was presumably pre-tectonic in origin, as much of the chlorite does not have a tectonite fabric. Examination of their fine structure has indicated that the beards which occur on the ends of grains formed by *in situ recrystallization* of the matrix chlorite. Boulter (1977) suggested a similar mode of origin for quartz-mica beards in Precambrian quartz arenites of the Burnie Formation (part of the Rocky Cape Geanticline) in northwest Tasmania. He interpreted these as having formed by recrystallization of diagenetic overgrowths. However, this mechanism may not be sufficient to explain the formation of all of the beard mica. Thus, in Fig. 4.15A, a felspar phenocryst appears to have suffered brittle fracture along a crystal cleavage, the opening fracture being filled with chlorite oriented similarly to that in the beards on the ends of the grains. This fracture infill presumably could not have originated by recrystallization, but rather must have required stress-controlled diffusion and precipitation of chlorite from solution.

4.4.3 Structure of the Denison Subgroup stratigraphic equivalent

This description is subdivided according to the coverage of two main subareas, SP1 and SP2, shown on Fig. 4.4.

(1) Subarea SP1

Examination of the bedding plot of Fig. 4.10A in conjunction with the structural map indicates that the dominant structure in this subarea is a major fold limb dipping at about 20° to the SSE, defined by the area within the central 10% contour on the bedding plot. This simple structure appears to have been complicated by refolding on N and NW trends, producing upright gently S and SE-plunging folds. The spread defined by the lower value contours in Fig. 4.10A has been interpreted in this way (shown by dashed great circles), although the characteristics of this pattern are not very definitive. Shallowly SE-plunging folding is more obviously indicated by a plot of bedding data from a smaller subarea, SP1(a), within subarea SP1 (see Fig. 4.10C, and Fig. 4.4 for coverage). The plot in Fig. 4.10D is of bedding data taken from the Tasmanian Department of Mines 1:63,360 Sheffield geological map sheet, on a traverse of the section of the Lea River which appears in the south-east corner of the Smiths Plains map. The data are a little thin, but folding on horizontal approximately WNW trending axes is indicated.

Cleavage development in the Denison Subgroup stratigraphic equivalent on the Smiths Plains map is patchy, dependent mainly on the presence of favourable lithologies. At most outcrops cleavage is either absent, or only a single cleavage is developed. Nevertheless, a plot of all cleavage readings in subarea SP1 indicates the presence of steeply dipping to vertical cleavages striking in two distinct directions, N and NNW (see Fig. 4.10B). These directions are parallel to strikes of the two definite cleavages recognized in the Mount Read Volcanics/Dundas Group stratigraphic equivalents to the north, discussed in the previous section.

Unfortunately, however, both cleavages in the Denison Subgroup stratigraphic equivalent are similar in style of development to the "stylolitic disjunctive" or "rough disjunctive" types of Powell (1979).

When two steeply dipping to vertical cleavages of this type occur together with an acute angle between their strikes, the effect produced as seen in the horizontal plane can be similar in appearance to the "anastomosing disjunctive" type of Powell. In such cases the possibility arises of erroneous visual averaging of the strikes of two cleavages which should have been measured as two separate features. Such errors may have lead to an artificially close grouping and overlap between the two modes in Fig. 4.10B. The problem is particularly pronounced in the coarse conglomerates, as even a single disjunctive cleavage will anastomose around the pebbles. Nevertheless, there are some localities in subarea SP1 where two definite cleavages, of N and NNW strike respectively, have been measured at a single outcrop. The best examples are near 4172/4082 and 4175/4068 (see Map 3). For this reason, the two modes which appear on the stereoplot (Fig. 4.10B) are assumed to represent two separate generations of cleavage, correlated respectively with the "West Coast Range/Valentines Peak trend" (N) and "Deloraine/ Railton trend" (NW-NNW) of Williams (1978).

(2) Subarea SP2

The bedding plot (Fig. 4.10E) reflects the dominant folding on gently SSE-plunging axes in this subarea. As was the case with subarea SP1, this pattern is suggested to have resulted from refolding on NNW axes of a major fold limb dipping gently to between S and SSE. Effects of folding about N-trending axes are not obvious on this plot. However, steeply dipping to vertical cleavages with two distinct strikes (N and NW-NNW respectively) are again present. Minor folds with hinges approximately parallel to these two trends are present between 4128/4082 and 4140/4080 in the southwest corner of the map.

4.4.4 Minor structures in the Denison Subgroup stratigraphic equivalent

As seen in outcrop, cleavage in the quartz arenites and quartz wackes is often defined mostly by spaced, anastomosing cleavage domains with spacings of 0.5-2 cm, oriented at a high angle to bedding. In some cases the appearance in the horizontal plane is similar to the "anastomosing disjunctive" type of Powell (1979), but, as noted in the previous section, care must be taken to determine whether or not this is actually due to the presence of two steeply dipping cleavages with an acute angle between their strikes. In thin section the domains appear as more or less discrete narrow belts up to 0.5 mm wide, with lower modal quartz than the interdomain areas, and consisting of bunches of discontinuous to semicontinuous dark seams which anastomose around and truncate quartz grains, the latter having cuspate shapes indicative of pressure dissolution on their cleavage-parallel edges. The seams appear to consist of concentrations of opaque iron oxides and fine matrix mica.

A cross-section of a typical cleavage domain is illustrated in Fig. 4.16A and B. This is a horizontal section at a low angle to bedding and normal to the dominant cleavage (in this case a vertical cleavage of NNW strike). The rock is an argillaceous quartz wacke with abundant bedding-perpendicular worm burrows. Two separate distinct cleavages (of N and NNW strike, respectively) were recognized at this outcrop, but within the fields of view covered by Fig. 4.16A and B, the cleavage of NNW strike is dominant. The few short seams trending from lower left to upper right in the bottom left-hand corner of Fig. 4.16A may be a partial expression of the other cleavage. A cross-section of a bedding-perpendicular worm burrow occupies the central part of Fig. 4.16B, and the cleavage domain is widened and enhanced where it crosses the burrow. This may be related to the observation that the pre-cleavage matrix:grain ratio was probably higher within the burrow. Fig. 4.16B illustrates

FIGURE 4.16

A. Cross-section of a cleavage domain in a worm-burrowed argillaceous quartz wacke from 4169/4075, near Devonport Mine. Horizontal section normal to cleavage and at a low angle to bedding. A flattened cross-section of a worm burrow occupies the central part of the photo. Trace of dominant cleavage runs left to right. Specimen UTGD 48402. PPL.

B. Enlargement of area outlined in A, above. PPL.

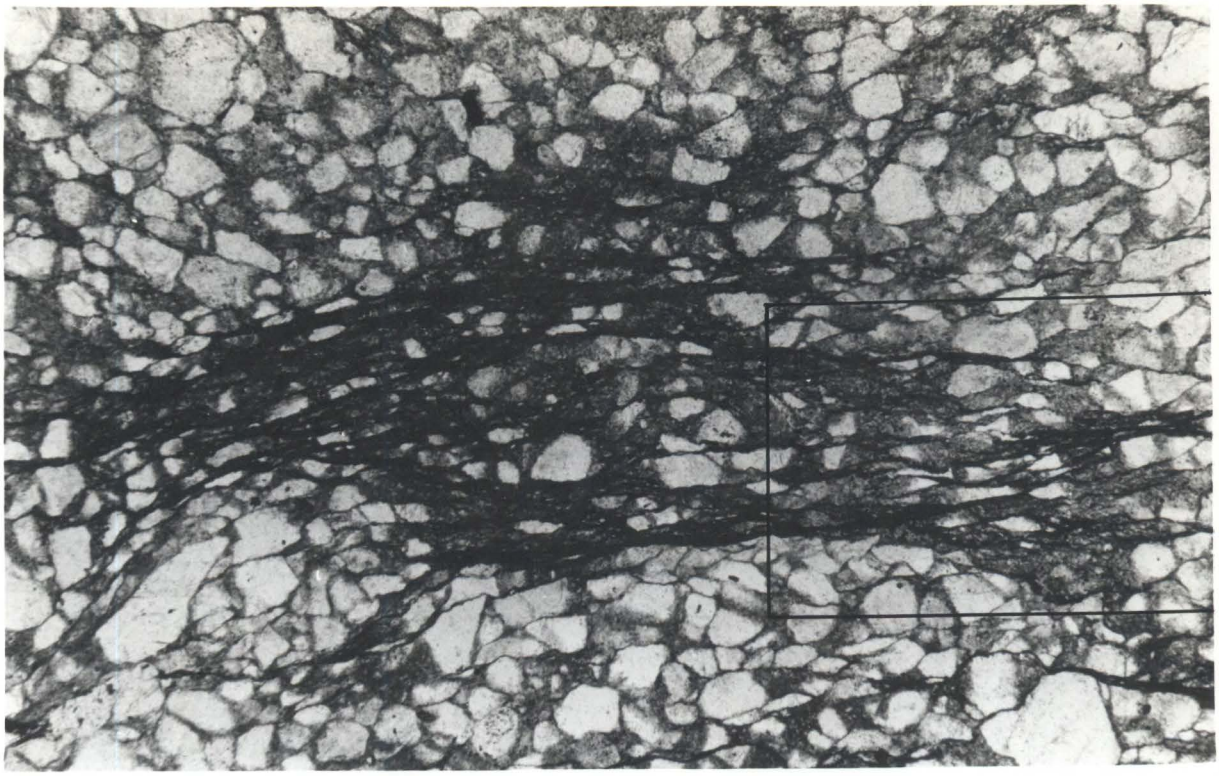

FIGURE 4.16A

0.5 mm

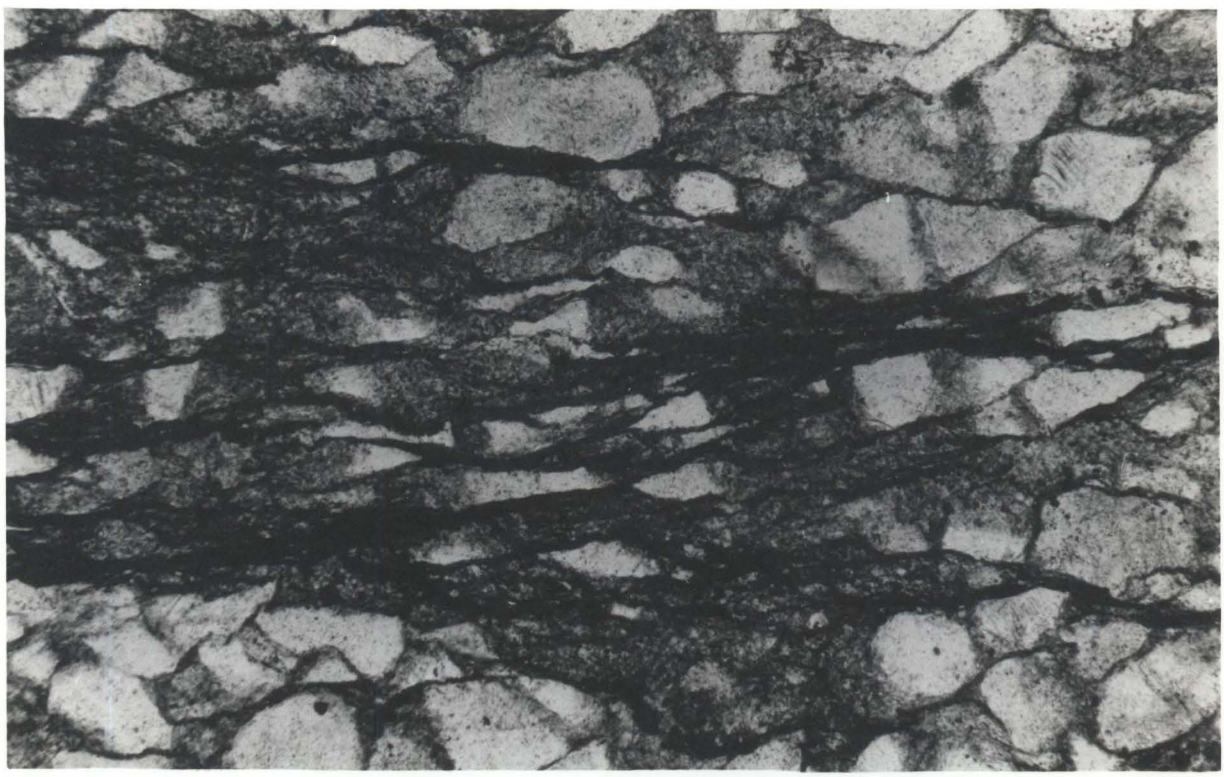

FIGURE 4.16B

0.25 mm

clearly the effects of pressure dissolution on quartz grains within the cleavage domain.

In some cases the cleavage is defined solely by the domains described above. However, particularly in the more strongly cleaved and/or more argillaceous rocks, a variably developed tectonite fabric is also present in the microlithons between the domains. This fabric is best seen on vertical sections normal to the cleavage, and is defined mostly by preferred orientation of fine matrix mica, but also by elongation of quartz grains (Fig. 4.17). The latter may be a result of pressure dissolution on cleavage-parallel edges, passive rotation and intragranular strain, in suggested order of decreasing relative importance.

The type of cleavage development described in the preceding paragraphs does not fit exactly into the classification scheme of Powell (1979), although the total fabric probably approximates to "rough disjunctive" cleavage, perhaps with more pronounced development of more widely spaced domains. It is much closer in appearance to the "type C rough cleavage" of Gray (1978) (see Fig. 4.7 herein). Remarkably similar cleavage development was reported by Geiser (1974) in a similar lithology (burrowed quartz arenite) in the Bloomsburg Formation in the folded Appalachian Mountains. Other examples of similar cleavages in quartz arenites were figured by Beach (1974, Fig. 1; 1977, Fig. 12) and Nickelsen (1979, Plate 3). All of these authors rated pressure dissolution of quartz as a major process in the formation of the cleavage domains.

In the lithic wacke conglomerates of Lithofacies I occupying the basal parts of the Denison Subgroup stratigraphic equivalent in places, tectonic strain has sometimes been selectively absorbed by the incompetent lithic fragments, which now appear to be wrapped around and squeezed

FIGURE 4.17

Detail of tectonite fabric in microlithons between the main cleavage domains shown in Fig. 4.16. Vertical section normal to dominant cleavage, the trace of which runs left to right in photo.
Specimen UTGD 48402. XPL.

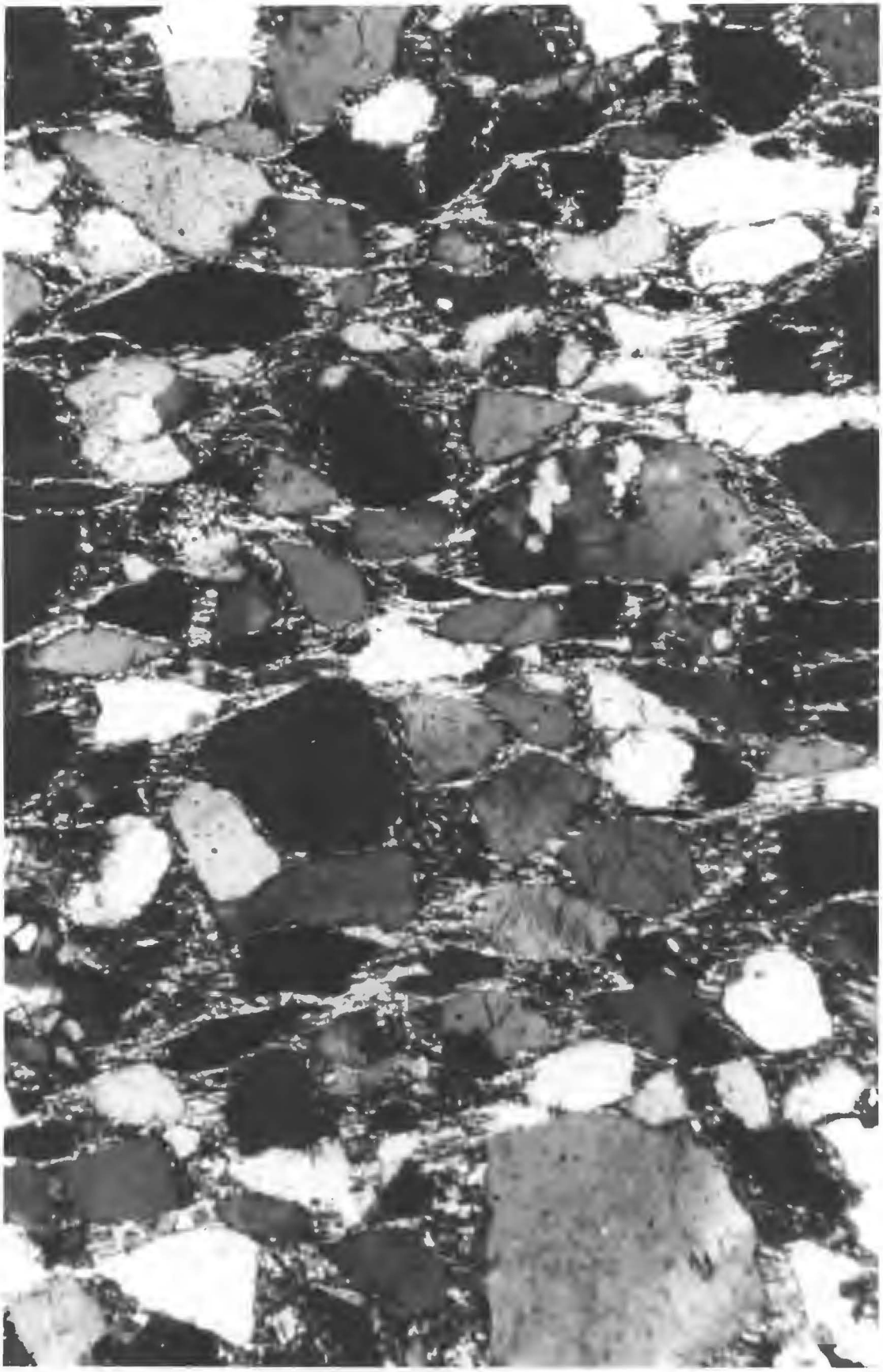

FIGURE 4.17

0.2 mm

FIGURE 4.18

A. Inhomogeneous strain selectively absorbed by the less competent lithic clasts in a lithic wacke fine conglomerate. Quartzose clasts show relatively little internal strain but quartz-hematite-(minor mica) beards have formed on their ends. Vertical section normal to cleavage, trace of which runs left to right. Specimen UTGD 48403. PPL.

B. Detail of quartz-hematite-(minor mica) beard on large quartzose clast. Same section as in A, above. PPL.

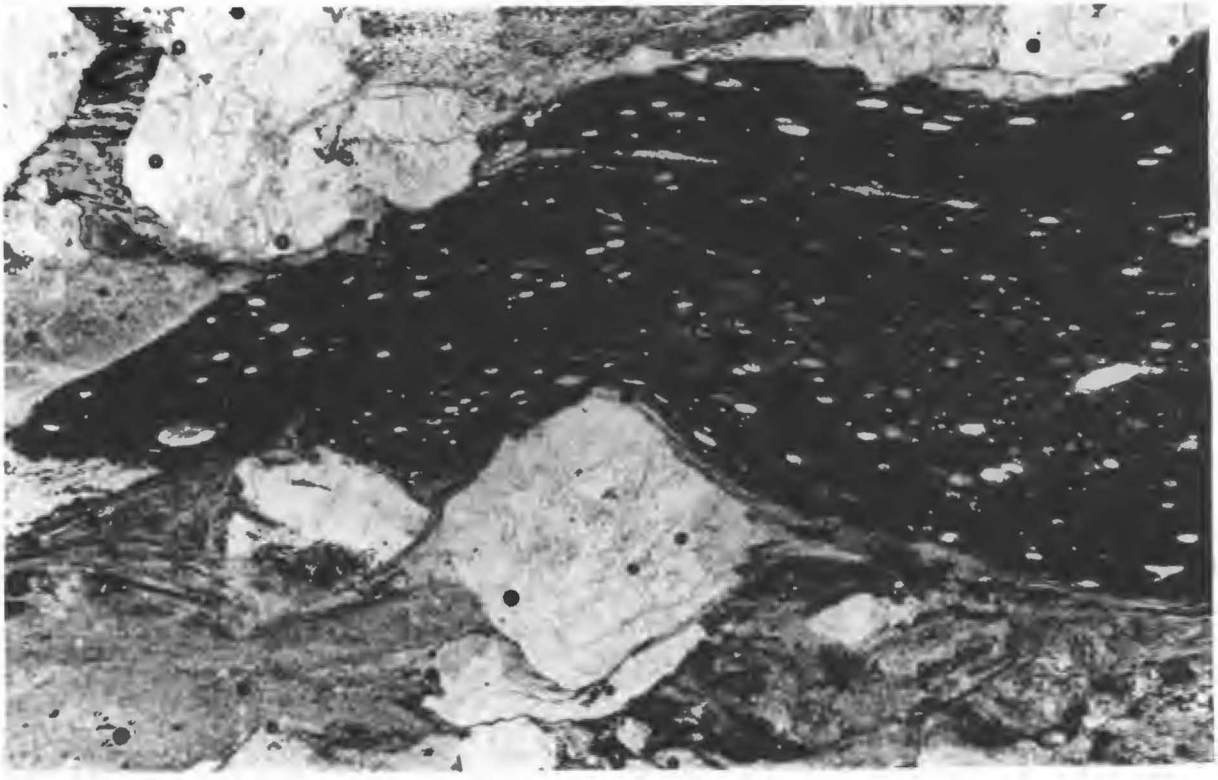

FIGURE 4.18A

0.5 mm

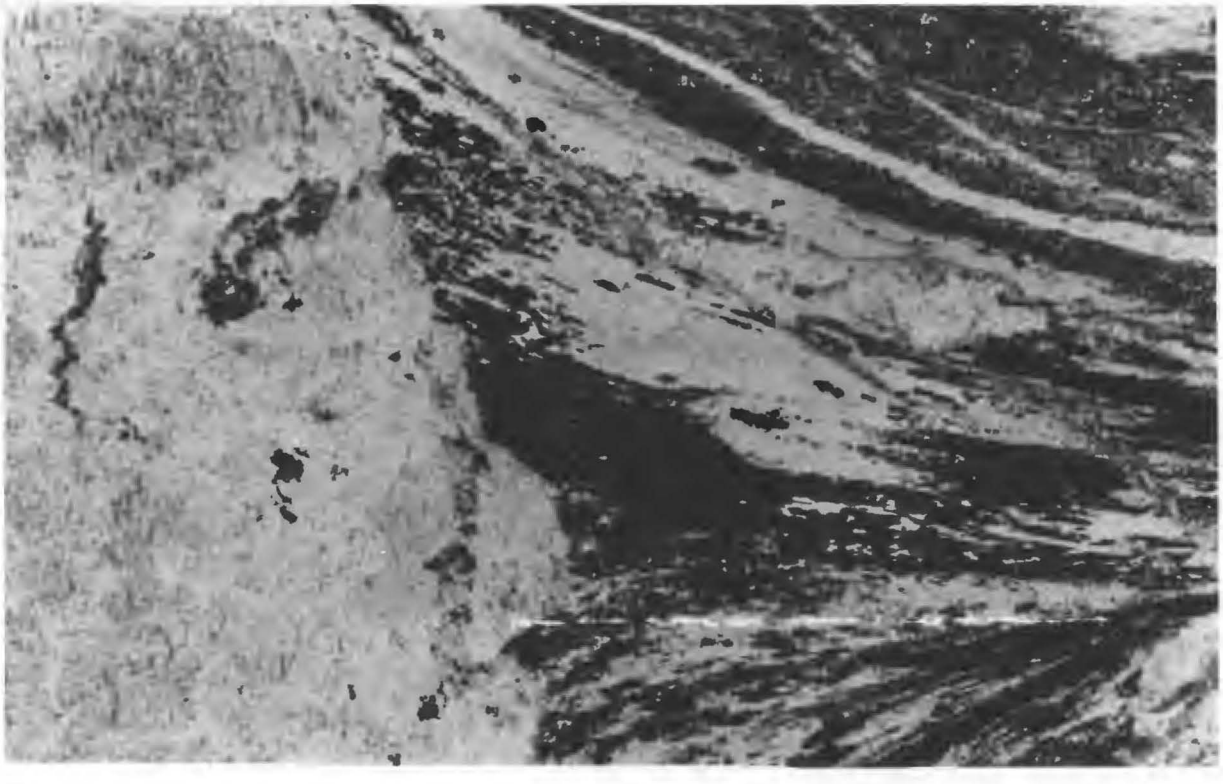

FIGURE 4.18B

0.25 mm

between the more rigid quartz clasts. An example is illustrated in Fig. 4.18A. Where the lithic fragments are argillaceous, they have often developed a strong internal preferred orientation of fine mica parallel to the overall rock cleavage. The quartz clasts, on the other hand, usually display little apparent internal strain effects but have well developed triangular shaped beard structures formed on their top and bottom ends (as viewed on a vertical section normal to steeply dipping cleavage). Hematite in the rock matrix has apparently been involved along with quartz and (minor) mica in the formation of the beards visible in Fig. 4.18A and illustrated at higher magnification in Fig. 4.18B.

4.5 BLACK BLUFF STRUCTURAL MAP

4.5.1 Structure of the Mount Read Volcanics/Dundas Group stratigraphic equivalent

These rocks occupy three main outcrop areas on the Black Bluff map (See Map 4):-

(1) A roughly triangular shaped area approximately 1 km north of the summit of Black Bluff, which is bounded at its eastern edge by the major NNW-trending Loongana Fault, discussed in Section 4.3 herein. No detailed mapping has been carried out in this area.

(2) A downthrown fault block apparently occupying the core of a gently N-NNE plunging open upright syncline in the vicinity of 4100/4125 at the central northern boundary of the map. Two vertical cleavages, of N and NNW strike respectively, are expressed as preferred orientations of fine sericitic mica in the matrix of lithic wackes near 4078/4126. The cleavage of NNW strike is later (see specimen UTGD 48407).

(3) The large area to the west and southwest of Mt. Tor. The stratigraphy of this area was discussed in Section 3.2.3 herein. The available bedding information is consistent with a moderately to steeply SE-dipping and younging sequence apparently unrelated to Tabberabberan structures. However, a steeply dipping to vertical N-striking cleavage is present at most outcrops, and is correlated with the "West Coast Range/Valentine Peak trend" of Williams (1978). In the vicinity of 4059/4106, this cleavage crenulates an earlier cleavage which strikes NE and dips steeply SE, sub-parallel to layering in interlayed thin bedded quartz-felspar crystal tuffs and mudstones (see specimen UTGD 48409 and UTGD 48415). This earlier cleavage is correlated with a group of NE-trending Tabberabberan structures which dominate the Vale of Belvoir (North) and (South) maps and are also evident in the southern half of the Black Bluff map. These structures are referred to herein as the "Belvoir trend". They were not recognized as a separate distinct set by Williams (1978), who in fact grouped them together with the "West Coast Range/Valentines Peak trend".

The only other structures in this area are minor folds with SE-plunging axes near the bridge over the Leven River at 4044/4122, and at 4050/4111, and steeply dipping cleavage of the same strike at 4060/4122. The relative age of these structures is uncertain, but they may possibly be correlated with the "Deloraine/Railton trend" of Williams (1978). They are parallel to strikes of steeply dipping faults which offset the basal surface of the Denison Subgroup stratigraphic equivalent south-southwest of Mt. Tor. Possible drag effects around 4090/4052 indicate sinistral strike-slip movement on these faults.

4.5.2 Structure of the Denison Subgroup stratigraphic equivalent

Discussion in this section mainly concerns two subareas, BB1 and BB2, coverage of which is shown on Fig. 4.4. Lack of time has precluded detailed mapping of the Denison Subgroup stratigraphic equivalent west of these subareas, and the structure of the unmapped area has been interpreted from aerial photographs.

(1) Subarea BB1

The plot of bedding data for the whole subarea (Fig. 4.19A) indicates that the dominant feature is folding on gently SW-plunging axes. Examination of Map 4 confirms the presence of open upright folds on this trend, with half-wavelengths of the order of 1-2 km, although photo interpretation of the area immediately northwest of subarea BB1 has indicated fold plunge to the NE. This folding is correlated with the "Belvoir trend" of this study. However, the pattern in Fig. 4.19A also suggests the presence of folding on axes which plunge gently to between SE and SSE. This is confirmed by a plot of bedding data from a smaller subarea, BB1(b), within subarea BB1 (see Fig. 4.19C, and Fig. 4.4 for areal coverage). Folding on this trend is correlated with the "Deloraine/Railton trend" of Williams (1978). Fig. 4.19B is a plot of bedding data from another smaller subarea, BB1(a), which covers approximately the northern half of BB1. The pattern is similar to that in Fig. 4.19A, except that there is some indication of folding on approximately S-trending axes. The latter is correlated with the "West Coast Range/Valentines Peak trend" of Williams (1978).

The most commonly developed cleavage in subarea BB1 is steeply dipping to vertical and strikes N (see Map 4). Minor upright horizontal folding on the same trend is present in thin bedded quartz arenites at 4119/4107, at the northwest end of the summit ridge of Black Bluff. This cleavage is also correlated with the "West Coast Range/Valentines

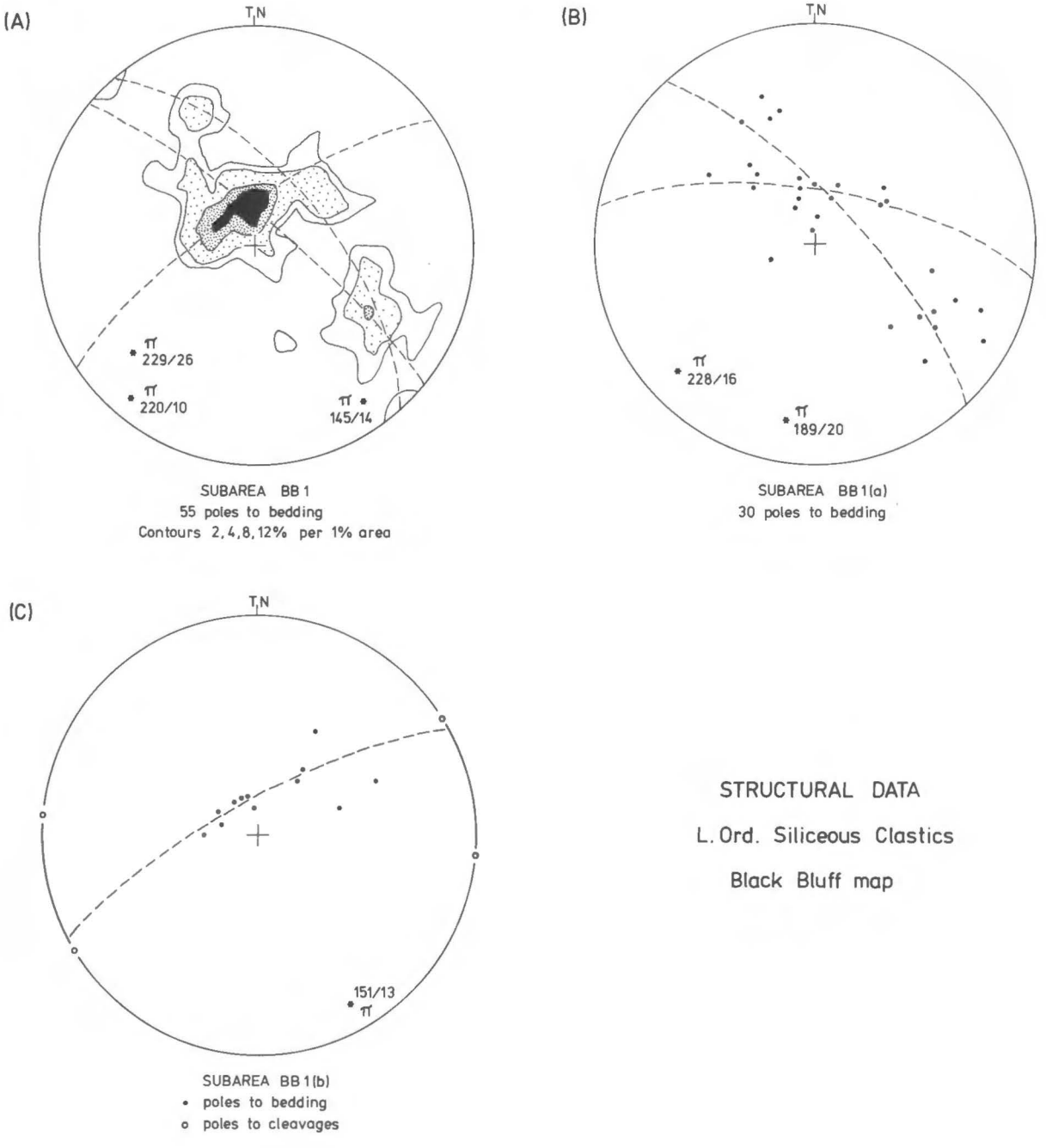
(A)
T,N
π 229/26
π 220/10
π 145/14
SUBAREA BB 1
55 poles to bedding
Contours 2,4,8,12% per 1% area
(B)
T,N
π 228/16
π 189/20
SUBAREA BB 1(a)
30 poles to bedding
(C)
T,N
151/13 π
SUBAREA BB 1(b)
• poles to bedding
o poles to cleavages
STRUCTURAL DATA
L. Ord. Siliceous Clastics
Black Bluff map

FIGURE 4.19

Peak trend" of Williams (*ibid.*). Cleavage of "Belvoir trend" (NE strike) is apparently absent. Two steeply dipping or vertical cleavages, of approximately N and NW strike respectively, are present in quartz arenites at 4112/4109 and 4114/4097. The NW-striking cleavage at these two localities is later, and is correlated with the "Deloraine/ Railton trend" of Williams (*ibid.*).

(2) Subarea BB2

Fig. 4.20A shows the dominant folding on SW-SSW trending axes in this subarea. Steeply dipping to vertical cleavage of similar strike also begins to appear in places (see Map 4), and minor folding on the same trend is present at 4102/4077 and 4104/4070. Folding on this trend is more clearly demonstrated by a plot of bedding data and minor fold hingelines from a smaller subarea, BB2(a), within subarea BB2 (see Fig. 4.20B, and Fig. 4.4 for coverage). All of these structures are correlated with the "Belvoir trend" of this study.

The only other cleavage recorded in this subarea is steeply W-dipping or vertical and strikes N, and is correlated with the "West Coast Range/Valentines Peak trend" of Williams (1978). The pattern of the bedding plot in Fig. 4.20A suggests that folding on NW-SE trends persists into this subarea, although no associated cleavage has been recognized. Another small subarea, BB2(b), in the vicinity of 4077/4064 within subarea BB2, displays minor folding on gently plunging W-WNW trending axes. The correlation of this folding is problematical, as the only other major structures of similar trend in the Black Bluff region are those developed in the limestone of the Gordon Subgroup at Loongana.

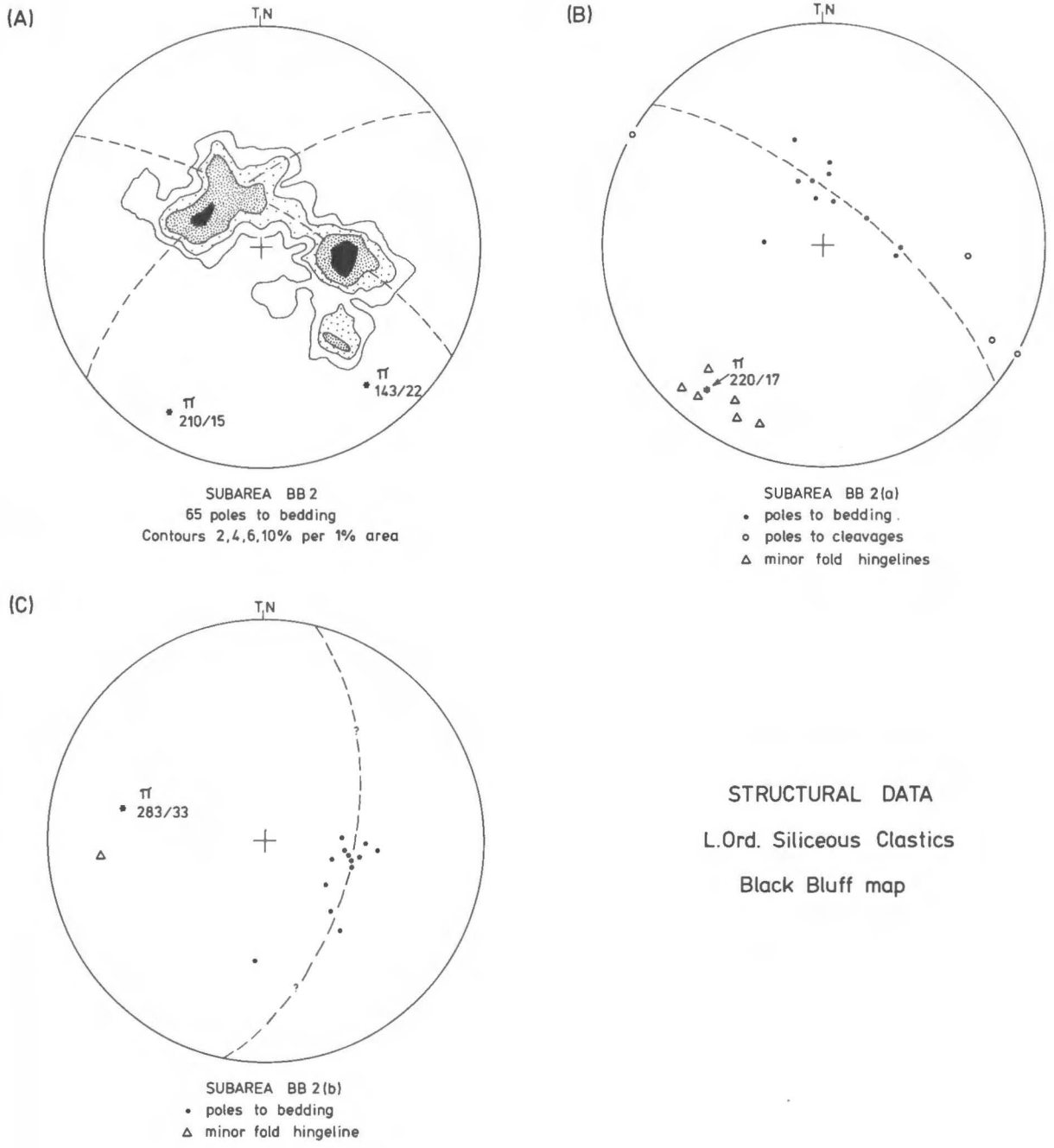
(A)
T N
π
210/15
π
143/22
SUBAREA BB 2
65 poles to bedding
Contours 2,4,6,10% per 1% area
(B)
T N
π
220/17
SUBAREA BB 2(a)
• poles to bedding.
o poles to cleavages
△ minor fold hingelines
(C)
T N
π
283/33
SUBAREA BB 2(b)
• poles to bedding
△ minor fold hingeline
STRUCTURAL DATA
L.Ord. Siliceous Clastics
Black Bluff map

FIGURE 4.20

4.5.3 Minor structures in the Denison Subgroup stratigraphic equivalent

Cleavage is not extensively developed in these rocks on the Black Bluff map, its presence apparently being mainly controlled by the existence of favourable lithologies. The best development of cleavage is seen in fine volcanic wacke conglomerates of Lithofacies I, close to the base of the sequence near 4131/4103 just southwest of Paddys Lake. These rocks have a single steeply dipping cleavage of NW-NNW strike ("Deloraine/Railton trend"), which consists of two main fabric elements:-

(1) Short, discontinuous dark seams (cf. "cleavage folia" of Powell, 1969, 1977) which anastomose around and truncate the edges of the clastic grains.

(2) Very well developed preferred orientation of intergrown quartz and sericitic mica (including "beards" on the clastic grains) in the matrix of the parts of the rock between the dark seams.

The overall fabric is very similar to the intermediate stage between "rough disjunctive" and "smooth disjunctive" cleavage of Powell (1979) (compare Fig. 4.21 with Fig. 4.6), and is also similar to the fabrics described and illustrated by Powell (1969, 1977) from the Early Proterozoic Siamo Slate, northern Michigan, U.S.A. The quartz-mica beards are so well developed as to be at least equal in importance with the seams in defining the appearance of cleavage in outcrop and hand specimen.

As was the case in certain tuffs in the Mount Read Volcanics/Dundas Group stratigraphic equivalents on the Smiths Plains map, discussed in Section 4.4.2, some of the oriented quartz-mica intergrowth in these rocks appears to have formed as extensional fracture infill. Thus, different segments of the volcanic quartz clasts in Fig. 4.22A and B appear to have moved relative to each other, the opening spaces being filled with oriented quartz-mica. In the case of the grain in Fig. 4.22B

FIGURE 4.21

Anastomosing cleavage folia and quartz-mica beards in volcanic wacke near base of Denison Subgroup stratigraphic equivalent at 4131/4103. Single steeply dipping cleavage of "Deloraine/Railton trend" (NW-NNW strike) is present, and this section is vertical and perpendicular to it. Note that the beards are actually intergrown with the margins of the quartz clasts in some cases.
Specimen UTGD 48406. PPL.

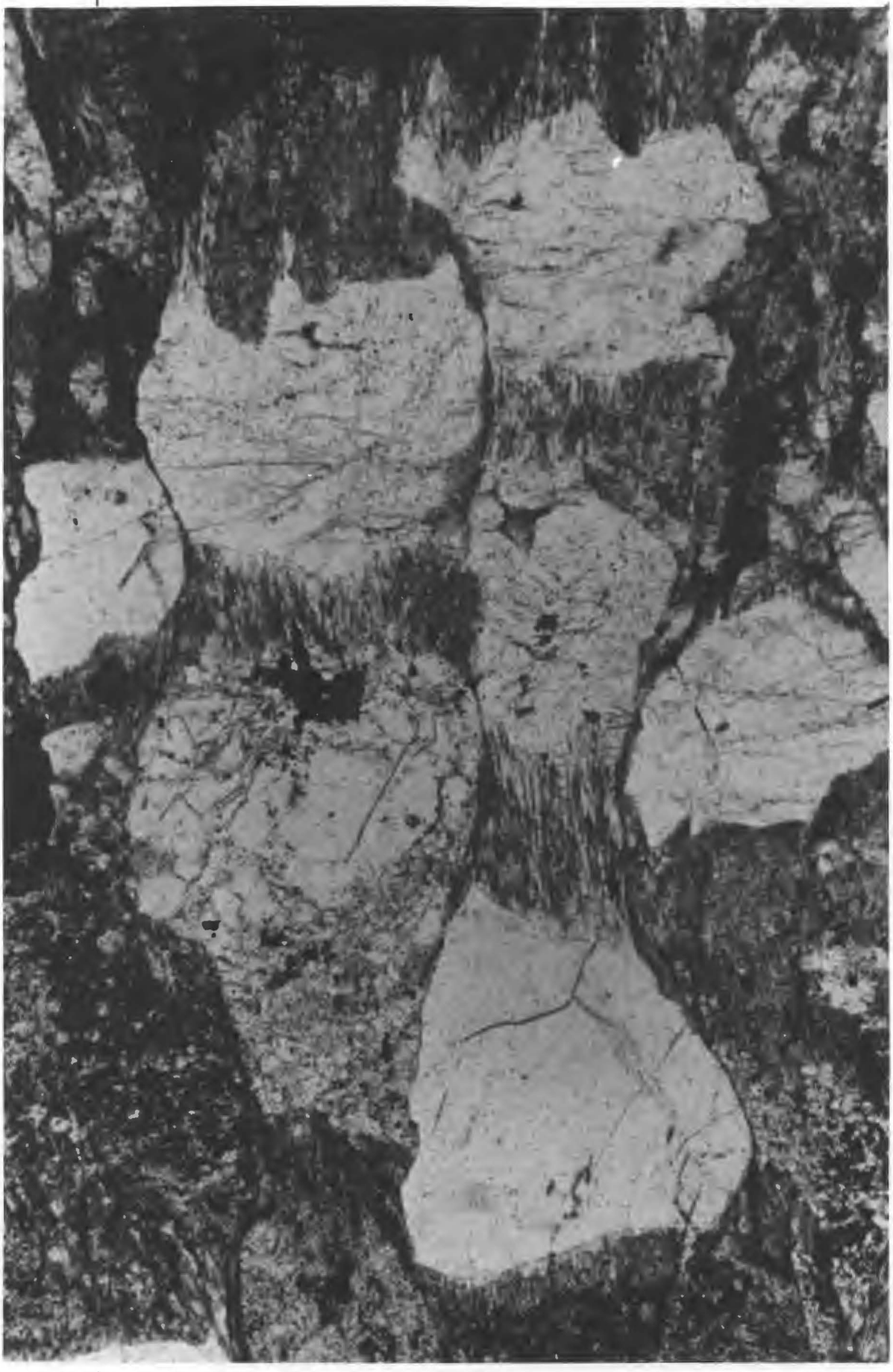

S_1

FIGURE 4.21

0.25 mm

FIGURE 4.22

A. Oriented quartz-mica intergrowth which appears to have formed partly by recrystallization of material filling embayments in a volcanic quartz clast. Same rock as in Fig. 4.21. The clast has disaggregated into five segments, two of which have moved relative to the rest. Section is vertical and perpendicular to single steeply dipping cleavage of NW-NNW strike. Specimen UTGD 48406. PPL.

B. Brittle tensional failure of a volcanic quartz clast, the opening fractures being filled with oriented quartz-mica intergrowth. Same specimen and section as in A, above. Specimen UTGD 48406. PPL.

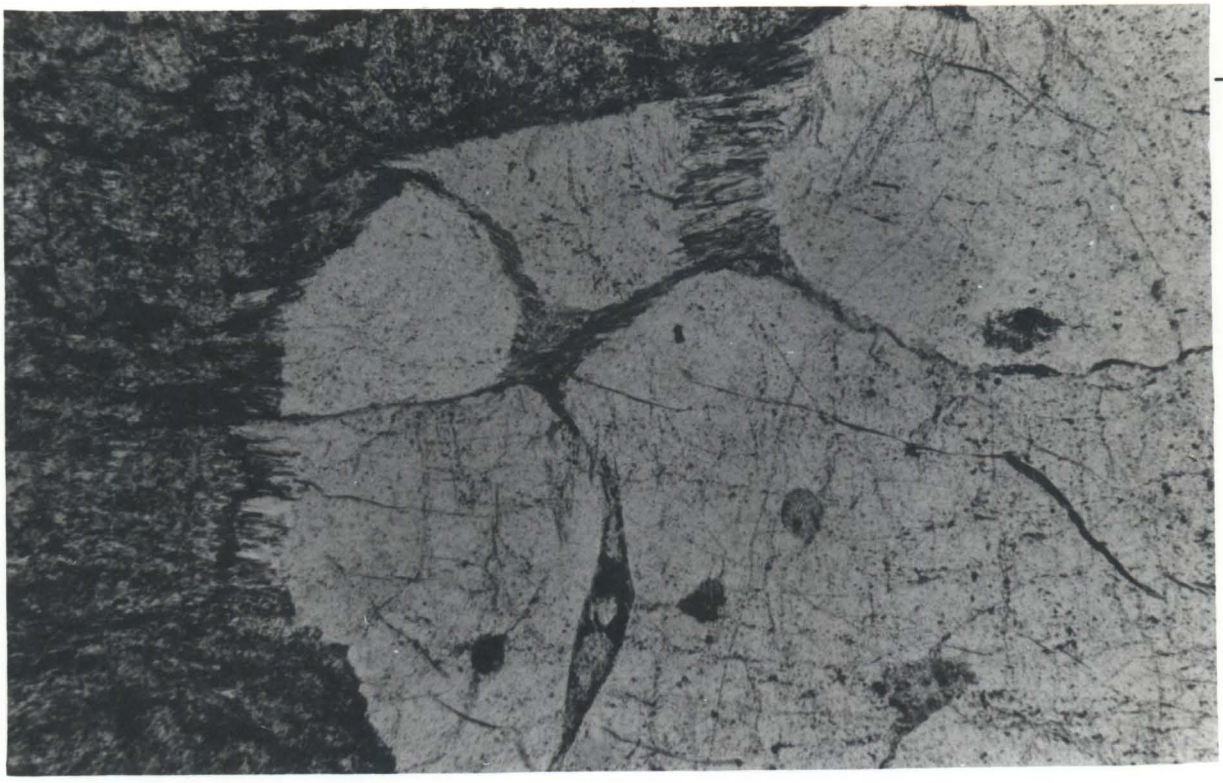

FIGURE 4.22A

0.25 mm

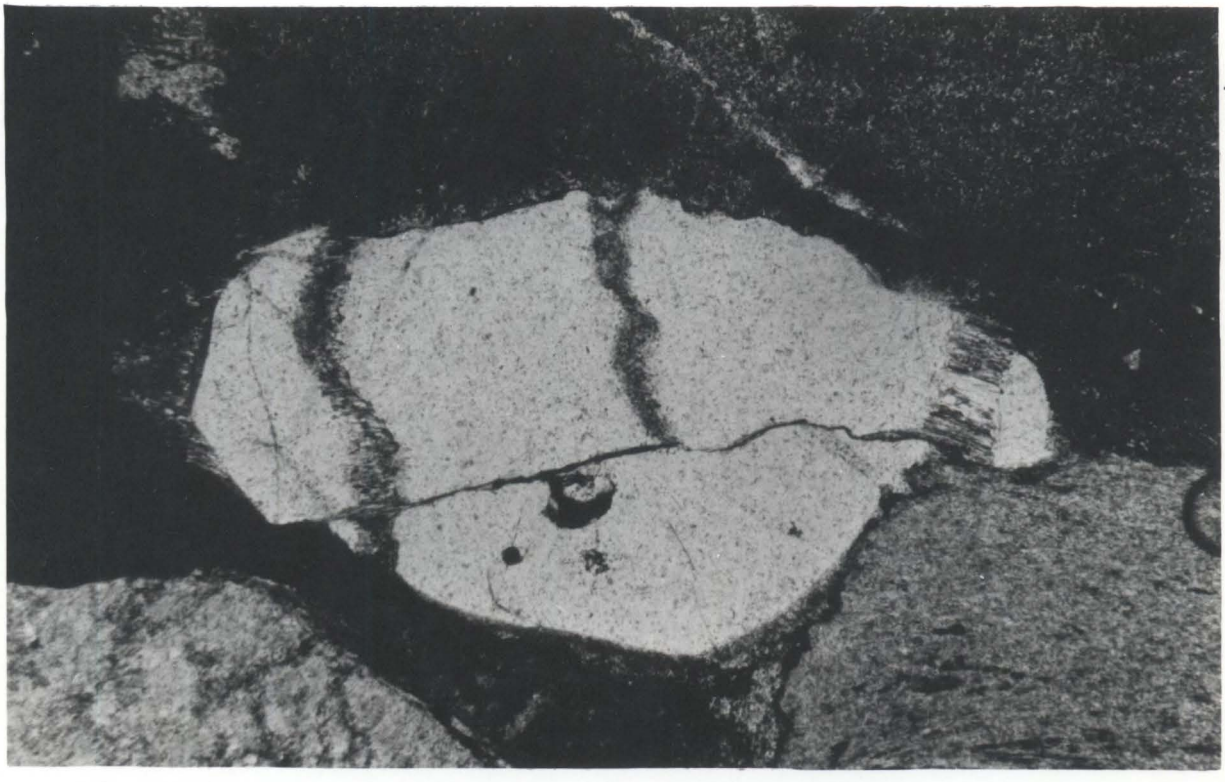

FIGURE 4.22B

0.25 mm

this appears to have followed brittle tensional failure. The seam running sub-parallel to the length of the grain appears to be a pressure dissolution surface (tectonic stylolite). The grain in Fig. 4.22A however, appears to have been an embayed volcanic quartz clast, and the areas of oriented quartz-mica now occurring within it may have partly formed by recrystallization of the embayment material rather than purely by extensional fracture infilling. There has however been some relative extensional strain, especially between the two smaller segments of the grain.

Some of the quartz-mica beards appear to be actually intergrown with the edges of the quartz grains which they abut against. This effect can be seen on the lower boundary of the large quartz grain in Fig. 4.23. The formation of the beards in this case appears to have involved quartz of the original detrital grains, i.e. not just quartz in diagenetic overgrowths, as was the case with the beard structures described by Boulter (1977). It may even be possible that some reaction mechanism of the matrix clays with the quartz clasts was involved. Note that the beard on the top side of the large quartz grain in Fig. 4.23 becomes progressively more quartz-rich as the boundary of the grain is approached. This points to active diffusion of quartz away from the clast during formation of the beards. Diffusion transfer of quartz has also considerably modified a group of smaller quartz clasts just above the large quartz grain in Fig. 4.23. The diffused material is seen in Fig. 4.23 as elongate dark areas consisting of fine granoblastic quartz, extending between the group of small grains and the large grain below. For comparison, a remarkably similar fabric was illustrated by Cowan (1974, his Fig. 3A) in "metagraywacke semischist" from the Franciscan Complex, California.

FIGURE 4.23

Detail of quartz-mica beards in the matrix of a volcanic wacke near the base of the Denison Subgroup stratigraphic equivalent at 4131/4103. Section vertical and perpendicular to single steeply dipping cleavage of NW-NNW strike. Note diffusion transfer of quartz, particularly in a narrow dark band extending between the large grain and a group of smaller grains above it. Note also intergrowth of the beard material with bottom edge of the large grain.
Specimen UTGD 48406. XPL.

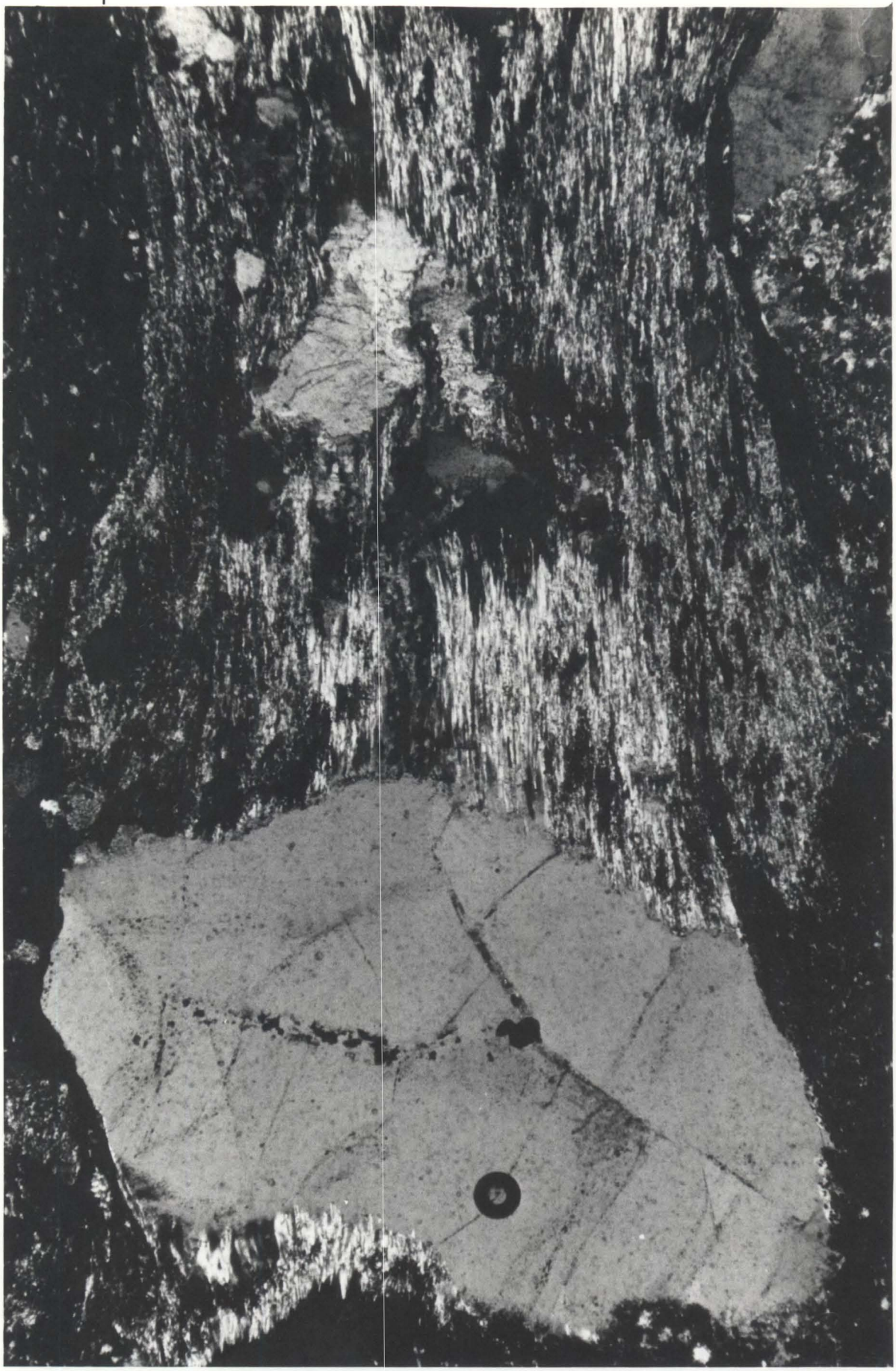

S_1

FIGURE 4.23

0.25 mm

FIGURE 4.24

A. Quartz-mica-hematite beard structure in the matrix of a hematitic fine chert breccia in the Denison Subgroup stratigraphic equivalent at 4138/4089. Section is vertical and perpendicular to single vertical cleavage of NW-NNW strike. Specimen UTGD 48405. PPL.

B. Enlargement of part of Fig. 4.24A, above.

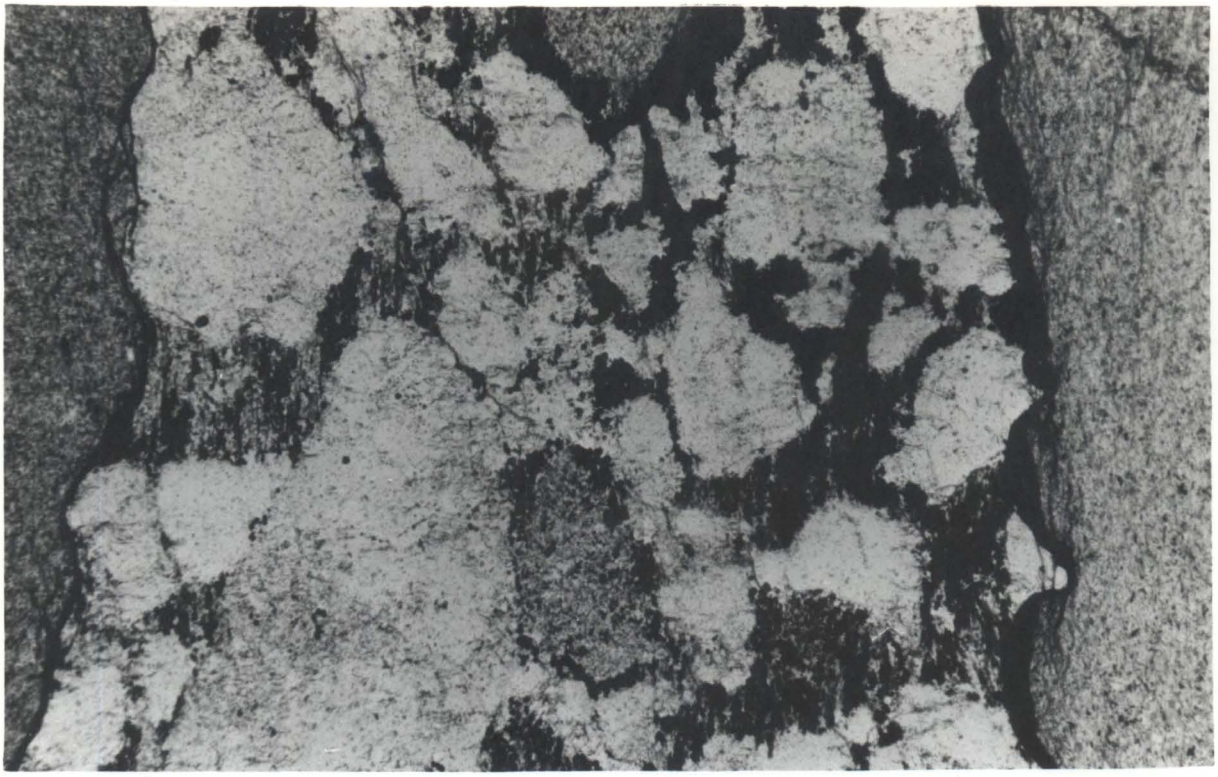

S_1

FIGURE 4.24A

0.25 mm

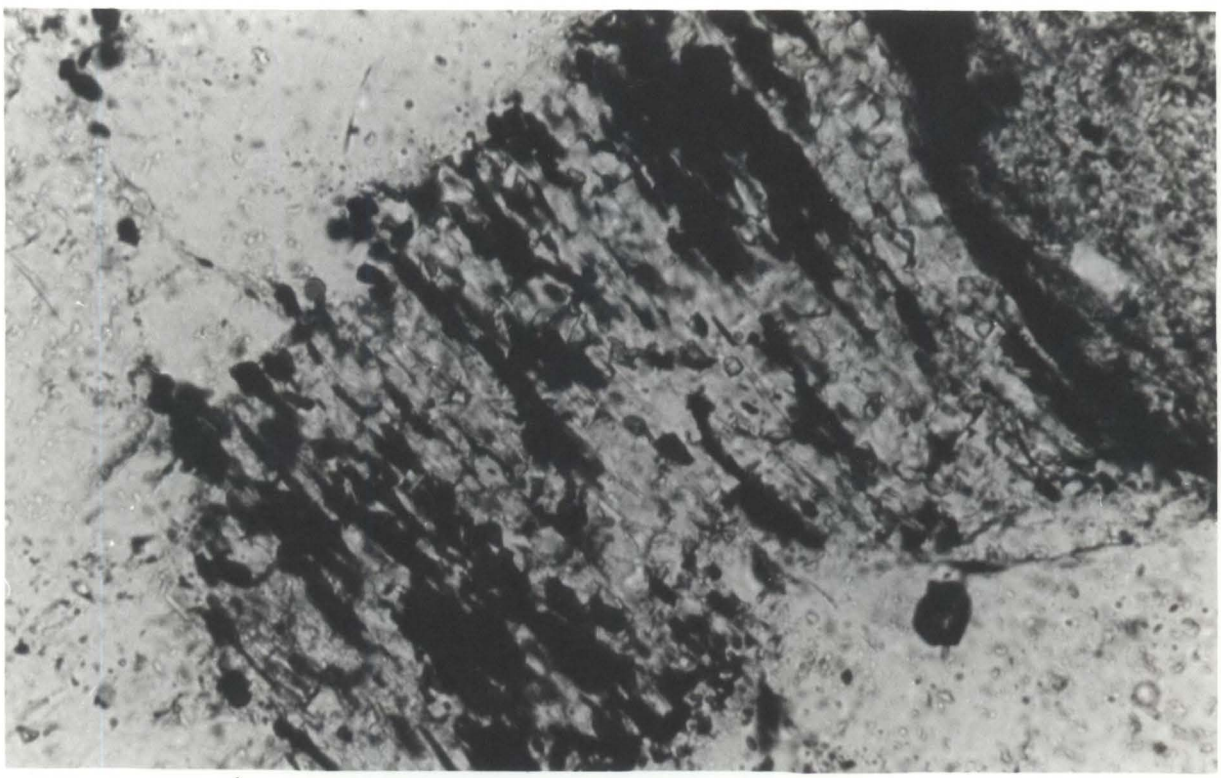

S_1

FIGURE 4.24B

0.05 mm

In some of the more hematitic rocks, matrix hematite has apparently also been involved in the formation of beards. Fig. 4.24A and B show quartz-mica-hematite beards which have formed in the matrix of a hematitic fine (?)chert breccia with quartz arenite matrix (Lithofacies III) from 4138/4089, 2 km southeast of the summit of Black Bluff. A single vertical cleavage of NW-NNW strike is present at this outcrop.

4.6 VALE OF BELVOIR (NORTH) STRUCTURAL MAP

4.6.1 Structure of the Mount Read Volcanics stratigraphic equivalents

These rocks occupy two isolated outcrops on the Black Bluff Range, and extensive areas on and to the east of Bonds Range. The structure of the basal parts of the Denison Subgroup stratigraphic equivalent around the boundaries of the two outcrop areas on the Black Bluff Range suggest that they occupy the cores of structural domes. These domes are suggested to have arisen by oblique cross-folding on NE and N trends, inferred partly from the presence, in the southern outcrop area, of vertical cleavages parallel to these two trends (see Map 5). The dominant cleavage on the Black Bluff Range is vertical to steeply NW-dipping and strikes approximately NE. This cleavage is correlated with the "Belvoir trend" of this study. Where the cleavage of N strike also occurs, it is later than the cleavage of NE strike, and is correlated with the "West Coast Range/Valentines Peak trend" of Williams (1978).

On Bonds Range the dominant cleavage in quartz porphyries in the Mount Read Volcanics stratigraphic equivalent is once again vertical to steeply NW-dipping with NE strike. Cleavage of N strike has not been detected in these rocks anywhere on this part of Bonds Range. However, at the northern end of the range, a second, later, vertical cleavage striking approximately ENE occurs in addition to the cleavage of NE strike.

The two cleavages and the relationship between them are particularly visible in outcrops in the vicinity of 4123/4040 (specimen UTGD 48427). Dome and basin structure in the Denison Subgroup stratigraphic equivalent at the northern end of Bonds Range is suggested to be due to folding on trends parallel to the strikes of the two cleavages.

4.6.2 Minor structures in the Mount Read Volcanics stratigraphic equivalents

As noted in Section 3.2.4 herein, the dominant rock type in the Mount Read Volcanics stratigraphic equivalent on Bonds Range and the southern Black Bluff Range is altered coarse quartz porphyry, some of which may represent hypabyssal intrusive material. The fine grained groundmass in these rocks has commonly suffered considerable pre-tectonic sericitic alteration. This fine groundmass sericite has often developed a tectonite fabric during the later cleavage development, in a similar manner to that described in the Mount Read Volcanics/ Dundas Group stratigraphic equivalents on the Smiths Plains map (Section 4.4.2). The large quartz phenocrysts have usually absorbed considerably less strain than the incompetent matrix, with the result that the foliation defined by crystallographic preferred orientation of fine sericite in the matrix "wraps" around the phenocrysts.

The large quartz phenocrysts themselves appear to have deformed by a number of different mechanisms. Brittle fracture is a common feature, and is very obvious in the grains illustrated in Figs. 4.25A and 4.26. Many of the fractures appear to be of tensile type, and have subsequently opened during continuing strain. The fractures in the grain in Fig. 4.25A, and those which are oriented at a high angle to the prism faces of the grain in Fig. 4.26, appear to be of this type. However, the fracture whose overall trend is sub-parallel to the prism faces in Fig. 4.26 is oriented at a high angle to the local compressive strain

FIGURE 4.25

A. Brittle failure of a quartz phenocryst in an altered quartz porphyry in the Mount Read Volcanics stratigraphic equivalent, from 4071/4038 on the Black Bluff Range. Section is vertical and perpendicular to local S_1, which is vertical cleavage of NE strike, and is expressed as patchy preferred orientation of (001) of fine sericite in the matrix.
Specimen UTGD 48420. PPL.

B. Same section as in A above, showing quartz fibre vein with overall trend normal to cleavage. Preferred orientation of quartz grain long axes in the vein parallels cleavage trace on this section and forms a lineation pitching at 90^{o} in the section parallel to cleavage. Specimen UTGD 48420. XPL.

S_1

0.5 mm

FIGURE 4.25A

S_1

FIGURE 4.25B

1 mm

FIGURE 4.26

Brittle failure of a quartz phenocryst in an altered quartz-felspar porphyry in the Mount Read Volcanics stratigraphic equivalent at 4059/4032 on the Black Bluff Range. Section is vertical and perpendicular to local S_1, which is vertical cleavage of NE strike. Those fractures oriented at a high angle to the maximum principal extension direction have opened, and are filled with quartz-sericite intergrowth with lattice preferred orientation parallel to the cleavage trace. Specimen UTGD 48422. XPL.

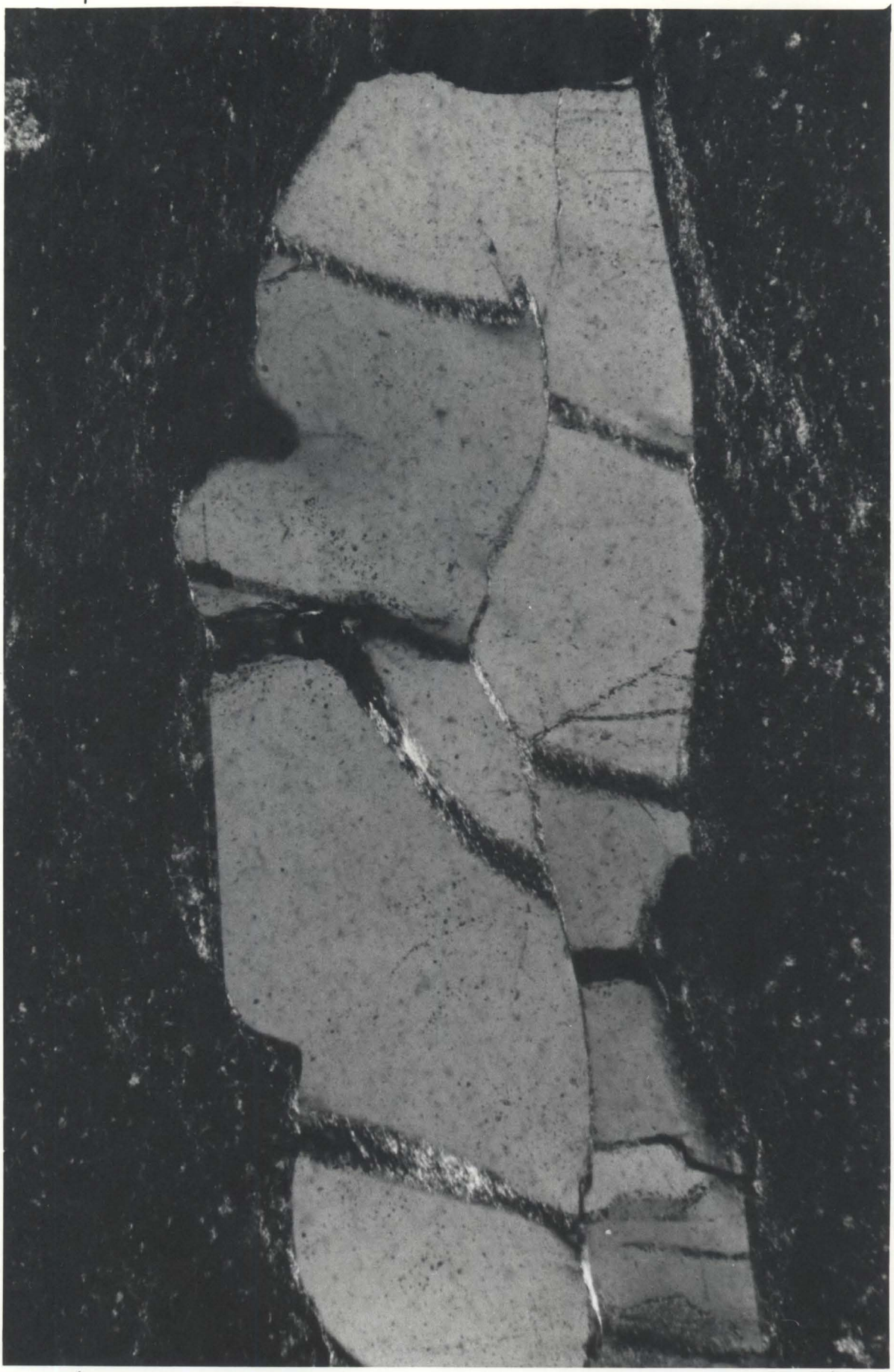

S_1

FIGURE 4.26

0.2 mm

(Z) direction, and relative simple shear movements have taken place along it. In some cases, later pressure dissolution has occurred along fractures with such orientations, changing their morphologies to that of tectonic stylolites. It is notable that the material filling the extensional fractures in the grain in Fig. 4.26 is oriented quartz-sericite intergrowth, probably with essentially the same bulk composition as the rock matrix. This points to the operation of pressure solution processes (including dissolution, solution transfer and reprecipitation) in the matrix.

Not all sites of reprecipitation contain quartz-mica intergrowth, however. Some sub-planar veins consist of essentially pure quartz, in fibrous form with grain preferred orientations sub-perpendicular to the vein walls (see Fig. 4.25B). The overall attitude of such veins is usually perpendicular both to cleavage and to the dip direction in the cleavage surface. The veins probably represent reprecipitation sites of silica dissolved from the matrix, and from favourably oriented grain boundaries and internal microfracture surfaces of the large quartz phenocrysts.

Brittle failure is not the only deformation mechanism in the large quartz phenocrysts. Thus, in phenocrysts with mean grainsize of 5 mm in altered quartz porphyries on the northern part of Bonds Range, intragranular strain has often been absorbed by formation of deformation lamellae in two or more crystallographic orientations (see Figs. 4.27 and 4.28). It is notable that these grains are heavily embayed, and are also loaded with primary fluid inclusions which are often concentrated along growth zones. In the grain in Fig. 4.27, the deformation lamellae appear to be partly localized by the embayments, which implies that the presence of the latter had the effect of mechanically weakening the grain.

FIGURE 4.27

Deformation lamellae in two crystallographic orientations in large embayed quartz phenocrysts in an altered coarse quartz-(?)felspar porphyry in the Mount Read Volcanics stratigraphic equivalent at 4137/4046 at the northern end of Bonds Range. Section is vertical and perpendicular to single vertical cleavage of ENE strike ("Bonds Range trend"). The deformation lamellae appear to be partly localized by the embayments. Specimen UTGD 48432. XPL.

FIGURE 4.27

0.2 mm

FIGURE 4.28

Detail of quartz-sericite-iron oxide beard structure developed in matrix between two large quartz phenocrysts in altered quartz-(?)felspar porphyry in the Mount Read Volcanics stratigraphic equivalents at 4112/4030, middle Bonds Range. Section is vertical and perpendicular to local S_1, which is vertical cleavage of NE strike ("Belvoir trend"). Note deformation lamellae in phenocrysts, and quartz-rich bands within the beard structure. Specimen UTGD 48426. XPL.

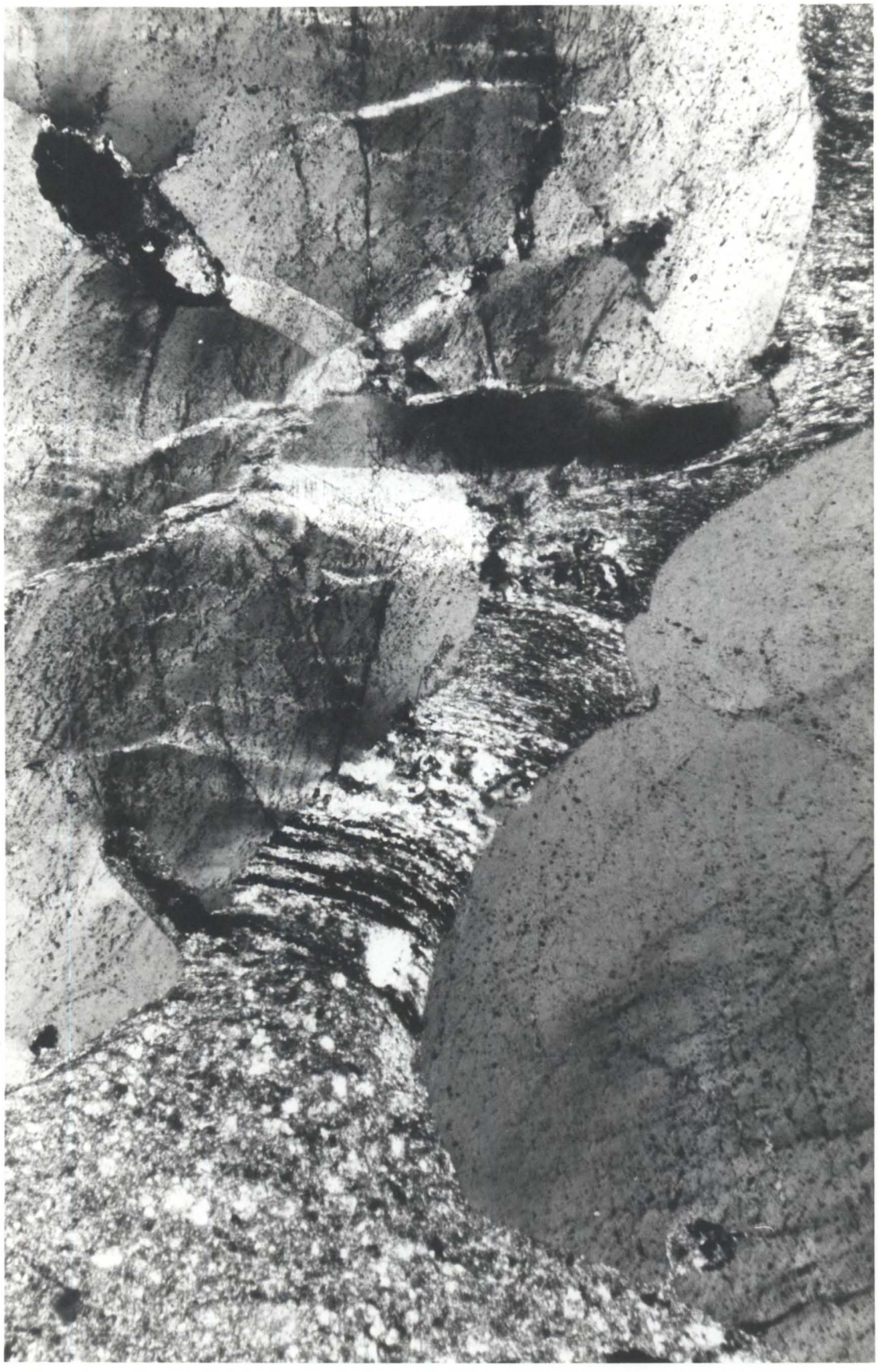

FIGURE 4.28

The grains may have also been hydrolytically weakened by the presence of the copious fluid inclusions. However, these very coarse phenocrysts are the only quartz grains in the Mount Read Volcanics/Dundas Group stratigraphic equivalents in the whole Black Bluff region in which this type of intragranular strain effect has been observed. This suggests that the dominant control may be grainsize in the manner suggested by the analysis of deformation mechanism maps by White (1976). Examination of White's diagrams indicates that at particular conditions of temperature and differential stress, coarse grained quartz may fall in the field of dislocation creep, while fine quartz falls in the field of Coble Creep (which may be partly or completely replaced by a field of pressure solution, as demonstrated by Rutter, 1976).

Some of the large phenocrysts, most noticeably in quartz porphyries on Bonds Range east of Lake Lea (e.g. specimen UTGD 48426) appear to have also suffered considerable diffusion of quartz, particularly on crystal faces oriented at a high angle to the cleavage trace on vertical sections perpendicular to cleavage. A similar effect was noted in Section 4.5.3 in discussion of quartz-mica beards in volcanic wacke conglomerates at the base of the Denison Subgroup stratigraphic equivalent near Black Bluff. However, the diffusion is much more pronounced in these rocks. A commonly occurring texture is illustrated in Fig. 4.29, where an almost hourglass-shaped area of diffused and recrystallized quartz has formed in the area between two adjacent large phenocrysts. Much of the recrystallized quartz has a granoblastic fabric with only weak grain elongation fabric, but it is intergrown with presumably recrystallized matrix mica and opaques having strong lattice preferred orientation. The quartz content of the hourglass-shaped area decreases away from each of the two phenocrysts and is at a minimum approximately at the midpoint between them.

FIGURE 4.29

Quartz-sericite-iron oxide beard structure developed in matrix between two large quartz phenocrysts in altered quartz-(?)felspar porphyry in the Mount Read Volcanics stratigraphic equivalents at 4112/4030, Bonds Range. Section is vertical and perpendicular to S_1, which is vertical cleavage of NE strike ("Belvoir trend"). Specimen UTGD 48426. XPL.

S_1

FIGURE 4.29

0.5 mm

It is doubtful that the structure illustrated in Fig. 4.29 is purely a dilational feature; that is, it is definitely not envisaged that the two phenocrysts were originally together. The amount of extensional strain in the space between the phenocrysts is probably only a small to moderate fraction of the present distance between them. The main reason for this conclusion is the observation that the strong preferred orientation of mica, opaques and, to a less extent, quartz, in the hourglass-shaped area rapidly becomes very much weaker laterally away from the area between the phenocrysts. It is therefore suggested that the structure has formed mainly by *in situ* recrystallization of the rock matrix during moderate extensional strain, with stress-controlled diffusion of quartz away from the boundaries of the two phenocrysts towards the mid-point between them. A similar mode of origin is envisaged for the quartz-mica-iron oxide beard structure between the two large quartz phenocrysts in Fig. 4.28, although in this case the dilation may be a higher percentage of the present space between the phenocrysts.

Tectonic preferred orientations of fine matrix sericite are best developed in rare sedimentary parts of the Mount Read Volcanics stratigraphic equivalent on the Vale of Belvoir (North) and (South) maps. The best developed examples occur in strongly cleaved volcanic quartz wackes near 4123/4040 on the northern Bonds Range. Two sub-vertical cleavages, respectively of NE strike (local S_1, "Belvoir trend") and NNE strike (local S_2, "Bonds Range trend"), are present in outcrops at this locality. The appearance of the sericite fabrics is illustrated in Fig. 4.30A and B. The development of mica films between the quartz clasts in Fig. 4.30A appears to have been associated with concomitant mutual pressure dissolution of the quartz grain boundaries. The sections in A and B are vertical and perpendicular to the dominant cleavage

FIGURE 4.30

A. Two sericite fabrics defining two steeply dipping cleavages with an acute angle between them, in the matrix of a quartz wacke in the Mount Read Volcanics stratigraphic equivalents at 4123/4040, northern Bonds Range. Section is vertical and normal to dominant cleavage (S_1). Local S_1 has NE strike ("Belvoir trend"), local S_2 has ENE strike ("Bonds Range trend"). Specimen UTGD 48427. XPL.

B. Same section as in A, above. Note domainal nature of the mica fabrics. Specimen UTGD 48427. XPL.

FIGURE 4.30A

0.2 mm

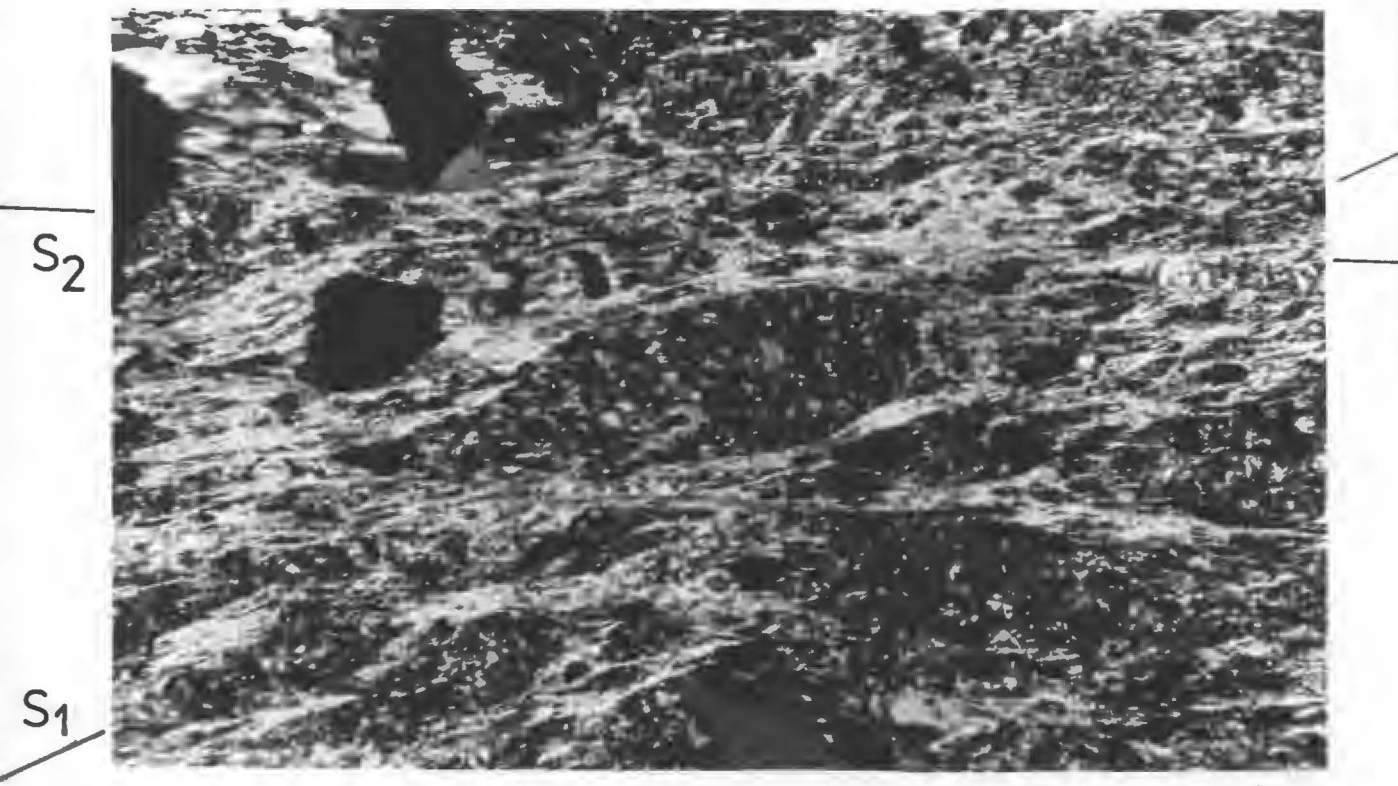

FIGURE 4.30B

0.2 mm

(that of NE strike). On such sections, detection of two mica fabrics with an acute angle between them, corresponding to the two cleavages, may be expected if the cleavages are not exactly vertical. The initial impression of a single anastomosing mica fabric in Fig. 4.30B is almost certainly a product of the presence of two such fabrics, and on close examination it is possible to determine the order of development indicated on the photo. Both of the fabrics are somewhat domainal on a small scale. In the centre of Fig. 4.30B, an interdomainal area contains minor oriented sericite which may partly be filling micro-fractures produced during extensional strain.

4.6.3 Structure of the Denison Subgroup stratigraphic equivalent

Subarea analysis of bedding data in these rocks on the two Vale of Belvoir maps is presented in Fig. 4.31. The coverage of the subareas is shown on Fig. 4.4.

(1) Subarea VB1

This subarea approximately covers the area of Denison Subgroup stratigraphic equivalents appearing on the Black Bluff Range on the Vale of Belvoir (North) map. Fig. 4.31A reflects the dominant folding on NE or "Belvoir trend" in this area. The major structure is a slightly asymmetric (SE verging) open NE-trending anticline with 1.5-2 km half-wavelength whose axial trace is just northwest of the crest of the Black Bluff Range. However, the structure is not simple, a well developed dome and basin pattern apparently being present. As proposed in Section 4.6.1, this pattern appears to have arisen by interference of the folds on NE trends with later cross-folds on N trends. The latter are correlated with the "West Coast Range/Valentines Peak trend" of Williams (1978).

The evidence for the relative timing of the two deformation events in this subarea has mainly come from examination of cleavages in the

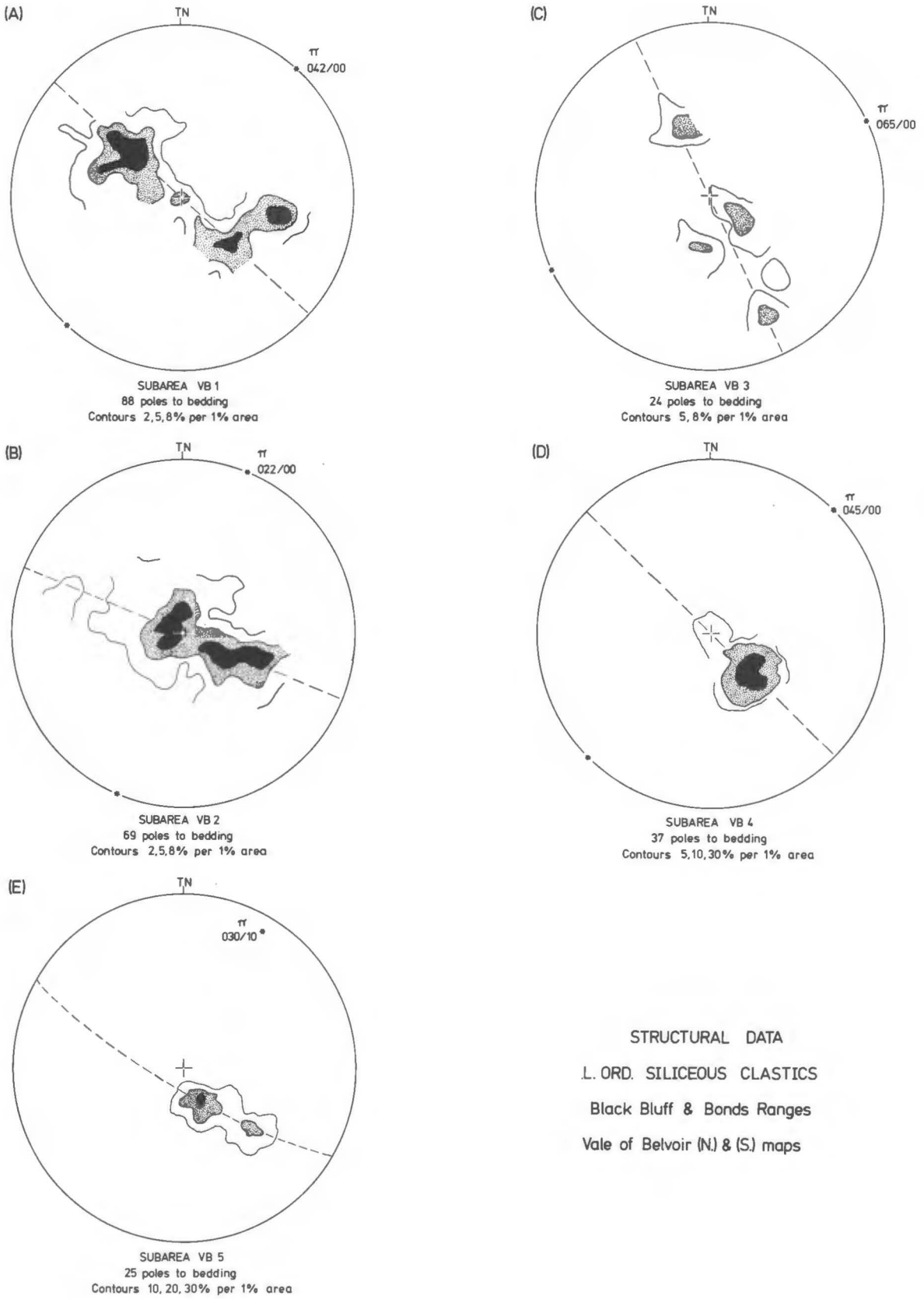
(A)
TN
π
042/00
SUBAREA VB 1
88 poles to bedding
Contours 2,5,8% per 1% area
(B)
TN
π
022/00
SUBAREA VB 2
69 poles to bedding
Contours 2,5,8% per 1% area
(C)
TN
π
065/00
SUBAREA VB 3
24 poles to bedding
Contours 5,8% per 1% area
(D)
TN
π
045/00
SUBAREA VB 4
37 poles to bedding
Contours 5,10,30% per 1% area
(E)
TN
π
030/10
SUBAREA VB 5
25 poles to bedding
Contours 10,20,30% per 1% area
STRUCTURAL DATA
L. ORD. SILICEOUS CLASTICS
Black Bluff & Bonds Ranges
Vale of Belvoir (N.) & (S.) maps

FIGURE 4.31

Mount Read Volcanics stratigraphic equivalents. The cross-folding may have resulted in the formation of conical closures, especially around the boundaries of the two outcrop areas of Mount Read Volcanics stratigraphic equivalents on the Black Bluff Range. The pattern of the bedding plot in Fig. 4.31A is in part suggestive of such non-cylindrical fold geometry. Lithologies in the Denison Subgroup stratigraphic equivalent in subarea VB1 are only rarely cleaved, but where cleavage is present it is usually steeply dipping to vertical with NE strike ("Belvoir trend").

(2) Subarea VB3

This subarea covers the northeastern end of Bonds Range, from a point near the northern end of Lake Lea. Dome and basin pattern in this area is attributed to interference of open upright horizontal folds on NE or "Belvoir trend" with later folds of comparable style on ENE or "Bonds Range trend". The folding on ENE trends tends to dominate, resulting in the relatively simple appearance of the plot of bedding data in Fig. 4.31C. Once again, information relating to the relative timing of the two folding events has mainly been obtained from overprinting relationships of associated axial cleavages developed in the Mount Read Volcanics stratigraphic equivalents. Cleavage is generally absent or very weakly developed in the Denison Subgroup stratigraphic equivalent in this subarea.

(3) Subarea VB4

This covers the part of Bonds Range between subarea VB3 and the southern boundary of the map. Structurally it is the simplest subarea of VB1, 3 and 4. Examination of Fig. 4.4 and Map 5 shows that it lies across the major strikes from subarea VB1, and covers the SE limb of a large slightly asymmetric (SE verging) horizontal syncline of NE trend, the core of which is occupied by limestone of the Gordon Subgroup stratigraphic equivalent in the Vale of Belvoir. This syncline has

approximately 2 km half-wavelength just southwest of Lake Lea, but progressively tightens further to the southwest, as will be seen on Map 6.

The bedding plot in Fig. 4.31D reflects the relatively simple structure of a limb dipping to the northwest at 25-30° in this subarea. There is still some suggestion of dome and basin pattern in the vicinity of 4100/4020. However, only a single generation of cleavage is evident in Mount Read Volcanics and Denison Subgroup stratigraphic equivalents over most of the subarea. This cleavage has NE strike ("Belvoir trend") and is vertical to steeply NW-dipping, the latter reflecting the asymmetry of other structures of this trend. The southernmost occurrence of the later cleavage of ENE strike is near 4109/4028.

4.7 VALE OF BELVOIR (SOUTH) STRUCTURAL MAP

4.7.1 Structure of the Mount Read Volcanics stratigraphic equivalents

These rocks outcrop in a small window on the southern Black Bluff Range, approximately 1.5 km northeast of Mayday Mt., and in more extensive areas on the southern extension of Bonds Range. The dominant rock type is massive fine to medium grained quartz porphyry, sometimes with flow banding. Crystal tuffs with compositional layering occur near 4038/3983, and strongly altered quartz-crystal vitric tuff (possibly of ashflow origin) occurs near 4051/3972 (specimen UTGD 48434).

The dominant cleavage in these outcrops is vertical to steeply NW-dipping with NE strike, and is parallel to cleavage in the overlying quartzose clastics of the Denison Subgroup stratigraphic equivalent. It is correlated with the "Belvoir trend" of this study. However, near 4052/3972 on the southern extension of Bonds Range, a second, later,

N-striking vertical cleavage occurs. This is parallel to second-phase cleavage occurring in the Denison Subgroup stratigraphic equivalent 1 km to the northeast (in the vicinity of 4060/3977), and is correlated with the "West Coast Range/Valentines Peak trend" of Williams (1978). All of the cleavages in the Mount Read Volcanics stratigraphic equivalents are defined mainly by patchy preferred orientations of fine sericite in the altered matrix.

4.7.2 Structure of the Denison Subgroup stratigraphic equivalent

(1) Subarea VB2

This subarea covers the part of the Black Bluff Range appearing on Map 6 (see Fig. 4.4 for coverage). The plot of bedding data in Fig. 4.31B indicates that the statistically defined fold hinge is horizontal and NNE-trending. Note that this is rotated anticlockwise somewhat from that defined in subareas VB1 and VB4. This dominant folding is correlated with the "Belvoir trend". Examination of the map indicates that dome and basin structure is still present. This is particularly obvious near 4043/3997, where a small structural basin can be seen, and in the vicinity of 4038/3982, where Mount Read Volcanics stratigraphic equivalents outcrop in the core of what appears to be a small structural dome. Interpretation of the origin of this dome and basin structure is made difficult by the general absence or very weak development of associated cleavages in this subarea. The only cleavages recognized in fact have NE strikes ("Belvoir trend") and dip steeply to the NW.

However, in thin bedded quartz arenites (Lithofacies VI) occurring on a small ridge running north from Mayday Mt., between 4033/3978 and 4035/3982, minor folds with NE-trending axes have visibly been refolded

on N-trending axes. As a result, the NE-trending folds have undulating hingelines, with plunges both to the NE and SW. As was the case in subarea VB1, it is therefore concluded that the structure in this subarea is a result of two deformation events. The earlier event produced folds and minor cleavage development on NE or "Belvoir trend", while the later event (which is correlated with the "West Coast Range/Valentines Peak trend" of Williams) involved refolding on N trends.

(2) Subarea VB5

This subarea covers a small ridge on the southeastern extension of Bonds Range, immediately to the south of the Vale of Belvoir (see Fig. 4.4). The plot of bedding data (Fig. 4.31E) is relatively simple and shows that the dominant folding is on a trend just east of NNE, with a gentle plunge in that direction. However, the influence of two phases of deformation is indicated by the presence of two generations of cleavage in quartz arenites of Lithofacies IV and V in the vicinity of 4060/3978. The first generation cleavage is mostly vertical with NE strike, and is correlated with the "Belvoir trend". The second is also vertical but strikes N, and is correlated with the "West Coast Range/Valentines Peak trend" of Williams (1978). As noted in the previous section, both cleavages also appear in the underlying Mount Read Volcanics stratigraphic equivalents in the near vicinity.

The style of cleavage development has presented some problems in separating the two generations of cleavage. This problem was also discussed in Section 4.4.3 herein. Fig. 4.32A shows the intersection of the two cleavages on a sub-horizontal outcrop surface in burrowed quartz arenite of Lithofacies V. The cleavage development lies somewhere between the "stylolitic disjunctive" type of Powell (1979) and the "type C rough cleavage" of Gray (1978) (compare with Figs. 4.6 and 4.7).

FIGURE 4.32

A. Spaced seams defining two subvertical cleavages, as seen on gently dipping bedding surface in burrowed quartz arenites near 4060/3977, on southern extension of Bonds Range. Local S_1 strikes between NE and NNE ("Belvoir trend"), S_2 strikes N ("West Coast Range/Valentines Peak trend").

B. Single set of en échelon quartz veins, possibly representing relative simple shear strain due to differential flattening between cleaved and uncleaved lithologies. Near 4059/3976, on southern extension of Bonds Range.

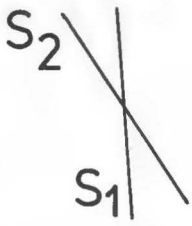

FIGURE 4.32A

10 cm

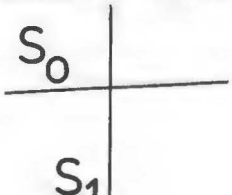

FIGURE 4.32B

10 cm

In some cases initial examination of a pattern such as that in Fig. 4.32A may give the impression of a single anastomosing cleavage. However, asymmetric crenulation of the seams defining S_1 can be clearly seen, and the crosscutting seams defining S_2 have the expected geometric relationship to the crenulations. On close examination of Fig. 4.32A it is seen that the pattern of asymmetric crenulations of S_1 is repeated on a fine scale in shorter discontinuous seams in the parts of the rock between the main cleavage folia.

4.7.3 Minor structures in the Denison Subgroup stratigraphic equivalent

The style of folding in these rocks can only rarely be examined at outcrop scale, due to the usually large size of even the smallest folds. Outcrop-scale minor folds generally only occur in the less competent and/or more thin-bedded lithologies, such as those occurring in Lithofacies VI. Fig. 4.33 shows such a fold closure from 4033/3978 on the southern Black Bluff Range. The fold style is close to parallel (Class 1B; Ramsay, 1967), although the hinge zones sometimes show some signs of flattening (Class 1C; Ramsay, *ibid.*). The quartz arenite layers often appear to have folded largely independently of one another, either by becoming detached from each other by the formation of bedding joints, or due to the fact that interlayered incompetent siltstone beds have deformed in a manner which accommodates the relative movement between the arenite beds.

In sequences dominated by well bedded arenites, flexural slip along bedding planes appears to have been operative during folding. Evidence for this is provided by the occurrence of bedding-parallel quartz veins on the limbs of upright horizontal folds. These veins often contain fibrous quartz with a slickenside texture, the long axes of the

FIGURE 4.33

Minor fold in thin bedded quartz arenites, near 4033/3978 on the southern Black Bluff Range.

FIGURE 4.33

20 cm

FIGURE 4.34

A. En échelon quartz vein set in thick bedded quartz arenites near 4050/3973, on bank of Vale River southwest of Vale of Belvoir. View is of bedding surface dipping at 45°.

B. Detail of A., above.

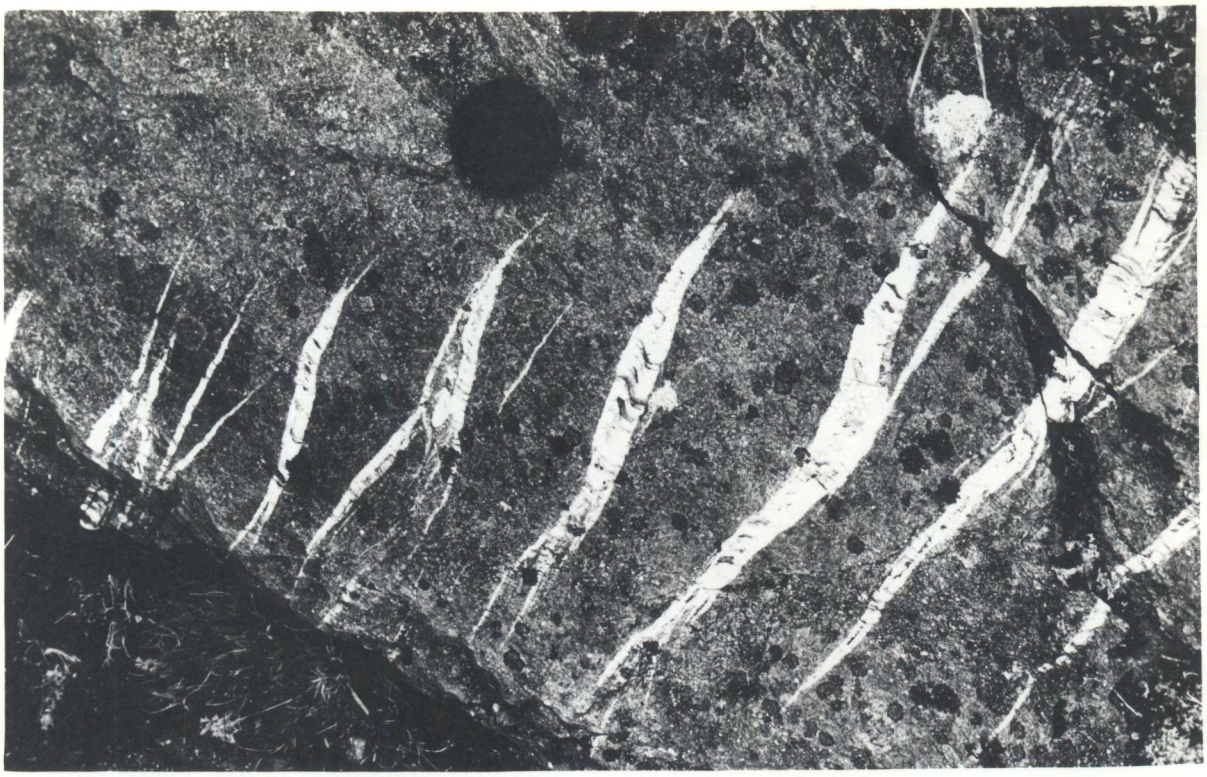

FIGURE 4.34A

10 cm

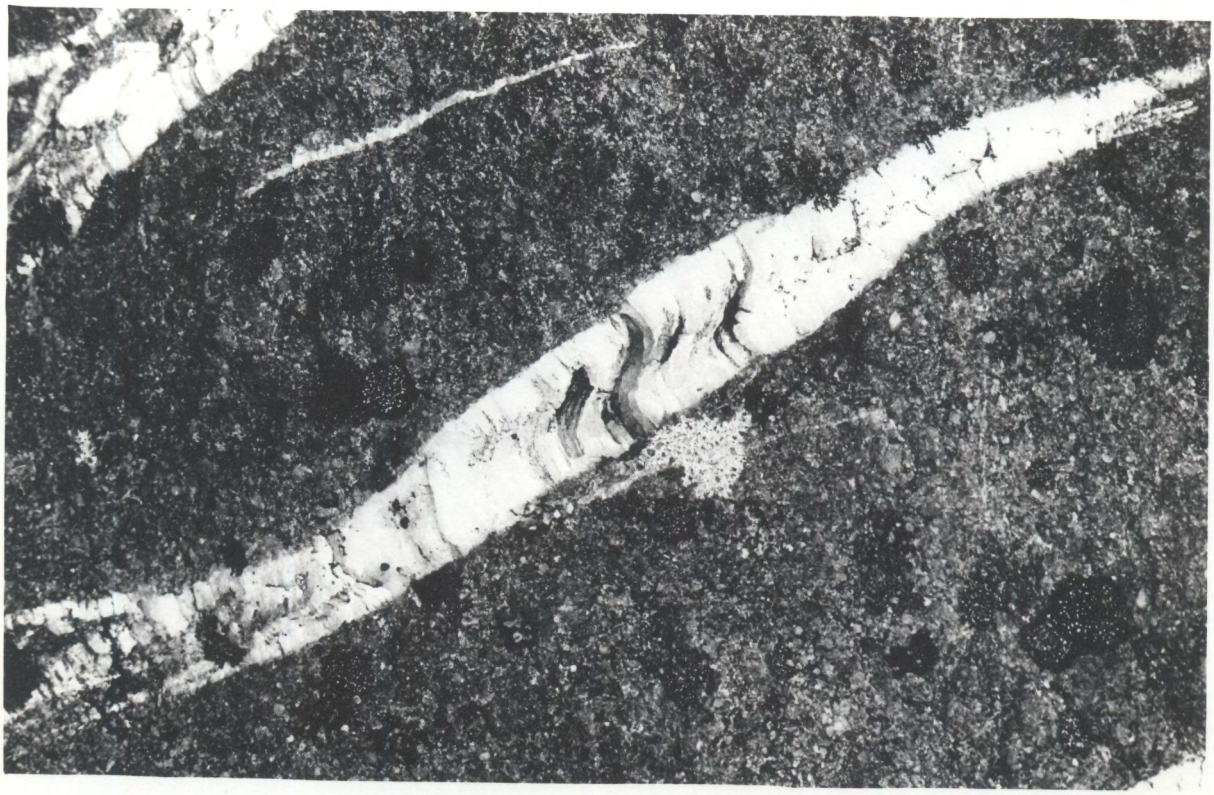

FIGURE 4.34B

5 cm

fibres having preferred orientation in the down-dip directions on the fold limbs.

Quartz veining is very common in the quartzose clastics of the Denison Subgroup stratigraphic equivalent throughout the Black Bluff region. The veins often occur in *en echelon* sets (see Fig. 4.34), which in turn comprise a number of distinct structural associations. The most important of these are:-

(1) Conjugate pairs of *en echelon* sets geometrically related to cleavage, as seen on vertical sections perpendicular to cleavage. The intersection of the bounding surfaces of the two sets is parallel to sub-parallel to the strike of the cleavage, and the apparent σ_1 direction is approximately normal to cleavage (see Fig. 4.35A).

(2) Single *en echelon* sets, the bounding surfaces of which tend to follow the boundaries between lithologies of apparently differing competence (see Fig. 4.35B). They appear to represent accommodation of simple shear strain which was a result of differential flattening of the material above and below. They commonly follow boundaries between cleaved and uncleaved lithologies in the Denison Subgroup stratigraphic equivalent (see Fig. 4.32B) and also appear along Jukesian-type unconformities in places where the rocks below are more strongly cleaved than those above. In the latter situation, a thrust fault following the unconformity sometimes passes laterally into an *en echelon* vein set representing the same sense of relative movement.

(3) Conjugate pairs of *en echelon* sets seen on bedding planes on steeply dipping to vertical fold limbs, the intersection of the bounding surfaces of the two sets being approximately normal to bedding. The σ_3 direction is in the downdip direction in bedding, and the σ_1 direction is sub-parallel to strike of bedding. A typical example is

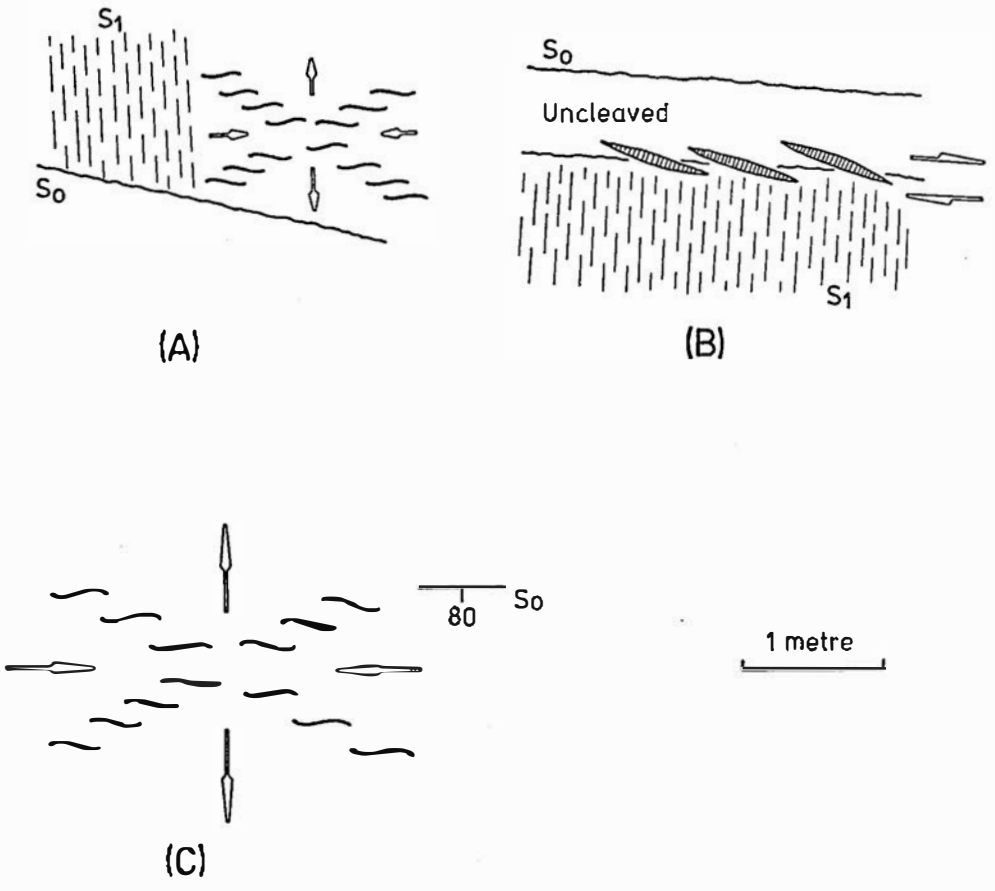

STRUCTURAL ASSOCIATIONS OF
EN ECHELON QUARTZ VEINS

Denison Subgroup strat. equiv.

FIGURE 4.35

FIGURE 4.36

Extensional quartz veins in coarse quartzose conglomerate, near 4068/4054 on the Black Bluff Range. View of section parallel to bedding which is vertical.

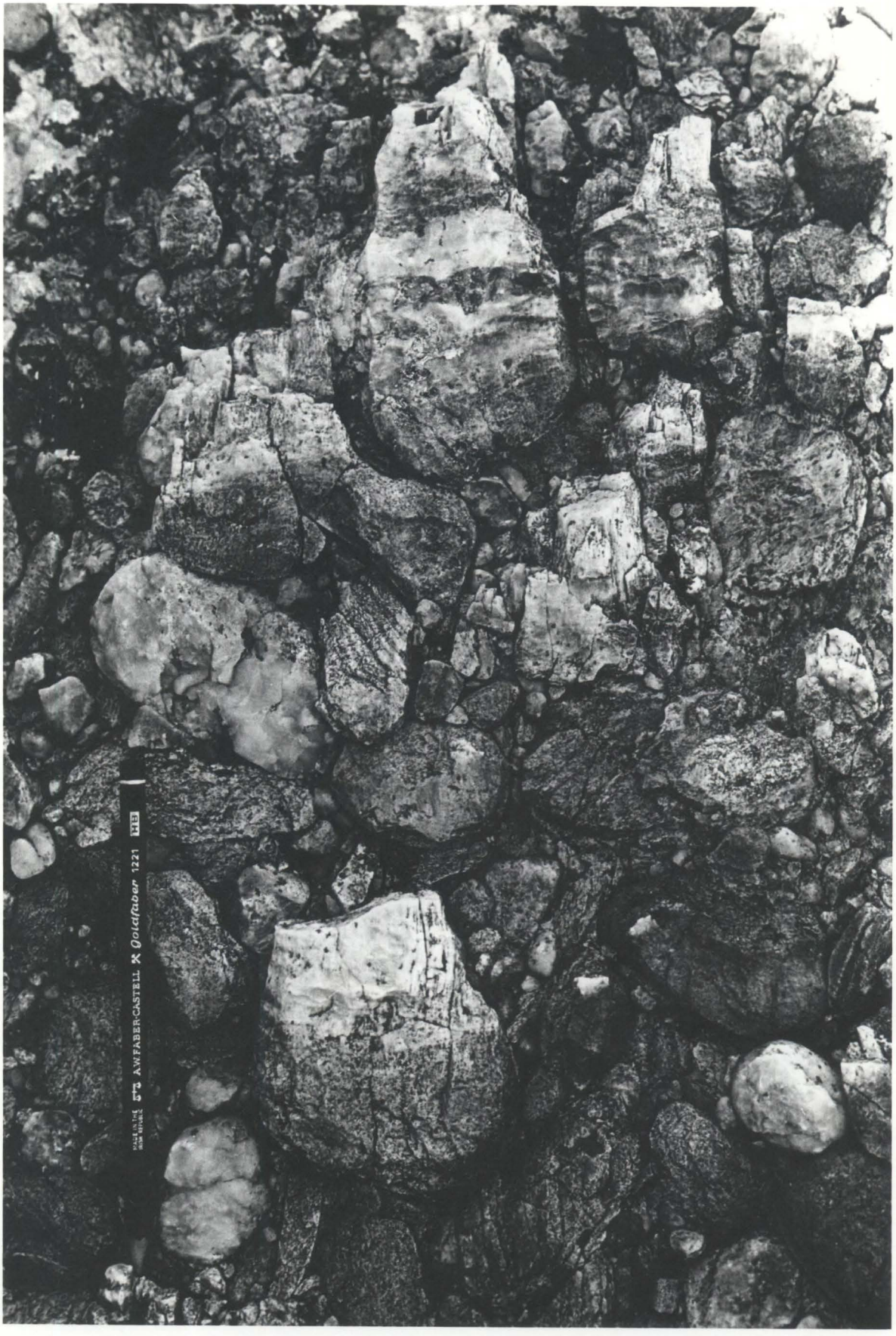

FIGURE 4.36

5 cm

illustrated in Fig. 4.35C, which is a view of a section parallel to bedding. These veins are suggested to have arisen by extension in the downdip direction in bedding on fold limbs which have rotated to high limb dips in the late stages of folding. Not all veins in such situations occur in *en echelon* sets. Fig. 4.36 shows sub-parallel simple dilational quartz veins with approximately horizontal attitude in coarse quartzose conglomerate on a vertical fold limb, giving the appearance of a "stretched pebble" conglomerate. The fibrous quartz in these veins has a grain preferred orientation which is approximately vertical.

(4) The converse of the situation described in (3) above is often seen on sections parallel to bedding in folds with gentle to moderate limb dips. That is, the intersection of the bounding surfaces of the two sets is still normal to bedding, but the apparent σ_1 and σ_3 directions are interchanged. These most probably formed during early layer-parallel shortening prior to most of the folding, and were rotated with bedding during the folding.

4.7.4 Structure of the Gordon Subgroup stratigraphic equivalent

The dominant structure in the limestone in the Vale of Belvoir is a strongly asymmetric SE-verging horizontal syncline with a statistically defined axis trending between NNE and NE (see plot of bedding data, Fig. 4.37A). The asymmetry is such that the main synclinal closure appears to be close to the western side of the Vale, so that very little of the NW limb of the structure is seen in field outcrops. Although the sense of vergence is the same (i.e. to the SE), the degree of asymmetry in the limestone structure suggests some discordance with that in the underlying rocks of the Denison Subgroup stratigraphic equivalent.

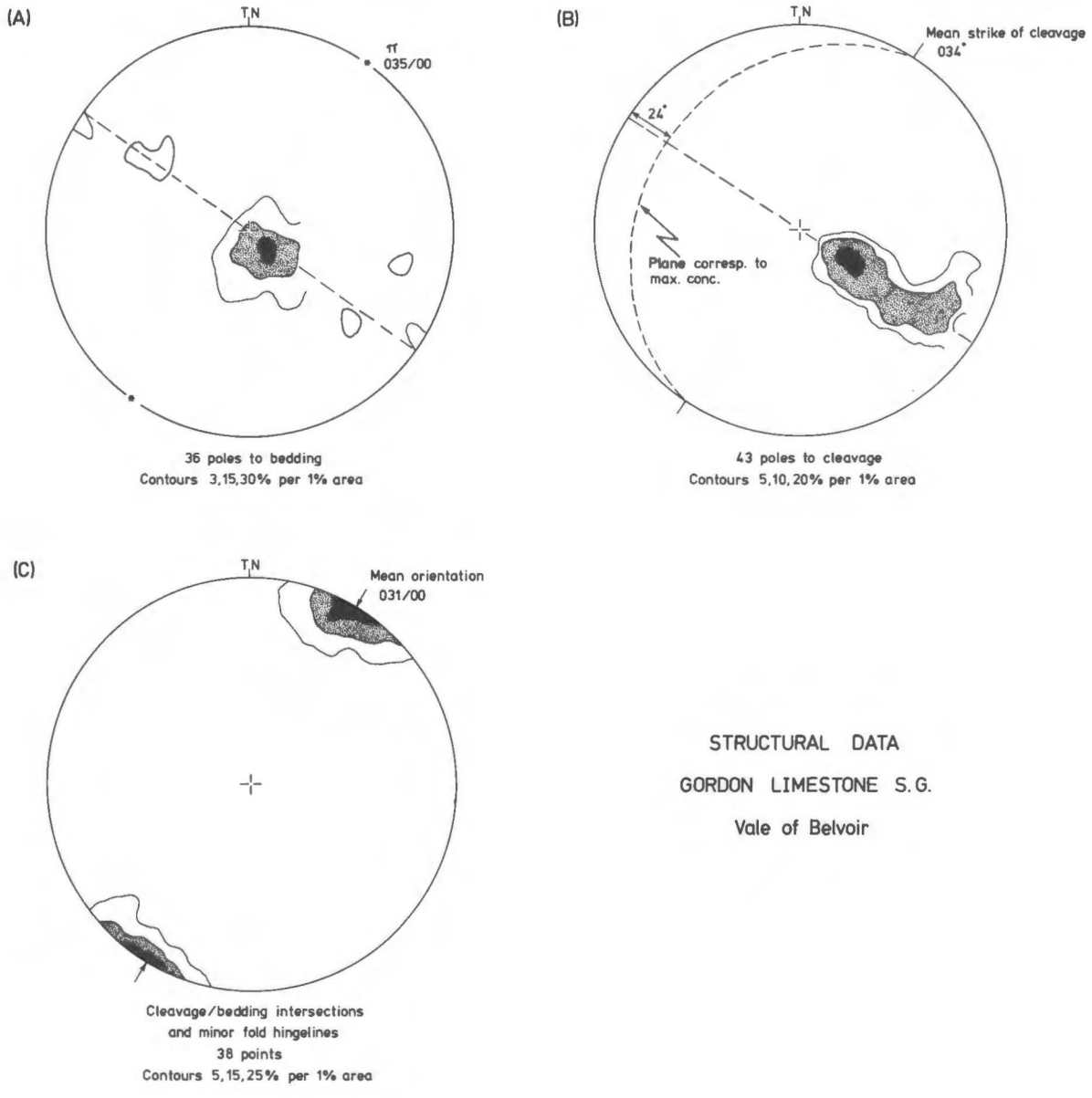
(A)
T.N
π
035/00
36 poles to bedding
Contours 3,15,30% per 1% area
(B)
T.N
Mean strike of cleavage
034°
24°
Plane corresp. to
max. conc.
43 poles to cleavage
Contours 5,10,20% per 1% area
(C)
T.N
Mean orientation
031/00
Cleavage/bedding intersections
and minor fold hingelines
38 points
Contours 5,15,25% per 1% area
STRUCTURAL DATA
GORDON LIMESTONE S.G.
Vale of Belvoir

FIGURE 4.37

The dominant cleavage in the limestone is very strongly developed and strikes parallel to the trend of the statistically defined fold axis (see Fig. 4.37B). Its dip is variable but is always to the NW, reflecting the asymmetry of the overall structure. Most outcrops in the Vale of Belvoir are situated on the long SE limb of the main synclinal structure, such that cleavage and bedding both dip to the NW, the dip of cleavage generally being the steeper. Cleavage/bedding intersections and minor fold hinges cluster around a line which is very close to the statistically defined fold hinge (see Fig. 4.37C).

All of the structures described in the above paragraphs are correlated with the "Belvoir trend" of this study. The only evidence of other phases of deformation detected in the limestone in the Vale of Belvoir is the appearance of a second, later cleavage in calcarenite channel fill near 4073/3997. This cleavage is steeply W-dipping and strikes N, and is tentatively correlated with the "West Coast Range/Valentines Peak trend" of Williams (1978).

4.7.5 Minor structures in the Gordon Subgroup stratigraphic equivalent

Cleavage in the limestone in the Vale of Belvoir is very strongly developed, sometimes to the point where the attitude of bedding is difficult to ascertain. The degree of cleavage development is quite strongly controlled by lithology, being weakest in calcarenites and strongest in micrites with low dolomite content (see Fig. 4.38A). The cleavage in a typical micrite within Unit 1 of the Vale of Belvoir sequence (see Section 3.5.2 herein), consists of continuous *planar* tectonic stylolites with spacing of 2-5 mm, and strong grain preferred orientation of microcrystalline calcite in the micrite matrix comprising the microlithons between the stylolites. The closest analogy in the terminology of Powell (1979), is "smooth disjunctive cleavage" (see

FIGURE 4.38

A. Control of cleavage development by lithology in limestone of the Gordon Subgroup strat. equiv., Vale of Belvoir. Dolomicrite above, calcarenite below.

B. Thin planar calcite veins parallel to cleavage in limestone of the Gordon Subgroup strat. equiv., Vale of Belvoir. Section vertical and normal to cleavage/bedding intersection.

S_0

S_1

FIGURE 4.38A

0.5 m

S_0

S_1

FIGURE 4.38B

5 cm

Fig. 4.6 herein). At the highest stages of cleavage development in the micrites, thin syntectonic calcite veins which are exactly parallel to cleavage are occasionally present (see Fig. 4.38B). As seen on the cleavage surface, these veins sometimes have a fibrous fabric, the grain preferred orientation forming a lineation which plunges down the dip of the cleavage.

The acute cleavage-bedding angle at most outcrops in the Vale of Belvoir has resulted in skewed final geometry of bedding-parallel diagenetic stylolites, due to the considerable flattening strain associated with the cleavage development. The example illustrated in Fig. 4.39A is from an outcrop near 4073/3999, and is estimated to represent an average degree of cleavage development for the limestone in the area. An estimate of two-dimensional strain was obtained from this photograph by assuming initial orthogonal symmetry of the stylolite, and that the cleavage trace represents the maximum principal extension direction on the section. The two-dimensional strain ratio obtained was $R_s = 3.30$. The section is vertical and normal to the strike of the cleavage. It also contains the grain elongation lineation seen on the cleavage surfaces. By assuming that the section represents an XZ section of the finite strain ellipsoid, the following limits can be placed on the three-dimensional strain:-

Assumption	X	Y	Z
Plane strain (const.vol.)	+82%	0	-45%
Pure flattening (const. vol.)	+49%	+49%	-55%
Intermediate between plane strain and pure flattening.	+67%	+18%	-49%

Minor folding is only rarely seen at outcrop scale in the

FIGURE 4.39

A. Skewed bedding - parallel diagenetic stylolite in limestone of the the Gordon Subgroup strat. equiv., Vale of Belvoir. Section normal to cleavage/bedding intersection.

B. Folded bedding - parallel chert lens in limestone of the Gordon Subgroup strat. equiv., Vale of Belvoir. Section normal to cleavage/bedding intersection.

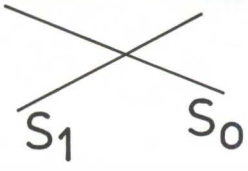

FIGURE 4.39A

5 cm

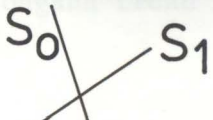

FIGURE 4.39B

5 cm

limestone. However, useful statistical hingeline data were obtained from small folds in discontinuous elongate chert lenses which are concentrated at certain horizons. These lenses appear to have behaved relatively competently during the strain. Fig. 4.39B shows an example from the steeply SE-dipping common limb of an asymmetric SE-verging medium scale fold (half-wavelength ~30 m) near 4065/3989. Cleavage is at a high angle to bedding on this limb, resulting in symmetric small scale folds in the chert lenses.

4.8 STRUCTURAL SYNTHESIS

4.8.1 Summary of results of structural mapping

The critical structural features recognized on each of the structural maps are summarized in the following notes. For brevity, the major stratigraphic units are referred to by the dominant lithology which they contain, i.e.,

Mt. Read Volcanics/Dundas Group	:	volcanics
Denison Subgroup	:	quartzose clastics
Gordon Subgroup	:	limestone

Reference to the different trend groups of structures is as follows:

Loongana trend	:	WNW	
Belvoir trend	:	NE-NNE	
Bonds Range trend:		ENE	
West Coast Range/ Valentines Peak trend	:	N	(Williams, 1978)
Deloraine/Railton trend	:	NW-NNW	(Williams, 1978)

Map 2 : Loongana

The Loongana trend is expressed in the limestone as an asymmetric

NNE-verging horizontal syncline, with associated axial plane cleavage which mostly dips steeply to the SSW. The relationship of this structure to other trends in the Black Bluff region is somewhat obscure due to lack of overprinting relationships in the Loongana area. However, the Loongana Syncline is transected by later NW-NNW trending faults, which are probably steep thrusts associated with the Deloraine/Railton trend of Williams (1978). The Loongana Syncline may be of the same generation as the synclinal structure in the Gordon Subgroup stratigraphic equivalent in the Gunns Plains area, some 11 km to the north-northeast. The latter structure is more gentle than the Loongana Syncline, with only minor cleavage development. However, the mapping of Hughes (1957) showed that the Gunns Plains Syncline has a horizontal axis trending 300° (as opposed to 290° for the Loongana Syncline), and displays similar asymmetry, with vergence to the NNE.

Map 3 : Smith Plains

Two generations of steeply dipping to vertical cleavage were recognized in the volcanics, belonging respectively to the West Coast Range/Valentines Peak trend (earlier) and the Deloraine/Railton trend (later). These two cleavages also occur in the quartzose clastics, together with upright folding on the same two trends. In the area immediately to the south of the major east-west trending belt of volcanics around Smiths Plains, the latter folding appears to have overprinted a pre-existing major limb which dipped SSE at ~20°. The relative timing of the two cleavages is the same in the quartzose clastics as that recognized in the volcanics.

Map 4 : Black Bluff

In a downthrown fault block of volcanics in the vicinity of 4100/4125, vertical cleavages of West Coast Range/Valentines Peak trend

(earlier) and Deloraine/Railton trend (later), are present. In the larger area of volcanics west and southwest of Mt. Tor, dominant vertical cleavage of West Coast Range/Valentines Peak trend shows overprinting relationships with earlier steeply SE-dipping cleavage of Belvoir trend, near 4059/4106.

In the quartzose clastics the dominant folding is on Belvoir trend, producing open upright horizontal to gently plunging folds with half-wavelengths of 1-2 km. However, cleavage of similar trend only begins to appear in the southern part of the map. Smaller scale upright folding on West Coast Range/Valentines Peak trend and Deloraine/Railton trend is also present. The most commonly developed cleavage is vertical and of West Coast Range/Valentines Peak trend, but later vertical cleavage of Deloraine/Railton trend is present in the north-eastern quadrant of the map.

Map 5 : Vale of Belvoir (north)

On the Black Bluff Range, two generations of cleavage have been recognized in the volcanics. The first is vertical to steeply NW-dipping with NE strike (Belvoir trend), while the second phase cleavage is vertical and of West Coast Range/Valentines Peak trend. The cleavage of Belvoir trend also occurs in the volcanics on Bonds Range, at the northern end of which it is overprinted by a later vertical cleavage of ENE strike (Bonds Range trend).

The dominant folding in the quartzose clastics is of Belvoir trend, represented by asymmetric SE-verging open horizontal NE-trending folds with 1.5-2 km half wavelength. However, dome and basin pattern on the Black Bluff Range is suggested to be due to interference of these folds with later cross-folds of West Coast Range/Valentines Peak trend.

On the other hand, dome and basin structure at the northern end of Bonds Range appears to be due to interference of folds of Belvoir trend with later crossfolds on ENE-trending axes (Bonds Range trend).

Map 6 : Vale of Belvoir (south)

The dominant cleavage in the volcanics on this map is vertical to steeply NW-dipping with NE strike (Belvoir trend). However, on the southern extension of Bonds Range this is overprinted by a second, later vertical cleavage of West Coast Range/Valentines Peak trend. Both cleavages also occur with the same relative overprinting relationship, in the quartzose clastics in the near vicinity.

The dominant folding in the quartzose clastics is again of Belvoir trend, although some anticlockwise rotation of axes (i.e., from NE to NNE) is evident relative to Map 5. Dome and basin structure is still present on the Black Bluff Range, and is attributed, as before, to interference of folds on Belvoir tend and West Coast Range/Valentines Peak trend. This is supported by the presence near Mayday Mt. of minor folds with NE-trending axes, which have visibly been refolded on N-trending axes.

The main structure in the limestone is a *strongly* asymmetric SE-verging horizontal syncline of Belvoir trend. The degree of asymmetry of this fold appears somewhat discordant with the structure in the underlying quartzose clastics, although the sense of vergence is the same. The dominant cleavage in the limestone is very strongly developed and strikes NE, with variable dips to the NW. Near 4073/3997 it is overprinted by later steeply W-dipping cleavage of West Coast Range/Valentines Peak trend.

4.8.2 Structural sequence

The various overprinting relationships described above have lead to recognition of the following suggested sequence of development of structures on the different trends:

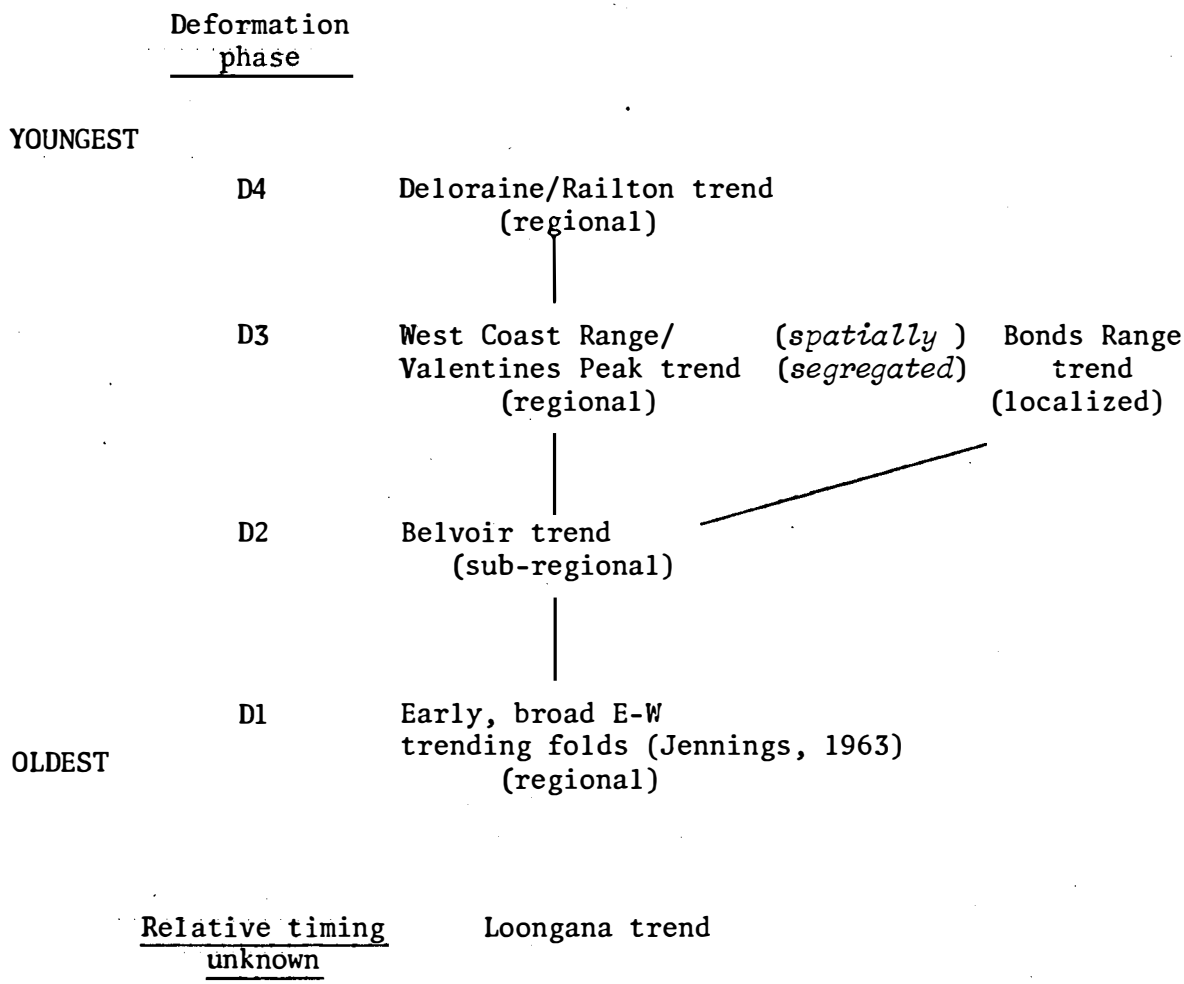

The folds identified as representing D1 have been included in the proposed sequence mainly for completeness, in recognition of the conclusions of Jennings (1963) and Pike (1964). In actual fact, the existence of D1 in the Black Bluff region has proven difficult to evaluate because of the structural complication caused by overprinting during the later folding. A possible remnant of this fold tend may be the approximately E-W trending N-dipping limb in the quartzose clastics

forming the northern boundary of the area of volcanics west of Mt. Tor (see Fig. 3.1).

The relationship of the Loongana trend to the other sets of structures is problematical. Previous workers (e.g., Pike, 1964) appear to have considered the Loongana Syncline and the Gunns Plains Syncline to the north to be a result of D1. However, the mapping carried out during this project has demonstrated that the axis of the Loongana Syncline actually trends WNW. This also appears to apply to the Gunns Plains Syncline. The degree of cleavage development in the limestone at Loongana also seems out of character with the supposed gentle development of the D1 structures (Jennings, 1963).

The Bonds Range trend appears to be only locally developed, and as such its place in the structural sequence has only been determined relative to the Belvoir trend. However, the gently SSE-dipping limb which appears to predate folds on West Coast Range/Valentines Peak trend and Deloraine/Railton trend in the quartzose clastics southwest of Smiths Plains, may have been a result of folding on Bonds Range trend. If this interpretation is correct, the latter may fit between the Belvoir trend and the West Coast Range/Valentines Peak trend in the structural sequence.

The dating of the Tabberabberan Orogeny in Tasmania must now be reconsidered in terms of the recognized structural sequence. Unfortunately the relationship between the deformation phases recognized herein and those defined by Burns (1963, 1964) in the Eugenana area is by no means clear. To reiterate, Burns demonstrated the existence of horizontal to gently plunging N-trending open upright folds with associated axial plane cleavage (his "Eugenanan phase"), and later superposed oblique cross-folds on NE trends (his "Loongana phase"). These two trends are parallel respectively to the West Coast Range/Valentines Peak trend (D3)

and Deloraine/Railton trend (D4) distinguished herein in the Black Bluff region, but are in the *reverse* order of development. Williams (1978) in fact appears to have correlated the "Eugenanan phase" of Burns with the Deloraine/Railton trend (see Map 1). However, in the present author's opinion it is unclear at present whether Williams' correlation is correct, or whether in fact the "Eugenanan phase" is of the same generation as the West Coast Range/Valentines Peak trend, as redefined herein. Resolution of this problem may require further detailed structural mapping in the region between Eugenana and the area covered during this project.

4.8.3 Conditions of deformation

A detailed analysis of pressure/temperature conditions in the Cambro-Ordovician rocks during the Devonian deformation has fallen outside the scope of this project. However, some potentially useful palaeotemperature data was obtained by Burrett (1978) on the basis of conodont geothermometry. This was based on work of Epstein *et al.* (1977) who showed that conodonts darken with increasing temperature due to carbonization of organic material in the interlamellar spaces. They established five "Colour Alteration Indeces" defined by progressively darkening colour, the maximum C.A.I (indicated by black colour) corresponding to temperatures of >300°C. Epstein *et al.* showed that pressure does not affect C.A.I., but that water in combination with confining pressure and heat considerably retards carbonization. This implies that the temperatures derived from C.A.I. should be regarded as minimum values.

Burrett (*ibid.*) measured C.A.I. values of medium sized specimens of elements of 4 conodont genera from the base and top of the Gordon

Subgroup in northwest, west and southwest Tasmania. Specimens from the Vale of Belvoir, Loongana and Claude Creek were supplied by the present author. Contoured geographical plots of C.A.I. showed positive geographic correlation with:

(1) The Palaeozoic sedimentary troughs surrounding the Tyennan Geanticline.

(2) The Devonian fold trends superimposed on the Palaeozoic rocks.

(3) The degree of deformation of the strata (samples from Mole Creek, Claude Creek, Eugenana, Loongana and the Vale of Belvoir all yielded conodonts with C.A.I.5).

There was no apparent correlation with distribution of Tertiary basalts, Jurassic dolerite or Devonian granites, all of which were recognized as possible heat sources. There was also no apparent correlation with the greatest thickness of Ordovician and post-Ordovician rocks. For example, C.A.I.5 was obtained from the base of the limestone at Eugenana (441434, Map 1) and Flowery Gully (486431), where the Ordovician limestone sequences and the younger cover rocks are relatively thin. In fact, at Eugenana, post-Ordovician rocks are unlikely to have exceeded 1 km in thickness. Even at Mole Creek, a maximum figure (and probably an over-estimate) for the greatest depth of burial of the base of the limestone is 4.5 km, yet the conodonts yielded C.A.I.5, indicating temperatures of >300°C.

The conodont C.A.I. data therefore suggested that high temperatures had occurred at fairly shallow depths principally in central northern Tasmania. Burrett (*ibid.*) suggested that this was due to high heat flows which developed in this region in post-Middle Ordovician times. In fact, the high heat flow was thought to be Devonian and most likely Middle

Devonian because:

(1) Lower Devonian conodonts which are unlikely to have been buried to any appreciable depth were metamorphosed.

(2) A C.A.I. gradient was observed between conodonts at the *stratigraphic* base and top of *dipping* limestone sequences at several localities. If the high heat flow was post-tectonic such gradients should not be observed.

(3) K-Ar ages of Upper Devonian granites have not been reset by subsequent heat induced leakage of argon. However, K-Ar ages of Upper Cambrian granites have been reset to Ordovician ages (McDougall and Leggo, 1965), presumably by Devonian heating.

The alternatives to the suggestion of high surface heat flow are:

(1) Great thicknesses of Cambrian and Siluro-Devonian sediments have been eroded from the region.

(2) Concealed granites are present at shallow depths beneath the localities where the high C.A.I. values were obtained.

(3) Conodont geothemometry needs revision, and in particular a pressure effect must be postulated.

In the absence of evidence for extensive removal of cover sediments, and/or experimental work suggesting that C.A.I. values can be altered by pressure, Burrett proposed very high heat flows for the north of the state at all crustal levels during the Devonian. It is herein suggested that this high heat flow (with consequent temperatures of >300°C at the base of the limestone at Mole Creek, Claude Creek, Eugenana, Loongana and the Vale of Belvoir) was pre- and syntectonic with the Tabberabberan deformation.

CHAPTER 5

STRAIN ANALYSIS

5.1 INTRODUCTION

This chapter describes the results of a separate subsection of the overall project, involving an examination of the use and abuse of certain established methods of geological finite strain analysis. The end result has been twofold:-

(1) An increased awareness of the potential errors involved in the use of certain established methods of geological strain analysis.

(2) Some degree of quantification of the flattening strain associated with single-phase cleavage development in limestones of the Gordon Subgroup stratigraphic equivalent.

The occurrence of potentially useful ellipsoidal strain markers (oolites and oncolites) near the base of the Gordon Subgroup stratigraphic equivalent at Mayberry (vicinity of 422398, Map 1 and Fig. 3.1) was exploited by Seymour (1975), as part of a general structural analysis of the Ordovician rocks in the area. As noted in Section 4.1 herein, the geological structure of the area is dominated by upright horizontal to gently plunging folds on WNW to NW trends, with associated development of steeply dipping to vertical single-phase cleavage with similar strike (see Figs. 4.1 and 4.2). This dominant folding and cleavage development is correlated with the "Deloraine/Railton trend" of Williams (1978). The results presented in this chapter represent an extension of the strain analysis work of Seymour (1975) based on further sampling of the Mayberry localities, and also of similar material at the base of the Gordon Subgroup stratigraphic equivalent at Claude Creek (4295/4065, Fig. 3.1). In addition

to the analysis based on oolites and oncolites, an attempt has also been made to evaluate the potential use of stromatolites as tectonic strain markers, using material from the Mayberry area.

Strain analysis methods which utilize ellipsoidal markers such as oolites and oncolites are critically dependent on knowledge of the initial pre-tectonic fabrics of the markers. The importance of this fact was clearly demonstrated by Boulter (1976). A desire to quantify this dependence lead to the initiation of a pilot project, the results of which are summarized in Section 5.2 herein. These results are of general importance in the field of geological strain analysis, and have been published in conjunction with Dr. C.A. Boulter (Seymour and Boulter, 1979). A reprint of this paper is included herein, and it is recommended that it be read in conjunction with Section 5.2.

It was originally anticipated that quantitative finite strain analysis could also be carried out using somewhat less satisfactory markers, which were potentially available in the stratigraphic equivalents of the Mt. Read Volcanics/Dundas Group and Denison Subgroup in the Black Bluff region. The possible markers included lapilli and altered felspar phenocrysts in the volcanics, and argillaceous chert clasts in Lithofacies III of the Denison Subgroup stratigraphic equivalent. However, examination of the microfabrics of these rocks quickly indicated that the anticipated markers had behaved relatively incompetently, absorbing much more strain than the bulk of the rock. In the case of the volcanics this was apparently due to the fact that the lapilli and felspar phenocrysts had been selectively altered during the hydrothermal alteration (see Fig. 4.14 for an example). It was therefore expected that the analysis would grossly overestimate the true bulk strain which these rocks had suffered. The volcanics also presented the further problem

that the most favourable lithologies were not situated in structurally simple areas. Thus, the total strain ellipsoid in lapilli tuffs and agglomerates of Unit 4 of the Smiths Plains sequence (described in Section 3.2.2 herein) was estimated to be a product of an initial bedding-parallel diagenetic compaction fabric, and two episodes of tectonic flattening, associated with the development of two cleavages with an acute angle between them. The accurate separation and quantification of three such strain components appeared impossible with existing methods. For the reasons listed, it was therefore decided to restrict the quantitative finite strain analysis to the structurally simple limestone sequences at Mayberry and Claude Creek.

5.2 A CRITIQUE OF STRAIN ANALYSIS METHODS APPLICABLE TO SUITES OF ELLIPTICAL MARKERS

5.2.1 Introductory comments

The flattening strain apparently associated with the formation of rock cleavage in a natural material domain has usually been described in terms of a finite strain ellipsoid, a triaxial (in the most general case) ellipsoid representing the change in shape of an initial reference sphere within the material domain, due to a homogeneous strain. Reference to this finite strain ellipsoid herein, uses the system adopted by Ramsay (1967, Chapter 4) and Wood (1974, p. 373), whereby the three mutually perpendicular principal axes of the ellipsoid are labelled X, Y and Z, where $X \geq Y \geq Z$.

In order to uniquely determine the orientation and magnitude of the principal axes of the finite strain ellipsoid in three dimensions, determinations are required of the two-dimensional strain ratios on any three non-parallel sections of the ellipsoid (Ramsay, 1967, p. 147).

However, calculations are simplified if the three cuts are made mutually perpendicular and parallel to the principal places, XY, YZ and XZ. If this procedure is followed, an internal check of consistency on the two-dimensional strain ratios measured on the three sections is provided by the relationship:

$$(X/Y) \cdot (Y/Z) = (X/Z)$$

This method, of course, requires the initial identification of the orientations of the principal planes in hand specimen, and the first step usually taken is to assume that the cleavage is parallel to the XY plane of the finite strain ellipsoid. Later determination of whether or not this assumption was justified depends on the accuracy and precision of the strain analysis method(s) used to determine the orientation and axial ratio of the finite strain ellipse on each of the three two-dimensional sections.

The next step after the cutting of the plane parallel to cleavage (assumed XY plane) is the identification in the cleavage plane, of the direction of the X principal axis of the finite strain ellipsoid. This may be assumed to be parallel to a marked grain elongation lineation in the matrix of samples with strongly developed cleavage. However, at low strain states such a lineation on the cleavage plane may be rather weak and ill-defined. In such cases resort may be made to syntectonic quart and/or calcite fibrous overgrowths ("beards") on clastic grains, and to syntectonic veins with fibrous structure. In situations where the strain history has been rotational, the fibrous crystals in these structures often have curved geometry, similar to that shown in Fig. 5.1A. Wickham and Elliott (1970), Wickham (1973), Durney and Ramsay (1973), Phillips (1974) and Wickham and Anthony (1977) have equated the growth direction of such fibres at each increment of growth with the X axis of

FIGURE 5.1

A. Syntectonic quartz-calcite overgrowth with curved fibre geometry. Vertical section perpendicular to cleavage on a fold limb in limestone of the Gordon Subgroup strat. equiv., Mayberry. Approximate XZ section of tectonic finite strain ellipsoid. Spec. No. UTGD 44350. XPL.

B. Syntectonic calcite-quartz fibre vein with straight fibre geometry, as seen on cleavage-parallel section of same rock as in A., above. Approximate XY section of tectonic finite strain ellipsoid. Spec. No. UTGD 44350. XPL.

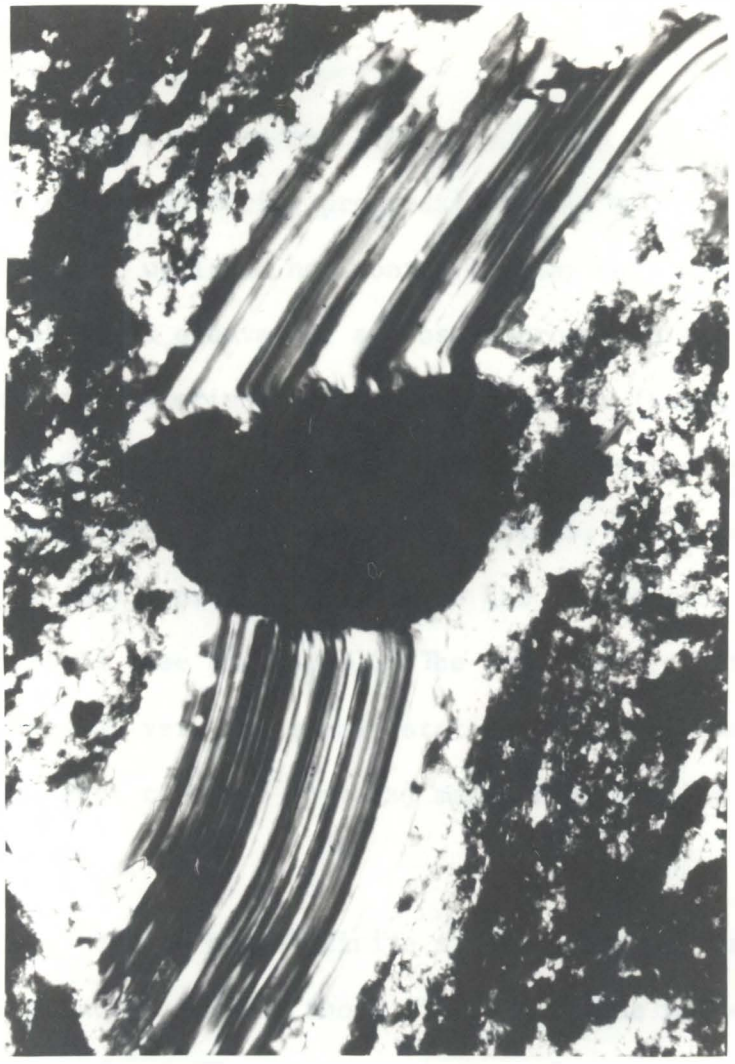

FIGURE 5.1A

0.1mm

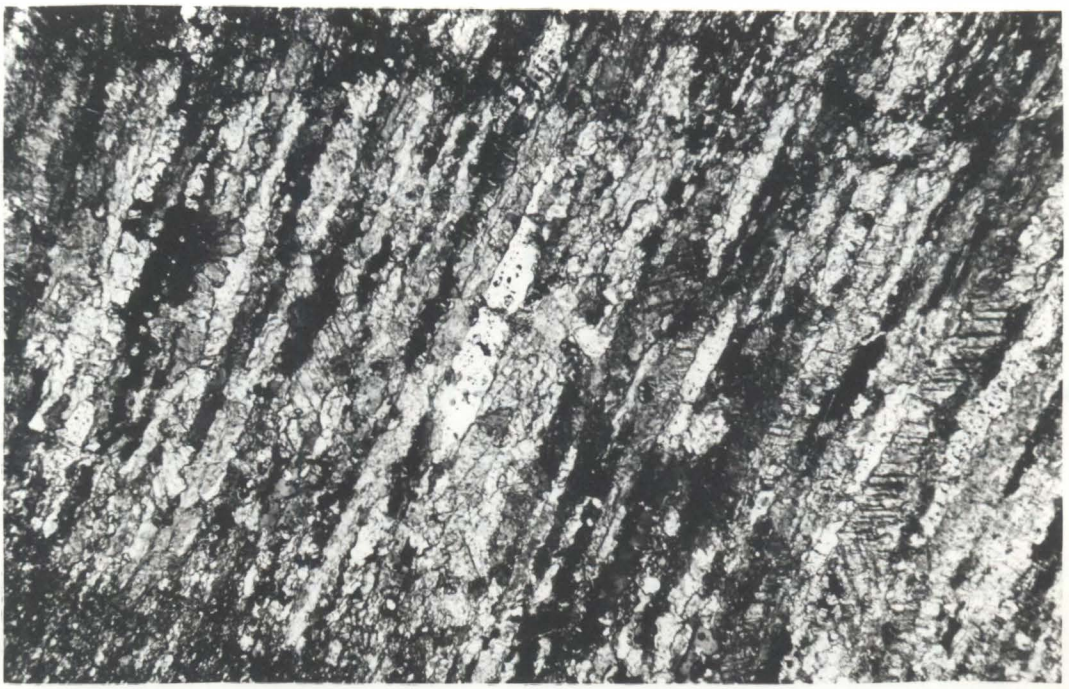

FIGURE 5.1B

0.2mm

the *incremental* strain ellipsoid. Curved fibres may thus preserve a partial or complete record of the changing relative orientation of the incremental strain ellipsoid during progressive deformation. However, in situations of simple, upright, horizontal folding with associated development of axial plane cleavage , a close approach to irrotational two-dimensional strain histories may be expected on XY (assumed cleavage-parallel) sections. Therefore, where the fibres are observed to be straight and constant in orientation throughout such sections, it appears reasonable to assume that they approximately define the X direction of the *finite* strain ellipsoid (see Fig. 5.1B). The appearance of fibrous overgrowths and veins at very low strain states (i.e., well below the strain at which distinct cleavage appears) makes them particularly useful in this regard.

Once the X direction of the finite strain ellipsoid has been identified in the manner described above, it is a simple matter to orient cuts parallel to the XZ and YZ principal planes. In the case of small markers such as oolites, thin sections are then made parallel to all three cuts. If possible, all of the thin sections are positioned close to the corner produced by the intersection of the three mutually perpendicular cuts, thus minimizing effects of inhomogeneous strain on the scale of the specimen. When using oncolites as markers, the same principle operates but larger areas are needed, and photographs of polished sections are generally used.

Following determination of the orientations of the principal planes XY, YZ and XZ and the cutting of sections parallel to them, the next part of the problem involves derivation of the axial ratios and orientations of the finite strain ellipses on each two-dimensional section. In early strain analysis studies (e.g., Cloos, 1947, 1971), such deter-

minations were made based on the assumption that the two-dimensional sections of the marker particles were all initially close to circular in the unstrained state (the equivalent assumption in three dimensions being that the marker particles were all originally close to spherical). Thus, the finite strain ratio in each section was taken to be equal to the mean of particle axial ratios. However, if the assumption of originally circular marker particles is exactly correct, and the usual assumption of homogeneous strain on the scale of the sample also holds, then all of the deformed particles in a two-dimensional section will have identical long axis orientations and axial ratios. The geometry of each deformed particle will be a replica of the finite strain ellipse in the section. In fact, Cloos (*ibid.*) recognized variable orientations (which he termed "fluctuation") of the long axes of the deformed oolites he measured, which immediately throws some doubt on the assumption. The "fluctuation" was observed to decrease with increasing strain ratio, in two-dimensional section.

The assumption of initially spherical markers may be applicable to certain objects, the most notable being reduction spots in slates (e.g., Wood, 1971, 1974). However, in most geological situations, the pattern of cross-sections (approximated to ellipses) of markers seen on any one of the three principal planes represents a modification of a two-dimensional section of an initial sedimentary or post-diagenetic fabric (with variable initial axial ratios and orientations) by the superimposed shape changes represented by the strain ellipse (with assumed constant axial ratio and orientation), in the plane. The problem at this stage therefore reduces to the separation of two effects, one due to initial fabric and the other to superimposed tectonic strain.

5.2.2 The methods

The strain analysis methods of Dunnet (1969), Mimran (1976), Shimamoto and Ikeda (1976) and Robin (1977), are designed for use on two dimensional sections of suites of strained elliptical markers, whose fabric was random in the unstrained state. The first of these is essentially a graphical method, which in the present author's experience is less sensitive to small deviations from the assumption of initially random fabric than are algebraic methods, of which the other three quoted are examples. The Dunnet method has been found to operate satisfactorily for the strain analysis of oolites in the Gordon Subgroup stratigraphic equivalent.

The Rf/ϕ method of two-dimensional strain analysis described by Dunnet (1969) is essentially an extension of theory developed by Ramsay (1967, pp. 209-211). Mathematical equations are derived which define the final shapes and orientations of any two-dimensional suite of elliptical particles with *initially random axial ratios and orientations*, after a finite homogeneous strain:-

$$\phi = F(Ri, Rs, \theta)$$

$$Rf = F(Ri, Rs, \phi)$$

$$\text{Cos } 2\phi = \frac{Ri(Rf^2+1)(Rs^2+1) \pm 2(Ri^2+1)RsRf}{Ri(Rf^2-1)(Rs^2-1)}$$

where

Ri = initial undeformed particle axial ratio

Rf = final deformed particle axial ratio

Rs = finite strain axial ratio

θ = angle from the Ri long axis to the maximum principal extension direction in the section

ϕ = angle from the Rf long axis to the maximum principal extension direction in the section

$$(-90° \leq \theta \text{ or } \phi \leq +90°)$$

This equation relates the two measurable parameters Rf and ϕ of each particle to its initial shape ratio (Ri) and the strain ratio (Rs). For set values of Ri and Rs the locus of Rf/ϕ will reflect only variation in the initial orientation (θ) of the particles. Therefore, a suite of particles of constant initial shape but variable orientations will have, after deformation, Rf/ϕ parameters lying on a hyperbolic curve around the finite strain value (Fig. 5.2). If the initial elliptical shapes had variable ratios Ri, the points on the Rf/ϕ graph will cover a field whose outer boundary is the Rf/ϕ locus corresponding to the highest Ri values in the undeformed distribution. Substitution of specific values of Ri and Rs into the above equation enables construction of a set of theoretical Rf/ϕ curves which can then be directly compared to Rf/ϕ plots of measured data; the curves are plotted on log/linear paper. Some useful corollaries of the mathematics of the Rf/ϕ method are:-

(1) Curves can be constructed which pass through the value of Rs on the ϕ = 0 line on the Rf/ϕ graph, and which split the field of plotted data points in two, with 50% of the points above and 50% below the curve (provided that the assumption of an initially random fabric is valid). The equation of the curve is:

$$\phi = \tfrac{1}{2} \operatorname{artan} [2Rs\ (Ri^2 - 1)/(Ri^2 + 1)(Rs^2 - 1)]$$

This curve can be used as an independent check on the best-fit Rf/ϕ curve.

(2) The maximum and minimum values of Rf (for a given Ri and Rs) are:

$$Rf\ max = Rs\ Ri$$

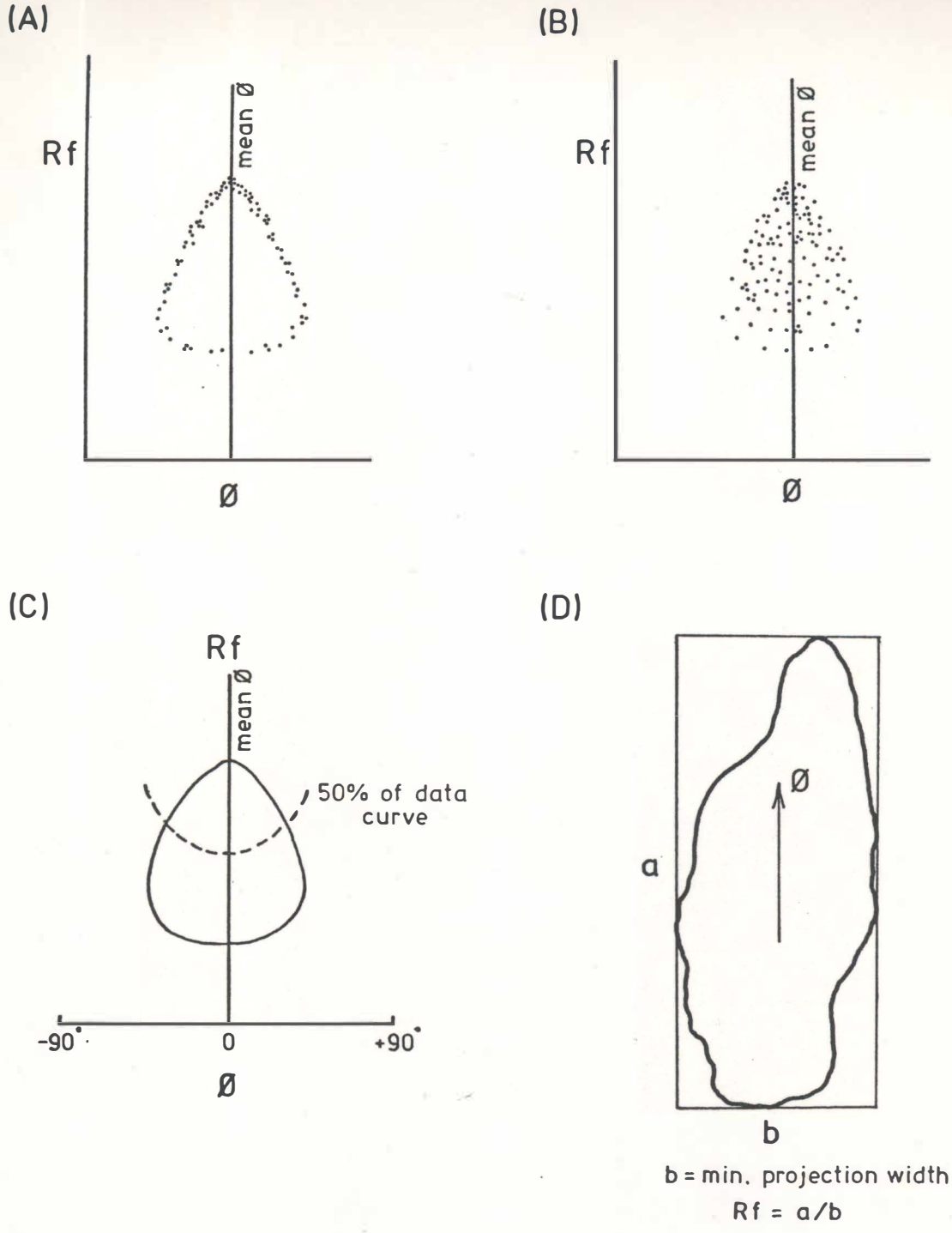

FIGURE 5.2

A. Dunnet (1969) Rf/ϕ plot of deformed elliptical particles which had random initial orientations and constant initial axial ratios.

B. As for A, but particles had randomly variable initial axial ratios.

C. Rf/ϕ graph showing 50% of data curve.

D. Measurement method for irregular particles.

$$Rf\ min = Rs/Ri$$

(3) The logmean of the Rf values is a better approximation to Rs than is the arthmetic mean of Rf (as used by Cloos, 1947, 1971).

The Dunnet method also permits the definition of criteria which should hold if the assumption of random initial fabric is valid. These criteria are:

(1) The mean of the ϕ values should correspond to the orientation of the maximum principal extension direction on the section.

(2) There should be no plot asymmetry about the maximum principle extension direction, i.e., there should be an equal number of data points to the left and right of this direction on the Rf/ϕ plot.

(3) Once the best-fit Rf/ϕ curve has been visually chosen to enclose the field of data points, there should be an equal number of points above and below the corresponding 50% of data curve.

It should be noted at this point that criteria (1) and (2) may also hold in situations where the principal extension direction is parallel or orthogonal to the trace of a preferred orientation which existed in the initial fabric. Such situations may arise, for example, in the hinge zones of upright horizontal folds with axial plane cleavage, where an initial preferred orientation parallel to bedding was present. Orthogonality of the bedding trace and maximum principal extension direction may be expected on both XY and XZ sections in this case. However, criterion (3) would not hold if the initial fabric was strongly anisotropic.

Preliminary strain analyses carried out on oolitic limestones from the Gordon Subgroup stratigraphic equivalent at Mayberry by Seymour (1975), supported the conclusion that the approach of the initial

pretectonic fabrics of these rocks to ideal randomness was such that no major errors would be expected in the use of the Dunnet (1969) Rf/ϕ method. The evidence on which this conclusion was based is:

(1) Mean ϕ was always within 5° of the assumed maximum principal extension direction (cleavage trace on XZ and YZ sections) in each principal plane. The small deviations observed could be equally due to errors in positioning the principal plane cuts as to any real deviation. In fact, it was estimated that the shape fabric defined by the oolites themselves could have been confidently used to *define* the cut orientations, an observation which may be useful in the analysis of low strain samples with only incipient cleavage development.

(2) All of the Rf/ϕ plots were highly symmetric left and right of mean ϕ.

(3) The strain values derived from the Rf/ϕ curve and 50%-of-data curve fits were always within 0.05 Rs units of each other. For either curve fit the *precision* of the method was also to 0.05 Rs, in the range up to Rs = 3.00.

(4) The error in the three-dimensional closure, X/Y . Y/Z = X/Z, was always $\leq$ 10%. In half of the analyses the misclosure was < 5%.

In addition to this indirect evidence bearing on the nature of the pretectonic fabrics, Seymour (1975) also carried out some limited examination of the fabrics of actual unstrained oolitic and oncolitic limestones, analogous to the lithologies used for strain analysis in the Gordon Subgroup. Due to the lack of suitable completely undeformed material in the Subgroup in Tasmania, these samples were all taken from localities elsewhere, carefully chosen to avoid any possibility of

tectonic modification. This followed on from the work of Boulter (1976), and is discussed more fully in Section 5.2.3 herein.

As concluded above, the method of Dunnet (1969) appears to operate satisfactorily for strain analysis of the oolitic lithologies. However, Seymour (1975) also began some preliminary work using oncolites as markers. These are larger, more irregular particles which often appear to have nucleated on quite elongate cores, e.g., blade-shaped pieces of fossil shell debris. It was therefore anticipated that some tendency towards anisotropic depositional fabric may have been developed, and that the assumption of random pretectonic fabric may break down. In fact, this quickly became obvious during the first attempt to use the Dunnet method on such an oncolitic limestone. Not only were the plots markedly asymmetric, with mean ϕ deviating considerably from the cleavage trace on XZ and YZ sections, but the three-dimensional misclosure was also too high to be acceptable. It was particularly notable that on the cleavage-parallel section (XY), a lineation defined by preferred orientation of long axes of oolites in the matrix, deviated from the mean orientation of oncolite long axes. It was therefore concluded that some pretectonic anisotropy, such as bedding-parallel preferred orientation or imbrication, had been present in the fabrics of these rocks. Initial attempts at application of a more appropriate strain analysis method used the graphical technique introduced by Elliott (1970) which is described below.

The main advantage of the Elliott method over that of Dunnet (1969) is that it hopes to enable the recognition, in the deformed state, of the presence of various different pretectonic sedimentary fabrics. It is therefore not tied solely to the assumption of initially random fabric. The changes in shape of individual ellipses in the distribution

during homogeneous strain are described by the equations:-

$$\cosh 2\varepsilon f = \cosh 2\varepsilon s \cosh 2\varepsilon i + \sinh 2\varepsilon s \sinh 2\varepsilon i \cos 2\theta$$

$$\tan 2\theta = \frac{\sinh 2\varepsilon i \sin 2\theta}{\sinh 2\varepsilon s \cosh 2\varepsilon i + \cosh 2\varepsilon s \sinh 2\varepsilon i \cos 2\theta}$$

where θ and ϕ are defined as before but transformations of the form $\varepsilon f = \frac{1}{2} \ln (Rf)$ have been introduced. The second equation was listed incorrectly by Elliott (1970, p. 2235, eq. 24), and has been recalculated to its correct form here.

Elliott introduced a polar graph on which axial ratio/orientation data for undeformed or deformed fabrics may be plotted. On this graph, the angles (θ or ϕ) are doubled and plotted as positive or negative according to a convention (Elliott, 1970, p. 2222), while εi or εf as defined above is used as the measurement of radial distance from the origin of the graph. The plotted points are contoured using the method of Mellis (as described by Flinn, 1958), with a size of measuring circle which "best brings out the character of the distribution".

On theoretical grounds, Elliott predicted that various different non-random undeformed sedimentary fabrics would have certain characteristic shapes on the polar graph (Table 5.1). For example, a moderately developed bedding-parallel fabric would, in the undeformed case, yield a plot with a delta or heart shape if measurements were made on a section perpendicular to bedding. The bedding trace would be the line of bilateral symmetry of the plot, and the intersection of the bedding trace and the base of the delta would lie at the origin of the graph (Elliott, 1970, p. 2225).

Elliott demonstrated that the shapes of plots of the theoretical initial distributions listed in Table 5.1 would retain their distinguishing features to quite high strains, the field of points simply moving

TABLE 5.1

(Elliott, 1970)

	Orientation: Axial Ratio Combination	Initial Pattern on Polar Graph	Final Pattern after Strain on Polar Graph
	Circular particles	Point Maxima at origin	Point Maxima away from origin (to right hand half of Grid)
	Random orientation of various axial ratios	Circular pattern of contours centered at origin	Egg-shaped pattern. (off-center to right, line of symmetry parallel Maximum Principal Direction)
Unimodal Orientation	Thin ellipses most strongly oriented	Deltas and hearts; base and line of symmetry at origin	Deltas and hearts (off-center to right)
Unimodal Orientation	Extreme orientation of various axial ratios	Linearly elongate maxima one end at origin	Linearly elongate maxima, both ends off origin (to right hand side of grid)
Unimodal Orientation	Extreme orientation of identical axial ratios	Point Maxima not at origin	Point Maxima, could be anywhere
Bimodal Orientation	90° between modes	Cigars and ovals; centered at origin	Cigars and ovals (off-center to right)
Bimodal Orientation	Less than 90° between modes	Banana centered at origin; mirror line passing through origin	Banana, off-center to right

to the right on the plot and rotating slightly, while the bedding trace moves clockwise in the upper half of the plot and anticlockwise in the lower half, according to the formula.

$$e^{2\varepsilon s} = \tan \theta'/\tan \phi' \qquad \text{(after Harker, 1885)}$$

where

ϕ' = post-strain orientation of bedding trace

θ' = pre-strain orientation of bedding trace

Theoretically, then, the shape characteristics of the contoured Elliott plot for the deformed state should allow identification of the type of pre-tectonic fabric which was present, and location of the position of the *initial circle point* (ICP), the point which would have plotted at the origin of the graph in the undeformed state. If this point can be accurately identified, the true maximum principal extension direction (which may not necessarily be parallel to its previously assumed orientation) in the plane being considered is given by the line joining the origin to the ICP. The finite two-dimensional tectonic strain is given by the distance between the origin and the ICP. If all three principal planes are analyzed, the check of three-dimensional internal consistency may be rewritten,

$$\varepsilon s(XY) + \varepsilon s(YZ) = \varepsilon s(XZ)$$

The main problem with the use of the Elliott strain analysis method, as discussed by Boulter (1976), is that when actual examples of tectonically unmodified sedimentary fabrics are measured in two-dimensional sections and plotted on the graph, the geometric characteristics of the resultant contoured plots often do not compare well with those predicted on theoretical grounds by Elliott. For instance, the ICP on such a plot commonly lies *inside* the contoured distribution in cases

where, from the plot shape, it would have been expected to be at the edge. The obvious inference is that when interpreting an Elliott plot of data from a naturally deformed rock, the ICP may be erroneously located in attempting to fit the contoured pattern to one of Elliott's theoretical types.

The problem described above appears to be aggravated by the fact that the shape of the Elliott plot is more sensitive to small aberrations than is the Rf/ϕ graph of Dunnet (1969). Thus, Seymour (1975) found that when the same oolite data which had been satisfactorily analysed using the Rf/ϕ technique was replotted on the Elliott graph, the contoured plot shapes generally did not conform to the simple egg-shape representing a deformed random distribution (see Table 5.1). The plot outlines were often quite irregular, as shown in the examples given by Boulter (1976, Fig. 4). Seymour found that reasonable correspondence with the results from the Rf/ϕ method could be obtained by placing the ICP's at the geometric centres of the plots, but this effectively involved ignoring the original guidelines on the use of the method listed by Elliott. The Elliott method was therefore abandoned in favour of the Rf/ϕ technique for strain analysis of oolites.

For strain markers other than oolites, the procedure evolved by Seymour (1975) in conjunction with C.A. Boulter involved a modification of the Elliott method as originally proposed. An important conclusion was that the uncertainties caused by the vagaries of initial sedimentary fabrics were such that the orientation of the maximum principal extension direction on each section of the deformed material being analyzed, must be *assumed* as an *a priori* control on the position of the ICP on the Elliott probe. This immediately destroys the usefulness of the method for *determining* the principal plane orientations. Thus, it is

proposed that the angular differences between the XY principal plane and slaty cleavage reported by Etheridge and Lee (1975), based on Elliott strain analysis of quartz dolomite-rich blebs, are just as likely to be a result of poor knowledge of the pretectonic fabric of the markers as to any actual lack of correspondence between the two planes.

Given this control on ICP position, the modified Elliott technique essentially involves artificial removal of the tectonic strain effect from the data until a closest match is attained with an estimated *optimum* or *average* tectonically unstrained fabric for that particular lithology. The matching involves three different parameters, namely, ICP position with respect to the edge of the contoured plot, bedding trace orientation, and actual plot shape. These are listed in *decreasing* order of importance. Destraining may be carried out either graphically using the Shape Factor Grid produced by Elliott (1970), or algebraically by using transformation equations in inverse form. The "average unstrained fabrics" are determined by examination of analogous material from sites carefully chosen to avoid effects of tectonic strain. The technique described was used for the preliminary strain analysis of deformed oncolitic limestone from Mayberry by Seymour (1975) and for analysis of deformed quartz arenites from the metamorphosed Precambrian of Tasmania by Boulter (1978). The publication of Tobisch *et al.* (1977) indicates that they independently evolved an almost identical modification of the Elliott technique, applied in their case to accretionary and lithic lapilli, breccia fragments and ashflow ellipsoids in pyroclastics and reduction spots in mudstones. The whole procedure was incorporated into a computer program.

Due to the uncertainties associated with the use of the Elliott method, it was hoped that independent checks could be provided by analysing

the same data sets using alternative techniques. As originally proposed, the strain analysis methods of Dunnet and Siddans (1971) and Matthews *et al.* (1974) were designed to handle fabrics which in their unstrained states were characterised by preferred orientation parallel to bedding, and the former method should also allow analysis of fabrics which were imbricate. The two methods are thus based on more restrictive assumptions than the Elliott method , and a desire to estimate potential errors caused by various deviations from these assumptions formed the basis for the tests outlined in Section 5.2.4 herein.

The Dunnet and Siddans (1971) strain analysis method is designed for use with data from sections on which the maximum principal extension direction is known; orientations of elliptical markers are referred to this direction. The basic principle of the method is that ellipse axial ratio-orientation data, measured on a two-dimensional section in the strained state, will plot on an Rf/ϕ graph as a field of points which is either symmetric or asymmetric about the principal strain direction (taken as the cleavage trace on sections perpendicular to cleavage). For example, on a section where the cleavage trace is at an oblique angle to the bedding trace, the preferred orientation of ellipse long axes will lie somewhere between the cleavage and bedding traces, if the suite of elliptical markers had an original bedding-parallel fabric. This is due to the different mathematical equations governing the behaviour of a passive marker line (the bedding trace) vs. elliptical particles during strain (see previous discussion of the Elliott method). In cases where the bedding trace is parallel or perpendicular to the principal strain direction, the Rf/ϕ plot will be symmetric even when the initial fabric had a preferred orientation parallel to bedding. For this reason, the method cannot be used when cleavage is parallel or perpendicular to

bedding, and becomes imprecise when the angle between bedding and cleavage traces is very low or very high. The degree of symmetry of the plot is tested by examining the distribution of the field of points about the vector mean of ellipse orientations (vector mean of ϕ values, VMPHI) and the logmean of ellipse axial ratios (LOGMEAN Rf). According to Dunnet and Siddans, a symmetric plot implies that the fabric was random in the unstrained state, and the Dunnet (1969) method may be employed to determine the strain ratio. If the plot is asymmetric about the principal strain direction, the data are progressively mathematically unstrained in small increments, and the plot symmetry is re-examined after each increment. In the case where the fabric in the unstrained state had preferred orientation parallel to bedding, a stage will be reached where the field of points is symmetric about the bedding trace (i.e., plot symmetry is maximized and VMPHI = BDGTRACE, with the latter condition taking priority). The strain which has been removed at this point is taken as the required strain ratio. Material in which the orientation of bedding is unknown may be analyzed by determining the stage at which plot symmetry is maximized (e.g., Roberts and Siddans, 1971), while fabrics which were imbricate in the unstrained state may be accommodated by giving maximization of plot symmetry priority over VMPHI = BDGTRACE. All of the described computations were incorporated into the FORTRAN IV computer program STRANE by Dunnet and Siddans.

The strain analysis method of Matthews *et al.* (1974) is also intended for use with data from sections on which the principal strain direction is known. A feature of the method is that it is based on an alternative mathematical treatment which enables application of a test for an initially random fabric and calculation of the strain ratio, purely from calculations carried out on the axial ratio-orientation data

in the strained state. That is, no unstraining is required. The method is applicable to fabrics which were either random or bedding-symmetric in the unstrained state; fabrics which were imbricate, or which had some other non-random, non-bedding symmetric fabric in the unstrained state, cannot be used. Matthews *et al.* (*ibid.*) claim that deformed specimens without bedding traces can be analyzed, but, as this involves a further extension of untested assumptions, such a procedure must be considered unwise. Orientations of elliptical markers measured on sections of the strained material are referred to the bedding trace rather than the cleavage trace as in the Dunnet and Siddans method. The test for an initially random fabric (FORTRAN IV program XROT) as set up by Matthews *et al.*, involves moving the reference direction from parallelism with the bedding trace to 2° from the cleavage trace, all ellipse orientations being referred to the new reference. The reference direction is subsequently moved through 90° in steps of 2° in the quadrant that does not contain the bedding trace. At each position of the reference direction, a value of the parameter 'Rs' is calculated. If 'Rs' is invariant (or practically so) with position of the reference direction, a random fabric in the unstrained state is indicated and the invariant value of 'Rs' is the required strain ratio. If 'Rs' varies markedly with the rotation, and the assumption is made that the fabric in the unstrained state was bedding-symmetric, the strain ratio is the value of 'Rs' calculated when the bedding trace is the reference direction. Program XROT was modified slightly herein to rotate the reference through 180°, so that one of the positions would parallel the bedding trace to give the required strain value. The method of Matthews *et al.* also includes statistical estimation of the "error" (more correctly, the precision) in the strain determination due to the sample-size of

measured markers and the orientation of the reference direction. In the case where an initially random fabric is identified, the optimum value of the strain ratio is read off at the position of the reference direction where the calculated "error" is minimized.

5.2.3 Natural tectonically undeformed sedimentary fabrics

Figures 5.3 A-F are contoured Elliott (1970) polar graphs of axial ratio-orientation data measured on bedding-perpendicular sections of representative tectonically unstrained sedimentary rocks from a number of different localities. The trace of bedding on the section is used as the reference direction in all of the plots.

(1) Oncolitic limestone

Fig. 5.3A illustrates the fabric of small oncolites (maximum diameter ~12mm) in the Pea Grit (Jurassic) from the Cotswold Hills, England, where the regional dip is less than 1° and tectonic influence is negligible (Ager, 1956). The oncolites have mostly nucleated on plate-like pieces of fossil shell debris, resulting in relatively high axial ratios, of up to 3.5/1. The availability of completely weathered-out particles at this locality enabled some determination of the variation in their *individual* three-dimensional shapes. This is plotted in Fig. 5.4A, which is drawn in the form of the log-log triaxial strain graph used by Wood (1971, 1974) to record the shapes of tectonic finite strain ellipsoids, but with the $X \geq Y \geq Z$ principal axes replaced by $a \geq b \geq c$ of each individual particle. For comparison, the lower limit of the "field of slaty cleavage development" (Wood, 1971, 1974) is shown by the dashed line. The oncolite three-dimensional shapes are mainly in the oblate field, as is the mean shape (shown by the open circle). However there is a very wide range of shapes, and a few extremely

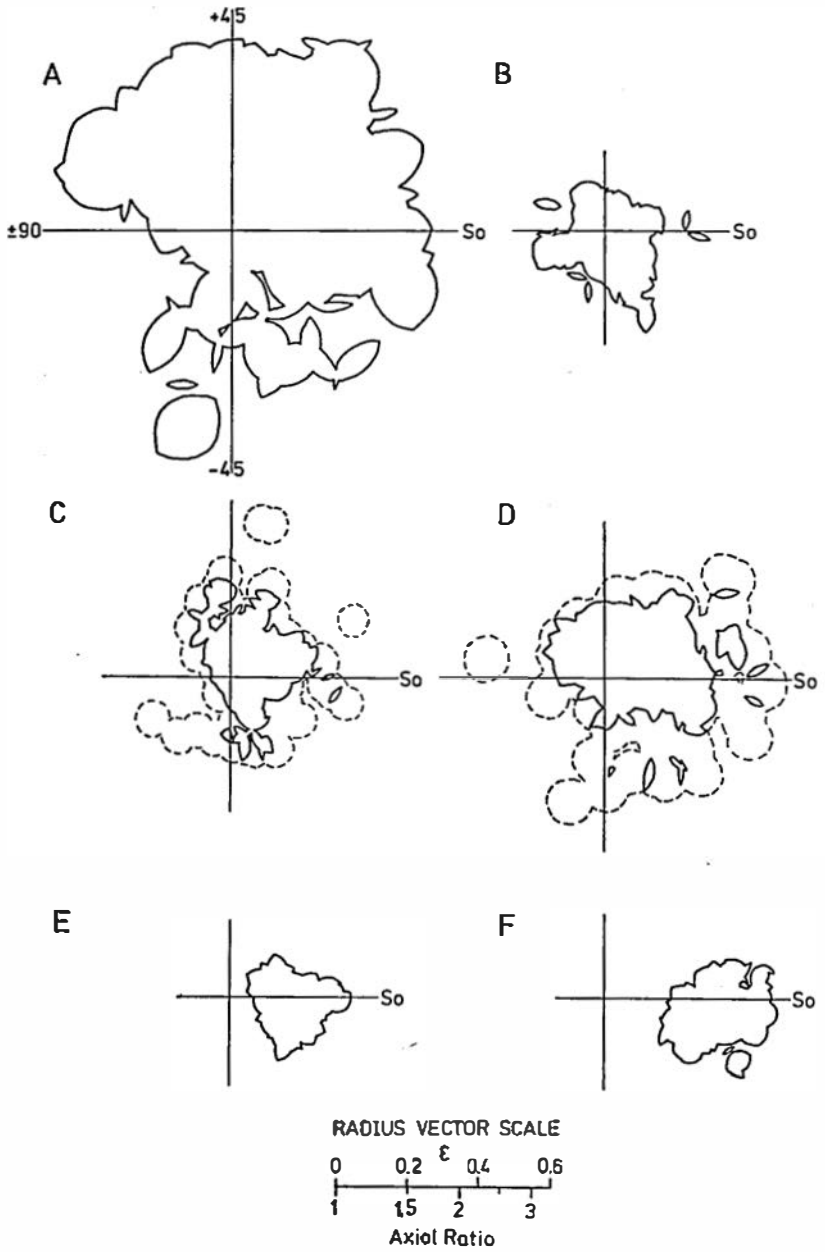

FIGURE 5.3

Contoured Elliott (1970) plots of the tectonically undeformed natural fabrics. All sections are bedding-perpendicular and the bedding trace is the reference. A. 75 small oncolites, 2 contour. B. 80 oolites, 2 contour. C. 80 quartz grains, Penrith Sandstone, 3 (solid line) and 1 (dashed line) contours. D. 75 quartz grains, Viking Sandstone, 3 (solid line) and 1 (dashed line) contours. E. 75 accretionary lapilli from the Brisbane Tuff, specimen (1), 2 contour. F. 76 accretionary lapilli from the Brisbane Tuff, specimen (2), 2 contour.

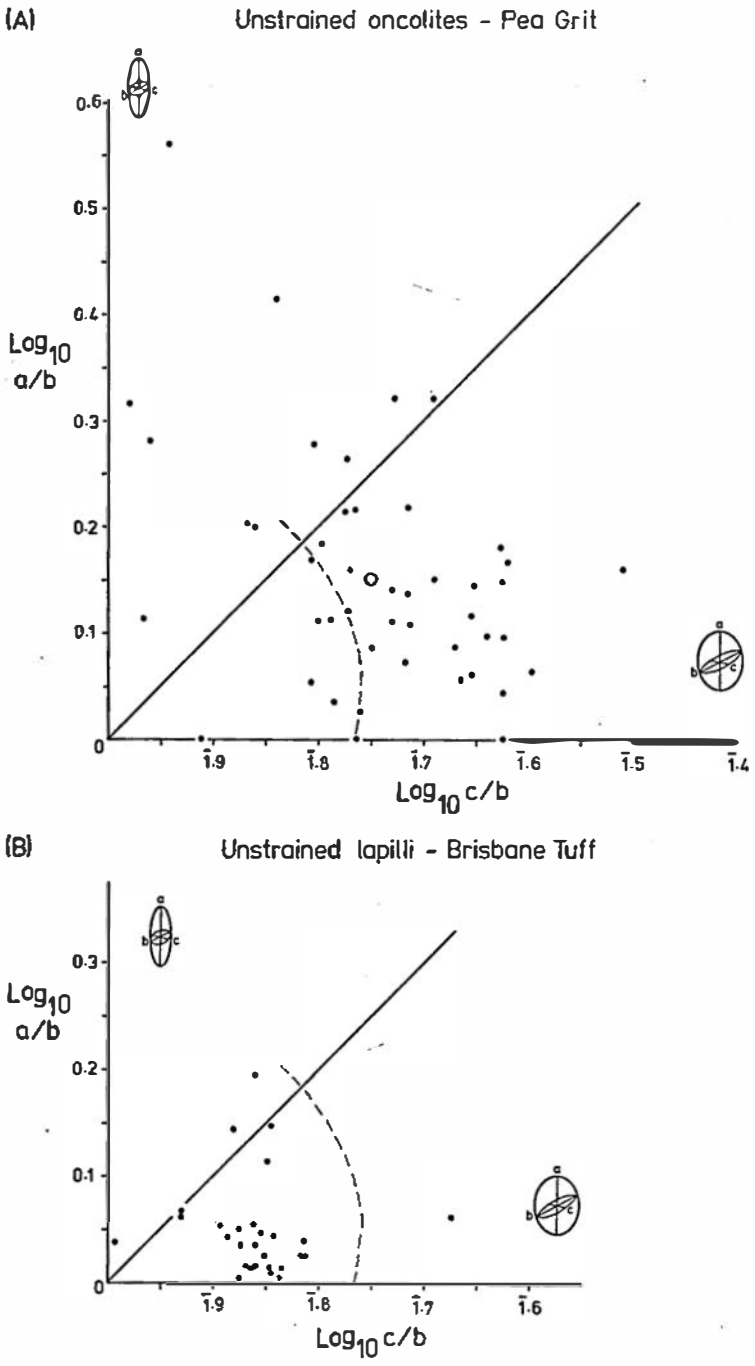

FIGURE 5.4 Individual three-dimensional shapes of natural tectonically undeformed ellipsoidal particles.

prolate particles occur. The problem of separating the tectonic strain effect from the original shape fabric effect in a deformed analogy of this rock may be foreseen from the overlap of unstrained oncolite shapes with the lower part of the field of slaty cleavage development.

The pattern on the Elliott plot in Fig. 5.3A is roughly delta-shaped with a line of symmetry at approximately +27° to the bedding trace and passing through the origin. It indicates the presence of a distinctly imbricate fabric. That is, most of the particle long axes are distributed in approximately a ±50° arc with respect to the line at +27° to the bedding trace. The pattern may be thought of as that representing a random fabric with a little under half of the points missing. The imbrication may have been partly due to the prevalence of particles with oblate three-dimensional shapes. It is notable that the origin of the graph (the ICP) falls *inside* the edge of the contoured plot. If the 2 contour shown is visually smoothed to a rough delta shape, the distance of the ICP inside the plot is approximately $\frac{1}{5}$ of the plot diameter along the symmetry lines, and about $\frac{1}{3}$ of the plot diameter along the horizontal axis of the graph.

The imbricate pattern was repeated on other bedding-perpendicular sections of oncolitic limestone from this locality, the ICP falling on average ⅛ of the plot diameter inside the plot edge along the line of symmetry. Sections parallel to bedding yielded similar sized and shaped plots, but with the ICP somewhat less off-centred, i.e., $\frac{1}{3}$ of the plot diameter inside the edge along the line of symmetry.

(2) Oolitic limestone

Fig. 5.3B is constructed from measurements of oolites, also in a specimen of Jurassic limestone from the Cotswold Hills. The section was cut in a direction down the dip of the foresets in a one

metre thick cross-bedded unit, in the hope that the most marked preferred orientations would be recorded. The point on the contour outline furthest from the origin represents axial ratios of approximately 1.8/1. The ICP is close to the geometric centre of the plot, but the contour outline is more irregular than the simple circular shape predicted by Elliott (1970) for a random fabric (Table 5.1 herein). Strictly, the plot represents a squat bimodal pattern with a dominant mode at -32° and a subsidiary mode at -80° to the bedding trace.

Measurement of fabrics of tectonically unstrained oolites from a number of different localities by both the author and C.A. Boulter (1978), has yielded contoured Elliott plots with similar dimensions to that in Fig. 5.3B, and with offsets of the ICP from the plot geometric centre varying between negligible and approximately ¼ of the plot diameter. An ICP positioned at or close to the plot edge, as suggested by the worked example of a tectonic strain analysis given by Elliott (1970, pp. 2230-2232), was only found on a single occasion. This was an "over-packed oolite" from the Upper Jurassic of Qatar, Arabia, illustrated by Wilson (1975, p. 431). A bedding-parallel preferred orientation in this rock was apparently due to diagenetic compaction. The plots of undeformed oolites can usually be almost completely enclosed within a circle about the origin of the Elliott graph with a radius representing particles with axial ratios of 1.50/1 (see Fig. 2 of Boulter, 1976). This is in agreeance with the Dunnet (1969) Rf/ϕ strain analysis of deformed oolites carried out by Seymour (1975), where the fields of data points on Rf/ϕ graphs were also neatly enclosed by standard curves representing the locus of particles with initial axial ratios of 1.50/1.

The work of Seymour (1975), and the results of the tests

reported in Section 5.2.4 herein, support the conclusion that minor fabric irregularities of the type indicated by the plot contour shape in Fig. 5.3B, do not lead to significant errors in the use of the Dunnet (1969) method. The same method also appears not to be seriously affected by the occasional small deviations of ICP's from Elliott plot geometric centres recognized in the analysis of actual unstrained oolites. This appear to be so because these deviations are small in absolute strain units. That is, the difference in the derived finite tectonic strain obtained by placing an ICP ¼ of the plot diameter in from the edge of an Elliott plot, versus placing it at the plot centre, is significant for an oncolite plot but generally not so for an oolite plot. All of these comments of course apply only to the Dunnet (1969) method. The algebraic methods of Dunnet and Siddans (1971) and Matthews *et al.* (1974) unfortunately appear to be far more sensitive to the described fabric irregularities of oolites.

(3) Quartz arenites

The depositional fabrics of quartz arenites might be expected to be markedly current-influenced, and therefore to display imbrication to varying degrees. Figures 5.3C and D (see also Boulter, 1976, Fig. 1) illustrate the characteristics of fabrics in bedding-perpendicular sections of the Permian Penrith Sandstone (northwest England; see Bennison and Wright, 1969, p. 263) and the Viking Sandstone (east of the Rocky Mountain Thrust Belt, Canada; see Zimmerle and Bonham, 1962). The two fabrics show apparent weak imbrication when the fairly high density three contour is examined; however, when all points are considered, as indicated by the one contour, the patterns are closer to bedding-symmetric. For the Penrith Sandstone, 47 points plot to the positive side of the bedding trace, and 28 to the negative side.

Corresponding figures for the Viking Sandstone are 41 and 30, reflecting the higher degree of symmetry seen on the Elliott plot.

The patterns of Figures 5.3C and D each represent a tendency towards an imbricate fabric, but the imbrication is considerably weaker than that in Fig. 5.3A.

(4) Accretionary lapilli tuff

This lithology, also referred to as pisolitic tuff, is one which has been considered to show the best approach to the assumption of an initial fabric characterized by preferred orientation parallel to bedding (see Dunnet and Siddans, 1971, example 3). The lapilli are thought to become easily flattened during diagenetic compaction, although Moore and Peck (1962, p. 191) noted that the shape fabric may be due to three factors, namely:

a) original formation of ellipsoidal lapilli which then naturally come to rest on their flat side;

b) flattening of lapilli on impact with the ground;

c) later flattening during compaction of the beds that contain the lapilli.

However, on the basis that most geologically Recent lapilli which have been described show little or no flattening, they concluded that factor c) was the most important.

In order to test the assumption concerning initial fabrics of these rocks, measurements were made on bedding-perpendicular sections of two specimens of the Triassic "Brisbane Tuff", from the banks of Tingalpa Creek at Castra, 19km east-southeast of Brisbane, Australia (Richards and Bryan, 1927). The marked difference in two-dimensional fabric on bedding-parallel and bedding-perpendicular sections of this material is shown in Fig. 5.5. The sediments at this locality are

FIGURE 5.5

A. Diagenetic compactional fabric as seen on bedding-perpendicular section of the Triassic Brisbane Tuff, Tingalpa Creek, Queensland. Two-dimensional compactional strain ratio on this section is 1.50/1 (0.20ε).

B. Same material as in A., but section is parallel to bedding. Note the isotropic two-dimensional fabric on this section.

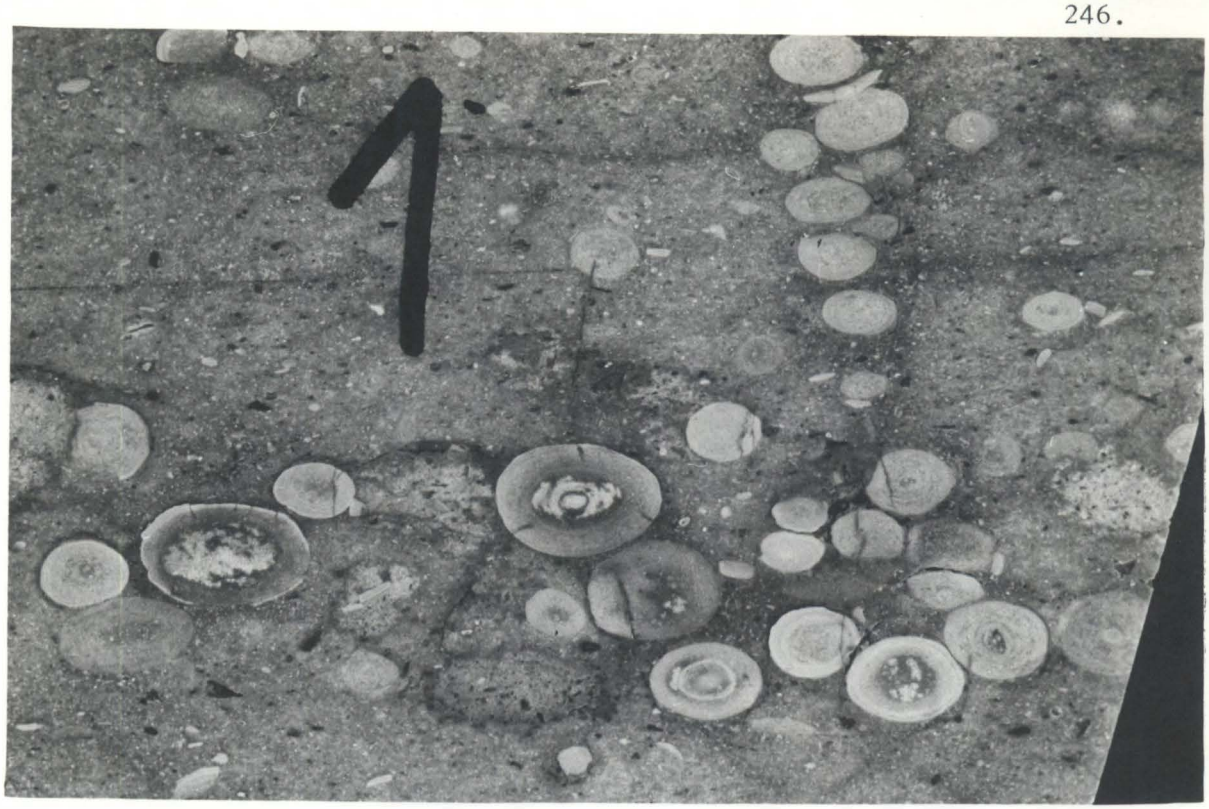

FIGURE 5.5A

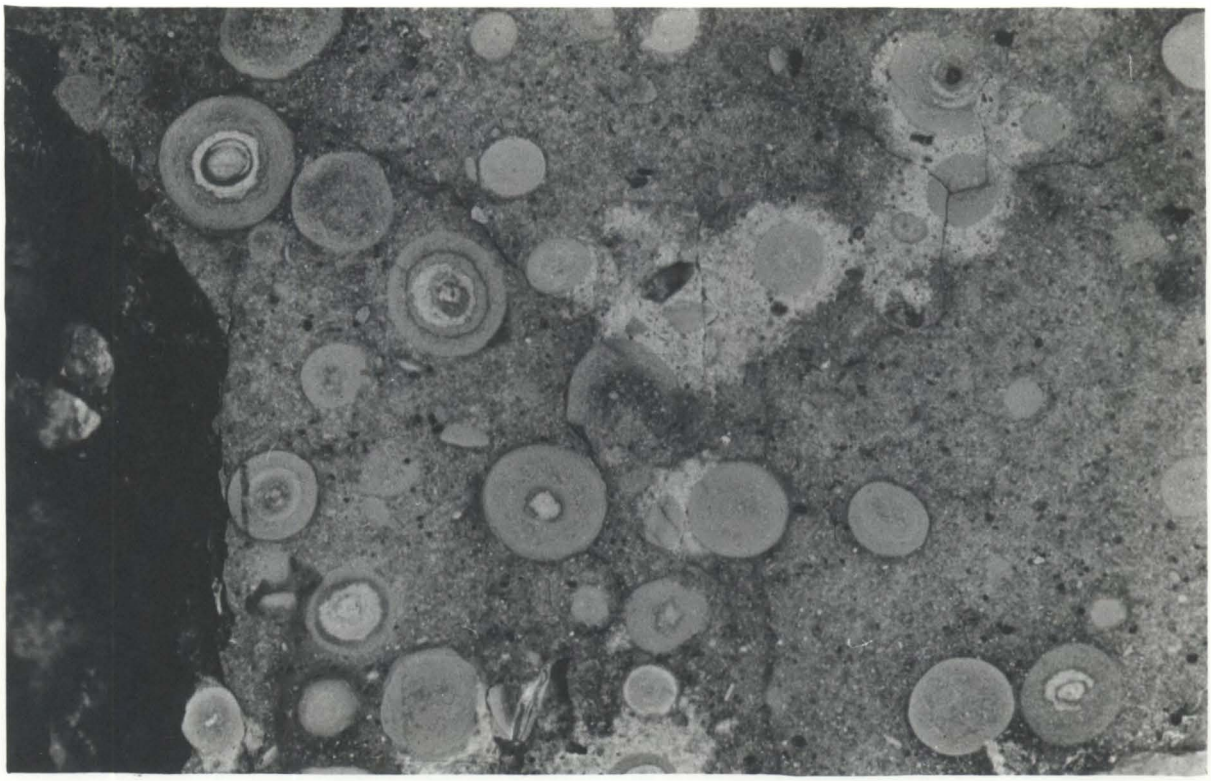

FIGURE 5.5B

flat-lying and show no evidence of tectonic modification. Accretionary lapilli are set in a matrix crowded with well-preserved glass shards; the fabric being very similar to that described by Sparks (1976). The more uniform three-dimensional shapes of the individual lapilli, as compared with oncolites, can be seen in Fig. 5.4B which was again constructed from measurements on completely weathered out particles.

Figures 5.3E and F are contoured Elliott plots of measurements of lapilli in the two bedding-perpendicular sections. The bedding trace on each section was identified by the presence of distinct lamination in the matrix. The most significant feature of the two plots is that they each show a small amount of asymmetry about the bedding trace. In fact, in Fig. 5.3E, 24 points plot to the positive side of the bedding trace, 3 points plot on the bedding trace, and 47 points plot to the negative side. The asymmetry is slightly more marked in Fig. 5.3F, where the corresponding figures are 20, 5 and 51. The observed asymmetry in the fabrics may be most readily attributed to some degree of initial dip. A situation is envisaged where the sediments are initially deposited non-horizontally (quite likely in this type of sedimentation) and subsequent compaction takes place vertically (in the strict sense, as it is gravity controlled), leading to a post-compaction fabric which is asymmetric about the depositional lamination defining bedding. The delta-shaped plot in Fig. 5.3E again demonstrates the problem associated with using plot shape to locate initial circle point. (cf., Elliott, 1970, and Boulter, 1976); the intersection of the line of symmetry and the base of the delta is 0.10 ε units from the origin.

If it is assumed that the precompaction fabrics of Figs. 5.3E and F were random, it is possible to estimate the two-dimensional finite compactional strain ratio for each of the two sections. Using

the standard Rf/ϕ curve technique of Dunnet (1969), and ignoring the slight asymmetry of the plots, the compactional strains were estimated to be 1.50/1 (0.20ε) and 1.95/1 (0.33ε) for Figs. 5.3E and F, respectively. These figures are somewhat high compared with those given by Tobisch *et al.* (1977) for two-dimensional compactional strains on bedding-perpendicular sections of tectonically undeformed accretionary lapilli tuffs, i.e., mean 0.14ε; standard deviation $\pm$0.06ε; total range 0.07-0.20ε. The latter data were based on a number of localities in North and Central America and Japan.

5.2.4 Tests of methods

In order to test the computerized strain analysis methods of Dunnet and Siddans (1971) and Matthews *et al.* (1974), either ideal theoretical or natural tectonically unstrained fabrics may be mathematically strained by set amounts and used as test input. It was considered preferable to use naturally occurring material in order to assess errors which may occur in the strain determinations if the natural fabrics in the unstrained state deviated from the assumptions made in the methods. To this end, the data derived from measurements of the natural unstrained fabrics described in the previous section, were input to a straining procedure built into programs XROT and STRANE, and which used the transformation equations:

$$\cosh 2\varepsilon f = \cosh 2\varepsilon s \cosh 2\varepsilon i + \sinh 2\varepsilon s \sinh 2\varepsilon i \cos 2\theta$$

(Elliott, 1970, p. 2235, eq. 23)

and

$$\cos 2\phi = \frac{\cosh 2\varepsilon s \cosh 2\varepsilon f - \cosh 2\varepsilon i}{\sinh 2\varepsilon s \sinh 2\varepsilon f}$$

(Dunnet and Siddans, 1971, p. 307, eq.1)

to superimpose set artificial two-dimensional tectonic strains on the

data, with the principal extension direction positioned at various angles to the bedding trace. These data were then subjected to normal XROT and STRANE analyses, and the "input" and "output" strain values compared. In order to cover the range of most commonly occurring geological situations, superimposed strain ratios of 1.4 and 5.0 were used with the principal extension direction set at angles of -75° to +75° (in steps of 25°) to the bedding trace in the unstrained state.

(1) Results - XROT

The results of the use of the straining procedure and program XROT on the six natural unstrained fabrics of Fig. 5.3 are shown in graphical form in Fig. 5.6A-F. Theta is the pre-strain angle between the bedding trace and the principal extension direction. The dotted lines are the "target" strain ratios, and the open or closed circles represent the strain determinations at each value of Theta. Statistically calculated precisions in the determined strain values are shown as bars; where no bars are given their length was greater than ±25% of the strain values. It was found that, for a particular set of data, and a given Theta, the percentage error in the strain determination (calculated from comparison of the "output" strain ratio with the target value) was independent of thetarget value. However, the largest errors tended to be associated with the least calculated precisions.

The smallest errors in the strain determination were obtained with the Cottswold Hills oolite, the Viking Sandstone and the lapilli tuff fabric of Fig. 5.3E. With these three fabrics, the errors in the strain values lay in the range of approximately ±10% of the target values. Apparently the latter two of these fabrics showed a sufficient degree of symmetry about bedding in the unstrained state for the method to work reasonably well. However, the program output for the oolite fabric of

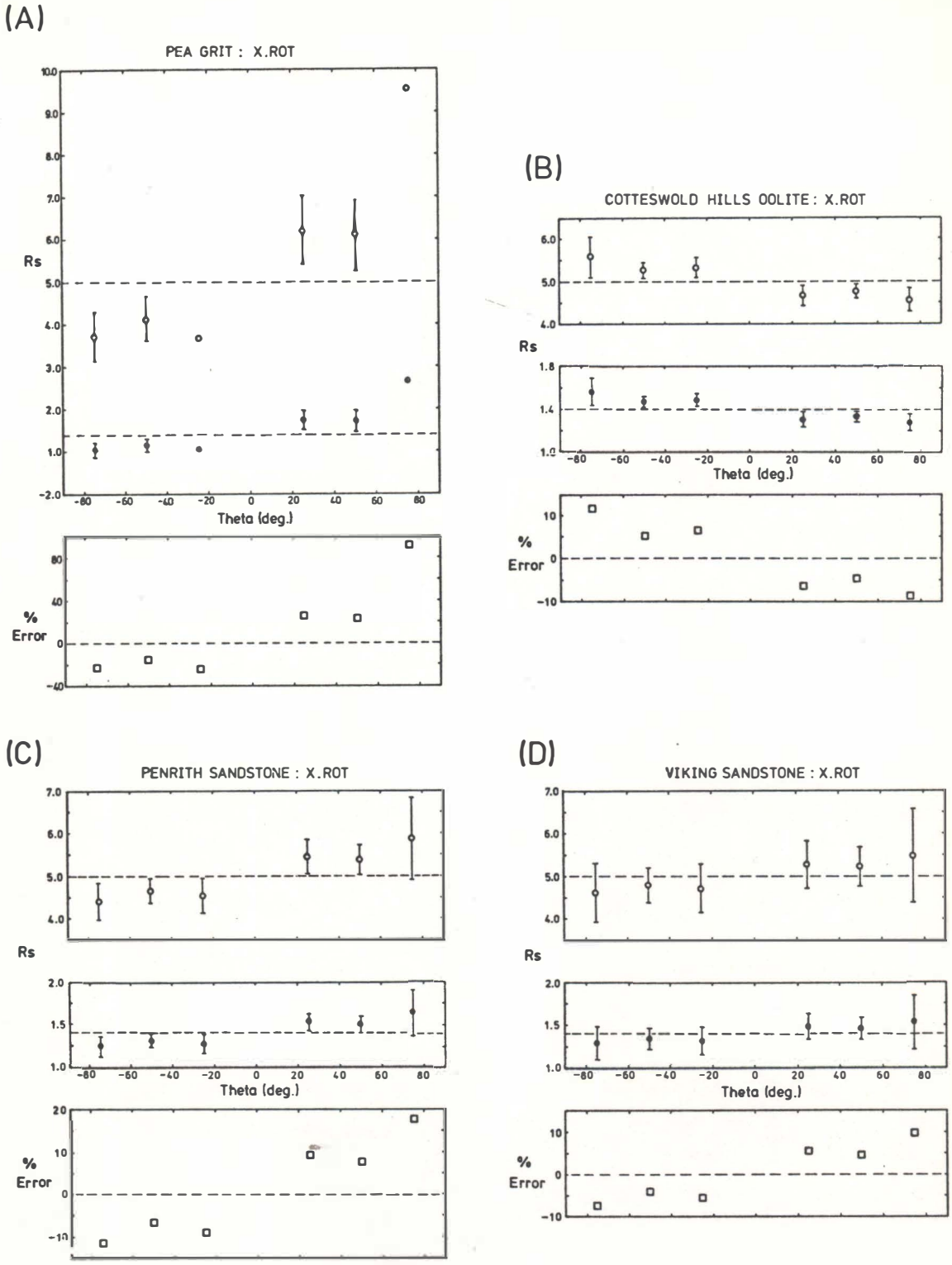

FIGURE 5.6 A - D

(see following page for caption)

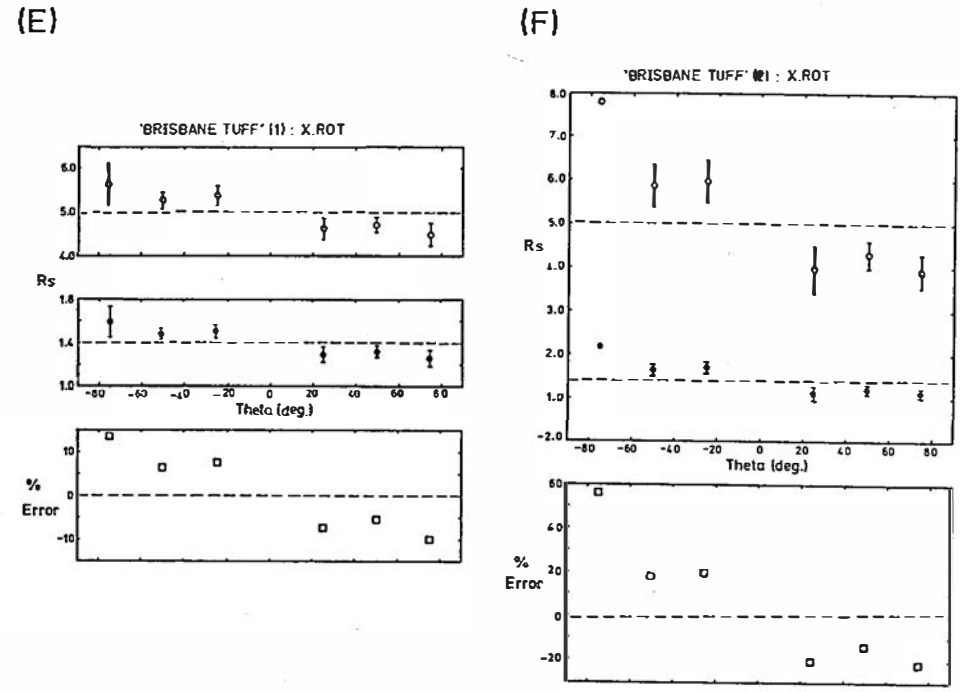

FIGURE 5.6

Results of use of the Matthews *et al.* (1974) strain analysis method, following artificial straining of the six natural fabrics. Target values shown by dashed line. Theta is the pre-strain angle between the bedding trace and the principal extension direction.

Fig. 5.3B proved somewhat difficult to interpret. It had been expected that the method would accept this fabric as a fair approximation to a random pattern, but examination of the variation of 'Rs' with rotation of the reference direction indicated otherwise. For instance, with Theta = -75° and a superimposed strain ratio of 1.4, 90° of rotation yielded a variation in 'Rs' from 0.75 to 1.99. The strain values plotted in Fig. 5.6B were therefore arbitrarily read off at the *Reference = Bedding trace* position, which amounts to the assumption that the initial fabric was bedding-symmetric. These values are compared below with those obtained by reading the values of 'Rs' corresponding to the optimum statistically calculated precisions, as recommended by Matthews *et al.* where an initially random fabric is identified. The figures in brackets are percentage errors in the strain determinations.

Target Rs = 1.4

Initial fabric assumption	Theta -75	-50	-25	25	50	75
Bedding-symmetric	1.56 (+11.4%)	1.47 (+5.0%)	1.49 (+6.4%)	1.30 (-7.1%)	1.33 (-5.0%)	1.28 (-8.6%)
Random	1.43 (+2.1%)	1.47 (+5.0%)	1.47 (+5.0%)	1.35 (-3.6%)	1.33 (-5.0%)	1.32 (-5.7%)

Errors in the strain determinations obtained using the fabric of the Penrith Sandstone (Fig. 5.3C) were rather similar to those resulting from the runs with the Viking Sandstone, except that an error of +17.5% resulted at one of the Theta values; at all other five positions errors were again in the approximate range of ±10%. Perhaps the least expected results were the rather large errors generated by the second lapilli tuff fabric (Fig. 5.3F). An error of +56% occurred at one value of Theta, with errors at the other five positions falling in the

range of ±20%. The largest errors in the strain determinations occurred, as anticipated, with the markedly bedding-asymmetric fabric of the Pea Grit (Fig. 5.3A). The absolute values of the errors were never less than 17% and varied up to +91%, a figure which is quite disastrous regardless of the "target" strain value. The strained states of the Pea Grit fabric could in theory be accurately analyzed by program STRANE, giving priority to maximization of plot symmetry. However, this was prevented by a basic mathematical problem which came to light during testing of program STRANE (see later discussion).

An elegant illustration of the failure of program XROT in analysis of a fabric which was imbricate in the unstrained state, can be obtained from a graph of 'Rs' against PHS, the angle between each successive reference direction and the principal strain direction. Such a graph is shown in Fig. 5.7 for the Pea Grit fabric, with Theta = -50° and a "target" strain ratio of 5.0. So' is the position of the bedding trace in the strained state, calculated using the formula given in the discussion of the Elliott (1970) method in Section 5.2.2 herein. Si' was calculated using the same formula, but represents the post-strain position of a line which was parallel to the preferred orientation of the elliptical markers in the unstrained state. It may be thought of as the post-tectonic position of the trace of the "plane of imbrication" of the markers. The interesting point is that the intersection of Si' with the 'Rs'/PHS curve in fact gives the correct tectonic strain ratio (5.0), as opposed to the intersection of the bedding trace So' with the curve, which gives a value of 4.14. The method has therefore treated this fabric as if it had a bedding trace parallel to the imbrication in the unstrained state. This conclusion is only of academic interest however, as there is no practical way of identifying the position of

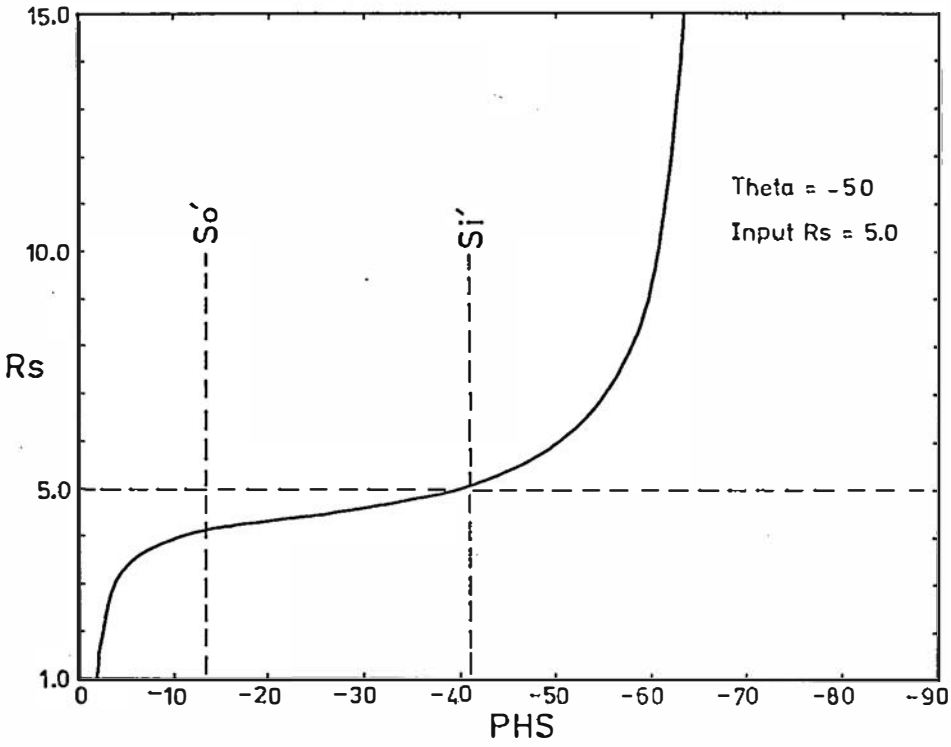

FIGURE 5.7

Graph of 'Rs' against PHS (the angle between each successive reference direction and the principal strain direction) for one of the XROT analyses using the oncolite fabric of the Pea Grit.

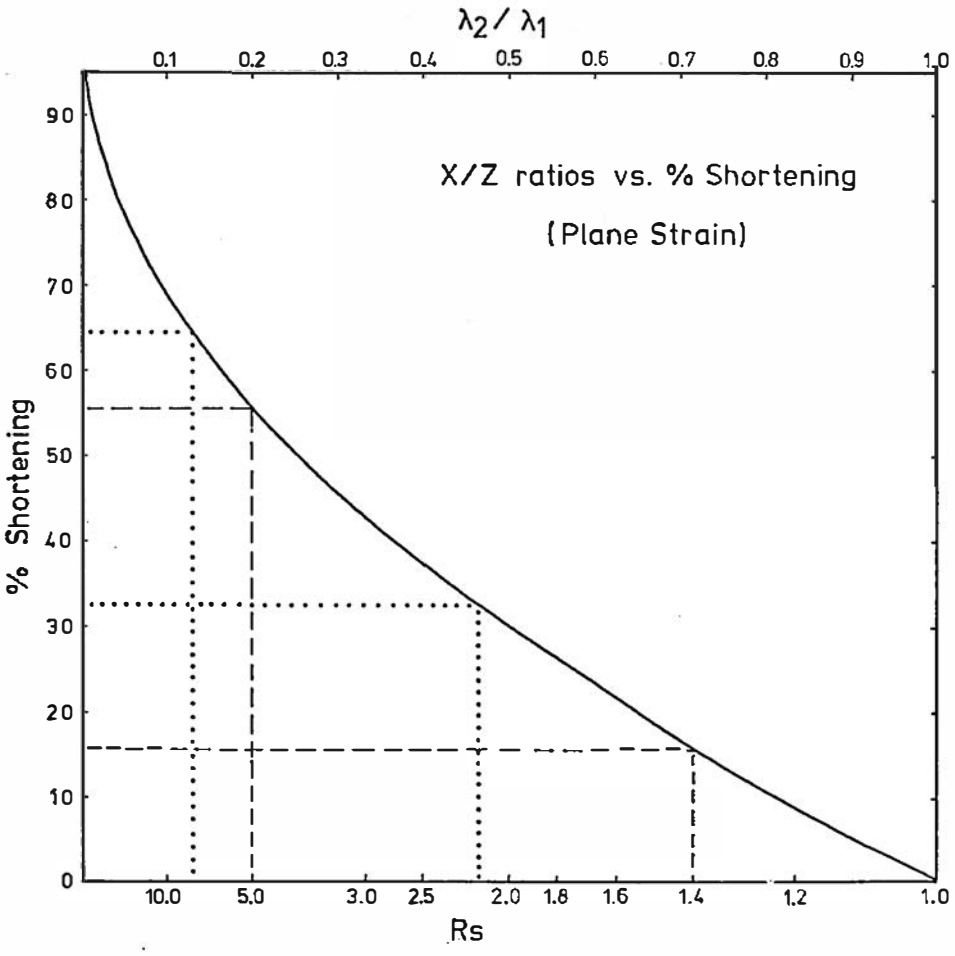

FIGURE 5.8

Graph of % shortening in X vs. X/Z strain ratios, assuming a plane strain condition. Strain estimate (dotted lines) and "target" values (dashed lines) are given for two XROT analyses using the fabric of the Brisbane Tuff, specimen (2).

Si' in the deformed material. That is, it is not a recognizable plane of anisotropy as is bedding, nor is it parallel to the preferred orientation of elliptical markers in the strained state.

Some understanding of the consequences of the errors outlined above can be gained by reference to Fig. 5.8 where the strain values are taken as X/Z ratios in plane strain, and plotted against the percentage shortening in X which they represent. The strains represented are the target values (dashed lines) and estimates (dotted lines) for the run using the second lapilli tuff fabric (Fig. 5.3F), with the principal extension direction set at -75° to the bedding trace in the unstrained state. The error in the strain determination was +56%. In the high strain situation (target strain ratio 5.0) the shortening represented by the target and estimated X/Z ratios is 55.5% and 64.5%, respectively. However, in the low strain state, the difference is much more marked, the % shortening approximately doubling from 15.5 to 32, from the target strain value to its estimate. This effect is a product of the shape of the % shortening - X/Z ratio curve. One can well imagine the effects of such large errors at low strain states on, for example, attempts to determine the amount of shortening corresponding to the first appearance of cleavage.

(2) Results - STRANE

During checks of the correct functioning of the modified XROT and STRANE programs with the included straining procedure, test runs were carried out with the idealized bedding-symmetric unimodal unstrained test fabrics shown on Elliott plots in Fig. 5.9. Using the straining procedure and XROT, the system worked perfectly, i.e., the superimposed "target" strain ratios were identified exactly by XROT at all six set angles (Theta) between the bedding trace and principal strain direction. However, a

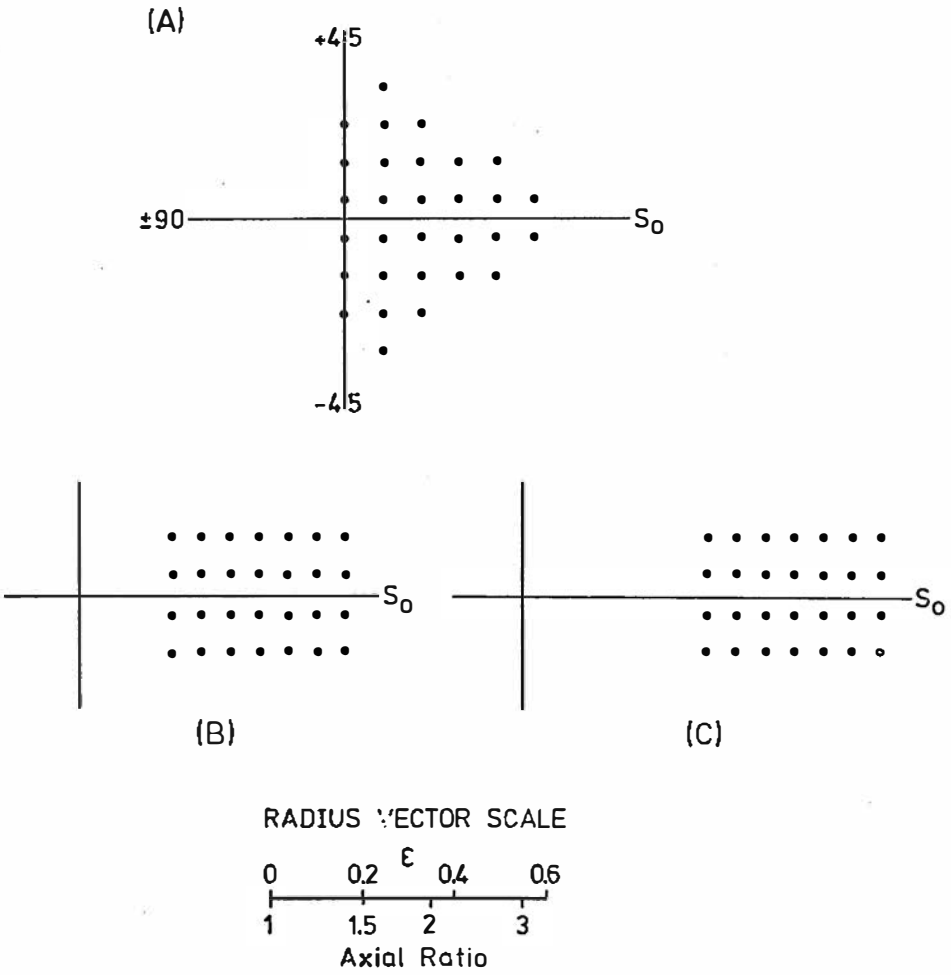

FIGURE 5.9

Uncontoured Elliott plots of idealized unstrained test fabrics. S_o is the bedding trace.

TABLE 5.2

Results of use of idealized bedding-symmetric unimodal unstrained test fabrics with program STRANE and straining option.

Test fabric	Target strain	Theta -75	-50	-25	25	50	75
1 (Fig.5.9A)	1.4	7.0	1.9	1.4	1.4	1.9	7.0
	5.0	7.0	6.6	5.0	5.0	6.6	7.0
2 (Fig.5.9B)	1.4	1.7	1.4	1.4	1.4	1.4	1.7
	5.0	6.0	5.0	5.0	5.0	4.0	6.0
3 (Fig.5.9C)	1.4	1.4	1.4	1.4	1.4	1.4	1.4
	5.0	5.0	5.0	5.0	5.0	5.0	5.0

problem was encountered when the same procedure was applied to program STRANE, in that when the particular value of Theta being used caused the set of ellipse orientations (referred to the principal strain direction) to contain both positive and negative angles, the method usually failed to accurately reproduce the superimposed strain ratios. This occurred at all but two of the Theta values with the fabric in Fig. 5.9A, and at two of the Theta values with Fig. 5.9B. The results of these test runs are set out in Table 5.2. Priority was given to VMPHI = BDGTRACE.

The situations where this apparent restriction on program STRANE will occur can also be identified in material in the deformed state. This is, if ellipse orientations, restricted to the range -90° to +90° with respect to the principal strain direction, are not all (or nearly all) of the same sign (as was the case with Test Fabric 3), the method will almost certainly suffer a basic mathematical failure, even if the assumptions concerning the nature of the pretectonic fabric are valid. The problem was traced to a breakdown in the calculation of VMPHI in such cases. In the exercise presented here, it was estimated that this difficulty could be avoided by using the straining procedure with program STRANE only on the two lapilli tuff fabrics shown in Fig. 5.3E and F.

In the analysis of the two lapilli fabrics, it was decided to compare the results from program STRANE, giving priority to VMPHI = BDGTRACE (MIN.DIFF. criterion), or to maximization of plot symmetry (MAX.SYM. criterion). This provides an analogy to analysis of strained material in which the orientation of bedding is known and unknown, respectively. The results obtained using the MIN.DIFF. criterion were almost identical to those obtained from XROT (see Fig. 5.10A and B). Both the ranges of errors and their magnitude and direction (i.e., underestimate or overestimate) at each value of Theta were similar. Some understanding of

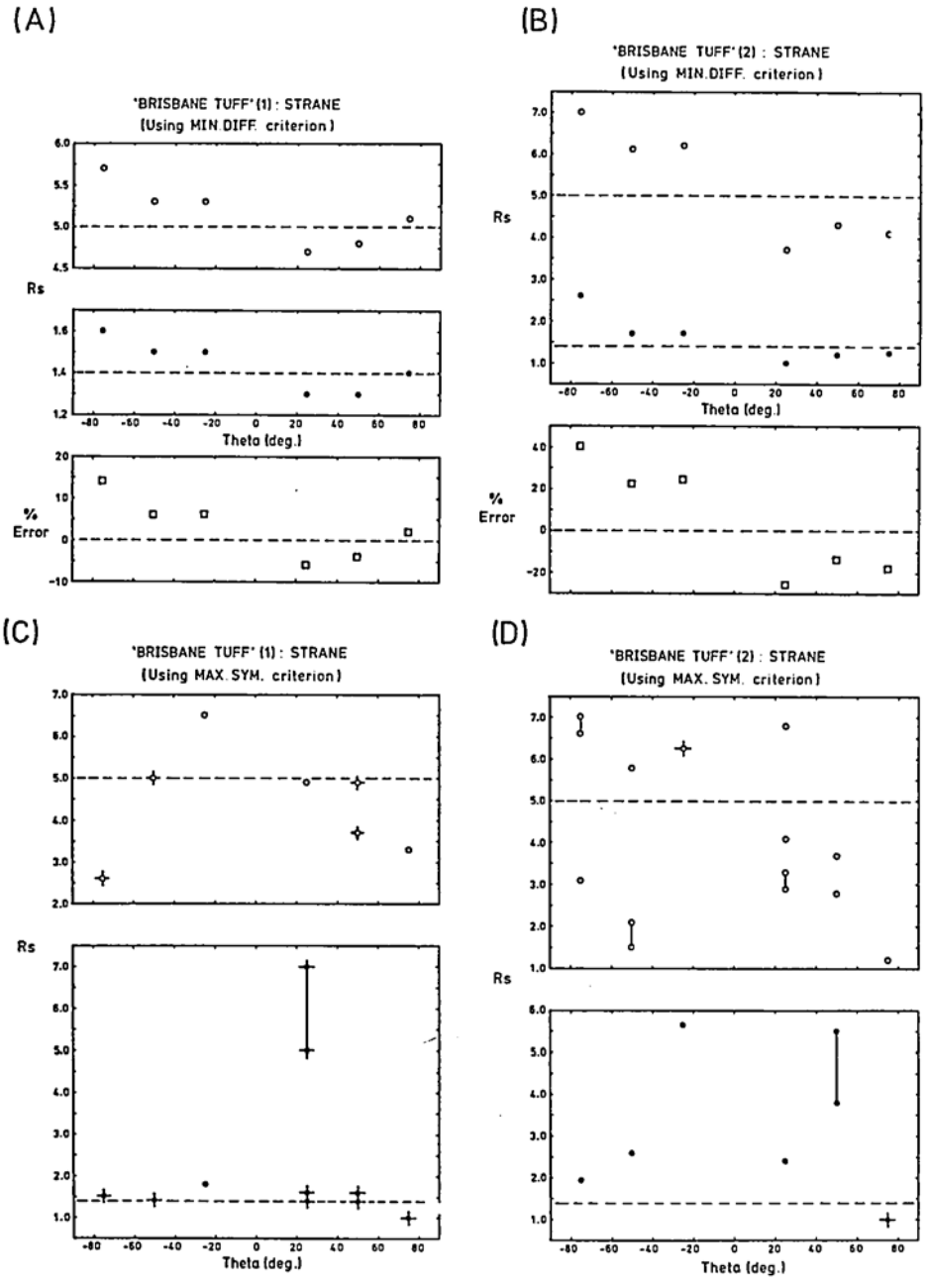

FIGURE 5.10

Results of use of the Dunnet and Siddans (1971) strain analysis method, following artificial straining of the two Brisbane Tuff fabrics. Target values shown by dashed lines.

the influence of the slight initial asymmetry of the fabrics on the errors produced may be gained by reference to Fig. 5.11, which summarizes the case with the largest error. Here, with the second lapilli tuff fabric, the principal extension direction was set at -75° to the bedding trace in the unstrained state, and the target strain ratio was 5.0. Fig. 5.11A is an Elliott polar graph of the fabric in the strained state, the bedding trace being indicated by the dashed line, while Fig. 5.11B is the situation after removal of the target strain (Rs = 5.0). However, to remove the residual asymmetry about bedding, unstraining had to continue to the position seen in Fig. 5.11C, where a strain of Rs = 7.0 has been removed. At this point both the MIN.DIFF. and MAX.SYM. criteria were satisfied. Assuming that Fig. 5.11C represents the true tectonically unstrained state, the amount of diagenetic compactional strain which must be removed to restore the fabric to a completely random one was estimated to be 2.55/1 (0.47ε) using the method of Dunnet (1969). This contrasts with the figure of 1.95/1 (0.33ε) obtained from the *actual* unstrained fabric of Fig. 5.11B. In this case, therefore, an analysis of the fabric of Fig. 5.11A to determine its tectonic and diagenetic strain components (e.g., as carried out by Roberts and Siddans, 1971) would have resulted in considerable overestimation of both.

By contrast with the results obtained from program STRANE using the MIN.DIFF. criterion, use of the MAX.SYM. criterion alone was, on the whole, a failure. Fig. 5.10 C and D illustrate the broad scatter of results. At several values of Theta the same maximum value of the symmetry variable occurred at several widely differing strain values, making it impossible to determine which was the "true" value if MAX.SYM. was being used alone. In other cases (and particularly with the first lapilli tuff fabric) the arbitrary minimum value of the symmetry

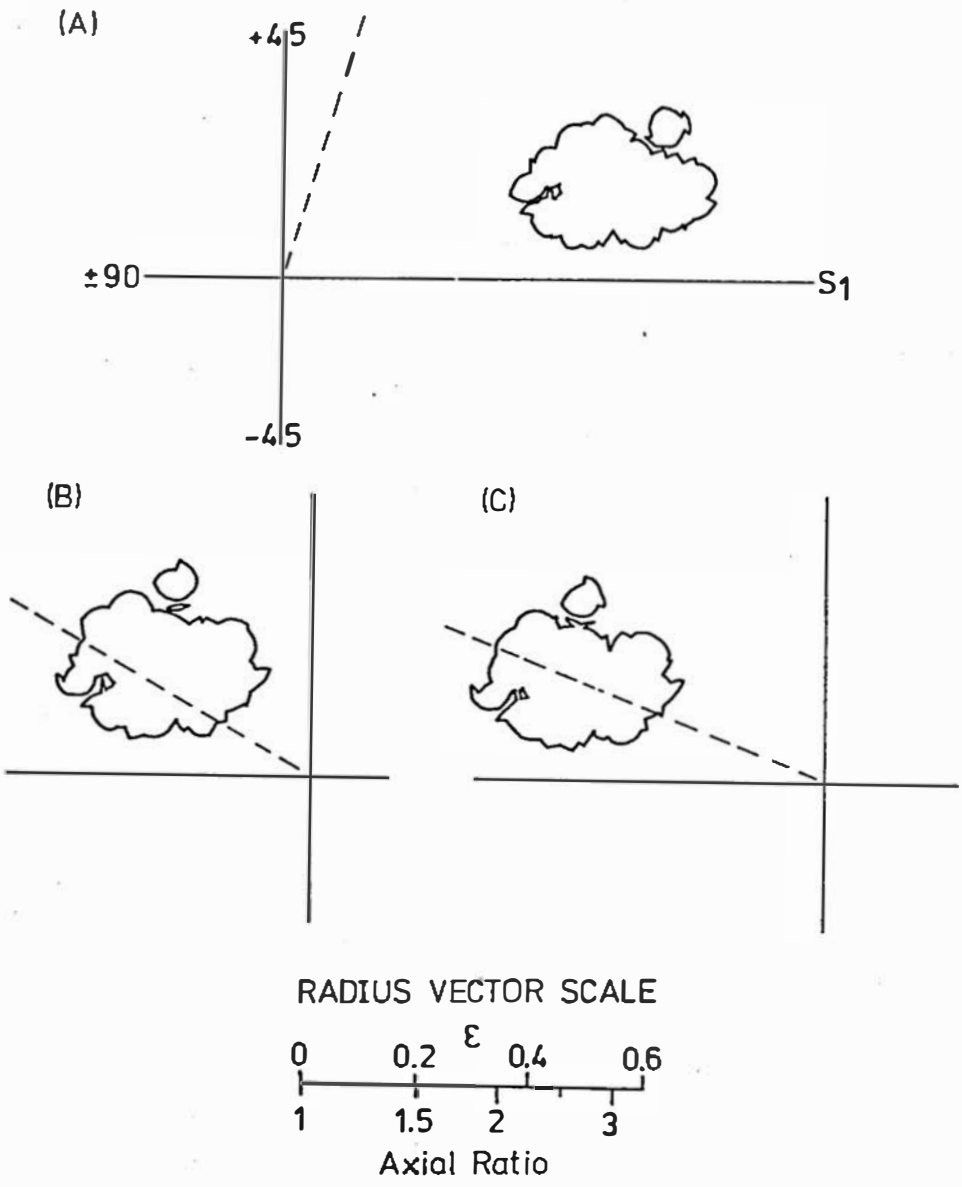

FIGURE 5.11

Contoured Elliott plots illustrating the unstraining carried out in one of the runs using the fabric of Brisbane Tuff specimen (2) and program STRANE.

variable (98%) required for the MAX.SYM. criterion was never attained; in such cases the strain value was read off at the maximum available symmetry position. The analyses where this occurred are indicated by crossed points on Fig. 5.10C and D. The only run using MAX.SYM. which was anywhere near satisfactory was that using the first lapilli tuff fabric with a target strain ratio of 1.4.

5.2.5 Conclusions about the methods

The exercise described in Sections 5.2.3 and 5.2.4 has highlighted the dangers involved in the use of strain analysis methods which make very specific assumptions about the nature of the sedimentary fabrics in the unstrained state. The *limited* examination of actual unstrained fabrics undertaken here has shown that such assumptions may be in error even in lithologies such as the Pea Grit and the lapilli tuffs, in which they had intuitively been expected to hold. There is a need for wider characterization of the variations which may occur in actual unstrained sedimentary fabrics. Deviations from the assumptions made in the strain analysis methods may cause large errors in the strain determinations, particularly where fabrics which were imbricate in the unstrained state are used with the mistaken assumption that they were bedding-symmetric. On the other hand, it is difficult to recognize that such errors have occurred; computerization of the methods can make matters worse, in that the user tends to accept the output strain values without question.

The best recommendation which can be made with regard to this problem is that two-dimensional strain analyses should always be carried out on all three principal sections, so that the three-dimensional check of internal consistency ($X/Y \cdot Y/Z = X/Z$) can be made. In some cases this may require the use of different strain analysis techniques on

different sections (e.g., where the bedding trace is perpendicular to the principal strain direction on one of the sections). It has been found a very useful practice to examine fabrics used in strain analysis on Elliott polar graphs, both in the strained state and after removal of a tectonic strain estimated by one of the available methods. Such a procedure not only enables a better visualization of the de-straining procedure and detection of obvious errors,but may also demonstrate radical differences in fabric characteristics on different sections of one specimen, leading to a more complete awareness of complicating factors arising from the complexities of initial sedimentary fabrics.

5.3 STRAIN ANALYSIS RESULTS FROM THE GORDON SUBGROUP STRATIGRAPHIC EQUIVALENT

5.3.1 The material

Limestone samples used for the tectonic finite strain analysis reported in this section were collected from close to the base of the Gordon Subgroup stratigraphic equivalent at three localities:-

(1) Grunter Hill, Mayberry (440400, Fig.3.1). Deformed oolitic and oncolitic limestones at this locality are exposed in a section across an open upright symmetric anticline with ~300m half-wavelength, and which plunges gently to just east of SE (see Fig. 4.2D for a plot of structural data from Grunter Hill). The structure has associated weakly to strongly developed axial plane cleavage, which is distributed in an upward-diverging fan with dips of 70-75° on the limbs.

(2) Weakly deformed incipiently cleaved oolitic limestone was collected in the vicinity of the entrance to Kubla Khan Cave, 1 km southwest of locality (1), above.

(3) Very strongly cleaved oncolitic limestone was obtained from small remnant outcrops in the bed of Claude Creek (431405, Fig.3.1). The limestone here occurs in a tight, upright, symmetrical synclinal closure in the hinge zone of the Claude Creek Synclinorium (Jennings, 1958), which plunges gently to the NW. An extremely well developed semi-continuous cleavage, axial planar to the synclinal closure, is present in most of the limestone lithologies. The degree of cleavage development is considerably greater than that observed in most of the limestone in the Mayberry area, and is similar to the most strongly deformed material in the Vale of Belvoir.

The structures described at the three localities all belong to the "Deloraine/Railton trend" of Williams (1978). All of the samples used for strain analysis have spar cements, and are therefore oosparites and oncosparites in the terminology of Folk (1962).

Strain analysis of the oosparites was accomplished satisfactorily with the method of Dunnet (1969), as outlined in Section 5.2.2 herein. The sample volume required for a complete three-dimensional analysis of one of these specimens was approximately 24cm^3. Between 50 and 70 individual oolites were measured on each principal section. As observed in Section 5.2, other strain analysis methods (particularly the more algebraic methods) were found to be over-sensitive to the minor initial fabric irregularities of oolites. However, it was estimated that the Matthews *et al.* (1974) XROT technique could have been used, if the strain ratio was read off at the position of the reference direction (PHS) corresponding to the optimum calculated precision. This however involved ignoring considerable variation of 'Rs' with PHS. Results of the use of the Dunnet (1969) and Matthews *et al.* (1974) methods on one of the Grunter Hill oosparites are compared below:-

Specimen No. UTGD 44360

Method	X/Y	Y/Z	X/Z	(X/Y.Y/Z)	Misclosure
Dunnet (1969)	1.65	1.60	2.90	2.64	9.0%
XROT	1.59	1.59	2.89	2.53	12.5%
Logmean Rf	1.64	1.57	2.95	2.57	12.9%

The main different types of oolites present can be seen on a typical XY section (parallel to cleavage), shown in Fig. 5.12A. Oolite type 1 has a coarsely recrystallized core which appears to have absorbed relatively little strain; measurements of such markers would almost certainly underestimate the bulk strain of the rock. Type 2 has a concentrically layered mantle surrounding a coarser grained radially structured core which has a lower axial ratio (and has therefore presumably absorbed less strain) than the overall grain. Type 3 is concentrically layered throughout and is probably the closest approach to a marker which will reflect the bulk strain. Wherever possible measurements were therefore restricted to oolites of type 3. Note that the assumption of initially random fabric implies that the X direction on this XY section of the tectonic finite strain ellipsoid is defined by the preferred orientation of long axes of the oolite cross-sections. A YZ section of an oosparite from Grunter Hill is shown in Fig. 5.12B. On this section the Y direction defined by preferred orientation of oolite long axes is parallel to the overall trend of the traces of tectonic stylolites, against which some of the oolites show truncation due to pressure dissolution. The wavy, anastomosing tectonic stylolites in this specimen are generally spaced ½-2cm apart, and in three dimensions display overall parallelism with each other and with the XY plane of the finite strain ellipsoid, as defined by the oolites.

FIGURE 5.12

A. XY section (parallel to cleavage) of a deformed oosparite from Grunter Hill, Mayberry. X direction of finite strain ellipsoid defined by preferred orientation of oolites. Strain ratio on this section 1.80; 3-d finite strain (+67.5%X, -7%Y, -36%Z), which is close to plane strain. Note different types of oolites, 1, 2 and 3 present (see text for details). Spec. No. UTGD 48358. PPL.

B. YZ section of a deformed oosparite from Grunter Hill. Y direction of finite strain ellipsoid, defined by preferred orientation of oolite long axes, is parallel to overall trend of the traces of tectonic stylolites, against which oolites are truncated due to pressure dissolution. Strain ratio on this section, 1.45; 3-d finite strain (+71%X, -8%Y, -36%Z). Spec. No. UTGD 48357. PPL.

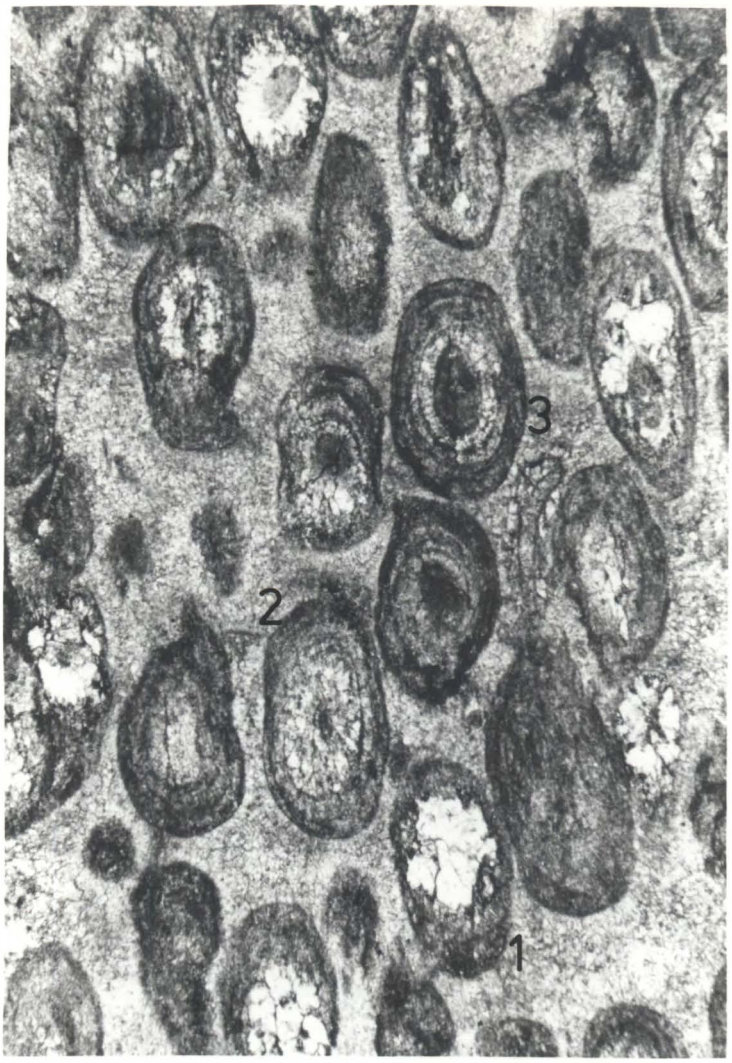

X

1 mm

FIGURE 5.12A

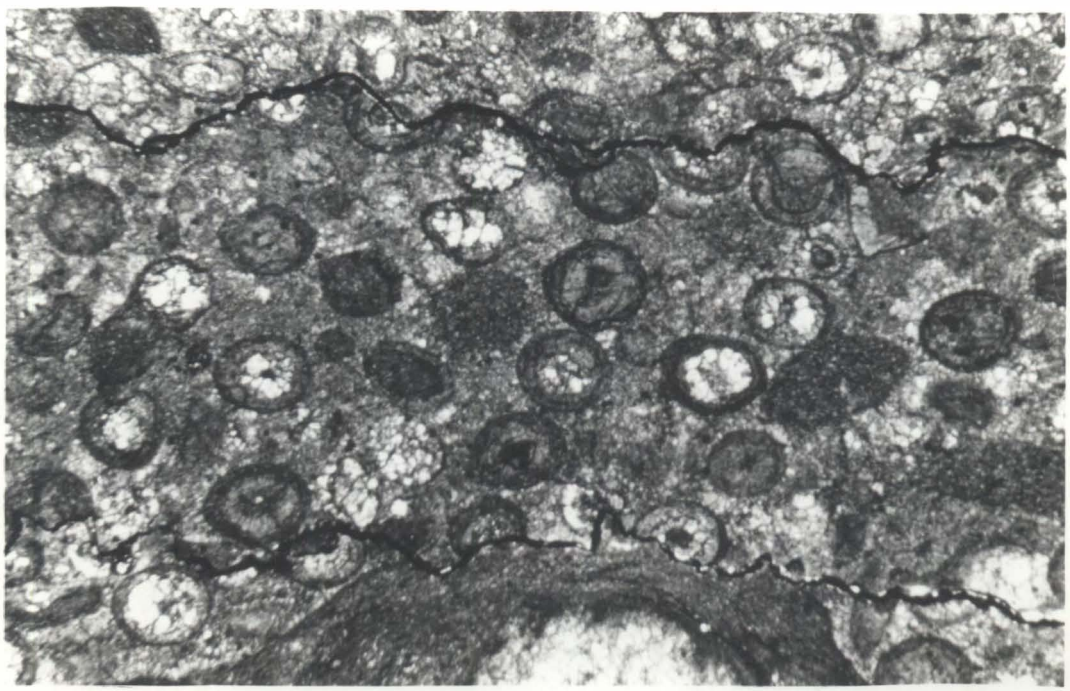

S_1

FIGURE 5.12B

1 mm

The larger size of oncolites, and the larger number of individual particles (70-90) measured on each section, required larger measurement areas than those needed for the oolites. Equivalent sample volumes varied between 1700 and 3400cm^3, depending on the size of the markers. An XY section of one of the lower strain Grunter Hill oncosparites is illustrated in Fig. 5.13. The preferred orientation of oncolite long axes on such a section cannot necessarily be used to define the principal extension direction, because of the probable existence of non-random pretectonic fabrics. Instead, the usual procedure was to use the preferred orientation of long axes of oolites which were usually present in the matrix of these rocks. This could be backed up by the use of calcite fibre veins and fibrous overgrowths on sections such as that in Fig. 5.13, where the principal extension direction is at a high angle to the bedding trace, and a close approach to irrotational strain history may be expected. A YZ section of one of the high strain oncosparites from Claude Creek is shown in Fig. 5.14. Samples from this locality often showed marked inhomogeneous strain effects in the vicinity of large rigid fossil shell fragments, one of which can be seen in Fig. 5.14. Features such as this had to be avoided when choosing areas for measurement.

It had originally been planned to use the Dunnet and Siddans (1971) computer program STRANE, with priority given to maximization of plot symmetry, to analyze the deformed oncolite fabrics from Grunter Hill and Claude Creek. This was due to the possibility that the fabrics had been imbricate in the unstrained state. However, it was estimated that the basic mathematical problem (associated with calculation of VMPHI) discovered in the program during the tests described in Section 5.2.4, would cause unpredictable errors in addition to any errors associated with initial fabric irregularities. On the other hand, the Matthews *et al.*

FIGURE 5.13

XY section (parallel to cleavage) of deformed oncosparite from Grunter Hill, Mayberry. X direction shown cannot necessarily be assumed parallel to preferred orientation of oncolite long axes, due to probable presence of non-random pretectonic fabric. Instead, the X direction is given by preferred orientation of oolites in matrix, and by lineation of calcite crystals in fibre veins and fibrous overgrowths. The latter are parallel to X on sections such as this, where irrotational strain history may be expected. Strain ratio on this section 1.53; 3-d finite strain (+45%X, -5%Y, -27%Z), close to plane strain.
Spec. No. UTGD 48360.

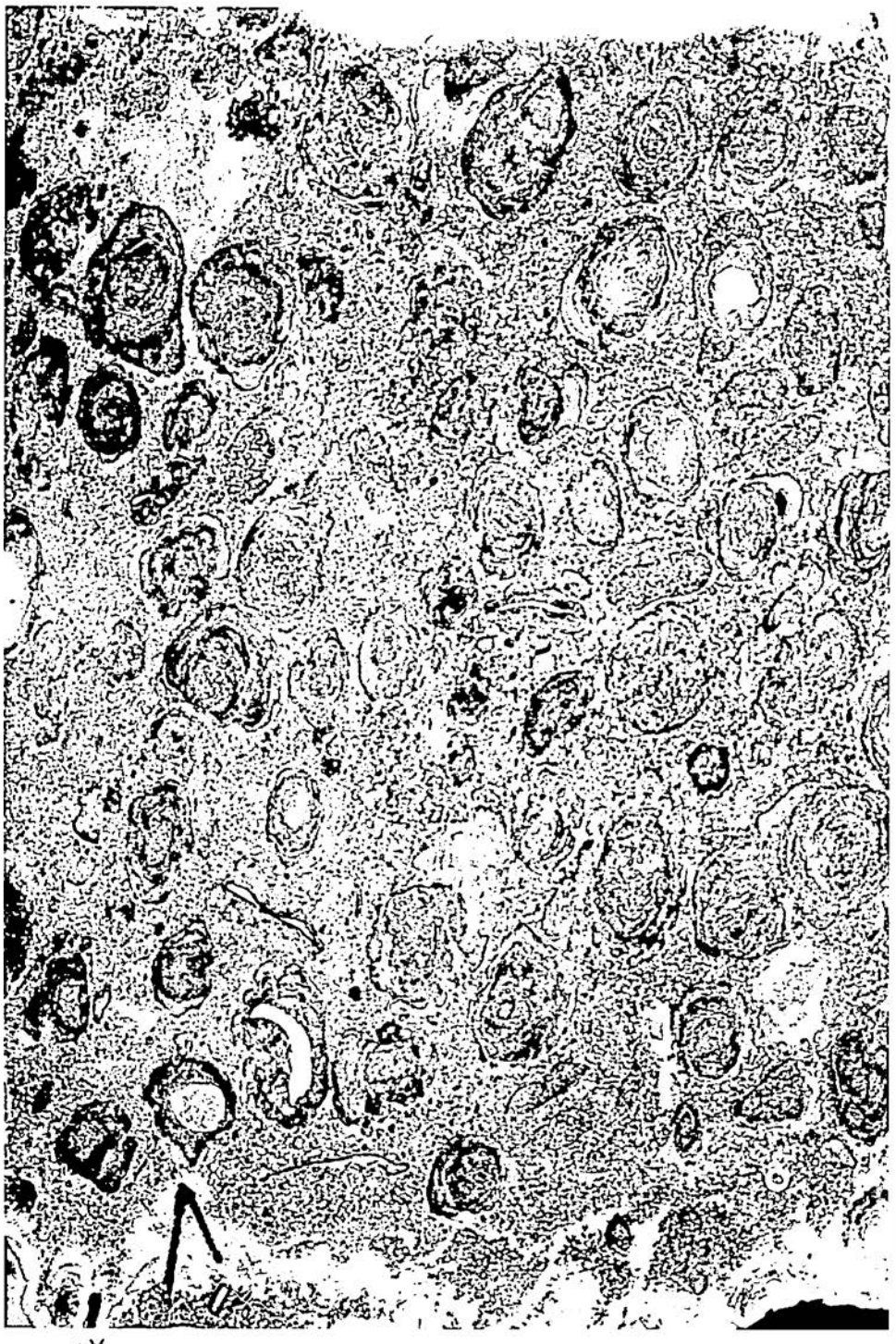

FIGURE 5.13

FIGURE 5.14

YZ section of a strongly deformed oncosparite from Claude Creek. Section is sub-horizontal and almost parallel to bedding. S_1 is local very strongly developed vertical cleavage of NW strike ("Deloraine/Railton trend"). Marked inhomogeneous strain effects around rigid fossil fragments, such as that in the lower part of the photo, must be avoided when making strain analysis measurements. Strain ratio on this section, 4.53; 3-d finite strain (+163%X, +31%Y, -71%Z).

Spec. No. UTGD 48362.

S_1

FIGURE 5.14

1 cm

(1974) XROT method does not immediately lend itself to analysis of fabrics which were imbricate in the unstrained state. The deformed oncolite fabrics were therefore analyzed using the graphical method of Elliott (1970) in its modified form (Seymour, 1975; Boulter, 1978), as described in Section 5.2.2. Thus, in positioning the ICP on Elliott plots of these fabrics on each principal plane, two main controls were used:-

(1) The ICP was constrained to lie on or very close to the *assumed* trace of the principal extension direction; i.e., the cleavage trace on XZ and YZ sections, and the direction defined by preferred orientation of matrix oolites and/or elongation of crystals in irrotational calcite fibre veins and fibrous overgrowths on XY sections.

(2) On sections at a high angle to bedding, the ICP was then positioned such that it lay ~¼ of the plot diameter inside the contoured plot edge along a line of plot symmetry. On sections at low angles to bedding, the same procedure applied but $\frac{1}{3}$ of the plot diameter was used.

Use of controls (1) and (2) sometimes lead to two possible ICP positions on a particular plot. If this occurred on all 3 principal planes, permutations and combinations of six possible strain ratios had to be considered. However, some of the ICP positions could usually be eliminated by the fact that they gave unlikely fabrics on unstraining (e.g., preferred orientation perpendicular to the bedding trace). If, after exercise of this control, there still remained two possible ICP positions on one of the plots, one of these could usually be eliminated by the final three-dimensional internal closure check, X/Y . Y/Z = X/Z.

5.3.2 Results

The results of tectonic finite strain analyses of limestones from

TABLE 5.3

Spec.No.	X/Y	Y/Z	X/Z	(X/Y.Y/Z)	Misclosure	X %	Y %	Z %
Oosparite - Kubla Khan Cave entrance								
48359	1.30	1.20	1.55	1.56	0.6%	+26.6	-2.6	-18.8
Oosparites - Grunter Hill								
48357	1.85	1.45	2.60	2.68	3.1%	+70.6	-7.8	-36.4
48358	1.80	1.45	2.50	2.61	4.4%	+67.5	-7.0	-35.8
44359*	1.55	1.50	2.15	2.33	8.1%	+53.3	-1.1	-34.1
44360*	1.65	1.60	2.90	2.64	9.0%	+63.3	-1.1	-38.1
44361*	1.60	1.20	1.90	1.92	1.1%	+45.4	-9.1	-24.3
44355*	1.55	1.50	2.40	2.33	2.9%	+53.3	-1.1	-34.1
44362*	1.75	1.40	2.55	2.45	3.9%	+62.5	-7.2	-33.7
Oncosparites - Grunter Hill								
44358*	1.90	1.75	3.25	3.33	2.5%	+84.9	-2.7	-44.4
48360	1.53	1.30	1.96	1.99	1.5%	+44.9	-5.3	-27.1
48361	1.69	1.77	3.15	2.99	5.1%	+71.6	+1.5	-42.6
Oncosparites - Claude Creek								
48362	2.00	4.53	9.37	9.06	3.3%	+162.7	+31.3	-71.0
48363	2.05	3.00	6.00	6.15	2.5%	+132.7	+13.5	-62.2

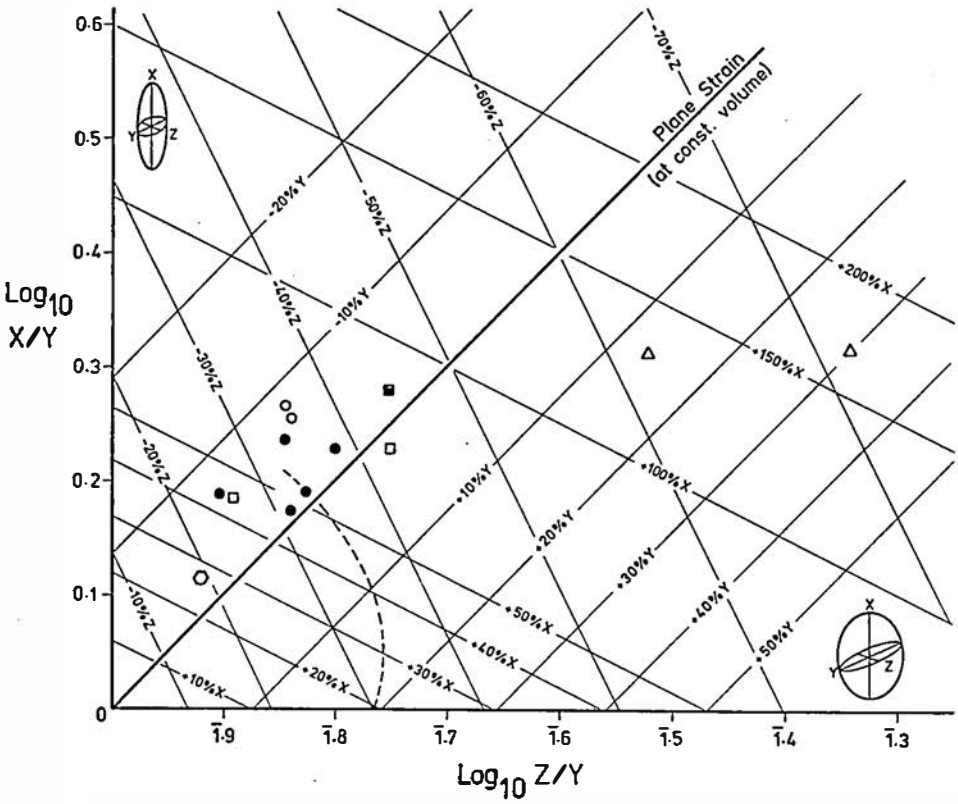

FINITE STRAIN ANALYSES
GORDON LIMESTONE S.G.

Oosparites

- ● Grunter Hill (Seymour, 1975)
- o " " new data
- ○ Kubla Khan Cave

Oncosparites

- ■ Grunter Hill (Seymour, 1975)
- □ " " new data
- △ Claude Creek

FIGURE 5.15

the Gordon Subgroup stratigraphic equivalent are listed in numerical form in Table 5.3, and are plotted on the log-log triaxial strain graph of Wood (1971, 1974) in Fig. 5.15. The results obtained by Seymour (1975) are included (see asterisks, Table 5.3). The Wood plot assumes constant volume deformation. The lower limit of the "field of slaty cleavage deformation" defined by Wood is shown by the dashed line. This field was defined on the basis of 5200 strain determinations in true slates from the Cambrian Slate Belt of Wales and the Taconic Slate Belt of New England.

Some difficulties were encountered with both positioning of principal plane cuts and the actual analysis, in low strain specimens of oncolitic limestone. Although several such specimens were collected, only one was satisfactorily analyzed at a strain state representing shortening in Z of less than 30%. However, no such problems occurred with the oosparites, and even the lowest strain specimen (UTGD 48359, from the Kubla Khan Cave locality) was easily and accurately analyzed, the three-dimensional misclosure being less than 1% (see Table 5.3). In general, the strain analysis results from the oosparites are considered to be more reliable than those from the oncosparites. Fig. 5.16 shows the small magnitude of the errors in principal plane cut orientations for Specimen UTGD 48359, despite the fact that the cuts were positioned by eye purely on the basis of the shape fabric of the particles (the specimen was uncleaved). The strain ratio on the YZ section was only 1.20, yet even at this low two-dimensional strain a quite distinct preferred orientation of oolite long axes was developed (Fig. 5.16). On the XY section, the preferred orientation of the particles was close to the line pitching down the dip of XY (marked by $\phi = 0$). This situation was repeated for all of the oosparite samples, and also for matrix oolites

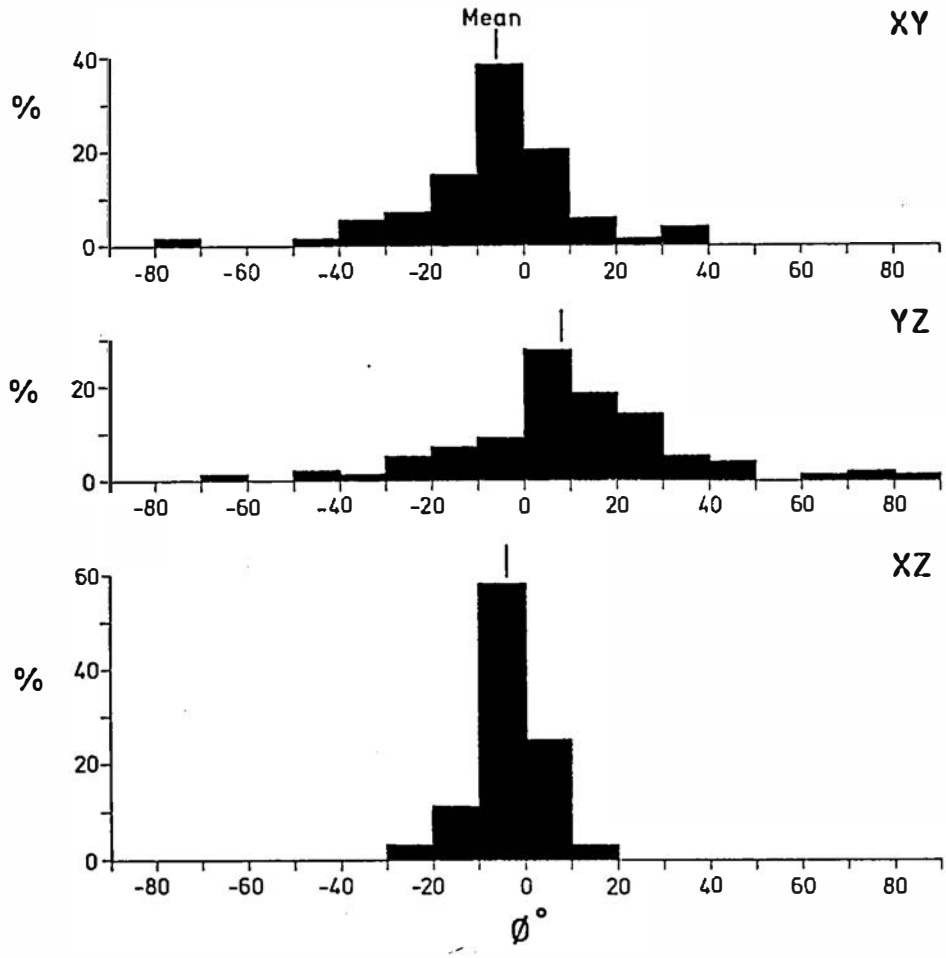

Oosparite, Kubla Khan Cave entrance

Angular distribution of ooid long axes in principal planes

Finite strain, +26%X, -2%Y, -19%Z

FIGURE 5.16

in the oncosparite samples. The lineation defined by orientations of crystals in irrotational calcite fibre veins and fibrous overgrowths on cleavage-parallel sections, also commonly pitched at close to 90° in the cleavage plane. It was therefore concluded that the Y direction was usually sub-horizontal and close to the fold axes.

Assuming that the true bulk strain is represented (see discussion, next section), analysis of the material from Grunter Hill and the nearby Kubla Khan Cave locality define an apparent strain path which is slightly on the constrictional side of plane strain, with tectonic flattening across the cleavage varying between 19% and 45%. There is generally a small amount of shortening in the Y direction, averaging 4%. Extension in X varies between 27% and 85%. As cleavage is at a high angle to bedding at most of the Grunter Hill and Kubla Khan Cave localities, the latter two figures also represent the approximate range in tectonic exaggeration of stratigraphic thicknesses. It was estimated that Wood's lower boundary of the "field of slaty cleavage deformation" was also approximately valid for the Grunter Hill and Kubla Khan Cave samples. That is, cleavage was absent or only very incipiently developed in the 5 samples plotting below or on the boundary in Fig. 5.15, while distinct moderately to strongly developed cleavage was present in the 6 samples plotting abovethe boundary. The results indicate that the onset of cleavage at outcrop scale in these rocks corresponded to shortening in Z of between 30 and 35%.

Cleavage in the limestone at Claude Creek is very strongly developed and planar, the style of development varying between the "smooth disjunctive" and "fine continuous" types of Powell (1979). It is similar to cleavage in the Gordon Subgroup stratigraphic equivalent in the Vale of Belvoir. The two samples analyzed from Claude Creek appear to

contrast markedly with the Grunter Hill/Kubla Khan Cave material. The results plot in the field of flattening (i.e., between the plane strain line and the abcissa of the triaxial strain graph). They also plot close to the central part of the "field of slaty cleavage deformation" of Wood (1971, 1974). The maximum indicated flattening across the cleavage is 71%, and extensions in Y for the two samples are 13.5% and 31.3%.

5.3.3 Strain Analyses and bulk strain

A totally different approach to interpretation of natural strain in oolitic limestones was adopted by Donath and Wood (1976). This involved rejection of the concept of homogeneous strain on the scale of the assemblage of measured markers. Rather, strain was assumed to be heterogeneous on the scale of individual oolites, because of variable behaviour among the particles and variation in their volume density relative to matrix of slightly different ductility. In fact, the authors proposed that the final shape fabric of the markers could be used to derive *strain paths* for the material. A further assumption involved was that each fabric component experiences a similar strain history but, at any given time, different components may reflect different stages of that history. Donath and Wood state (p. 188):-

> "Ideally, one would like to have rock specimens comprised of closely packed spherical objects which would deform by one or another of several possible deformation mechanisms depending upon the conditions imposed. Oolitic limestone seems to meet these requirements best in that (1) it includes spherical objects having similar properties and behaviour as the enclosing cement, and (2) calcite deforms by a variety of fracture and frictional mechanisms (cataclasis) and intra-crystalline gliding mechanisms under different conditions of deformation...."

The variable axial ratios seen on a two-dimensional section

of a deformed oolitic limestone were therefore assumed by Donath and Wood to represent inhomogeneous strain on a particle to particle scale, rather than an expression of initial pre-tectonic fabric of the markers. The actual calculation of strain paths was based on a method outlined by Wood (1974, p. 391). Individual measurements of oolite axial ratios in each principal plane were sorted into order of increasing departure from circular, and then into 10% or 20% groups, each of which was averaged. Complete three-dimensional ellipsoids were then calculated, based on the assumption that the most deformed objects in one symmetry plane should be associated with the most deformed objects in another symmetry plane. This yielded strain paths for each specimen consisting of either 5 or 10 points. Donath and Wood calculated such strain paths for five naturally deformed oolitic limestones from Wales, Scotland and Maryland (U.S.A.), and concluded that:

> "The data ... suggest that naturally deformed limestones may characteristically deform in a manner closely approximating plane strain."
>
> (Donath and Wood, 1976, p. 190)

The described technique was attempted herein with axial ratio data from the three principal planes of one of the Grunter Hill oosparites. It was found, however, that considerable three-dimensional misclosure occurred at all but one of the 20% of data groups (the 60-80% group). The three individual strain paths shown in Fig. 5.17 were therefore calculated using the three principal planes in pairs. The "whole sample strain analysis" shown by the shaded error triangle is that derived by the Dunnet (1969) Rf/ϕ method, based on the conventional assumption of *homogeneous* strain on the scale of the sample, and represents a strain state of (+53%X, -1%Y, -34%Z). Only one of the calculated strain paths has the appearance of a reasonable result,

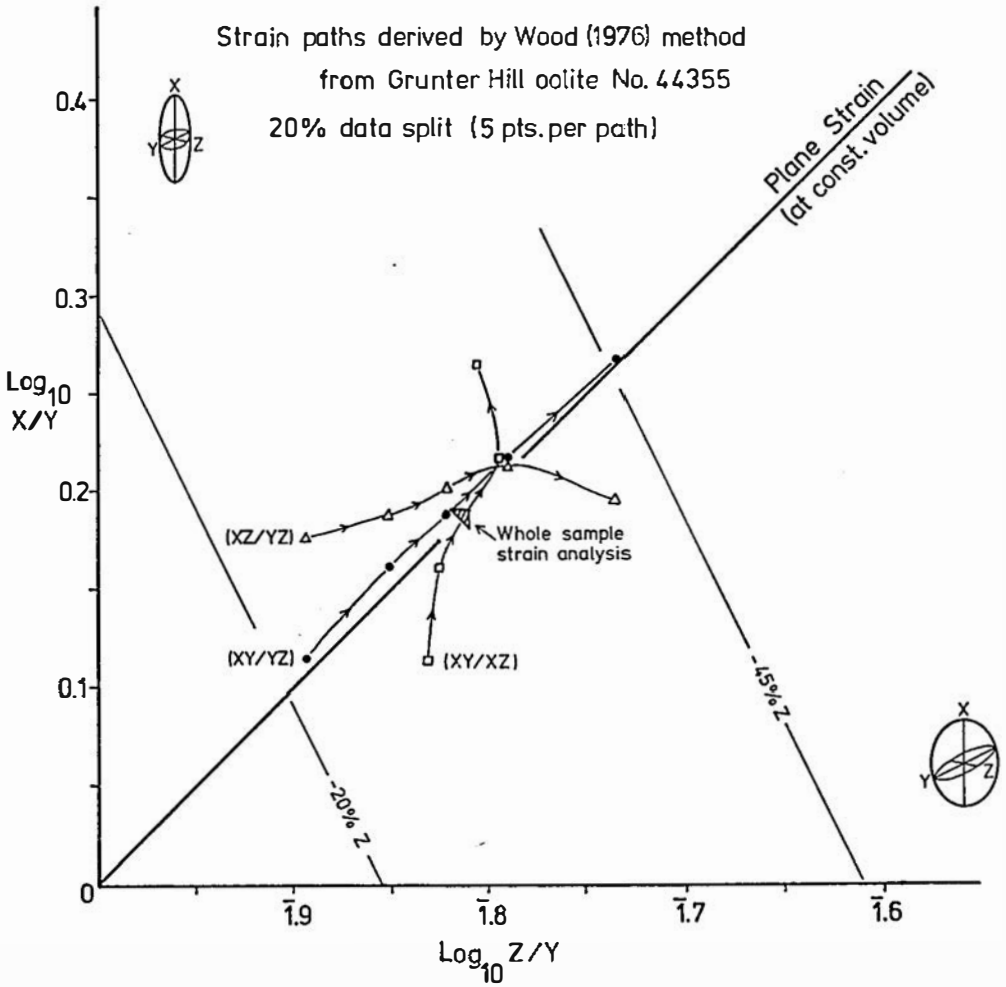
Strain paths derived by Wood (1976) method
from Grunter Hill oolite No. 44355
20% data split (5 pts. per path)
X
Y
Z
Plane Strain
(at const. volume)
0.4
0.3
0.2
0.1
0
Log10 X/Y
(XZ/YZ)
Whole sample
strain analysis
(XY/YZ)
(XY/XZ)
-45% Z
-20% Z
1.9
1.8
1.7
1.6
Log10 Z/Y

FIGURE 5.17

namely that derived from the XY and YZ sections in combination. If this was accepted as a true strain path for the material, it would indicate a range of shortening in Z *within the specimen* of ~20% to 45%, along a path which is close to plane strain. However, the failure in three-dimensional closure in this analysis has lead to rejection of the concept on which the Donath and Wood method was based. In fact, the proposal is also questioned on more basic grounds, with respect to initial pretectonic fabrics of oolites. The examination of actual unstrained oolitic limestone described in Section 5.2.3 herein indicated that perfectly spherical particles are rare in such material. Axial ratios in two-dimensional sections in fact commonly varied in an approximately random fashion up to a maximum of ~1.50. The results of Dunnet Rf/ϕ analyses on the deformed oosparites from Mayberry are also consistent with the presence of approximately random initial pretectonic fabrics, with axial ratios varying up to 1.50. Thus, the variable axial ratios and orientations of oolites observed on a two-dimensional section in the deformed state are fully accounted for by the superposition of a finite *homogeneous* tectonic strain on an initial fabric. Strain paths such as those shown in Fig. 5.17 are therefore considered to be invalid. Nevertheless, in view of the comments of Donath and Wood with respect to the deformation behaviour of limestones, it is interesting to note that the finite strain analyses reported in Section 5.3.2 appear to define a *collective* strain path for the Grunter Hill/Kubla Khan Cave material which is close to plane strain. This does not however extend to the higher strain Claude Creek material.

If it is therefore accepted that the suites of measured strain markers have undergone homogeneous strain, there still remains the question of the relationship between the finite strain indicated by

the markers, and the true bulk strain of the rock. This depends on the amount of competence contrast between the particles and their matrix. Referring back to Fig. 5.12A, it can be seen that the oolitic limestones consist of markers which are mostly composed of material similar in composition and grainsize to that comprising the rock matrix, i.e., medium-coarse grained sparry calcite. The outer layers of the oolites are composed of recrystallized micrite, i.e., now micro-spar with a finer grainsize than either the cores of the oolites or the matrix. Comparative axial ratios of the core and the whole particle for the three numbered oolites in Fig. 5.12A are:-

Oolite type	Rf	Rf_{core}	difference
1	1.95	1.22	37%
2	1.89	1.72	9%
3	1.62	1.50	7.5%

Interpretation of bulk strain in the oosparites thus presents an interesting problem. On the one hand, the above figures suggest that the oolites may have behaved in a similar fashion to that described by Tan (1974), with particles deforming around relatively competent nuclei. Tan showed that in such situations the three-dimensional strain derived from the markers may be more constrictional in shape than the true bulk strain. In strain analysis of oolitic limestones from Windgällen, Switzerland, Tan (1976) attempted to avoid this effect by measuring only oolites which had been cut off-centre and showed no nucleus or very small nuclei in thin sections. This procedure was prevented in the Grunter Hill/Kubla Khan Cave oosparites because such cross-sections were found to be rather fuzzy in outline and consequently difficult to measure. In fact, cross-sections with no or very small

cores were rare, due to the fact that even in Type 3 oolites, the average core diameter was $\sim\frac{3}{4}$ of the whole particle diameter. This brings the argument to another point, namely, that the micrite coatings of the oolites in the Grunter Hill/Kubla Khan Cave samples may only constitute some 15-20% of the bulk rocks, the remainder approximating to medium-coarse grained sparry calcite. From the work of Gay (1968), one might conclude that the high volume concentration of medium-coarse sparry calcite in all of the oosparite samples, indicates that the three-dimensional strain values derived from the markers should be close to the true bulk strains. However, this conclusion must be balanced against the work of Schmid and Paterson (1976, 1977) and Schmid *et al.* (1977), who predicted that superplastic flow may be important in the very fine grained calcite (micrite) coatings of oolites at geological strain rates and temperatures. If this had occurred, measurements of the oolites would overestimate the bulk strain of the rocks.

The approach of the oolite strain analyses to the bulk strain can be checked using the d-α method of Ramsay (1967, pp. 195-197). This is a particularly useful method, because it relies on the initially uniform distribution of particles throughout the rock. Thus, in two dimensional section, the distances (d) between the centres of adjacent particles are measured in conjunction with the orientations (α) of the lines joining the centres. Because only the relative displacements of *points* within the material are measured, the method treats the material as an homogeneous whole, and should thus yield the bulk strain. A d-α plot for the XY principal section of one of the Grunter Hill oosparites (UTGD 44355) is shown in Fig. 5.18. The Dunnet Rf/φ analysis for this specimen plotted approximately in the middle of the Grunter Hill/Kubla Khan Cave *collective* strain path in Fig. 5.15, and also

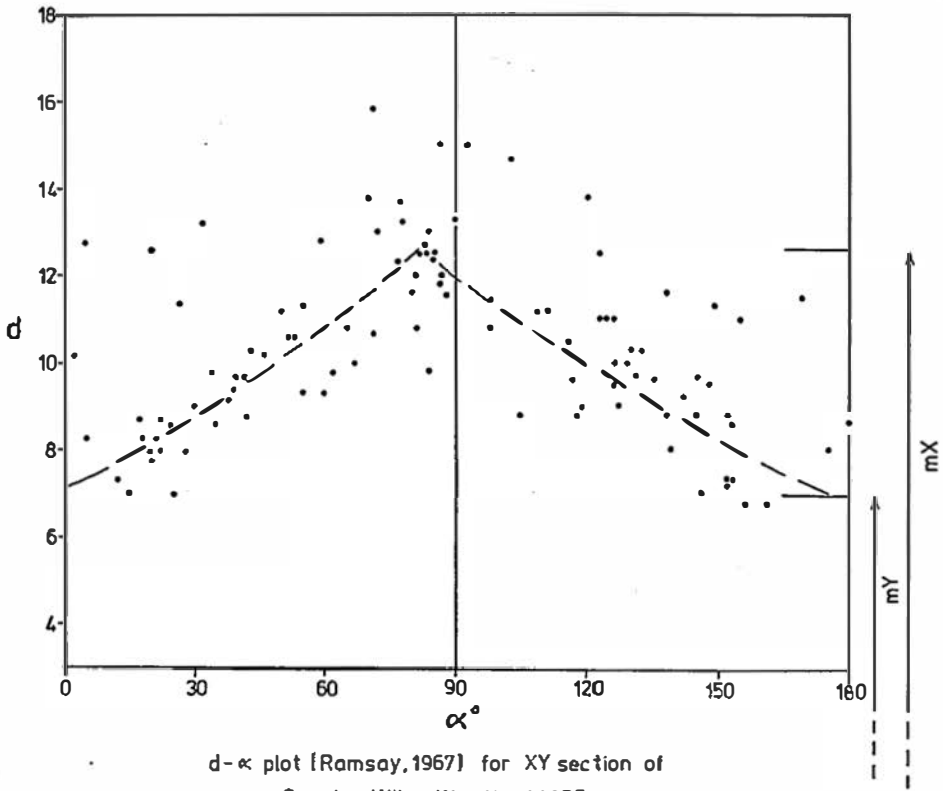

d-∝ plot [Ramsay, 1967] for XY section of
Grunter Hill oolite No. 44355
104 link network involving 61 ooliths
Strain ratio from this method. Rs = mX/mY
= 1.80

From Dunnet [1969] method.
Rs = 1.55

FIGURE 5.18

lay on the lower limit of Wood's "field of slaty cleavage deformation". The precision of the d-α strain estimate was estimated to be ±0.10 Rs, and the indicated strain ratio is thus 1.80 ± 0.10. This figure is 16 (±6)% *higher* than the strain ratio derived by the Dunnet method. The suggestion, based on the work of Schmid *et al.*, that Dunnet strain analysis of the oolites overestimates the bulk strain, is therefore rejected. On the other hand, it is possible that the oolite strain analyses have underestimated bulk strain ratios by the order of 10-20%. The significance of this difference in terms of X, Y and Z is indicated in the calculation below, where the 16% difference in two-dimensional strain ratio observed on the XY strain of UTGD 44355 is assumed to also apply on the other two principal planes:

	X %	Y %	Z %
Marker strain (Dunnet, 1969)	+53.3	-1.1	-34.1
True bulk strain (?)	+77.3	-1.5	-42.7

This adjustment moves the analysis to close to the top of the collective Grunter Hill/Kubla Khan Cave strain path in Fig. 5.15.

By contrast with the oolites, the oncolites generally do not have relatively rigid cores, and are usually composed almost entirely of micrite (see Figs. 5.13 and 5.14). These markers may in fact have a negative competence contrast relative to their sparry calcite matrix, and may therefore be expected to slightly overestimate the bulk strain. This may explain why the two highest strain samples from Grunter Hill are oncosparites. Alternatively, the volume concentration of these markers (usually between 30 and 40%) may have given the oncosparites a higher micrite content than the oosparites, leading to an overall lower competence for the bulk rock. This is supported by the observation

that the most strongly cleaved lithologies at Grunter Hill were oncosparites. An important result of the Grunter Hill strain analyses is that the oncosparites yield the same *type* of three-dimensional strain as the oosparites, despite the fact that the oncolites are mostly uncored particles of effectively homogeneous internal composition. This implies that the effect predicted by Tan (1974), whereby analysis of cored oolites yields an apparent three-dimensional strain of more constrictional type than the bulk strain, has *not been important* in the oosparites. It is therefore concluded that the true bulk strain for the Grunter Hill/Kubla Khan Cave material is close to plane strain in character, but that the amount of strain may have been slightly underestimated by the oolite analyses, and slightly overestimated by the oncolite analyses.

On the basis of mean finite strain ellipsoids calculated from a number of published analyses from various orogenic belts, Tobisch *et al.* (1977) recognized two mean deformation paths. Their Path I approximately bisects the "field of slaty cleavage deformation" of Wood (1971, 1974), while Path II approximates to plane strain. The importance of plane strain as a deformation path in various orogenic belts has also been pointed out by Burns and Spry (1969) and Wood (1973, Fig. 10, Path C). Tobisch *et al.* proposed that one possible constraint leading to plane strain deformation is the buttressing effect of thick, relatively competent bodies of quartzite. This situation may apply to the limestones of the Gordon Subgroup, which are effectively sandwiched between competent quartzose clastics of the Denison Subgroup below and the Eldon Group above. These competent lithologies presumably underwent little extension parallel to Y during folding. However, the geometry of deformed stromatolites higher in the Gordon Subgroup in the Mayberry area indicates three-dimensional strain of flattening type with

considerable extension in Y (see next section), as do the strain analyses of the Claude Creek oncosparites. It seems feasible that the plane strain condition may have held at low strain states and close to the boundaries of the competent units, but that at higher strains and/or away from the latter boundaries, increasing extension in Y occurred to give three-dimensional finite strains in the field of flattening. The situation at Claude Creek, with considerable extension in Y in limestones close to the base of the Gordon Subgroup, may imply the existence of a décollement between the limestone and the underlying competent sandstones and orthoquartzites of the Moina Sandstone.

The major remaining factor which has not been taken into account in the strain analyses is pressure solution strain (e.g., see Mitra, 1976, 1978). This represents additional shortening in Z (by the formation of tectonic stylolites) and concomitant extension in X (by formation of fibre veins and fibrous overgrowths). However, none of the samples used for strain analysis has tectonic stylolites developed to the extent shown in the sample illustrated in Fig. 5.19. The extra shortening in Z represented by the stylolites on this XZ section was estimated at 14%. It is interesting to note that this shortening by pressure dissolution does not appear to be balanced by extra extension in X due to reprecipitation of calcite in fibre veins (marked fv in Fig. 5.19). There has therefore been some volume loss from the overall sample, possibly represented by precipitation of calcite in large irregular "sweatouts" observed in the near vicinity in the field. This volume loss is not distributive throughout the sample however, and there is no need to adjust strain estimates for the interstylolite domains for a uniform homogeneous volume loss (Ramsay and Wood, 1973). The controls on degree of tectonic stylolitization of the limestones are somewhat

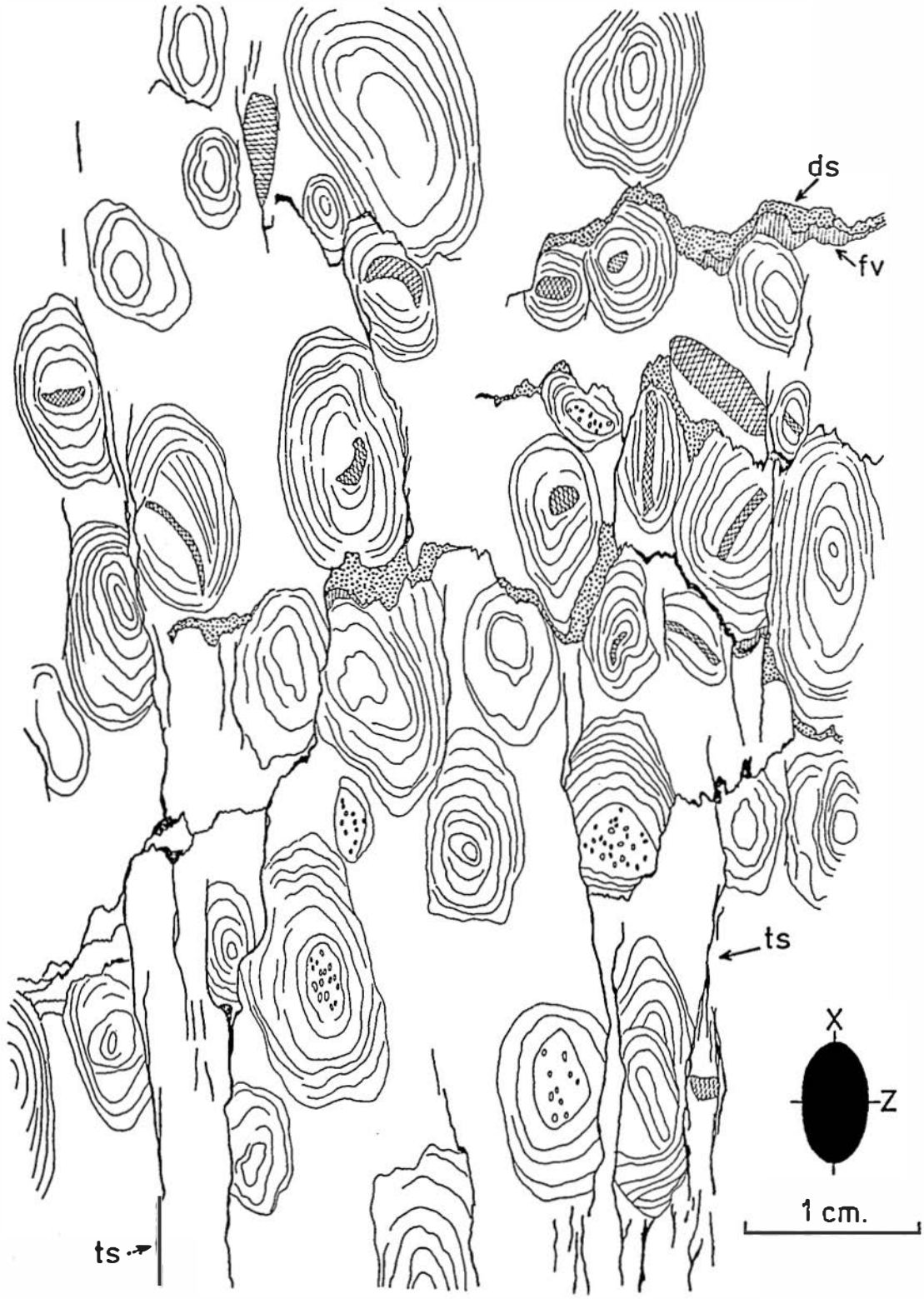

FIGURE 5.19

Deformed oncosparite with strong development of tectonic stylolites, from Grunter Hill, Mayberry. Tectonic stylolites ts, syntectonic calcite fibre veins fv, dolomitized diagenetic stylolites ds. Strain ellipse shown has axial ratio 1.81, and represents the strain indicated by the deformed oncolites only. It does not take into account the extra strain represented by the tectonic stylolites and fibre veins.

obscure. The oncosparites tend to be more commonly stylolitized than the oosparites, but in the former there is no apparent relationship between degree of development of tectonic stylolites and the strain in the interstylolite domains. Thus, the heavily stylolitized sample illustrated in Fig. 5.19 has an approximate three-dimensional strain as indicated by the oncolites, of only (+37.5%X, -4%Y, -24%Z), while the very high strain oncosparites from Claude Creek are virtually unstylolitized. The most likely control on stylolitization is suggested to be variation in the original insoluble residue content of the limestones. It is estimated that the weak development of tectonic stylolites and fibre veins in the samples used for the strain analyses reported herein would add a maximum of 10% to the estimates of shortening in Z and extension in X if the bulk strains were considered.

5.3.4 Tectonic modification of stromatolite morphology

Stromatolites are common organosedimentary structures in limestones in general and have several important geological uses (e.g., P.F. Hoffman, 1967). Knowledge of the amount of change of shape of a particular stromatoid due to tectonism could be important when attempting to use it for:

(1) Correlation and age determination.

(2) Derivation of palaeocurrent directions and shoreline orientations.

(3) Measurement of past tidal ranges.

Fossil fish, brachiopods, trilobites, etc. have all been used for tectonic strain determinations, almost from the inception of quantification in deformation studies. These fossils clearly display the effects of deformation by the loss of some fundamental symmetry. The deformation of stromatolites, on the other hand, is often by no means as obvious,

because of the wide variations in morphology they are known to show in the undeformed state (H.J. Hofmann, 1973). There is therefore a real danger of neglect of the importance of tectonic deformation in the production of the final shape observed. On the other hand, attempts should be made to estimate the amount of tectonic deformation if the morphologies of these structures are to be used in determinations such as (1)-(3) above.

A limited study of alteration of the geometries of algal stromatolites by homogeneous tectonic flattening has been carried out in the Gordon Subgroup stratigraphic equivalent in the Mayberry area. Two localities are considered, both of which have single phase steeply dipping to vertical cleavage of WNW strike ("Deloraine/Railton trend", Williams, 1978). Locality 1 is on the southern flank of the closure around the eastern end of the Standard Hill Anticline, near 4462/3982 (see Fig. 3.1). This locality is close to the base of the limestone sequence, but comprises algalaminated dolomicrites (some of which are stromatolitic), flat-pebble conglomerates and burrowed dolomicrites indicative of an intertidal sedimentary environment. It probably represents a lateral (shallowing) facies change relative to the subtidal oosparites and oncosparites of Grunter Hill/Kubla Khan Cave, 6 km to the west-northwest. It was estimated that the degree of cleavage development at Locality 1 was similar to that of average-strain material from Grunter Hill. Locality 2, near 4414/3981 (Fig. 3.1), has similar lithologies but is considerably higher in the Gordon Subgroup stratigraphy, and represents a vertical facies change relative to Grunter Hill. The cleavage at this locality is considerably more strongly developed than that at either Grunter Hill or Locality 1.

In order to provide at least some reference point in tectonically

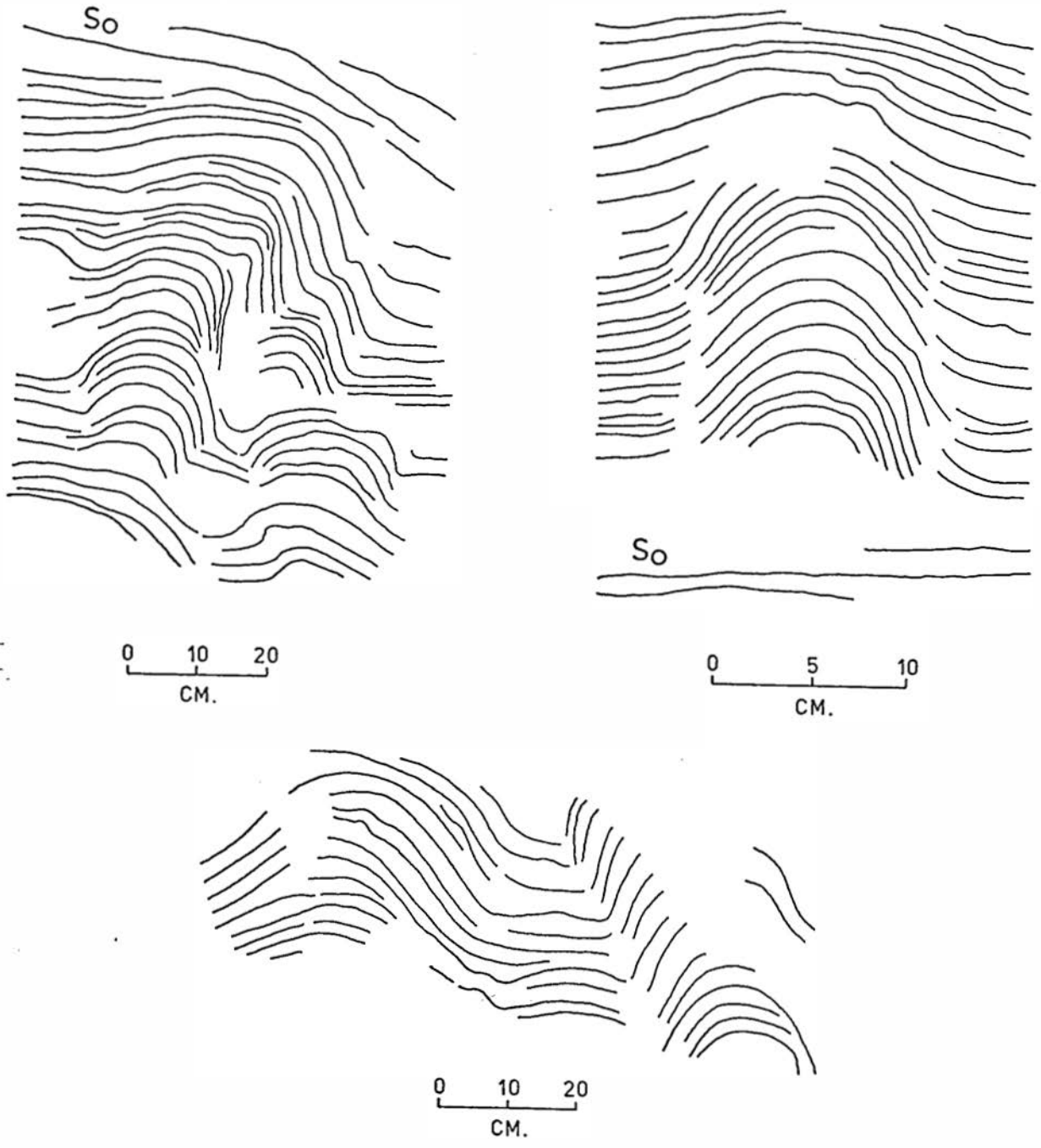

FIGURE 5.20

Longitudinal sections of tectonically unstrained stromatolites in the Gordon Subgroup in the Florentine Valley, southwest Tasmania. Bedding trace indicated by S_o.

unstrained material, stromatolitic lithologies were examined in the Gordon Subgroup in its type area in the Florentine Valley (454280, Map 1), southwest Tasmania. Here the geological structure is a large, gentle, upright horizontal syncline trending almost N-S, with little or no associated cleavage development. Field evidence, including the general lack of cleavage and tectonite fabrics except in some of the mudstones, the lack of deformation of fossils in the limestone, and the rarity of tectonic stylolites and veins, suggests that there has been little tectonic strain apart from the rotation associated with the folding. Bedding-perpendicular longitudinal sections of several columnar stromatolites from this area are shown in Fig. 5.20, and illustrate a certain amount of variation even in tectonically unmodified material. The geometries of these forms tend to be symmetric about lines perpendicular to the enveloping bedding surfaces (indicated by S_o).

In attempts at removal of the tectonic strain effects from the geometries of the Mayberry stromatolites, it has been assumed that the XY principal plane of the tectonic finite strain ellipsoid representing the flattening strain is parallel to cleavage, and that the strain was homogeneous and took place at constant volume. In addition, the X direction has been assumed to pitch at 90° in the cleavage plane (i.e., at a high angle to fold hingelines), based on parallelism with a lineation defined by preferred orientation of crystals in calcite fibre veins in cleavage-parallel thin sections at the two localities.

Thus, the vertical section perpendicular to cleavage at Locality 1, shown in Fig. 5.21, is assumed to represent an XZ principal section. Bedding (S_o) at this locality dips S at 30°, while cleavage (S_1) dips NNE at 75°. In the deformed state (Fig. 5.21A), the large

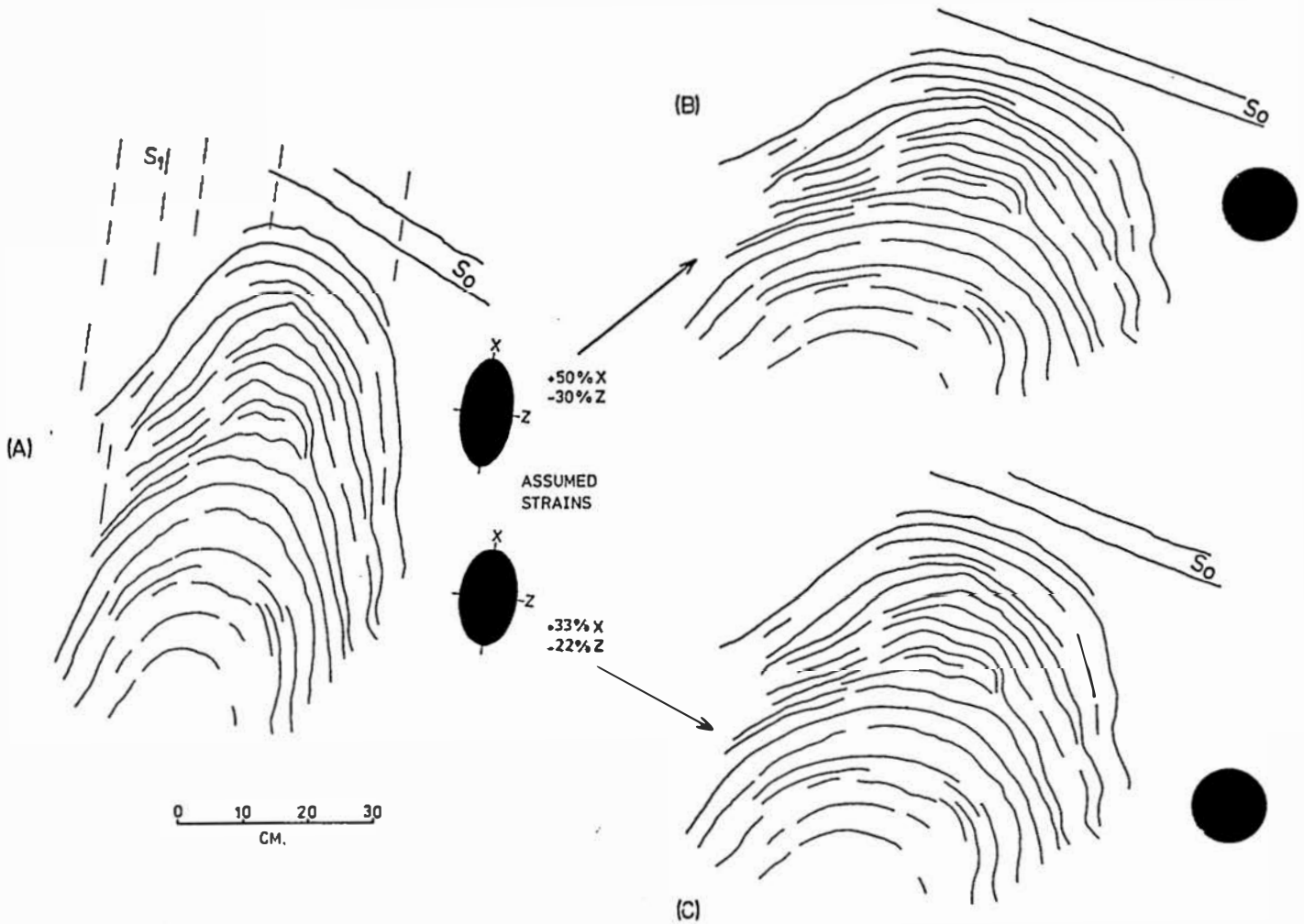

FIGURE 5.21 Destraining carried out on XZ principal section of deformed columnar stromatolite, Locality 1, Mayberry. Cleavage S_1, bedding S_o.

columnar stromatolite is markedly asymmetric with respect to both the cleavage trace and a line normal to the bedding trace, The bisector of the stromatolite form in fact lies between these two lines. As previously noted, it was estimated that the degree of cleavage development at Locality 1 was similar to that at average deformation states in the Grunter Hill/Kubla Khan Cave material. For this reason, the initial attempts at restoring the form to its pre-flattening geometry assumed a three-dimensional strain representing a point approximately in themiddle of the Grunter Hill/Kubla Khan Cave collective strain path (see Point 1, Fig. 5.22). The strain was (+50%X, -5%Y, -30%Z) yielding an X/Z two-dimensional strain ratio of 2.14. Fig. 5.21B shows the results of removal of this strain. The shape of the stromatolite is now much more similar to the actual unstrained examples in Fig. 5.20. However, it is notable that the line bisecting the form now lies clockwise from the normal to the bedding trace, whereas in the deformed state in Fig. 5.21A it was anticlockwise from it. This implies that the point at which these two lines were *parallel* was passed through during the destraining. The two-dimensional strain ratio which must be removed to produce the orthogonal geometry is in fact 1.71. If the three-dimensional strain is assumed to lie on the same Grunter Hill/Kubla Khan Cave strain path as that used in the first destraining attempt, it represents (+33%X, -3.6%Y, -22%Z). This is indicated by Point 2 on the triaxial strain graph in Fig. 5.22. The result of removal of this strain is shown in Fig. 5.21C. By comparison with the results of finite strain analysis at Grunter Hill/Kubla Khan Cave, it is suggested that the 22% shortening in Z assumed for this second destraining is a little low with regard to the degree of cleavage development at Locality 1. However, if the same two-dimensional strain ratio (1.71) is

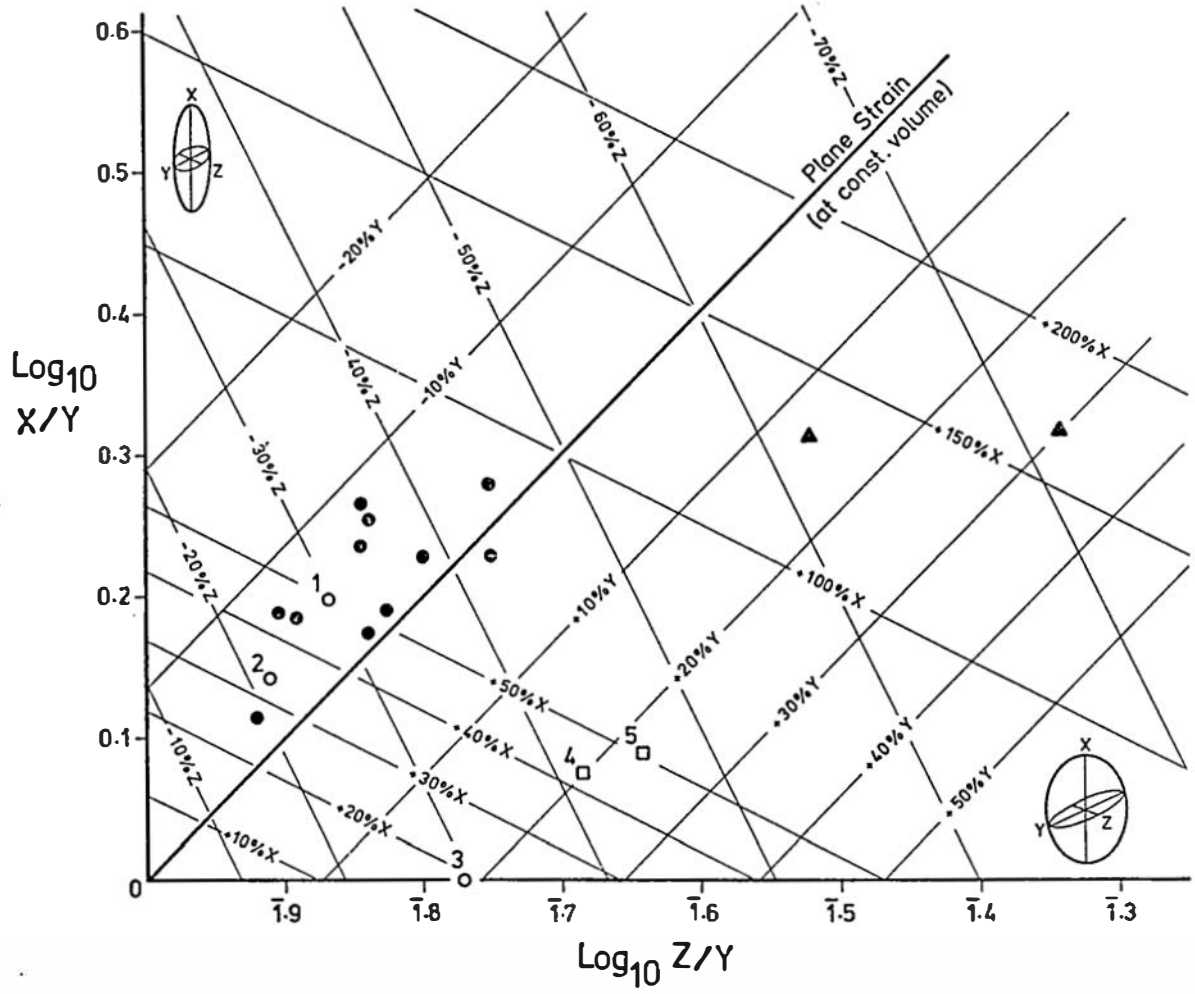

Strain Analysis of Deformed Stromatolites
Gordon Limestone S.G., Mayberry

- ● Finite strain data, oosparites & oncosparites, Grunter Hill
- ▲ Finite strain data, oncosparites, Claude Creek

Numbered points referred to in text

FIGURE 5.22

recalculated in three dimensions to a pure flattening strain (X = Y), the result is (+20%X, +20%Y, -30%Z) which brings the shortening in Z back up to a reasonable figure (see Point 3, Fig. 5.22). The possible pre-tectonic shapes of the stromatolite, represented by Figures 5.21B and C, fall within the range of shapes of the actual unstrained examples shown in Fig. 5.20. It is therefore suggested that boundary limits on the three-dimensional tectonic strain at Locality 1 are represented by Points 1 and 3 on Fig. 5.22. The destraining has reduced the height of the deformed stromatolite in Fig. 5.21A by 25 ± 3%, which has obvious implications in the use of such deformed objects for tidal range calculations (e.g., H.J. Hofmann, 1973).

At Locality 2 at Mayberry, the three-dimensional nature of the outcrop permits examination of the deformed stromatolites on sections parallel to all three principal planes. On the XY (cleavage-parallel) section, the similarity of the geometry of the stromatolite longitudinal sections with that of the actual unstrained examples in Fig. 5.20, lead to an initial assumption that the three-dimensional strain was close to a pure flattening type ($X/Y \approx 1$, and $X/Z = Y/Z$). On the YZ section, the stromatolites were exposed as cross-sections approximately normal to the axes of the columns (see Fig. 5.24A). On this section the assumption was made that the axial ratios and orientations of the column cross-sections were initially random. On this basis, a Dunnet (1969) Rf/ϕ analysis indicated a two-dimensional strain ratio, $Y/Z = 2.05$. Combining this with the assumption that $X/Y = 1$ yielding a three-dimensional strain of (+27%X, +27%Y, -38%Z). Removal of this strain from the YZ section yielded a result which appeared feasible, but on the XZ section (see Fig. 5.25A) there remained, after destraining, considerable residual clockwise asymmetry of the

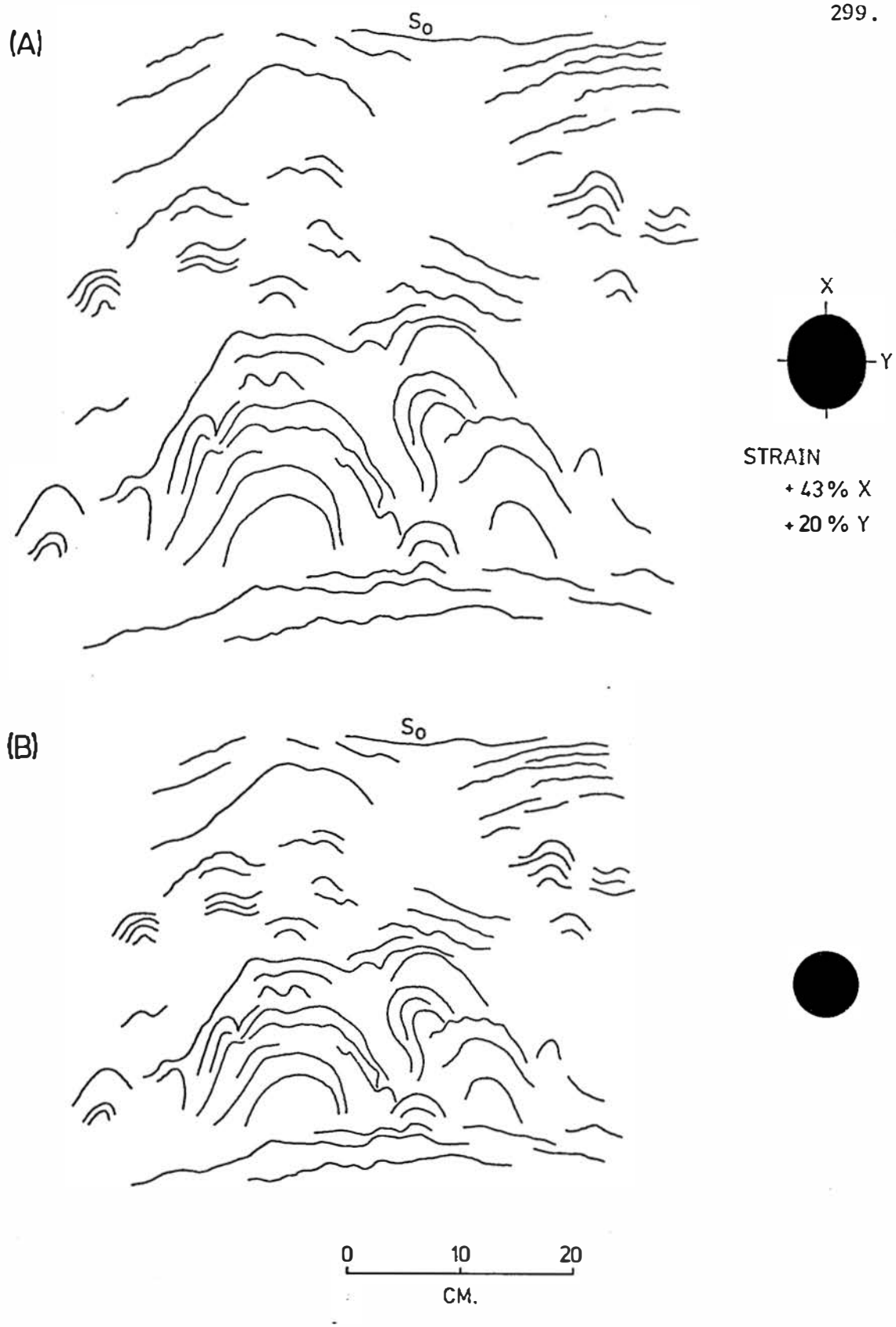

FIGURE 5.23

Destraining carried out on XY principal section of deformed stromatolites at Locality 2, Mayberry area. X/Y = 1.20.

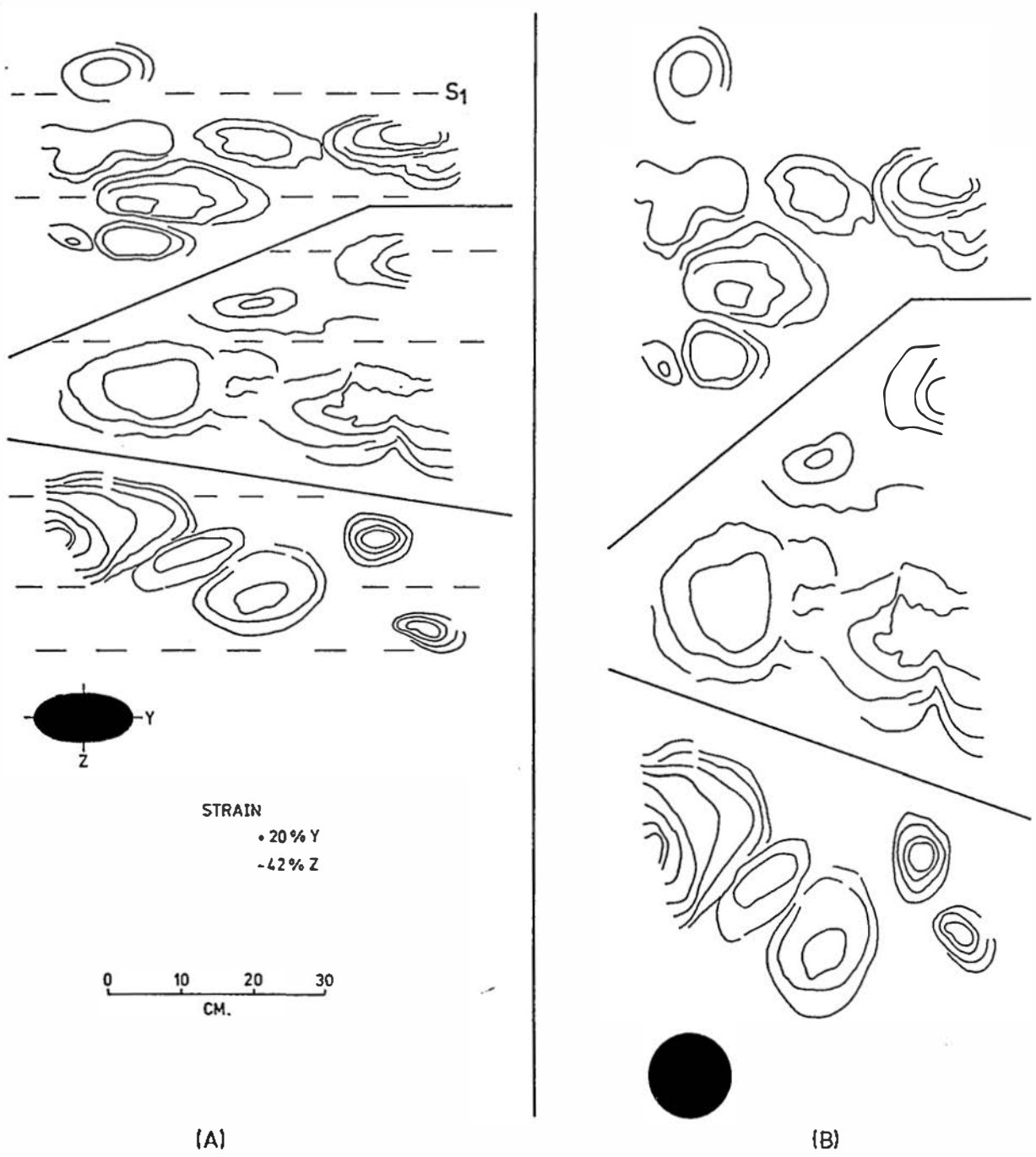

FIGURE 5.24

Destraining carried out on YZ principal section of deformed stromatolites, Locality 2, Mayberry area. Y/Z = 2.05.

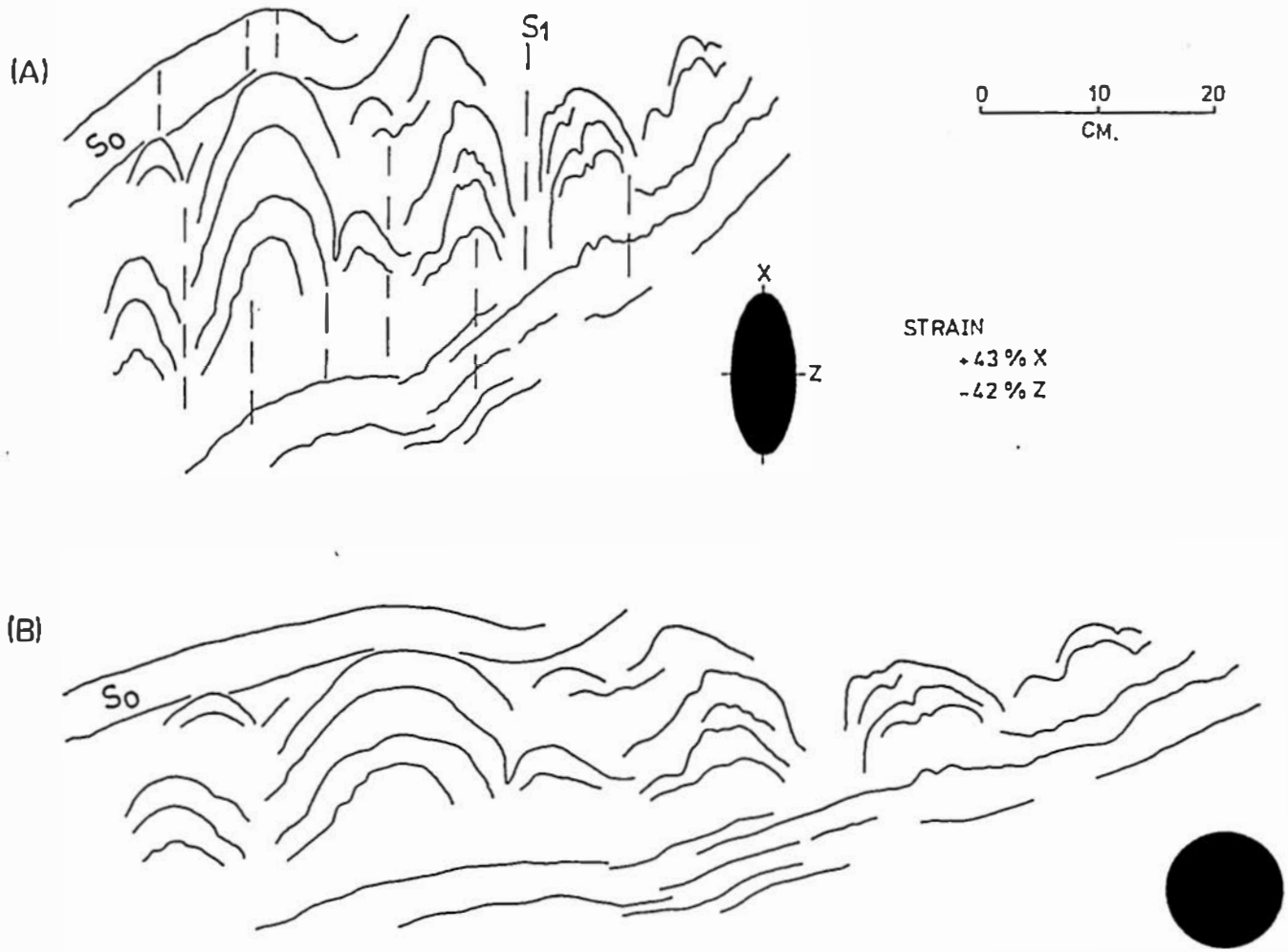

FIGURE 5.25 Destraining carried out on XZ principal section of deformed stromatolites, Locality 2, Mayberry area. X/Z = 2.47.

stromatolite columns with respect to lines normal to the bedding trace. It was found that the minimum strain ratio which had to be removed from the XZ section to restore reasonable orthogonal symmetry with respect to bedding, was 2.47. This implied that there was in fact a small amount of two-dimensional strain on the XY section in Fig. 5.23A, namely X/Y = 2.47/2.05 = 1.20. The three-dimensional strain was therefore recalculated to (+43%X, +20%Y, -42%Z), which is represented by Point 4 on the triaxial strain graph in Fig. 5.22. It is notable that the shortening in Z now approximately corresponds to that of the highest strain material from Grunter Hill, which is consistent with the strong cleavage development at Locality 2. This three-dimensional strain was used to carry out the destraining illustrated in Figs. 5.23-5.25.

Following destraining, the longitudinal sections of the stromatolite columns in Figs. 5.23B and 5.25B are now similar both to each other and to the actual unstrained examples in Fig. 5.20. On the YZ section analyzed in Fig. 24, it is notable that some of the column cross-sections are now elongate at high angles to the tectonically produced preferred orientation which was present in the field. This again has implications in the use of stromatolite cross-sections in deformed terrains for palaeocurrent analysis (P.F. Hoffman, 1967).

Stromatolites in one of the small outcrops at Locality 2 appeared to have undergone somewhat greater strain than those analyzed in Figs. 5.23-5.25. Only an XZ section was available, illustrated in Fig. 5.26A. The restoration of reasonable orthogonal symmetry and shape to these forms required a higher two-dimensional strain ratio than that used in Fig. 5.25, namely 2.80 rather than 2.47. A new three-dimensional strain value was calculated by assuming that it lay on

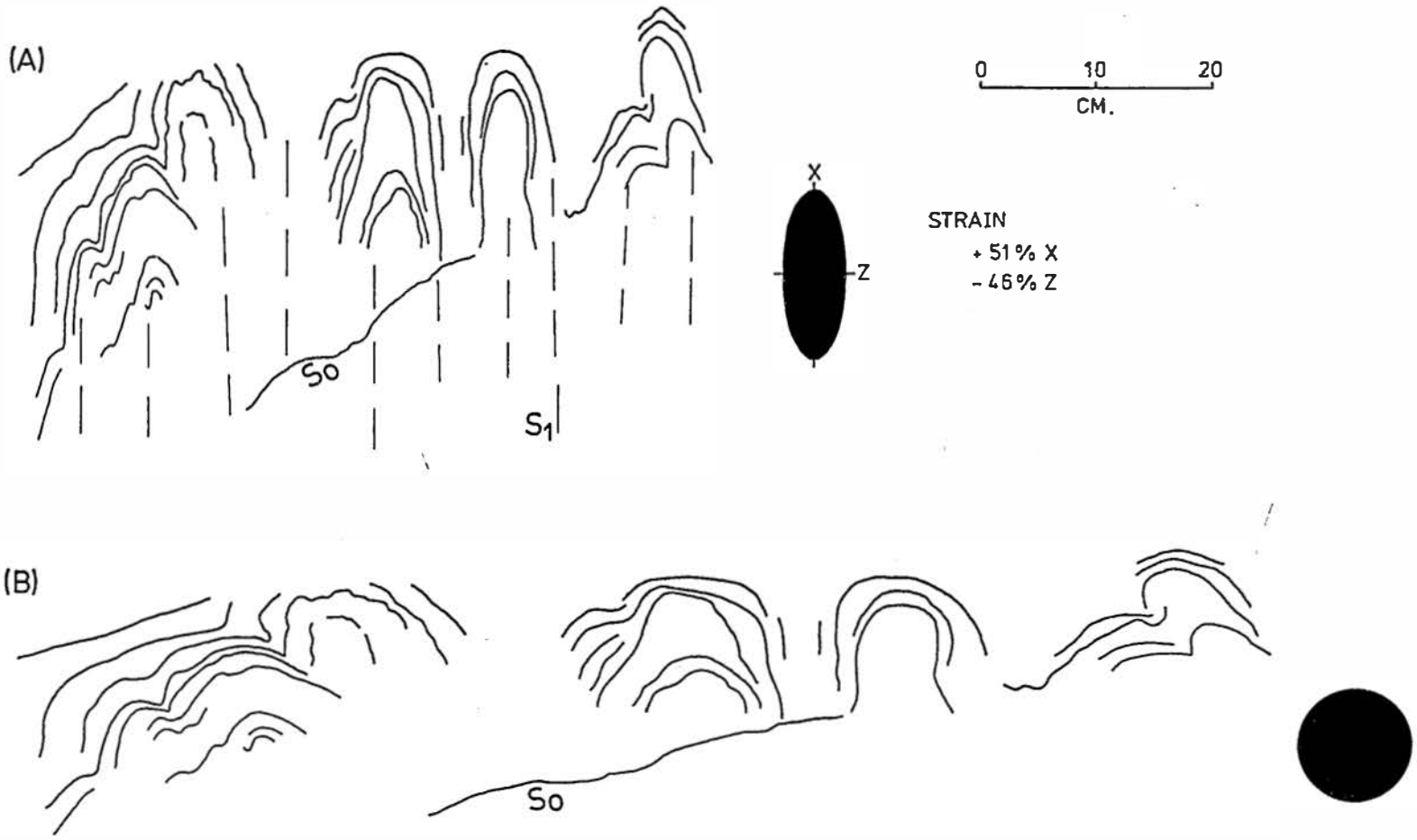

FIGURE 5.26 Higher strain XZ section of deformed stromatolites at Locality 2, Mayberry area. X/Z = 2.80.

the same strain path as that determined for the other stromatolites at Locality 2. The actual figures were (+51%X, +23%Y, -46%Z) represented by Point 5 on the triaxial strain graph (Fig. 5.22).

This exercise has given some indication of the degree of modification of stromatolite morphology which has occurred due to the flattening strain associated with cleavage development in the limestone at Mayberry. The question of whether stromatolites can be used as *strain markers* in deformed terrains is more difficult to answer. On sections at high angles to bedding it may be possible to derive two-dimensional strain ratios by assuming that *assemblages* of column axes had pretectonic preferred orientation normal to the bedding trace. This obviously would not apply to sections on which the principal extension direction is normal to the bedding trace. The two-dimensional strain ratio on sections at low angles to bedding may be derived by assuming that the cross-sections of the stromatolite columns had random orientations and axial ratios in the undeformed state. The assumptions made on both types of sections would need to be checked, preferably in equivalent tectonically unstrained material, as considerable morphological variation has been observed even in stromatolites which are known to be tectonically undeformed. In particular, the latter apparently sometimes exhibit preferred orientation of elongate column cross-sections parallel to currents and/or normal to shorelines (P.F. Hoffman, 1967). Sections at low angles to bedding in deformed equivalents of such material may be impossible to evaluate, because the only potentially precise strain analysis method which would be suitable is the Dunnet and Siddans (1971) STRANE method with MAX.SYM. criterion. However, the tests described in Section 5.2.4 herein showed that the STRANE computer program does not work well when used with the MAX.SYM. criterion alone.

CHAPTER 6

CONCLUSIONS

In the Black Bluff region, the stratigraphic equivalents of the Mt. Read Volcanics and the Dundas Group appear to display similar geographic distribution with respect to the Tyennan Geanticline as previously recorded in the Dundas Trough and the Fossey Mountain Trough. That is, volcanics are concentrated towards the margin of the Geanticline, with sediments becoming more prevalent away from it. The volcanics are dominated by pyroclastics of ashfall and ashflow type, with intermediate to acid composition. All of the volcanics are highly altered to quartz-albite-sericite-chlorite-(±carbonate) mineralogies. The sedimentary parts of the Mt. Read Volcanics/Dundas Group sequence essentially represent relatively minor intercalations between the volcanics, and mostly consist of volcaniclastic sediments, reworked tuffs and fine laminated siltstones. Further work is needed to obtain biostratigraphic data from these rocks in the Black Bluff region.

The available evidence suggests that the boundary between the Mt. Read Volcanics/Dundas Group stratigraphic equivalents and the overlying dominantly quartzose clastics of the Denison Subgroup stratigraphic equivalent, is a high angle angular unconformity in the Black Bluff region. However, there is no compelling evidence for pre-Devonian folding and/or cleavage development in the rocks underlying the unconformity. Rather, the movements responsible for the angular discordance appear to have produced steep tilting of the volcanosedimentary sequences. The provenance, palaeocurrent and thickness variation characteristics of the overlying Denison Subgroup sediments support the conclusion that these movements

were dominantly vertical and resulted in increased relief of the geanticlines of Precambrian rocks, which became source areas for the sediments overlying the unconformity.

The sediments comprising the Denison Subgroup stratigraphic equivalent are predominantly terrestrial quartzose clastics, much of the sequence apparently having been deposited in a variety of alluvial fan environments. The basal parts of the sequence are sometimes volcaniclastic. Marginal marine and marine sediments also occur, and progressively dominate the upper parts of the sequence in places. However, the simple subdivision of the Denison Subgroup stratigraphic equivalent into a lower terrestrial sequence and upper marine sequence reported in other parts of Tasmania, is not as clearcut in many parts of the Black Bluff region. The variety of lithofacies recognized in the Subgroup in the area of this study identify it as a potentially fruitful subject of further sedimentological research.

As is the case in most of northern Tasmania, the limestones of the Gordon Subgroup stratigraphic equivalent in the Black Bluff region are dominated by the products of deposition in intertidal carbonate sedimentary environments. Some of the carbonate lithofacies are distinguished from certain intertidal quartzose clastic sediments of the Denison Subgroup sequence only by relative lack of terrigeneous influx. This points to much reduced relief of the Tyennan Geanticline source area by the beginning of deposition of the limestones in the early-Middle Ordovician.

At least four main sequentially developed regional fold trends are now recognized as products of the Devonian deformation in the Black Bluff region. In order of development, the folds are on E (D1), NE (D2),

N (D3) and NW-NNW (D4) trends. Most of the folds are open, upright and horizontal, although vergence towards the Tyennan Block occurs close to its margins. The last three fold phases were associated with axial planar cleavage development in the less competent lithologies. In particular, the "West Coast Range/Valentines Peak trend" of Williams (1978) has been redefined to include only N-trending structures (D3 herein). Williams had included NE-trending folds and cleavage at the northwestern margin of the Tyennan Block, in his "West Coast Range/ Valentines Peak trend". However, these are now recognized as the expression of a separate deformation phase (D2 herein), which predates the N-trending structures. Thus, D4 ("Deloraine/Railton trend" of Williams, 1978) is now the only regional deformation phase which displays apparent deflection of fold trends against the margin of the Tyennan Block.

The place in the overall structural sequence, of local folding and cleavage development on ENE trends around the northern end of Bonds Range, is only definitely known relative to the second regional deformation phase, which it postdates. However, less conclusive evidence suggests that it occurred between D2 and D3. The relative time of development of folds and cleavage on WNW trends in the limestone at Loongana and Gunns Plains is uncertain at present. These structures were correlated with D1 by previous workers, but the degree of cleavage development at Loongana, the NNE-directed asymmetry of the folds and the fact that they do not trend exactly E-W are considered to be out of character with previous descriptions of the D1 folds.

In view of the newly recognized structural sequence, the lower limit on the age of the Tabberabberan deformation provided by the undeformed late-Middle Devonian cave deposits at Eugenana, may need to be

reconsidered. This is due to the fact that it now appears unclear whether the main cleavage-forming event in the limestone bedrock at Eugenana was a product of D3 or D4, as defined herein.

The present exposures of the Palaeozoic rocks represent high crustal levels at the time of the Devonian deformation. Depths of burial, even of the Cambrian rocks, were probably no greater than 4-5 km. However, conodont geothermometry indicates that temperatures of >300°C were developed at the base of the Gordon Subgroup. This indicates high crustal heat flow which is suggested to have been pre- and syntectonic with the deformation.

In the Cambrian volcanics, development of tectonite fabrics was dominantly by recrystallization and new grain growth of sericite and chlorite in the previously hydrothermally altered matrix and felspar phenocrysts. However, quartz phenocrysts deformed variously by brittle fracturing, stress-controlled dissolution and reprecipitation, and intragranular strain accomplished by the formation of deformation lamellae. Pressure dissolution of quartz, mica and calcite also played a major part in the formation of spaced cleavage domains (including tectonic stylolites) in the quartzose clastics and limestones of the Denison Subgroup and Gordon Subgroup. Reprecipitation of the dissolved material in these rocks is expressed in the form of syntectonic extensional fibre veins and fibrous overgrowths ("beards"). The deformation mechanisms responsible for pronounced tectonite fabrics in ultra-fine grained calcite (micrite) in certain lithologies in the Gordon Subgroup are uncertain, but may include superplastic flow (Schmid *et al.*, 1977).

Critical examination of strain analysis methods designed for suites of elliptical markers, has shown that the initial fabric effect

is probably the most important variable to be considered. Certain established strain analysis methods may need serious reconsideration on the basis of tests of their sensitivity to this variable, carried out during this project.

Results of tectonic finite strain analyses of incipiently to very strongly cleaved limestones in the Gordon Subgroup stratigraphic equivalent have indicated flattening across the cleavage varying between 19% and 71%, with concomitant extensions in X of 27% to 163%. The onset of obvious cleavage at outcrop scale in the limestone appears to correspond to flattening of 30-35%. In the oolitic limestones parallelism of cleavage with the XY principal plane of the finite strain ellipsoid representing the flattening, has been demonstrated to within an uncertainty of $\sim \pm 5°$. The three-dimensional shape of the finite strain ellipsoid in the analyzed samples was either of approximately plane strain type, or intermediate between plane strain and pure flattening, i.e., in the "field of slaty cleavage deformation" of Wood (1971, 1974).

REFERENCES

Ager, D.V. 1956: Field meeting in the Central Cotswolds. *Proc.Geol. Assoc.Can., 66:* 356-365.

Alvarez, W., Engelder, T. and Geiser, P.A. 1978: Classification of solution cleavage in pelagic limestones. *Geology, 6:* 263-266.

Baillie, P.W. and Williams, P.R. 1975: Sedimentary and structural features of the Bell Shale correlate (Early Devonian), Strahan Quadrangle, western Tasmania. *Pap.Proc.Roy. Soc.Tasm., 109:* 1-15.

Balme, B.E. 1960: Palynology of a sediment from Halletts Quarry, Melrose, Tasmania. *Palynol.Rep.Dep.Geol.Univ.W. Aust., 62.*

Banks, M.R. 1956: The Middle and Upper Cambrian Series (Dundas Group and its Correlates) in Tasmania, Pp. 165-212 *in: El Sistema Cambrico, 2, 20th Int.geol.Congr.*

_____ 1962a: Cambrian System. *In*: A.H. Spry and M.R. Banks (Eds.), The Geology of Tasmania. *Jour. geol.Soc. Aust., 9:* 127-145.

_____ 1962b: Ordovician System. *In*: A.H. Spry and M.R. Banks (Eds.), The Geology of Tasmania. *Jour. geol.Soc. Aust., 9:* 147-176.

_____ and Solomon, M. 1961: Cambrian succession in west Tasmania. *Aust.Jour.Sci., 23:* 337.

Barton, C.M. *et al.*, 1966: Geological Atlas 1 mile series. Zone 7 Sheet 44. Mackintosh. *Dept. of Mines, Tasm.*

Beach, A. 1974: A geochemical investigation of pressure solution and the formation of veins in a deformed greywacke. *Contrib.Mineral.Petrol., 46:* 61-68.

___ ___ 1977: Vein arrays, hydraulic fractures and pressure-solution structures in a deformed flysch sequence. *Tectonophysics, 40:* 201-226.

Bennison, G.M. and Wright, A.E. 1969: The geological history of the British Isles. London, Edward Arnold Ltd., 406pp.

Blissett, A.H. 1962: One mile geological map series. K/55-5-50. Zeehan. *Explan.Rep.geol.Surv.Tasm.*

Boulter, C.A. 1976: Sedimentary fabrics and their relation to strain-analysis methods. *Geology, 4:* 141-146.

_____ 1977: Cleavages in immature and mature arenites from the Precambrian of Tasmania. Au 3 *in*: B.M. Bayly, G.J. Borradaile, C. McA. Powell (Eds.), Atlas of Rock Cleavage (Provisional Edition). University of Tasmania.

_____ 1978: The structural and metamorphic history of the Wilmot and Frankland Ranges, Southwest Tasmania. Unpub. Ph.D. Thesis, University of Tasmania, 250pp.

Bradley, J. 1956: The geology of the West Coast Range of Tasmania, Part II. Structure and ore deposits. *Pap.Proc. Roy.Soc.Tasm., 90:* 65-129.

Brathwaite, R.L. 1972: The structure of the Rosebery ore deposit, Tasmania. *Proc.Aust.Inst.Min.Metall., 241:* 1-13.

Brown, A.V., Turner, N.J. and Williams, E. 1975: The basal beds of the Junee Group. *Pap.Proc.Roy.Soc.Tasm., 109:* 107-110.

Bull, W.B. 1972: Recognition of alluvial-fan deposits in the stratigraphic record. Pp. 63-83 *in*: J.K. Rigby and W.K. Hamblin (Eds.), Recognition of Ancient Sedimentary Environments. *S.E.P.M. Spec.Publ. No.16.*

Burns, K.L. 1963: The tectonic history of the Dial Range area, Tasmania. Unpub. Ph.D. thesis, University of Tasmania, 388pp.

_____ 1964: One mile geological map series. K/55-6-29. Devonport. *Explan.Rep.geol.Surv.Tasm.*

_____ and Spry, A.H. 1969: Analysis of the shape of deformed pebbles. *Tectonophysics, 7:* 177-196.

Burrett, C.F. 1978: Middle-Upper Ordovician conodonts and stratigraphy of the Gordon Limestone Subgroup, Tasmania. Unpub. Ph.D. Thesis, University of Tasmania, 342pp.

Campana, B. 1961: Comment on the note of Banks and Solomon. *Aust.Jour.Sci., 23:* 339.

_____, Dickinson, S.B., King D. and Matherson, R.S. 1958: The mineralized rift valleys of Tasmania. Pp. 41-60 *in*: F.L. Stillwell Anniversary Volume. *Aust.Inst. Min.Engrs.*

_____, King, D. and McKenna, D. 1960: Unconformable units of the Cambrian succession of West Tasmania. *Aust.Jour. Sci., 22:* 352-352.

_____ and King, D. 1963: Palaeozoic tectonism, sedimentation and mineralization in west Tasmania. *Jour.geol.Soc. Aust., 10:* 1-53.

Carey, S.W. 1947: Report of the Government Geologist. *Rept.Dir.of Mines, Tasm.*, for 1945, 21-29.

_____ 1953: Geological structure of Tasmania in relation to mineralization. *5th Emp.Min. and Metall.Congr., 1:* 1108-1128.

_____ and Banks, M.R. 1954: Lower Palaeozoic unconformities in Tasmania. *Pap.Proc.Roy.Soc.Tasm., 88:* 245-269.

Cloos, E. 1947: Oolite deformation in South Mountain Fold, Maryland. *Geol.Soc.Amer.Bull., 58:* 843-918.

_____ 1971: Microtectonics along the western edge of the Blue Ridge, Maryland and Virginia. Johns Hopkins Press, Baltimore and London. 234pp.

Corbett, K.D. 1970: Sedimentology of an Upper Cambrian flysch-paralic sequence (Denison Group) on the Denison Range, southwest Tasmania. Unpub. Ph.D. Thesis, University of Tasmania. 207pp.

_____ 1972: Features of thick-bedded sandstones in a proximal flysch sequence, Upper Cambrian, southwest Tasmania. *Sedimentology, 19:* 99-114.

_____, Banks, M.R. and Jago, J.B. 1972: Plate tectonics and the Lower Palaeozoic of Tasmania. *Nature Phys. Sci., 240:* 9-11.

_____ and Banks, M.R. 1974: Ordovician stratigraphy of the Florentine Synclinorium, southwest Tasmania. *Pap.Proc.Roy.Soc.Tasm., 107:* 207-238.

_____ and Banks, M.R. 1975: Revised terminology of the Late Cambrian - Ordovician sequence of the Florentine - Denison Range area, and the significance of the 'Junee Group'. *Pap.Proc.Roy.Soc.Tasm., 109:* 121-126.

_____, Reid, K.O., Corbett, E.B., Green, G.R., Wells, K. and Sheppard, N.W. 1974: The Mount Read Volcanics and Cambrian-Ordovician relationships at Queenstown, Tasmania. *Jour.geol.Soc.Aust., 21:* 173-186.

Cowan, D.S. 1974: Deformation and metamorphism of the Franciscan Subduction Zone Complex northwest of Pacheco Pass, California. *Geol.Soc.Amer.Bull., 85:* 1623-1634.

Crawford, A.R. and Campbell, K.S.W. 1973: Large-scale horizontal displacement within Australo-Antarctica in the Ordovician. *Nature Phys.Sci., 241:* 11-14.

Donath, F.A. and Wood, D.S. 1976: Experimental evaluation of the deformation path concept. *In*: A Discussion on Natural Strain and Geological Structure. *Phil.Trans. Roy.Soc.Lond., A283:* 187-201.

Dunnet, D. 1969: A technique of finite strain analysis using elliptical particles. *Tectonophysics, 7:* 117-136.

_____ and Siddans, A.W.B. 1971: Non-random sedimentary fabrics and their modification by strain. *Tectonophysics, 12:* 307-325.

Durney, D.W. 1972: Solution-transfer, an important geological deformation mechanism. *Nature, 235:* 315-317.

_____ 1976: Pressure-solution and crystallization deformation. *In*: A Discussion on Natural Strain and Geological Structure. *Phil.Trans.Roy.Soc.Lond., A283:* 229-240.

_____ and Ramsay, J.G.R. 1973: Incremental strains measured by syntectonic crytal growths. *In*: K.A. DeJong and R. Scholten (Eds.), Gravity and Tectonics. J. Wiley and Sons.

Elliott, D. 1970: Determination of finite strain and initial shape from deformed elliptical objects. *Geol.Soc.Amer. Bull., 81:* 2221-2236.

_____ 1973: Diffusion flow laws in metamorphic rocks. *Geol.Soc.Amer.Bull., 84:* 2645-2664.

Elliston, J.N. 1954: Geology of the Dundas District, Tasmania. *Pap.Proc.Roy.Soc.Tasm., 88:* 161-183.

Epstein, A., Epstein, J. and Harris, L.D. 1977: Conodont colour alteration - an index to conodont metamorphism. *U.S.Geol.Survey Prof.Paper, 995:* 1-27.

Etheridge, M.A. and Lee, M.F. 1975: Microstructure of slate from Lady Loretta, Queensland, Australia. *Geol.Soc.Amer. Bull., 86:* 13-22.

Flinn, D. 1958: On tests of significance of preferred orientation in three-dimensional fabric diagrams. *Jour.Geol., 66:* 526-539.

Flood, P.G. 1974: Lower Devonian brachiopods from the Point Hibbs Limestone of western Tasmania. *Pap.Proc.Roy.Soc. Tasm., 108:* 113-136.

Folk, R.L. 1962: Spectral subdivision of limestone types. Pp. 62-84 *In*: Classification of carbonate rocks. *Amer.Assoc. Petroleum Geologists, Memoir 1,* 279pp.

Gay, N.C. 1968: Pure-shear and simple-shear deformation of inhomogeneous viscous fluids. 2. The determination of the total finite strain in a rock from objects such as deformed pebbles. *Tectonophysics, 5:* 295-302.

Gee, C.E., Jago, J.B. and Quilty, P.G. 1970: The age of the Mt. Read Volcanics in the Que River area, western Tasmania. *Jour.geol.Soc.Aust., 16:* 761-763.

Gee, R.D. 1963: Structure and petrology of the Raglan Range. *Bull.geol.Surv.Tasm., 47.*

_____, Marshall, B. and Burns, K.L. 1970: The metamorphic and structural sequence in the Precambrian of the Cradle Mountain area, Tasmania. *Rep.geol.Surv.Tasm.,11.*

Geiser, P.A. 1974: Cleavage in some sedimentary rocks of the Central Valley and Ridge province, Maryland. *Geol.Soc.Amer.Bull., 85:* 1399-1412.

Gray, D.R. 1978: Cleavages in deformed psammitic rocks from south-eastern Australia: their nature and origin. *Geol.Soc. Amer.Bull., 89:* 577-590.

Harker, A. 1885: On slaty cleavage and related rock structures, with special reference to the mechanical theories of their origin: *British Assoc.Adv.Sci.,* 813-852.

Harrington, H.J., Burns, K.L. and Thompson, B.R. 1973: Gambier-Beaconsfield and Gambier-Sorell fracture zones and the movement of plates in the Australia-Antarctic-New Zealand region. *Nature Phys.Sci., 245:* 109-112.

Hills, C.L. and Carey, S.W. 1949: Geology and mineral industry. *In*: Handbook for Tasmania. *Aust.Ass.Adv.Sci.,* Hobart.

Hoffman, P.F. 1967: Algal stromatolites: use in stratigraphic correlation and palaeocurrent determination. *Science, 257:* 1043-1045.

Hofmann, H.J. 1973: Stromatolites: characteristics and utility. *Earth Sci.Revs., 9:* 339-373.

Hughes, T.D. 1957: Loongana. Pp. 138-141 *in*: Limestones in Tasmania. *Geol.Surv.Min.Res. No.10, Dept.of Mines Tasm.*

Jago, J.B. 1972: The youngest recorded Tasmanian Cambrian trilobites. *Search, 3:* 173-174.

_____ 1973: Paraconformable contacts between Cambrian and Junee Group sediments in Tasmania. *Jour.geol.Soc.Aust., 20:* 373-377.

_____ 1976: Late Middle Cambrian Agnostid trilobites from the Gunns Plains area, north-western Tasmania. *Pap.Proc. Roy.Soc.Tasm., 110:* 1-18.

_____ 1977: A late-Middle Cambrian fauna from the Que River Beds, western Tasmania. *Pap.Proc.Roy.Soc.Tasm.,111:* 41-57.

_____ 1978: Late Cambrian fossils from the Climie Formation Western Tasmania. *Pap.Proc.Roy.Soc.Tasm., 112:* 137-153.

_____, Cooper, J.A. and Corbett, K.D. 1977: First evidence for Ordovician igneous activity in the Dial Range Trough, Tasmania. *Jour.geol.Soc.Aust., 24:* 81-86.

_____, Pike G.A. and Mills, D. 1975: Cambrian stratigraphy of the St. Valentines Peak area, north-western Tasmania. *Pap.Proc.Roy.Soc.Tasm., 109:* 85-90.

_____, Reid, K.O., Quilty, P.G., Green, G.R. and Daily, B. 1972: Fossiliferous Cambrian limestone from within the Mount Read Volcanics, Mount Lyell Mine area, Tasmania. *Jour.geol.Soc.Aust., 19:* 379-382.

Jennings, I.B. 1958: The Round Mount District. *Bull.geol.Surv.Tasm.,45.*

_____ 1963: One mile geological map series. K/55-6-45. Middlesex. *Explan.Rep.geol.Surv.Tasm.*

_____ and Burns, K.L. 1958: Geological Atals 1 mile series Zone 7 Sheet 45. Middlesex. *Dept. of Mines, Tasm.*

_____, Burns, K.L., Mayne, S.J. and Robinson, R.G. 1959: Geological Atlas 1 mile series. Zone 7 Sheet 37. Sheffield. *Dept. of Mines, Tasm.*

Kobayashi, T. 1940: Lower Ordovician fossils from Caroline Creek, near Latrobe, Mersey River District, Tasmania. *Pap.Roy.Soc.Tasm.,* (1939), 67-76.

Lewis, A.N. 1940: Geology of the Tyenna Valley. *Pap.Proc.Roy.Soc.Tasm.,* (1939): 33-59.

Loftus-Hills, G., Solomon, M. and Hall, R.J. 1967: The structure of the bedded rocks west of Rosebery, Tasmania. *Jour.geol.Soc.Aust., 14:* 333-338

Longman, M.J. and Matthews, W.L. 1962: Geology of the Bluff Point and Trowutta Quadrangles. *Tech.Rep.Dept.Mines Tasm., 6:* 48-54.

Matthews, P.E., Bond, R.A.B. and Van den Berg, J.J. 1974: An algebraic method of strain analysis using elliptical markers. *Tectonophysics, 24:* 31-67.

McClean, C.J. 1974: Structural petrology of the Davey River area, southwestern Tasmania. *Pap.Proc.Roy.Soc.Tasm., 107:* 57-63.

McDougall, I. and Leggo, P.J. 1965: Isotopic age determinations on granitic rocks from Tasmania. *Jour.geol.Soc.Aust., 12:* 295-332.

McNeil, R.D. 1961: Geological reconnaissance of part of the Arthur River area. *Tech.Rep.Dept.Mines Tasm., 5:* 46-59.

Mimran, Y. 1976: Strain determination using a density-distribution technique and its application to deformed Upper Cretaceous Dorset Chalks. *Tectonophysics, 31:* 175-192.

Mitra, S. 1976: A quantitative study of deformation mechanisms and finite strain in quartzites. *Contrib.Mineral. Petrol., 59:* 203-226.

_____ 1978: Microscopic deformation mechanisms and flow laws in quartzites within the South Mountain Anticline. *Jour.Geol., 86:* 129-152.

Moore, J.G. and Peck, D.L. 1962: Accretionary lapilli in volcanic rocks of the western continental United States. *Jour.Geol., 70:* 182-193.

Nickelsen, R.P. 1979: Sequence of structural stages of the Alleghany Orogeny, at the Bear Valley strip mine, Shamokin, Pennsylvania. *Amer.Jour.Sci., 279:* 225-271.

Opik, A.A. 1951: Cambrian fossils from Leven Gorge, Northern Tasmania. *Bur.Min.Res.Records,* 1951-56.

_____ 1956: Cambrian Palaeogeography of Australia. Pp. 239-284 *in: El Sistema Cambrico, 2, 20th Int.geol.Congr.*

Park, W.C. and Schot, E.H. 1968: Stylolites: their nature and origin. *Jour.Sed.Pet., 38:* 175-191.

Philips, W.J. 1974: The development of vein and rock textures by tensile strain crystallization. *Q.Jour.Geol.Soc. Lond., 130:* 441-448.

Pike, G. 1964: Geology of the Region around St. Valentines Peak, Tasmania. Unpub. B.Sc. Honours Thesis, University of Tasmania, 89pp.

Powell, C. McA. 1969: Intrusive sandstone dykes in the Siamo Slate near Negaunee, Michigan. *Geol.Soc.Amer.Bull., 80:* 2585-2594.

_____ 1977: Overgrowths and mica beards on rounded quartz grains enclosed by cleavage folia. Am 33 *in:* B.M. Bayly, G.J. Borradaile, C.McA. Powell (Eds.), Atlas

of Rock Cleavage (Provisional Edition). University of Tasmania.

_____ 1979: A morphological classification of rock cleavage. *Tectonophysics, 58:* 21-34.

Ramsay, J.G. 1967: Folding and Fracturing of Rocks. McGraw-Hill, 568pp.

_____ and Wood, D.S. 1973: The geometric effects of volume change during deformation processes. *Tectonophysics, 16*: 263-277.

Richards, H.C. and Bryan, W.H. 1927: Volcanic mud balls from the Brisbane tuff. *Roy.Soc.Queensland, 34:* 54-60.

Roberts, B. and Siddans, A.W.B. 1971: Fabric studies in the Llwyd Mawr Ignimbrite, Caernarvonshire, North Wales. *Tectonophysics, 12:* 283-306.

Robin, P. - Y.F. 1977: Determination of geologic strain using randomly oriented strain markers of any shape. *Tectonophysics, 42:* T7-T16.

Rutter, E.H. 1976: The kinetics of rock deformation by pressure solution. *In*: A Discussion on Natural Strain and Geological Structure. *Phil.Trans.Roy.Soc.Lond., A283:* 203-219.

Schmid, S.M., Boland, J.N. and Paterson, M.S. 1977: Superplastic flow in fine grained limestone. *Tectonophysics,43:* 257-291.

_____ and Paterson, M.S. 1976: An experimental study of the marker technique of strain determination using oolitic limestone. *Australian National University, Research School of Earth Sciences, Annual Report 1976,* 44-45.

_____ and Paterson, M.S. 1977: Strain analysis in an experimentally deformed oolitic limestone. *In*: S.K. Saxena and S. Battacharji (Eds.), Energetics of Geological Processes. Springer, Berlin.

Seymour, D.B. 1975: Deformation studies of Gordon Limestone and Moina Sandstone. Unpub. B.Sc. Honours Thesis, University of Tasmania. 113pp.

_____ 1977: Dissolution and precipitation during deformation. Au 13 *in*: B.M. Bayly, G.J. Borradaile, C. McA. Powell (Eds.), Atlas of Rock Cleavage (Provisional Edition). University of Tasmania.

_____ (In press): Pressure dissolution as a cleavage-forming process in quartz sandstone and limestone
and
Finite strain and pressure solution processes in a

deformed limestone. *In*: B.M. Bayly, G.J. Borradaile, C. McA. Powell (Eds.), Atlas of Rock Cleavage (Revised Edition). Springer-Verlag.

_____ and Boulter, C.A. 1979: Tests of computerized strain analysis methods by the analysis of simulated deformation of natural unstrained sedimentary fabrics. *Tectonophysics, 58:* 221-235.

Shimamoto, T. and Ikeda, Y. 1976: A simple algebraic method for strain estimation from deformed elliptical objects. I: Basic theory. *Tectonophysics, 36:* 315-337.

Solomon, M. 1957: Palaeozoic sedimentation, tectonics and mineralization in the Mt. Lyell area (Tasmania). Unpub. Ph.D. Thesis, University of Tasmania.

_____ 1962: The Tectonic History of Tasmania. *In*: A.H. Spry and M.R. Banks (Eds.), The Geology of Tasmania. *Jour.geol.Soc.Aust., 9:* 311-339.

_____ 1965: Geology and mineralization of Tasmania. *Publs. 8th Commonw.Min.Metall.Congr., 1:* 464-477.

Sparks, R.S.J. 1976: Grain size variations in ignimbrites and implications for the transport of pyroclastic flows. *Sedimentology, 23:* 147-188.

Spry, A.H. 1962: The Precambrian rocks. *In*: A.H. Spry and M.R. Banks (Eds.), The Geology of Tasmania. *Jour .geol. Soc.Aust., 9:* 107-126.

_____ 1963: The Precambrian rocks of Tasmania. Part V, Petrology and structure of the Frenchman's Cap area. *Pap.Proc. Roy. Soc.Tasm., 97:* 105-127.

Tan, B.K. 1974: Deformation of particles developed around rigid and deformable nuclei. *Tectonophysics, 24:* 243-257.

_____ 1976: Oolite deformation in Windgällen, Canton Uri, Switzerland.*Tectonophysics, 31:* 157-174.

Tobisch, O.T., Fiske, R.S., Sacks. S. and Taniguchi, D. 1977: Strain in metamorphosed volcaniclastic rocks and its bearing on the evolution of orogenic belts. *Geol.Soc.Amer.Bull., 88:* 23-40.

Wade, M. and Solomon, M. 1958: Geology of the Mount Lyell mines, Tasmania. *Econ.Geol., 53:* 367-416.

White, S. 1976: The effects of strain on the microstructures, fabrics, and deformation mechanisms in quartzites. *In*: A Discussion on Natural Stain and Geological Structure. *Phil.Trans.Roy.Soc.Lond., A283:* 69-86.

Wickham, J.S. 1973: An estimate of strain increments in a naturally deformed carbonate rock. *Amer.Jour.Sci., 273:* 23-47.

_____and Anthony, M. 1977: Strain paths and folding of carbonate rocks near Blue Ridge, Central Appalachians. *Geol.Soc.Amer.Bull., 88:* 920-924.

_____ and Elliott, D.E. 1970: Rotation and strain history in folded carbonates, Front Royal area, Northern Virginia (Abstract). *Trans.Amer.Geophys.Union, 51:* 422.

Williams, E. 1976: Tasman fold belt system in Tasmania. Explan. notes for the 1:500,000 structural map of pre-Carboniferous rocks of Tasmania. *Tasm.Dept.of Mines publication.*

_____ 1978: Tasman fold belt system in Tasmania. *Tectonophysics, 48:* 159-205.

_____, Solomon, M. and Green, G.R. 1976: The geological setting of metalliferous ore deposits in Tasmania. *Monogr.Ser.Australas. Inst.Min.Metall., 5:* 567-581.

_____, and Threader, V.M. 1971: Tectonic setting of ore deposits in Tasmania. *Section 3, 41st ANZAAS Congress, Brisbane.*

_____, and Turner, N.J. 1973: Geological Atlas 1:250,000 Series. SK 55-3. Burnie. *Dept.of Mines, Tasm.*

Williams, P.F. 1972: 'Pressure Shadow' structures in foliated rocks from Bermagui, New South Wales. *Jour.geol.Soc.Aust., 18:* 371-377.

Williams, P.R. 1975: The relationship between the Cambrian rocks and the correlate of the Junee Group at Misery Hill, near Zeehan. *Tech. Rep.Dept.Mines Tasm., 18:* 36-39.

Wood, D.S. 1971: Studies of strain and slaty cleavage in the Caledonides of north-west Europe and the eastern United States. Unpub. Ph.D. Thesis, Dept. of Earth Sci., University of Leeds. 182pp.

_____ 1973: Patterns and magnitudes of natural strain in rocks. *Phil.Trans.Roy.Soc.Lond., A274:* 373-382.

_____ 1974: Current views of the development of slaty cleavage. *Ann.Rev.Earth and Plan.Sci., 2:* 369-401.

Zimmerle, W. and Bonham, L.C. 1962: Rapid methods for dimensional grain orientation measurements. *Jour.Sed.Pet., 32:* 751-763.

APPENDIX A.

ROCK SPECIMEN COLLECTION

Except for the material used for strain analysis in the Gordon Subgroup stratigraphic equivalent, the following list is subdivided according to the structural map on which the localities occur. Grid coordinates are given to the nearest 100 metres in the order (east, north) and are prefixed by a letter representing the appropriate Tasmanian Government Lands Department 1:100,000 TASMAP, as follows:-

H	Hellyer	(sheet 8015)
F	Forth	(sheet 8115)
S	Sophia	(sheet 8014)
M	Mersey	(sheet 8114)

The preparation key is:-

T	Thin section
PT	Polished thin section

In many cases two or more mutually orthogonal thin sections were made, indicated by T x 2, etc. Most of the samples were field oriented, the orientation being indicated by a strike azimuth and dip symbol on a prominent flat surface on each specimen. All azimuths are relative to true north.

A1 STRAIN ANALYSIS MATERIAL (Gordon Subgroup strat. equiv.)

Catalogue No.	Grid Coords.	Preparations	Description
48357	M 4402/4001	T x 3	Weakly cleaved oosparite
48358	"	T x 3	" " "
48359	M 4396/3993	T x 3	Oosparite, slightly deformed, uncleaved
48360	M 4402/4001		Weakly cleaved oncosparite
48361	"		Cleaved oncosparite
48362	F 4305/4054		Strongly cleaved oncosparite
48363	"		" " "

A2 SMITHS PLAINS STRUCTURAL MAP

A2.1 Mount Read Volcanics/Dundas Group strat.equivs.

Catalogue	Grid Coords.	Preparations	Description
48364	F 4197/4121	PT x 2	Cleaved strongly altered volcanic wacke conglomerate or agglomerate
48365	"	PT x 2	Cleaved strongly altered volcanic wacke conglom. or crystal lithic tuff
48366	"	PT x 2	" " "
48367	"		Cleaved strongly altered volcanic wacke conglom. or agglomerate
48368	"	T	" " "
48369	"		" " "
48370	F 4198/4126		Cleaved volcanic wacke
48371	F 4187/4129	T	Thinly laminated argillaceous siltstone and fine quartz wacke
48372	"	T x 3	Lithic (felspar > quartz) crystal tuff (ashfall)
48373	"	T x 2	" " "
48374	F 4194/4101	T x 2	Cleaved hematitic fine lithic wacke conglomerate
48375	F 4180/4091	PT x 2	Strongly altered andesitic lava
48376	"	T x 2	Strongly altered quartz-(?) felspar porphyry (2 cleavages present)
48377	F 4180/4094		Altered flow-banded andesitic lava
48378	"	PT x 2	" " "
48379	"	T	Cleaved strongly altered quartz-(?)felspar porphyry (2 cleavages present)
48380	"	T x 2	Strongly cleaved heavily altered quartz-(?)felspar porphyry (2 cleavages present)
48381	F 4180/4094	T	Altered quartz-felspar porphyry
48382	F 4190/4101		Welded quartz crystal vitric tuff
48383	F 4193/4103	T x 2	Cleaved altered crystal vitric tuff (ashflow)
48384	"		Andesitic lava
48385	H 4159/4125		Cleaved coarse lithic crystal tuff (ashflow?) or agglomerate
48386	H 4160/4124		Thin bedded laminated siltstone and fine quartz wacke

Catalogue No.	Grid Coords.	Preparations	Description
48387	H 4161/4127		Thin bedded laminated siltstone and fine quartz wacke
48388	"		" " "
48389	H 4160/4124		Welded lithic crystal tuff in contact with 48386
48390	H 4161/4123		Quartz-felspar porphyry with fine dark green groundmass
48391	"		As for 48390 but with (?) autobrecciated texture
48392	F 4167/4087	T x 2	Altered quartz-(?)felspar porphyry (autobrecciated lava or coarse pyroclastic breccia)
48393	"	T	Cleaved strongly altered coarse quartz porphyry (originally ashflow tuff?)
48394	"	T x 2	Cleaved strongly altered quartz porphyry with coarse fragmental texture (ashflow tuff?)
48395	H 4156/4083		Cleaved altered crystal vitric tuff
48396	H 4153/4081	T x 2	Weakly cleaved strongly altered andesitic lava
48397	H 4148/4081		Cleaved fine quartz-crystal vitric tuff
48398	H 4132/4115	T x 2	Strongly cleaved altered quartz-felspar porphyry (crystal vitric tuff?)

A2.2 Denison Subgroup strat.equiv.

48399	F 4174/4083	T x 2	Cleaved pebbly quartz arenite
48400	F 4167/4087		Weakly cleaved laminated hematitic quartz siltstone
48401	"	T	Cleaved thin bedded hematitic quartz wacke siltstone
48402	F 4169/4075	T x 2	Cleaved bioturbated quartz wacke
48403	F 4169/4080	T x 2	Strongly cleaved hematitic fine lithic wacke conglomerate
48404	F 4179/4088	T	Cleaved hematitic fine quartz wacke
48405	H 4138/4089	T x 2	Weakly cleaved hematitic fine chert breccia (bimodal fabric)
48406	H 4131/4103	T x 2	Cleaved hematitic fine volcanic wacke congomerate

A3. BLACK BLUFF STRUCTURAL MAP (& WEST)

A3.1 Mount Read Volcanics/Dundas Group strat.equivs.

Catalogue No.	Grid Coords.	Preparations	Description
48407	H 4097/4126	T x 2	Strongly cleaved hematitic lithic wacke
48408	H 4044/4122		Felspar -crystal vitric tuff
48409	H 4059/4106	T x 2	Thin bedded quartz-felspar crystal tuff and mudstone (2 cleavages present)
48410	H 4008/4143		Laminated dark grey claystone and siltstone
48411	"	T	" " "
48412	"		" " "
48413	"	T	Cleaved thin bedded light green claystone
48414	"	T x 2	Altered crystal tuff(ashflow)
48415	H 4059/4106		(As for 48409)
48416	H 4059/4107	T x 2	Cleaved altered coarse lithic crystal tuff (ashflow?)

A3.2 Denison Subgroup strat.equiv.

48417	H 4104/4062	T x 2	Hematitic fine chert conglomerate (bimodal fabric)
48418	"	T x 2	" " "
48419	H 4077/4056		Thin bedded hematitic quartz arenite and mudstone with trilobite trace fossils

A4. VALE OF BELVOIR (NORTH) STRUCTURAL MAP

A4.1 Mount Read Volcanics strat.equiv.

48420	S 4071/4038	T x 2	Cleaved altered quartz-(minor felspar) porphyry
48421	"	T x 2	Strongly cleaved altered quartz-(?)felspar porphyry, possible flow banding (3 cleavages present)
48422	S 4059/4032	T x 2	Weakly cleaved altered quartz-felspar porphyry with flow banding (originally andesitic lava?)
48423	S 4056/4013	T x 2	Cleaved altered fine quartz-(?)felspar porphyry (2 cleavages present)

Catalogue No.	Grid Coords.	Preparations	Description
48424	S 4051/4015	T x 2	Cleaved altered quartz porpyry with (?) autobrecciated texture
48425	S 4099/4020	T x 2	Weakly deformed altered quartz-(?)felspar porphyry
48426	S 4112/4030	T x 2	Cleaved altered quartz-(?) felspar porphyry
48427	S 4123/4040	T x 2	Strongly cleaved quartz wacke (2 cleavages present)
48428	S 4072/4037	T x 2	Strongly cleaved altered quartz porphyry (2 cleavages present)
48429	S 4071/4038		(As for 48421)
48430	S 4067/4038	T	Cleaved altered quartz porphyry with (?) autobrecciated or fragmental texture
48431	S 4112/4030		(As for 48426)
48432	S 4137/4046	T x 2	Cleaved altered coarse quartz-(?)felspar porphyry
48433	S 4131/4043		Cleaved coarse quartz porphyry

A5. VALE OF BEVOIR (SOUTH) STRUCTURAL MAP

A5.1 Mount Read Volcanics strat. equiv.

48434	S 4051/3972	T x 2	Cleaved altered quartz-crystal (?) vitric tuff (ashflow?) (2 cleavages present)

A5.2 Gordon Subgroup strat.equiv.

48435	S 4073/3999		Very strongly cleaved dolomicrite
48436	S 4074/3997		Weakly cleaved channel-filling biosparite (calcarenite)
48437	"		" " "
48438	S 4072/3996		Cleaved channel-filling biosparite (calcarenite) (2 cleavages present?)
48439	S 4071/3994		Very strongly cleaved micrite
48440	S 4074/3997		(As for 48436 and 48437)